

CAPITAL UNIVERSITY OF SCIENCE AND  
TECHNOLOGY, ISLAMABAD



# Energy-Balancing with Sink Mobility in the Design of Underwater Routing Protocols

by

Zahid Wadud

A thesis submitted in partial fulfillment for the  
degree of Doctor of Philosophy

in the

Faculty of Engineering

Department of Electrical Engineering

2019

# Energy-Balancing with Sink Mobility in the Design of Underwater Routing Protocols

By  
Zahid Wadud  
(PE123002)

Dr. Leonard Barolli, Professor  
Faculty of Information Engineering, Fukuoka Institute of Technology,  
Japan

Dr. Kamran Munir, Associate Professor  
University of West of England (UWE), Bristol, UK

Dr. Sajjad Hussain  
(Thesis Supervisor)

Dr. Nadeem Javaid  
(Thesis Co-Supervisor)

Dr. Noor Muhammad Khan  
(Head, Department of Electrical Engineering)

Dr. Imtiaz Ahmed Taj  
(Dean, Faculty of Engineering)

DEPARTMENT OF ELECTRICAL ENGINEERING  
CAPITAL UNIVERSITY OF SCIENCE AND TECHNOLOGY  
ISLAMABAD  
2019

Copyright © 2019 by Zahid Wadud

All rights reserved. No part of this thesis may be reproduced, distributed, or transmitted in any form or by any means, including photocopying, recording, or other electronic or mechanical methods, by any information storage and retrieval system without the prior written permission of the author.

I would like to dedicate this thesis to my late father and mother whose upbringing taught me not to be complacent. My father was very serious about my studies and shaped his life and schedules in order that my healthy activities must not be compromised. After early death of my father, my mother did not leave any stone unturned to push me up and therefore somehow managed to shape successful future for me. At times their prayers were my only hope.



**CAPITAL UNIVERSITY OF SCIENCE & TECHNOLOGY  
ISLAMABAD**

Expressway, Kahuta Road, Zone-V, Islamabad  
Phone: +92-51-111-555-666 Fax: +92-51-4486705  
Email: [info@cust.edu.pk](mailto:info@cust.edu.pk) Website: <https://www.cust.edu.pk>

**CERTIFICATE OF APPROVAL**

This is to certify that the research work presented in the thesis, entitled “**Energy-Balancing with Sink Mobility in the Design of Underwater Routing Protocols**” was conducted under the supervision of **Dr. Sajjad Hussain**. No part of this thesis has been submitted anywhere else for any other degree. This thesis is submitted to the **Department of Electrical Engineering, Capital University of Science and Technology** in partial fulfillment of the requirements for the degree of Doctor in Philosophy in the field of **Electrical Engineering**. The open defence of the thesis was conducted on **April 18, 2019**.

Student Name: Mr. Zahid Wadud (PE123002)

The Examining Committee unanimously agrees to award PhD degree in the mentioned field.

**Examination Committee :**

- (a) External Examiner 1: Dr. Waseem Shahzad  
Professor  
FAST-NU, Islamabad
- (b) External Examiner 2: Dr. Asif Ullah Khan  
Associate Professor  
PIEAS, Islamabad
- (c) Internal Examiner : Dr. Amir Qayyum  
Professor  
CUST, Islamabad

**Supervisor Name :** Dr. Sajjad Hussain  
Assistant Professor  
CUST, Islamabad

**Name of HoD :** Dr. Noor Muhammad Khan  
Professor  
CUST, Islamabad

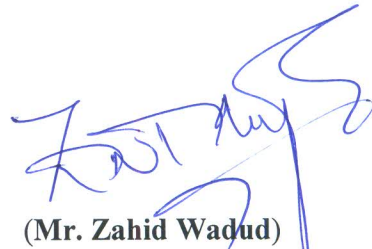
**Name of Dean :** Dr. Imtiaz Ahmad Taj  
Professor  
CUST, Islamabad

## AUTHOR'S DECLARATION

I, **Mr. Zahid Wadud (Registration No. PE-123002)**, hereby state that my PhD thesis titled, '**Energy-Balancing with Sink Mobility in the Design of Underwater Routing Protocols**' is my own work and has not been submitted previously by me for taking any degree from Capital University of Science and Technology, Islamabad or anywhere else in the country/ world.

At any time, if my statement is found to be incorrect even after my graduation, the University has the right to withdraw my PhD Degree.

Dated: 18<sup>th</sup> April, 2019



(Mr. Zahid Wadud)

Registration No : PE-123002

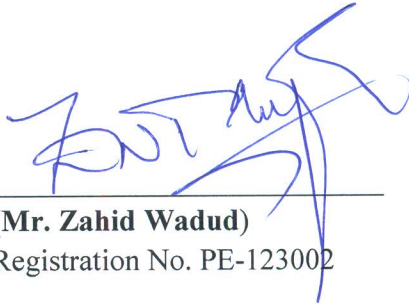
## PLAGIARISM UNDERTAKING

I solemnly declare that research work presented in the thesis titled “**Energy-Balancing with Sink Mobility in the Design of Underwater Routing Protocols**” is solely my research work with no significant contribution from any other person. Small contribution/ help wherever taken has been duly acknowledged and that complete thesis has been written by me.

I understand the zero tolerance policy of the HEC and Capital University of Science and Technology towards plagiarism. Therefore, I as an author of the above titled thesis declare that no portion of my thesis has been plagiarized and any material used as reference is properly referred/ cited.

I undertake that if I am found guilty of any formal plagiarism in the above titled thesis even after award of PhD Degree, the University reserves the right to withdraw/ revoke my PhD degree and that HEC and the University have the right to publish my name on the HEC/ University Website on which names of students are placed who submitted plagiarized thesis.

Dated: <sup>29</sup>18 April, 2019

  
\_\_\_\_\_  
(Mr. Zahid Wadud)  
Registration No. PE-123002

---

## *List of Publications*

It is certified that following publication(s) have been made out of the research work that has been carried out for this thesis:-

1. **Zahid Wadud**, Khadem Ullah, Sajjad Hussain, Xiaodong Yang, and Abdul Baseer Qazi. "DOW-PR DOLphin and Whale Pods Routing Protocol for Underwater Wireless Sensor Networks (UWSNs)." *Sensors* 18, no. 5 (2018): 1529.
2. **Zahid Wadud**, Nadeem Javaid, Muhammad Awais Khan, Nabil Alrajeh, Mohamad Souheil Alabed, and Nadra Guizani. "Lifetime Maximization via Hole Alleviation in IoT Enabling Heterogeneous Wireless Sensor Networks." *Sensors* 17, no. 7 (2017): 1677.
3. **Zahid Wadud**, Sajjad Hussain, Nadeem Javaid, Safdar Hussain Bouk, Nabil Alrajeh, Mohamad Souheil Alabed, and Nadra Guizani. "An Energy Scaled and Expanded Vector-Based Forwarding Scheme for Industrial Underwater Acoustic Sensor Networks with Sink Mobility." *Sensors* 17, no. 10 (2017): 2251.
4. Ahmed, Farwa, **Zahid Wadud**, Nadeem Javaid, Nabil Alrajeh, Mohamad Souheil Alabed, and Umar Qasim. "Mobile Sinks Assisted Geographic and Opportunistic Routing Based Interference Avoidance for Underwater Wireless Sensor Network." *Sensors* 18, no. 4 (2018): 1062.
5. Shah, Mehreen, **Zahid Wadud**, Arshad Sher, Mahmood Ashraf, Zahoor Ali Khan, and Nadeem Javaid. "Position adjustment based location error resilient geo-Opportunistic routing for void hole avoidance in underwater sensor networks." *Concurrency and Computation: Practice and Experience* 30, no. 21 (2018): e4772.

**Zahid Wadud**

(PE123002)



## *Acknowledgements*

Well, I feel proud to mention all those people who open heartedly facilitate me during my PhD studies. The people included are those who helped me with their brilliant ideas, and those who showed kindness and those who provided me with accommodation whenever I away from my homeland for the purpose of PhD and those who encouraged me to believe on my abilities. Sometimes discouraging emotions received from people which even helped me to re-organize my work and strengthened my focus and determination. Thank you very much to all those who took part in this journey.

At the outset, I would like to pay high tribute to my late father and mother whose upbringing taught me not to be complacent. My father was very serious about my studies and shaped his live and schedules in order that my healthy activities must not be compromised. After early death of my father, my mother did not left any stone unturned to push me up and therefore somehow managed to shape successful future for me. At times their prayers were my only hope.

I am extremely thankful to my brothers, Abid and Shahid and my sisters Tabasum and Tayyaba who strengthened me whenever I felt worried and trouble. A word of gratitude to my supervisor Dr. Sajjad Hussain and Co-Supervisor Dr. Nadeem Javaid are truly larger than life. Their dedication, patience, kindness, positivity, response time and eye for detail are unmatched. Dr. Nadeem Sir, can not express my emotions for your supervision, guidance and most important is your brotherly behavior will never be forgotten. I must acknowledge the guidance of Sir, Prof. Dr. Noor Khan at early research stage. Thank you very much to all of my supervisors.

I would also like to acknowledge the review committee members Prof. Dr. Imtiaz Taj (Dean faculty of Engineering, CUST), Prof. Dr. Amir Qayyum for their academic and moral support. I must also acknowledge the support of all my teachers at CUST. I am sure that dissertation would not be possible without encouragement of my child hood friends Prof. Dr. Muhammad Arif, Engr. Muhammad Adnan Khan, Engr. Muhammad Ibrahim Khan, Dr. Abdul Baseer Qazi.

Last but not least, my wife, Sajida. Publications usually have second authors and these can be anyone who has contributed. If the same would be possible in a PhD thesis, my wifes name would have definitely appeared on it. She stood by my side through thick and thin (and trust me there was more of thick than thin). She comforted me whenever I was worried and encouraged me whenever I lost hope.

She made up for any of the responsibilities which I, as a son, husband or father would neglect while analyzing loads of quantitative data. At times she singlehandedly took care of Sana, Hira and Hamana so that I could focus on completing this dissertation.

---

## *Abstract*

Underwater Wireless Sensor Networks (UWSNs) have been considered to provide efficient monitoring tasks and help in exploring aquatic environments. UWSNs composed of small size sensor nodes which are randomly or deterministically deployed in the desired sensing area. The focus of this thesis is energy balancing with sink mobility through the design of routing strategies for UWSNs. First and foremost, Dolphin and Whale Pods Routing (DOW-PR) routing, implements the adaptive transmission range adjustment into a number of power levels and at the same time select the next PFN from forwarding and suppressed zones. DOW-PR not only considers the packet upward advancement, but also takes into account the number of suppressed nodes and number of PFNs at the first and second hops. This research come up with another two schemes: geospatial division based geo-opportunistic routing for interference avoidance (GDGOR-IA) and Geographic routing for maximum coverage with sink mobility (GRMC-SM). The former one has opted depth based recovery and later one utilizes vertical and horizontal coordinate adjustment of deployed sinks to provide maximum coverage over an area. Furthermore, network field is divided into logical cubes by considering transmission range of sensor nodes. Both the schemes contribute to avoid fraction of local maximum nodes and improve packet delivery ratio (PDR). Also they can handle connectivity holes by their proposed recovery mechanisms. Additionally, Location Error resilient Transmission Range adjustment based protocol (LETR), Mobile Sink based LETR (MSLETR) and Modified MSLETR (MMS-LETR) for UWSNs are proposed. To successfully deliver data packets and maximize network throughput along with energy efficiency, LETR calculates Mean Square Error (MSE). This helps to cope with the inefficiency introduced by geographic routing (without considering location inaccuracy) in terms of energy consumption and network throughput. The packet delivery probability, packet advancement and MSE are used altogether in the selection of optimal forwarder node. Finally, an Energy Scaled and Expanded Vector-Based Forwarding (ESEVBF) scheme contributes the mitigation of duplicate packets generation due to imbalance of holding time difference and propagation delay between nodes. ESEVBF uses the residual energy of the node to scale and vector pipeline distance ratio to expand the holding time. Resulting scaled and expanded holding time of all forwarding nodes has a significant difference to avoid multiple forwarding, which reduces energy consumption and energy balancing in the network with less end to end delay.

# Contents

Author's Declaration	v
Author's Declaration	v
Plagiarism	vi
Plagiarism Undertaking	vi
List of Publications	vii
Acknowledgements	viii
Acknowledgements	viii
Abstract	x
List of Figures	xv
List of Tables	xviii
Abbreviations	xix
Symbols	xxi
<b>1 Introduction</b>	<b>1</b>
1.1 Wireless Sensor Networks . . . . .	2
1.1.1 Sensors Deployment Parameters . . . . .	2
1.1.2 WSNs Classification . . . . .	3
1.1.3 WSN Routing Classification . . . . .	4
1.2 Underwater Wireless Sensor Networks . . . . .	5
1.2.1 UWSNs Applications . . . . .	6
1.3 UWSN Routing strategies . . . . .	6
1.4 UWSN Challenges . . . . .	7
1.4.1 Research Questions . . . . .	8
1.5 Research Aims and Hypthesis . . . . .	9

---

1.6	Research Methodology . . . . .	10
1.7	Thesis Outline . . . . .	11
<b>2</b>	<b>Literature Review</b>	<b>13</b>
2.1	Introduction . . . . .	13
2.2	WSN . . . . .	13
2.3	Underwater Propagation Model . . . . .	17
2.3.1	Acoustic Signal Velocity in the Underwater Environment . . . . .	19
2.3.2	Acoustic Signal Reflection and Refraction in the Underwater Environment . . . . .	20
2.4	UWSN Routing Protocols . . . . .	21
2.4.1	Geographical Routing . . . . .	22
2.4.2	Sender and Receiver based Routing . . . . .	22
2.4.3	Depth based Routing . . . . .	23
2.4.4	Location Based Routing . . . . .	25
2.4.5	Energy Based Routing . . . . .	28
2.4.6	Pressure Based Routing . . . . .	29
2.4.7	Sink Mobility Assisted Routing . . . . .	30
2.5	Conclusion . . . . .	34
<b>3</b>	<b>DOW-PR Dolphin and Whale Pods Routing protocol for UWSNs</b>	<b>36</b>
3.1	Summary of the Chapter . . . . .	36
3.2	Introduction . . . . .	37
3.2.1	Contributions: . . . . .	38
3.3	Problem Statement . . . . .	40
3.3.1	Preliminaries . . . . .	41
3.3.2	Causes of Duplicate Packets . . . . .	43
3.4	Proposed Scheme . . . . .	44
3.4.1	Network Architecture . . . . .	44
3.4.2	Packet Types in the Dolphin and Whale Pods Routing . . . . .	45
3.4.3	Division of Transmission Range into Different Transmission Power Levels . . . . .	46
3.4.4	Selection of a Forwarding Node among Suppressed Nodes . . . . .	48
3.4.5	Holding Time Estimation . . . . .	48
3.4.6	Whale Pods Routing Protocol . . . . .	53
3.5	Simulation Analysis . . . . .	54
3.5.1	Simulation Setup . . . . .	56
3.5.2	Hop Count Mechanism . . . . .	61
3.5.3	Data Delivery Mechanism . . . . .	62
3.6	Performance Comparison and Analysis . . . . .	63
3.6.1	Simulation Results in the Dolphin Pods Routing Scenario . . . . .	66
3.6.2	Simulation Results in the Whale Pods Routing Scenario . . . . .	72
3.7	Conclusions . . . . .	76

---

<b>4</b>	<b>Mobile Sinks assisted Geographic and Opportunistic Routing based Interference Avoidance for UWSN</b>	<b>78</b>
4.1	Summary of the Chapter . . . . .	78
4.2	Introduction . . . . .	79
4.2.1	Contributions: . . . . .	81
4.3	Preliminaries . . . . .	82
4.3.1	Network Architecture . . . . .	82
4.3.2	Beacon Message Types . . . . .	83
4.3.3	Potential Neighbor Set Selection . . . . .	84
4.3.4	Geospatial Division Model . . . . .	84
4.4	GDGOR-IA . . . . .	85
4.4.1	Target Cube Selection . . . . .	86
4.4.2	Next-Hop Forwarder Set Selection Criterion . . . . .	87
4.5	GRMC-SM . . . . .	89
4.5.1	Data Forwarding and Routing in GRMC-SM . . . . .	90
4.5.2	Recovery Mode via Sink Mobility . . . . .	91
4.6	Mathematical Formulation Using Linear Programming . . . . .	93
4.6.1	Energy Consumption Minimization . . . . .	93
4.6.2	PDR Maximization . . . . .	98
4.6.3	Minimization of Average Delay . . . . .	99
4.7	Simulation Results and Discussions . . . . .	102
4.7.1	Simulation Settings . . . . .	103
4.7.2	Analysis of proposed Scheme Results against Existing State of the Art . . . . .	104
4.7.2.1	Fraction of Void Nodes . . . . .	105
4.7.2.2	Depth Adjustment . . . . .	106
4.7.2.3	PDR . . . . .	107
4.7.2.4	Energy Consumption . . . . .	109
4.7.2.5	End-To-End Delay . . . . .	110
4.7.2.6	Performance Trade-Offs . . . . .	111
4.7.3	Observations of the Research . . . . .	112
4.7.3.1	Performance Analysis Based on Varying Traffic Loads . . . . .	112
4.7.3.2	Performance Analysis of GRMC-SM by Varying Number of Sinks . . . . .	113
4.8	Conclusions . . . . .	116
<b>5</b>	<b>Position adjustment based location error resilient geo-opportunistic routing for void hole avoidance in UWSN</b>	<b>118</b>
5.1	Summary of the Chapter . . . . .	118
5.2	Introduction . . . . .	119
5.3	Problem Statement . . . . .	122
5.4	System Model . . . . .	124
5.4.1	Packet Delivery Estimation Model . . . . .	124
5.5	Proposed Protocols . . . . .	126

---

5.5.1	LETR	126
5.5.1.1	Controlled Beacons Algorithm	126
5.5.1.2	Neighbor Set Selection	128
5.5.1.3	Forwarder Set Selection	130
5.5.1.4	Controlled Depth Adjustment	134
5.5.2	Sink Mobility based Routing Protocols	134
5.5.2.1	MSGER	136
5.5.2.2	MSLETR	137
5.5.2.3	MMS-LETR	137
5.6	Performance Evaluation	141
5.6.1	Impact of varying node density on packet loss ratio	142
5.6.2	Impact of sink mobility on energy consumption	144
5.6.3	Impact of depth adjustment on energy consumption	145
5.6.4	Impact of data transmission on energy consumption	147
5.6.5	Impact of varying node density on fraction of void nodes	147
5.6.6	Impact of varying node density on node displacement	149
5.7	Conclusion	151
<b>6</b>	<b>An Energy Scaled and Expanded Vector-Based Forwarding Scheme for Underwater Acoustic Sensor Networks with Sink Mobility</b>	<b>153</b>
6.1	Summary of the Chapter	153
6.2	Introduction	154
6.2.1	Contributions	155
6.3	Proposed Scheme	157
6.3.1	Problem Statement	157
6.3.2	Preliminaries	160
6.3.3	Estimation of $HT_p^i$	161
6.4	Results and Analysis	166
6.4.1	Performance Metrics	168
6.4.2	Simulation Results in the Static Sink Scenario	169
6.4.3	Simulation Results in the Mobile Sink Scenario	181
6.5	Conclusion	188
<b>7</b>	<b>Conclusion and Future Work</b>	<b>190</b>
7.1	Conclusion	190
7.2	Future Work	193
	<b>Bibliography</b>	<b>194</b>

# List of Figures

1.1	Wireless Sensor Network . . . . .	2
1.2	Underwater Sensor Network . . . . .	5
2.1	Speed of sound vs. temperature. . . . .	19
2.2	Speed of sound vs. salinity. . . . .	20
2.3	Sensor Architecture . . . . .	21
2.4	Classification of existing routing protocols . . . . .	23
3.1	Forwarder node selection scenario . . . . .	41
3.2	Network architecture . . . . .	45
3.3	Division of transmission zones (TZ1–TZ6) . . . . .	47
3.4	Forwarder selection from the suppressed nodes . . . . .	49
3.5	Holding time scenario . . . . .	52
3.6	Network architecture for whale pods routing . . . . .	56
3.7	Network deployment with embedded sink $D_{EM}$ . . . . .	61
3.8	Hop count mechanism . . . . .	62
3.9	(a) PDR vs. number of nodes; (b) energy tax vs. number of nodes; (c) end-to-end delay vs. number of nodes; (d) APD vs. number of nodes. Comparison in Dolphin Pods using SET1, SET2, SET3. . . . .	64
3.10	(a) PDR vs. number of nodes; (b) energy tax vs. number of nodes; (c) end-to-end delay vs. number of nodes; (d) APD vs. number of nodes. Simulation results using arbitrary values in SET3. . . . .	69
3.11	(a) number of alive nodes vs. rounds; (b) number of alive nodes vs. rounds; (c) number of packets dropped with suppressed vs. number of nodes; (d) number of packets dropped without suppressed vs. number of nodes. Simulation results using arbitrary values in SET3. . . . .	72
3.12	(a) PDR vs. number of nodes; (b) energy tax vs. number of nodes; (c) end-to-end delay vs. number of nodes; (d) APD vs. number of nodes. Comparison of dolphin pods with whale pods/routing. . . . .	75
4.1	Network Architecture . . . . .	83
4.2	Cubical representation of target cube . . . . .	85
4.3	Schematic diagram of GRMC-SM . . . . .	90
4.4	Feasible regions (a) Feasible region for energy tax minimization (GDGOR-IA); (b) Feasible region for energy tax minimization (GRSM- MC). . . . .	97



---

4.5	Feasible regions. (a) Feasible region for throughput maximization (GDGOR-IA); (b) Feasible region for throughput maximization (GRMC-SM). . . . .	100
4.6	Feasible regions. (a) End to end delay: feasible region for GDGOR-IA; (b) End to end delay: feasible region for GRMC-SM. . . . .	103
4.7	Fraction of void nodes plots . . . . .	106
4.8	Depth adjustment plots . . . . .	107
4.9	PDR plots . . . . .	108
4.10	Energy consumption comparative plots . . . . .	109
4.11	End to end delay plots . . . . .	111
4.12	Performance parameters for GDGOR-IA. (a) PDR for GDGOR-IA; (b) Latency for GDGOR-IA; (c) Energy tax for GDGOR-IA. . . . .	114
4.13	Performance parameters for GRMC-SM. (a) Fraction of void nodes under different number of sonobuoys; (b) PDR under different number of sonobuoys; (c) End to end delay under different number of sonobuoys. . . . .	115
5.1	Network model for LETR . . . . .	122
5.2	Operation of LETR . . . . .	135
5.3	Sink mobility pattern of MSGER and MSLETR . . . . .	136
5.4	System model for MMS-LETR . . . . .	141
5.5	The ratio of packets lost during simulation . . . . .	144
5.6	Energy consumption in the network field . . . . .	145
5.7	Percent energy consumed in depth adjustment . . . . .	146
5.8	Percent energy consumed in communication . . . . .	148
5.9	Fraction of void nodes . . . . .	149
5.10	Depth adjustments in the network . . . . .	150
6.1	Holding Time and PFZ scenario . . . . .	159
6.2	Relationship between holding time difference and broadcast suppression in the underwater networks . . . . .	161
6.3	Holding time estimation parameters and scenario . . . . .	163
6.4	Mobile sink network scenario . . . . .	168
6.5	Number of data message copies forwarded in the network for different network size . . . . .	169
6.6	Number of data message copies forwarded in the network for different transmission range . . . . .	170
6.7	% reduced data packets by the proposed scheme for different $T_r$ and network size . . . . .	170
6.8	End-to-End delay between Source node that generated data message and Sink node versus the network size . . . . .	172
6.9	End-to-End delay between the source node that generated data message and Sink node versus transmission range . . . . .	172
6.10	The overall percentage less End-to-End delay achieved by the proposed scheme for different $T_r$ and network size . . . . .	173
6.11	Overall network energy consumption versus the network size . . . . .	175

---

6.12	Overall network energy consumption versus the transmission range .	175
6.13	Overall network energy consumption for varying number of data packets generated by the source nodes in the network . . . . .	176
6.14	Number of dead nodes for varying number of data packets generated by the source nodes in the network . . . . .	177
6.15	Average No. of Hops data messages traversed versus the network size	179
6.16	Average no. of hops data messages traversed versus transmission range . . . . .	179
6.17	Average packet delivery ratio versus the network size . . . . .	181
6.18	Average packet delivery ration versus the transmission range . . . . .	181
6.19	Total copies of data message forwarded in the network with and without Sink mobility for different (network size) . . . . .	182
6.20	Total copies of data message forwarded in the network with and without Sink mobility for different (transmission range) . . . . .	183
6.21	Average number of hops the data message needs to traverse in network to reach static and mobile Sink (Network with varying size) .	184
6.22	Average number of hops the data message needs to traverse in network to reach static and mobile Sink (Network with varying transmission range) . . . . .	184
6.23	End-to-end delay experienced by the data message in a network with static and mobile Sink for varying network size . . . . .	185
6.24	End-to-end delay experienced by the data message in a network with static and mobile Sink for varying transmission range . . . . .	185
6.25	Network energy consumption in the static and mobile Sink network scenario for varying network size . . . . .	186
6.26	Network energy consumption in the static and mobile Sink network scenario for varying transmission range . . . . .	186
6.27	PDR in the static and mobile Sink network scenario for varying network size . . . . .	187
6.28	PDR in the static and mobile Sink network scenario for varying transmission range . . . . .	187
6.29	PDR alleviated after the introduction of the mobile Sink in ESEVBF	188
6.30	PDR alleviated after the introduction of the mobile Sink in AHHVBG	189

# List of Tables

1.1	Comparison of average properties of WSN and UWSN . . . . .	6
2.1	Comparison of the State of the Art in WSNs . . . . .	17
2.2	Comparison of the State of the Art Work in UWSNs . . . . .	32
3.1	Actual number of PFNs mapped into arbitrary values . . . . .	58
3.2	Actual number of SUPs mapped into Arbitrary Values . . . . .	59
3.3	Parameters' settings . . . . .	60
3.4	Overall PDR improvement in dolphin pods routing compared to WDFAD-DBR . . . . .	73
3.5	Overall Energy saved in dolphin pods routing compared to WDFAD-DBR . . . . .	73
3.6	Overall End-to-End delay improvement of dolphin pods with WDFAD-DBR . . . . .	73
3.7	Performance trade-offs . . . . .	76
4.1	Analysis of performance parameters against GEDAR . . . . .	112
5.1	Network Simulation Parameters . . . . .	142
6.1	Overall energy saved by the proposed scheme compared to AHH-VBF	177

# Abbreviations

<b>ADV</b>	ADVancement
<b>ATF</b>	Average Traffic Load
<b>AWGN</b>	Additive White Gaussian Noise
<b>BER</b>	Bit Error Rate
<b>BPSK</b>	Binary Phase Shift Keying
<b>CC</b>	Current Cubes
<b>CCT</b>	Current Clock Time
<b>CSMA/CA</b>	Carrier Sense Multiple Access/Collision Avoidance
<b>DA</b>	Depth Adjustment
<b>DR</b>	Data Rate
<b>DFM</b>	Data Forwarding Mechanism
<b>E2E</b>	End to End delay
<b>EPA</b>	Expected Packet Advanced
<b>ECPN</b>	Energy Consumption Per Node
<b>ECDA</b>	Energy Consumed in Depth Adjustment
<b>ECAC</b>	Energy Consumed in Acoustic Communication
<b>GPS</b>	Global Positioning System
<b>HS</b>	Header Size
<b>IoT</b>	Internet of Things
<b>IUASN</b>	Industrial Underwater Acoustic Sensors Network
<b>MS</b>	Mobile Sonobuoy
<b>MSE</b>	Mean Square Error
<b>NN</b>	Normal Node
<b>NC</b>	Neighbor Cubes

<b>NADV</b>	Normalized ADVanced
<b>NPV</b>	Node Priority Value
<b>OR</b>	Opportunistic Routing
<b>PDR</b>	Packet Delivery Ratio
<b>PL</b>	PayLoad
<b>PFZ</b>	Potential Forwarding Zone
<b>PFN</b>	Potential Forwarding Node
<b>RSSI</b>	Received Signal Strength Indicator
<b>SN</b>	Super Node
<b>SNR</b>	Signal to Noise Ratio
<b>TC</b>	Target Cubes
<b>TEC</b>	Total Energy Consumed
<b>WSN</b>	Wireless Sensors Network
<b>UWSN</b>	Underwater Wireless Sensors Network

# Symbols

$u(f)$	Absorption Coefficient
$p_e()$	Error Probability
$(E_{tax})$	Energy Tax
$E_m$	Energy Cost
$\varepsilon_o$	Initial Energy
$N_o$	Noise Power Density
$\rho$	Node Density
$E_b$	per bit average transmission energy
$k$	Spreading Factor
$B$	Total Bandwidth
$t_s$	Moving time of a mobile sonobuoy
$T_p$	Throughput
$T_p(r)$	Number of packets received
$\alpha$	Lower Bound
$\beta$	Upper Bound
$\omega$	Constant
$HT_p^i$	Holding Time
$\mathcal{N}$	Set of nodes in the network
$D_j^i$	Euclidean Distance
$\gamma$	Distance of the potential forwarder towards the sink
$C_n$	Number of logical cubes
$N_n$	Total nodes deployed
$S_s$	A set of sonobuoys
$\Lambda$	Flag to indicate that latest neighbor information

---

$F_{set}$	Potential forwarder nodes set
$CC$	Current cube
$NC$	Neighbor cube
$TC$	Target cube
$P_{BER}$	Bit error rate probability
$P_{CR}$	Probability of collision rate
$ADV$	Advancement towards destination
$T_{proc}$	Processing time at each node
$T_p$	Propagation delay
$NADV$	Normalized advancement towards destination
$MS_n$	Number of mobile sonobuoys deployed in the network
$DFM$	Data forwarding
$E_{TX}$	Transmission energy
$E_{RX}$	Receiving energy
$D_{i,j}$	Straight line distance from node i to node j
$E_{consumed}$	Energy consumed
$DR$	Data rate
$E_{DA}$	Energy dissipated in data aggregation
$R_c$	Communication range of a node
$P_{TX}$	Transmission power for transmission data packet
$P_{RX}$	A power required to receive a data packet
$PDR$	Packet delivery ratio
$E_{th}$	Residual energy threshold
$D_{DT}$	Delay occur in transmitting data packet directly
$D_{MHT}$	Delay occur in delivering data packet through multiple hops
$T_{hold}$	Time required to hold a packet

---

# Chapter 1

## Introduction

The emergence of Internet has increased the connectivity of human beings at unprecedented scale. However, the rapid growth of short range networks including; Wireless Sensor Networks (WSNs) Bluetooth, Radio Frequency IDentification (RFID), Wireless Fidelity (WiFi), ZigBee, etc.; the interconnection between numerous devices is inevitable [1]. Now, it is obvious that the interconnection of the sensors lead to gather information from the environment and forward it to the fusion centers and that too is done with out humen effort. The sensor equipment could be different in term of thier processing speed, recognition characteristic etc. Characteristics of the sensors included their sensing abilities, processing capability, transmitting and receiving packet information through wireless communication [2]. The applications of the sensor networks are monitoring the environment, serveilance, gas leakage and temperature checks, traffic control, sensing through image processing and many more [3]. Wireless sensors networks are formed through deployment of small sensors called nodes that could be structured in different network topologies. The major cause of deployment of sensor networks is to connect data collection center to receive information. The battery usage must be considered while designing the network, as it is the primary interest to extend the lifetime of the network. The lifetime of the network must be extended through balancing data packet loads among sensor nodes [4].



## 1.1 Wireless Sensor Networks

Wireless sensor networks (WSNs) is the composition of homogeneous or/and heterogeneous interconnected nodes (Figure 1.1), which do communication and sensing from their surrounding nodes and environment. Sensor nodes cooperate with each other in order to merge individual sensor readings which result in high level of sensing. Wireless sensor network has many characteristics such as mobility, communication bandwidth, switching character and limited power of battery. The UWSNs and terrestrial wireless sensor networks are differ in many ways for example on the basis of communication, cost of single node, power generation, propagation delay, node deployment etc. Table 1.1 show the different properties of underwater sensor networks and terrestrial WSNs.

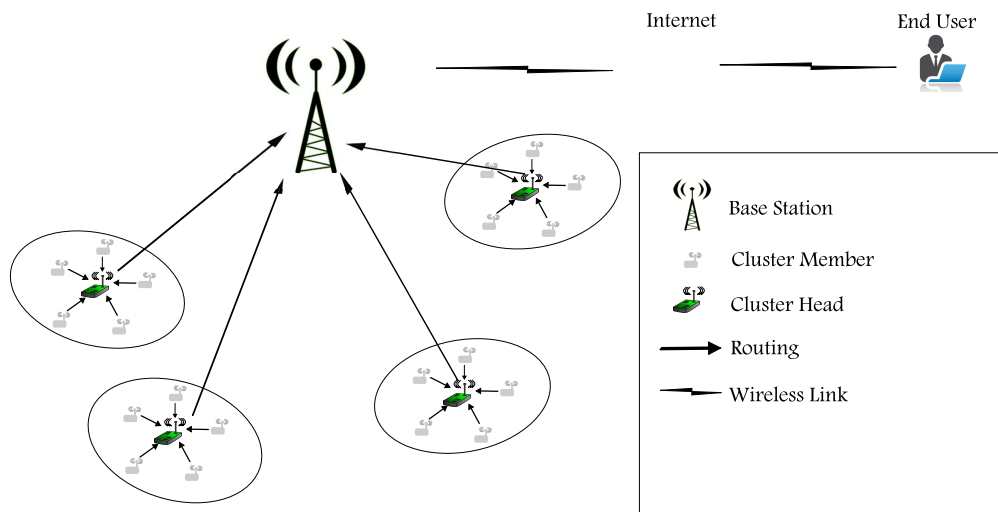


FIGURE 1.1: Wireless Sensor Network

### 1.1.1 Sensors Deployment Parameters

Wireless sensors deployment strategy have significant effect upon the performance of the Network. In order to optimize performance of the networks, the researchers describe different parameters which need to be addressed in designing the Networks. The performance parameters are:

1. **Sensing Range** is the maximum area or distance that a sensor can sense information sensing range. It depends upon the sensing capability of a node.
2. **Transmitting Range** is the Omni-directional region around the nodes that can transmit signal.
3. **Node Redundancy** is the amount of coverage region of interest in which one or more nodes are deployed as node redundancy. For instance if m number of sensors covering sensing area is called as m-coverage.
4. **Link Redundancy** is the degree of average number of links/paths availability for information routing. For instance if k number of nodes can forward packets with certain range than it is called as k-connectivity.
5. **Link Characteristics** is the physical property of the medium that have direct effect upon the quality and reliability of the communication between nodes. The range of the network is also dependent upon link characteristics, that's why it is important consideration while implementing sensors deployment strategies.
6. **Network Energy** Before deducing sensors deployment parameters it is highly desirable that the network must be energy conscious. The network energy conservation is an important parameter for designing deployment strategy.
7. **Obstacle awareness** The algorithms adopted to cater the interference of obstacles between the communication link of the sensor nodes.

### 1.1.2 WSNs Classification

WSNs can be classified in accordance with different properties of the network, for example homogenous and heterogeneous networks. In homogenous networks all the sensor nodes have same capabilities while in heterogeneous networks the nodes may have different capabilities. The capabilities may include initial energy, energy usage rate, processing efficiency and sensing region, etc. [5]. Beside the kind of the network, the routing strategy play important role to optimizes the performance

parameters. The following points must be considered while designing the routing protocol in order to optimize results.

- Least energy consumption route is the primary concern of the routing protocols.
- Optimal traffic load balancing contributes significantly to prolong the lifetime of the network. Nodes may deplete earlier if load distribution is uneven and a source of producing void holes.

### 1.1.3 WSN Routing Classification

To deal with the above mentioned challenges, significant efforts have been made by the researches to cater with the scarce energy resource of the sensor networks. Routing protocols can be divided into three basic categories it includes: flat, location based and hierarchical based routing. In flat networks, all the sensor nodes have same capabilities and perform forwarding of information through homogeneous network [6]. In location based routing, the geographic position of the nodes is estimated and routing path selected for data packet transfer [7]. In hierarchical based routing, the nodes form the small chunks of networks and then in turn these small network are interconnected each other. The advantage of those networks is that it is scalable in nature. The examples of hierarchical based routing are cluster routing and ring routing [8]. It uses greedy strategy for routing and it is delay efficient and scalable [9]. The itemized text below represent few benefits of ring routing:

- It focuses on restricted amount of broadcasting to achieve speedy packet delivery.
- Ring routing is appropriate for event driven applications.
- It is independent on the dynamic position of the sink.

## 1.2 Underwater Wireless Sensor Networks

UWSNs composed upon the limited capacity sensor nodes that are interconnected through acoustic links. The primary task of the sensor nodes is to collect data and communicated to the sink(s) that is/are floating at the sea surface that forward(s) data to the onshore monitoring station. Sensor nodes are deployed in underwater environment to form a SEA swarm architecture Figure 1.2. Communication in the underwater environment poses many challenges for all the communication approaches that have been considered [10] e.g., radio or electromagnetic [11],[12], optical [13],[14], and acoustic communication modes [15],[16]. UWSNs have been considered to provide efficient monitoring tasks and help in exploring aquatic environments.

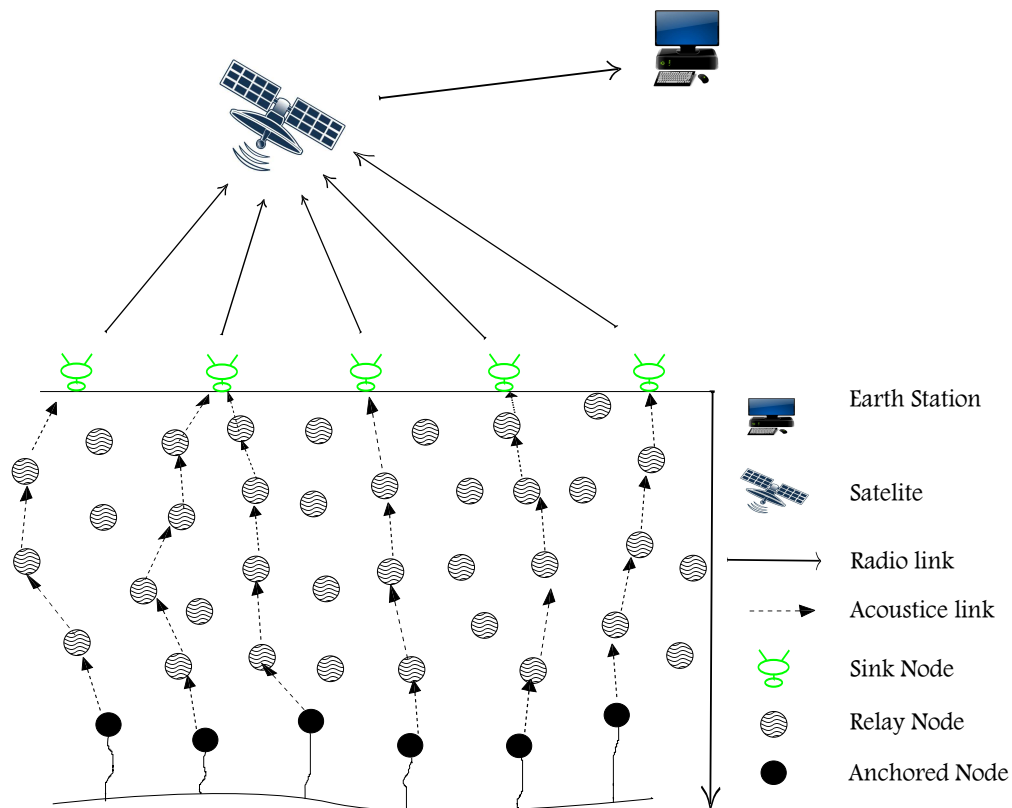


FIGURE 1.2: Underwater Sensor Network

TABLE 1.1: Comparison of average properties of WSN and UWSN

Features	UWSN	WSN
Signal	Acoustic	Radio
Bandwidth of signals	5kHz-15kHz	3kHz-300GHz
Speed of signals	1500 m/s	Speed of light
Node status	Mobile nodes	Static and Mobile nodes
Communication	Based on acoustic signals	Based on radio signals
Cost	Expensive	Less expensive
Battery power	Difficult recharge	Easily rechargeable

### 1.2.1 UWSNs Applications

There are several applications in UWSNs like monitoring aquatic life, underwater vehicles, tsunamis, seaquakes, floods, oilfields, pollution, mine recognition, military surveillance [17], harbor monitoring, oceanographic data collection, seaquakes monitoring, submarine tracking, and many others [18], [3], thus they have gained much attention of scientists and researchers.

## 1.3 UWSN Routing strategies

UWSNs routing strategies include **Geographic Routing** which is the most scalable and promising technique for UWSNs [19]. It does not require a complete route from source to destination. Also, there is no need to update routing states during each transmission [20]. In geographic routing, the nodes close to the destination are selected as next hop forwarders. In **Opportunistic Routing (OR)**, the selection of next hop forwarder node is done on the fly. In OR, group of nodes are selected that are assumed to become next hop forwarder nodes. The node which receives the packet continues to forward the packet towards next hop. The priorities assigned to each node are different using different metrics. While, the node with the highest priority among other nodes is selected first for forwarding data towards the destination. The node with next highest priority is chosen if the highest priority node fails to do so. The low priority nodes stop their scheduled

transmissions if they sense the successful data forwarding from the highest priority node. **Geo-opportunistic** routing is more useful underwater routing in terms of minimizing the energy consumption with high PDR, however, it has void hole problem [21]. The void hole occurs when a node fails to find next hop forwarder node within its transmission range and such node is called a void node due to its presence in communication void hole as it stops the data delivery towards the sonobuoy.

## 1.4 UWSN Challenges

Smart Coasts (SCs) are one of the key factors for the sustainable community [22]. Main objectives of the SC are to monitor the quality of water, the ecosystem, water pollution, seismic activity and management of the coastal zone(s). All of these objectives are hard to achieve without continuous detection, collection, monitoring, and management of the oceanographic parameters. This uninterrupted collection and communication of the aquatic parameters are not possible without Underwater Sensor Networks (USNs) [23], which is one of the key technology in the realm of SCs.

The goal of the any routing protocol is to compute the routing path that consume minimal energy of the network. To achieve this, the balancing of the network traffic is the primary concern. The nodes which are used more frequently for data transfer dead earlier. Underwater sensor networks undergoes through different challenges, few of them are identified below:

1. The underwater medium offers severe attenuation to radio and optical waves and therefore the strength of the signal disappeared at a very short distance. On the other hand optical waves require precise line of sight link between transmitter and receiver. It is commendable to opt the most feasible method of communication in underwater environment that is acoustic communication.

2. Nevertheless, acoustic communication also faces challenges like long propagation delays due to low speed of sound in underwater environment that is 1500 m/s.
3. High bit error rate and multipath fading is observed due to low data rate and high noise.
4. Limited bandwidth due to high attenuation and multipath effect in acoustic channel.
5. Moreover, sensor nodes are battery powered devices and replacement of batteries incurs high cost and complexity.
6. Water currents present in underwater environment cause additional energy expenditures due to node mobility.
7. Paths establishment and maintenance becomes one of an utmost importance for routing in the UWSNs [24].
8. Creating links between nodes has become a difficult task in UWSNs due to path loss, high attenuation and high error probability.
9. The deployment strategy of sensors and the imbalanced energy consumption results in void holes creation.
10. Global positioning systems provides an expensive and power consuming solution to the localization problem. However, erroneous nature of local positioning system affects communication between network nodes.
11. Communication void areas are major hurdles in successful data transmissions.

### 1.4.1 Research Questions

**Question 1** How efficient forwarding node selection is performed to alleviate coverage and energy holes?

**Question 2** Role of sink mobility in network for lifetime improvement. Do sink trajectories play any role in achieving maximized network lifetime?

**Question 3** How to maximize the network performance through designing a fast

and reliable routing protocol?

**Question 4** How linear optimization is proved to be effective in terms of minimizing the energy consumption of nodes?

**Question 5** Why geographic routing paradigm seems promising choice for data transmission in severely limited acoustic communication channel conditions?

**Question 6** If a node fails to find any neighbor node within its defined maximum transmission range level, than how it recovers communication void regions using depth adjustment technology?

**Question 7** How holding time suppresses data broadcasts? and how can it keep energy and delay fairness in the network?

**Question 8** Can energy efficiency and energy balancing are achieved by employing the normalized residual energy information of the neighboring nodes in the holding time and suppressing more number of packets?

**Question 9** How minimizing tradeoff between energy consumption and other important parameters that included PDR, E2ED, number of void holes, APD etc.?

This dissertation, limited in scope to routing only, aims at energy efficient solutions to prolong the lifetime of UWSNs. A few of the above mentioned research issues/questions have been investigated and resolved through state of the art routing protocols proposed in this research. Specifically, this research convincingly contributes towards the solution of problems of energy balancing (research question 8), void and energy holes (research question 1) and role of sink mobility (research question 3).

## 1.5 Research Aims and Hypthesis

Besides all minor goals, the main focus of this thesis is to:

*Analyze and design routing strategies that ensure significant energy conservation in UWSNs by reducing consumption. The energy or void hole reduction phenomena is also linked with the energy-rich routing algorithms. Moreover, all challenges mentioned in section 1.5 are positively addressed by the state of the art routing*



*protocol proposed in this thesis.*

The idea of the research is to deploy the sensor networks in underwater environment through simulation setup. The cooperative routing linkages between the sensor nodes around the local area are found to be effective in solving the energy scarcity problem. This thesis utilizes the sink mobility in area of interest along with power transmission level control in order to achieve precise and targeted goals. The research also presents the need of knowledge regarding the local neighbors of node in a network to make efficient routing decisions. The implementation of such energy-aware routing protocols can minimize the energy consumption and prolong the network lifespan. The fundamental hypotheses are then that:

*Sensor nodes are: i) capable to sense data from the environment, ii) share information with the surrounding sensor nodes iii) simple and complex linear optimization in calculating the holding time of packets received from the predecessor nodes, iv) capable of knowing its position relative to its neighbors in transmission range.*

Thus, the thesis utilizes the above mentioned hypotheses at the node level and it seems to be beneficial in balancing the traffic load and hence reducing the energy conservation in homogeneous underwater wireless sensor networks.

## 1.6 Research Methodology

1. In the initial phase, a comprehensive literature review of the related routing protocol in underwater sensor networks (UWSNs) has been conducted. Furthermore, research related to energy balancing with sink mobility in UWSNs has been extensively explored.
2. Critical examination of dependent parameters, that are directly affected by the implementation of energy and traffic load balancing in UWSNs routing protocols have been studied. This includes parameters such as energy tax, fraction of void nodes, throughput, computation overhead, end to end delay etc.

3. Furthermore, limitations and challenges of state-of-the-art UWSNs energy minimization and void hole routing protocols have also been explored and identified.
4. Development of a mathematical model for the abovementioned routing protocol that is based on energy balancing with sink mobility.
5. Extensive simulations have been conducted in order to measure the performance and efficiency of proposed routing techniques and thus validate the mathematical model. In addition, the comparison of the proposed method will be done with the existing techniques.

## 1.7 Thesis Outline

This thesis is organized as follows: Chapter 2 gives the detail of the literature review of the WSN and UWSN routing Protocols. In Chapter 3, to improve the performance of the existing WDFAD-DBR scheme, a routing protocol DOW-PR has been proposed. In DOW-PR protocol, the forwarding zone region is divided into small horizontal transmission levels. The forwarder is selected from potential forwarding and SUPs zones. The adaptive nature of transmission power level helps to reduce the significant amount of network energy. The other attractive feature of this protocol is to consider the number of hops involved for packet transmission from source to sink. In case, if there is unavailability of node in potential forwarding zone the protocol select forwarder from the suppressed region and therefore effectively cater with the void hole problem. In Chapter 4, geospatial division based geo-opportunistic routing scheme for interference avoidance (GDGOR-IA) assisted with void recovery mechanism has been proposed. Along with this the second scheme, geographic routing for maximum coverage with sink mobility (GRMC-SM) aims to provide maximum coverage over the interest field. Chapter 5 presents four routing protocols: Location Error resilient Transmission Range adjustment based protocol (LETR), Mobile Sink based GEographic and Opportunistic Routing (MSGER), Mobile Sink based LETR (MSLETR) and

Modified MSLETR (MMS-LETR). In Chapter 6, ESEVBF routing protocol uses the residual energy related to each individual sensor to stretch the holding time difference among the nodes. Consequently it is observed that the corresponding increase in holding time difference and therefore there are avoidance of duplicate packets. Hence significant amount of energy conservation saved and fair balancing in network energy resulted. Chapter 7 sum up the thesis and present precise conclusion of the research.

# Chapter 2

## Literature Review

### 2.1 Introduction

This chapter thoroughly discusses state of the art routing protocols. It contributes in finding out the research challenges and their respective solutions by critical examination of the dependent and independent performance parameters. It also reviews the energy efficient algorithms used in those protocols and their comparison on the basis of performance metrics like energy tax, packet delivery ratio, end-to-end delay etc. Moreover the limitations and tradeoffs are carefully investigated. This chapter is structured as follows: section 2.1 discusses the terrestrial WSN routing protocols in detail. To sum up the detailed discussion regarding WSN issues a comparison of various routing protocols are proposed in table 2.1. Section 2.3 explores the underwater wireless channel characteristics in detail. Section 2.4 discusses the classification of underwater routing protocols along with their comparison with one another.

### 2.2 WSN

A significant amount of research carried on to improve the wireless network efficiency using different routing protocols. HORA [25] protocol proposed by saho

et al. which addresses to the void holes problem through hole repair algorithm . The proposed algorithm considers the movement of sensor nodes. Each node checks its status whether it is Cross Triangles (CT), Hidden Cross Triangles (HCT) or Non Cross Triangle (NCT) in order to minimize overlapping region. Neighbor node with highest overlapping region will move towards coverage hole to fill the gap. HORA helps to improve network lifetime and maximizes the throughput but its application in delay sensitive area degraded due to hole repairing process.

Energy hole is one of the major factor which minimizes the network lifetime. Death of the nodes in the innermost region of the sink minimizes the network performance. Some of the proposed routing protocol adopted the different power levels for transmission of the packets, for example "Load Balancing Technique" (LBT) [26]. However, LBT do not considered the void or energy hole in the network. Khan et al. [27] proposed solutions to cater with energy/void holes with homogeneous and heterogeneous nodes in the network. After receiving the chunk of data by the super nodes then they schedule their energy levels and therefore significant energy is saved. Although, the energy is conserved but still void hole problem persists. To aim the balancing of energy consumption among the network nodes Li et al. [28] uses the ring topology and compute the energy and traffic load of a single node. It is observed from the simulation that, the nodes near in the vicinity of the destination need to bear a more load as compared to the nodes far away from the sink. It is therefore the near vicinity nodes depleted earlier and causes the energy hole. Moreover, Rasheed et al [29] also present model "Energy-efficient HOle Removing Mechanism" (E-HORM). To overcome energy hole. In the propose scheme sleep scheduling mode is adopted for energy saving. The nodes nearer to the destination are selected and transmission energy is computed based upon the distances. An energy threshold " $E_{th}$ " is defined. If a node energy level falls below this  $E_{th}$ , it cannot transmit data. The propose scheme able to maximize network lifetime and stability period in expense of delay. Jewel et al. [30] propose an "Improved Hole Detection Healing and Replacing Algorithm for optimal coverage in WSNs" (IHDHRA). The proposed protocol presents the energy efficient algorithm that utilizes the reduction of the probability for regeneration of packet

or loss of data. It also introduces the mechanism to replace the energy void node with other node in the network. It is observed that the protocol proposed is good enough to elongate the lifespan of the network. However the robustness degraded the performance of the network.

Fair energy distribution in the network nodes is proposed by Ekal et al. [31]. A corona based model is considered such that to balance the energy among the nodes. Required energy of every node is calculated based on its initial energy in respective corona and corona load. The proposed model aim to improve network lifetime. However extra energy is provided to these nodes which is not a best solution for lifetime maximization. Lu et al. [32] propose an“ Energy-Efficient Data Sensing and Routing in unreliable energy-harvesting WSNs” (EEDSRS) that carry the sensing mechanism and routing of the packets. Performs both data sensing and data routing. EEDRS presents the three stages of algorithm. Initially the link quality is calculated by using AEW algorithm. Second, a distributed energy efficient rate allocation is performed for data sensing and routing for lifetime maximization through optimal data sensing rate. In last, data is routed through the links via energy efficient path. The algorithm aims to optimize the network performance but it is purely a MAC layer protocol which increases the complexity. A mixed transmission strategy is propose in [33] for energy balancing. The most important parameter addressed in this protocol is to check the link reliability and immediate neighbor nodes amount. It in turns gave a better results to prolong the network age but had to compromise the end to end delay.

Kumar et al. [34] acheived improved network lifetime on the basis of location based algorithm.It mitigate rebroadcasting of the information packets through the Forwarding Search Space (FSS). Forwarder picked up among neighbors on the basis of its advancement distance to destination and angle. Due to greater number of calculations involve in selection of data forwarder it delays the performance of the network. Data aggregation is one of the useful concept in WSNs. To cater with repeated transmissions of a information packet, the researchers work on to resolved the issue and present the optimal solutions for energy minimization.Because of this cause an “Energy Efficient Ant Colony algorithm” (EEAC) is proposed by Lin et

al. [35] in order to collect information from the network nodes. In the propose algorithm the authors uses residual energy of the node to optimize the selection of the best forwarder. Although the scheme compromises the scalability of the network but on the other hand it prolong the age of the network. Liu. [36] present a transmission strategy called “An Optimal-Distance based Transmission Strategy for lifetime maximization of wireless sensor networks” (ODTS) using ant colony optimization technique. In this scheme, movement of the each ant between different circular regions of the coverage area is considered for information flow towards the sink. Two algorithms included MEED and MEBD are considered to pick the optimal energy efficient path. The proposed scheme works better in sparse network as compared to dense network.

Energy consumption is one of the major factor which decreases the performance of the network. An energy efficient routing protocol is must in this case. Ghaffari et al. [37] target the number of hop count towards the sink in order to select the next hop forwarder. It selects nodes that have minimum distance from the sink. Moreover it also identifies the link quality while selecting minimum hop counts. Network lifetime is improved in dense area network however its performance is degraded in sparse area network due to the unavailability of potential relay nodes in the upstream region. In order to maximize network performance Jin et al. [23] propose an “Energy Efficient tree based Data Collection Protocol” (EEDCP-TB) for data gathering using cascading time mechanism by efficiently allocating time slots in order to save nodal energy. EEDCP-TB helps in maximizing network lifetime in expense of delay. “Lifetime Maximizing Dynamic Energy efficient routing protocol” (LMDE) is proposed by Bhattachargee et al. [38] to optimize network performance. The routing mechanism use remaining energy of nodes for data forwarding. The scheme improves the network lifetime however fails to control the scalability and data redundancy. The authors in [36, 39–41], target the energy constraint and succeeded to improve the energy consumption of the node in the network through balancing.

TABLE 2.1: Comparison of the State of the Art in WSNs

Protocol	Technique Used	Metrics	Parameters Achieved	Parameters Compromised
HORA [25]	Multi-hopping	Energy and distance	Network lifetime	Transmission Delay, Energy tax
LBT [26]	Multi hop ring routing	Energy and Distance	Network lifetime	Energy Hole
NEHA [27]	Sleep schedule, multi-hopping	Energy and Distance	Network lifetime	Energy tax, E2E delay
E-HORM [29]	Sleep schedule, multi-hopping	Energy threshold, distance	Network lifetime	E2E delay increases
IHDHRA [30]	Node replacement	Forwarder function and energy	Network lifetime	Scalability and Robustness
EEDSRS [32]	Data sensing, Data routing	Link Quality	Network lifetime	MAC layer protocol
EEAC [35]	Ant colony optimization	Energy	less energy consumption	Scalability and Robustness
ODTS [36]	Ant colony optimization	Distance and Energy	Network lifetime	Performance degraded in dense area network
EEDCP-TB [42]	Data gathering Tree based Routing	TDMA	Network lifetime	E2E delay increases
LMDE [38]	Multi hop Routing	Energy	Network performance optimizes	Scalability issue

## 2.3 Underwater Propagation Model

This section, present the underwater propagation model from [43]. The path loss due to unobstructed propagation path for a signal having frequency  $f$  over a distance  $d$  is given as:

$$A(d, f) = d^k u(f)^d \quad (2.1)$$

Where  $k$  denotes the spreading factor. For cylindrical spreading,  $k = 1$ , value of  $k$  for practical scenario is 1.5 and for spherical spreading, value of  $k$  is 2.  $u(f)$



is the absorption coefficient generally described in dB/km. Thorp's formula [21], [44], [45] used in underwater to minimize the effect of noise:

$$10\log u(f) = \frac{0.11 \times f^2}{1 + f^2} + \frac{44 \times f^2}{4100 + f} + 2.75 \times f^2 + 0.003 \quad (2.2)$$

The average Signal to Noise Ratio (SNR) [21] is given as:

$$\Upsilon(d) = \frac{E_b/A(d, f)}{N_o} = \frac{E_b}{N_o d^{k_u}(f)^d} \quad (2.3)$$

Where  $E_b$  represents per bit average transmission energy,  $N_o$  is the noise power density in non-fading Additive White Gaussian Noise (AWGN) [21]. Rayleigh fading is used for small scale modeling. The purpose of using Rayleigh fading is to find out the dominant signal in case of multipath fading. Like [46], the probability distribution of SNR is given by:

$$p_d() = \int_0^\infty \frac{e^{-\Upsilon(d)}}{\Upsilon(d)} \quad (2.4)$$

Also the probability of error [21] is given as:

$$p_e(d) = \int_0^\infty p_e() p_d() d \quad (2.5)$$

Where,  $p_e()$  is the error probability for a random modulation for a defined SNR. BPSK modulation is widely adopted in [24], [47]. In BPSK, a bit is carried by each symbol. The bit error probability over a distance  $d$  taken from [47] is:

$$p_e(d) = \frac{1}{2} \left( 1 - \sqrt{\frac{\Upsilon(d)}{1 + \Upsilon(d)}} \right) \quad (2.6)$$

The packet delivery probability for  $m$  bits data transmitted is given by:

$$p(d, m) = (1 - p_e(d))^m \quad (2.7)$$

### 2.3.1 Acoustic Signal Velocity in the Underwater Environment

Different factors affect the speed of acoustic waves i.e., temperature variation, pressures at different layers of the sea and salinity of the water. Mathematically, it can be related as [48]:  $c = 1446.96 + 4.591T - 5.305 \times 10^{-2}T^2 + 2.374 \times 10^{-2}T^3 + 1.340(S - 35) + 1.63 \times 10^{-1}D + 1.675 \times 10^{-7}D^2 - 1.025 \times 10^{-2}T(S - 35) - 7.139 \times 10^{-13}TD^3$ , where  $c$  represents the velocity of the acoustic signal in m/s,  $T$  represent the temperature in degree Celsius,  $S$  is the salinity in parts per thousand and  $D$  represents the depth in meters. The sound speed increases with the increase in temperature as shown in Figure 2.1 and speed of sound variation with respect to salinity shown in Figure 2.2. The above Equation is valid for  $0 \text{ C} \leq T \leq 30 \text{ C}$ ,  $30 \leq S \leq 40$  PPT,  $0 \leq D \leq 8000 \text{ m}$ .

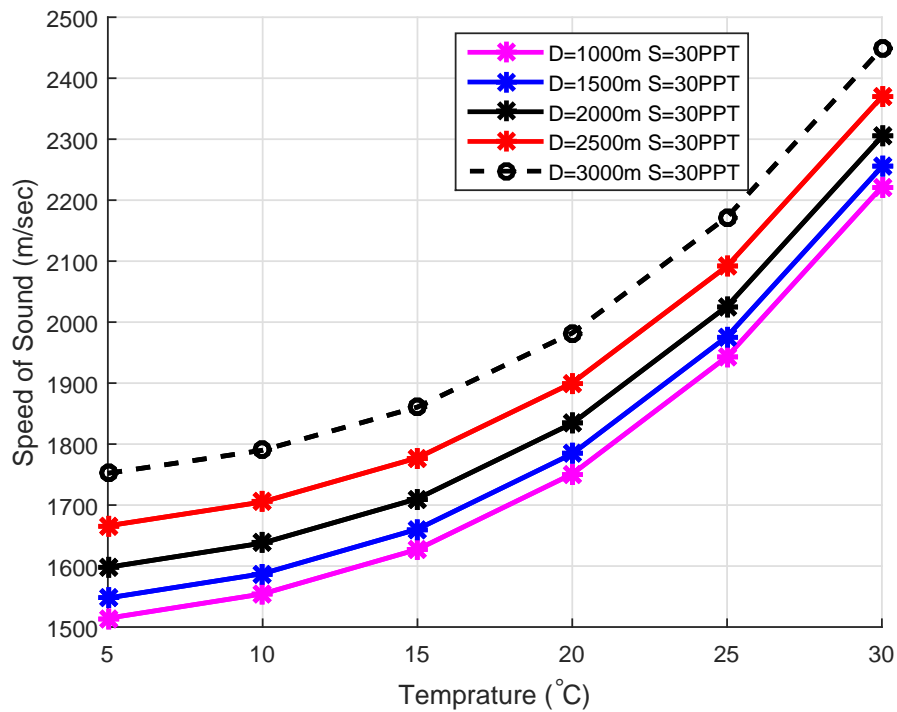


FIGURE 2.1: Speed of sound vs. temperature.

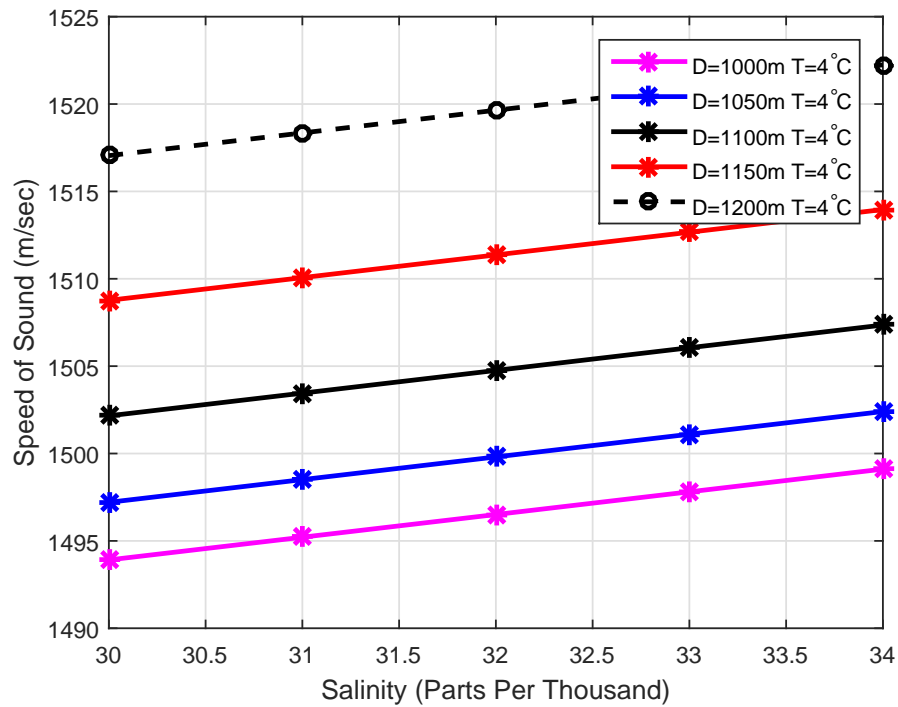


FIGURE 2.2: Speed of sound vs. salinity.

### 2.3.2 Acoustic Signal Reflection and Refraction in the Underwater Environment

Channel geometry and its reflection and refraction properties influence the impulse response of an acoustic channel. The total count of major paths for propagation and their relative delays and strengths are also determined by these characteristics. Strictly speaking, the number of signal echoes is infinitely large, but after discarding those which have undergone multiple reflections and thereby lost much of their energy, left with only a few significant paths. The longest path delay governs the total multipath spread, which is to the tune of tens of milliseconds. Such values are usually reported in shallow-water experiments [49]. The dispersion of individual paths is significantly lesser than the total multipath spread. Therefore, for systems with maximum frequencies significantly below the channel cutoff (several tens of kilohertz in simulations), it can be ignored. For systems currently in use, this is typically the case.

## 2.4 UWSN Routing Protocols

A multi-modal communication is proposed by O'Rourke *et al.* [50] using radio and acoustic communication simultaneously. Sensor nodes are equipped with acoustic communication modem (Figure 2.3). The information is delivered to sonobuoy through radio signal. An information is sent to node for the selection of data forwarder. The proposed algorithm helps in determining the set of surface nodes for data forwarding. The major disadvantage of the proposed mechanism is the high end to end delay due to movement of node at new depth until it reaches to the surface in order to transmit the data towards the destination. A distributed algorithm Hop-by-Hop Dynamic Addressing based protocol for monitoring of long range underwater pipeline is proposed by Abbas *et al.* [51] which assigns dynamic hop address to every node that participates in data forwarding process. It improves the PDR on the expense of high energy consumption. The comparison of the state of the art work in UWSNs is shown in Table. 2.2.

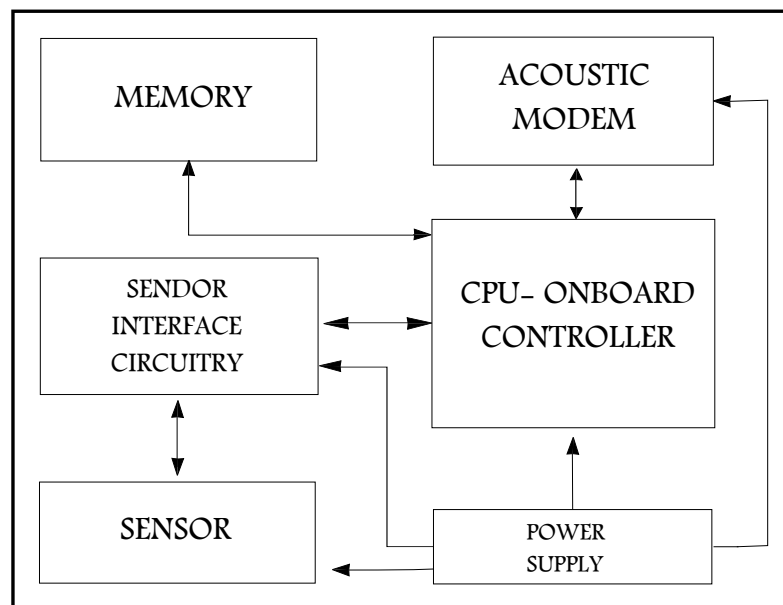


FIGURE 2.3: Sensor Architecture

### 2.4.1 Geographical Routing

Geographic routing utilizes location information for path establishment between source and destination. Geographic position information is used to send packet towards closer destination at each hop till packet reaches the sink. Unlike the proactive routing that bears large communication overhead due to full path discovery and maintenance, geographic routing relies on one or two hop information for routing tables. This feature enhances scalability of large sensor networks. In geographic routing, services like geo-casting can be used to get geographic information for data forwarding within a geographic region [52].

In existing literature, various routing schemes and protocols have used position information of sender and receiver node for routing purposes. Such as Vector Based Forwarding routes data within the confined pipeline along the virtual vector drawn from sender to receiver. Relative distance of sender node and virtual vector is taken within a threshold. Beyond a certain distance between node and virtual vector, sender node has to drop the packet. In dense network regions, a more number of nodes take part into forwarding process that leads towards redundant paths for improved packet delivery at the cost of high energy consumption. Considering this shortcoming, authors proposed self-adaption algorithm based on position information of sender node and receiver node with respect to virtual vector in a virtual pipeline. According to this information, suitability of a node is calculated for routing the data towards destination [53].

### 2.4.2 Sender and Receiver based Routing

Considering geographic information, this section categorize the existing protocols and schemes into two hierarchies: **sender based** and **receiver based** underwater routing protocols as tabulated in Table I. These hierarchies are further divided into two streams based on information type: either location information or depth information as shown in Fig. 2.4.

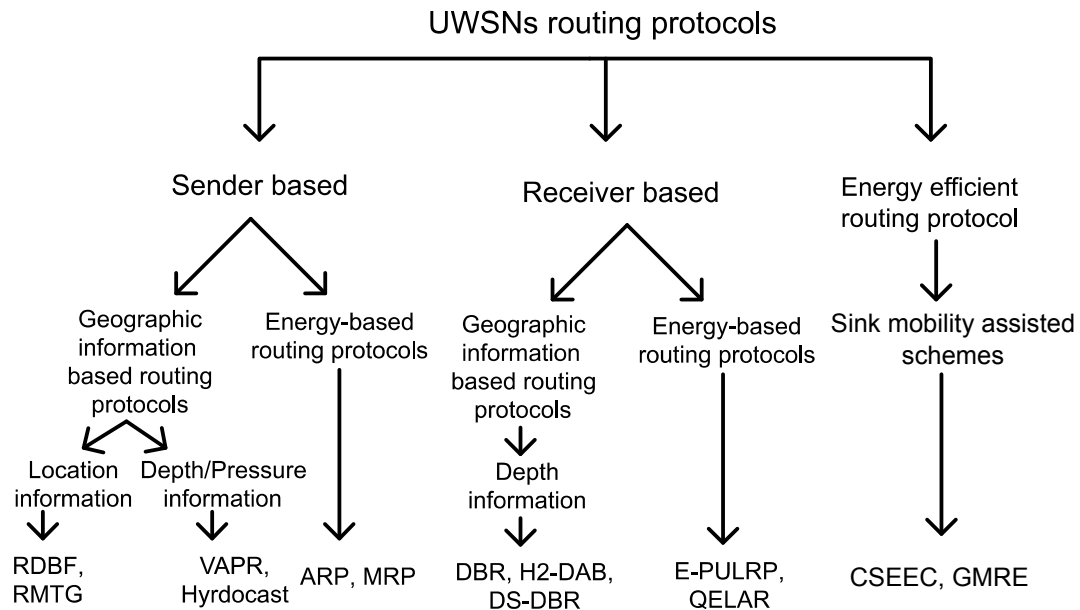


FIGURE 2.4: Classification of existing routing protocols

### 2.4.3 Depth based Routing

The existing receiver based underwater routing protocols using geographic information for routing are Depth Based Routing (DBR), Delay Sensitive Depth Based Routing (DSDBR), Hop 2 Hop Dynamic Addressing Based (H2-DAB) routing, etc. The sender based underwater routing protocols relying on geographic information for routing purpose are Relative Distance Based Forwarding (RDBF), Routing and Multicast Tree based Geocasting (RMTG), Adaptive Routing Protocol (ARP), Diagonal and Vertical Routing Protocol (DVRP), Void-Aware Pressure Routing (VAPR) protocol and HydroCast.

In [54], authors formulates holding time calculations to reduce latency in the network. This protocol is intended to reduce end to end delay for delay sensitive applications. H2-DAB routing protocol in [55] uses two part information: node ID and hop ID for routing the data packet. This protocol is energy efficient because it does not store complex routing information in routing tables. Whereas, it needs to update routing table on time for effective data transmission.

In [56], VAPR protocol exploits two hop depth information and hop counts to select next hop forwarder. It is easier to get depth information as compared to

location coordinates. VAPR opts two fold procedure: enhanced beaconing and opportunistic directional data forwarding. A node initiates a beacon containing information like its depth, data forwarding direction and hop count in the first phase of communication. In the second phase, sensors relay the data packets on the basis of direction of flow at first and second hops. The mechanism ensure the flow of the data packets on the upward direction towards the sink. Due to efficient beaconing, VAPR is robust against failures and node mobility. In [45], hydrocast routing protocol uses pressure information of sender node, neighbor nodes and two hop neighboring distance. During forwarding process, hydrocast selects a set of neighboring nodes based on greedy advancement towards destination, considering hidden terminal problem as well. Both VAPR and hydrocast maintain routing path to avoid void holes at the cost of high energy consumption.

DBR [57] is proposed by Yan *et al.* that consider the depth of nodes to find the next hop forwarder nodes. Low pressure nodes are selected as neighbor nodes for data transmission. The proposed scheme minimizes the energy consumption of the network, however it fails to optimize network performance when void node appears in the network. The node fails to find forwarder node in its transmission range thus the performance of the network is degraded due to presence of void nodes. To extend the idea of DBR [57], RPR [58] uses encryption and decryption mechanism. In RPR, the payload and packet header are encrypted. A pair of keys (public and secret keys) are given to each node and a generated pair of key certificate is issued to nodes by a trusted party. Information shared between nodes is encrypted using the Network wide Security Key (NSK). During the data forwarding phase, the packet payload is encrypted with a Gateway Pubic Key (GPK) and encryption of packet header at each forwarder node is done using NSK. After a node successfully receives a packet, it decrypts the header and checks whether the packet is signed by a valid node or not. Only the packet with a proper signature is accepted for routing.

The authors in [59], propose a Weighting Depth and Forwarding Area Division DBR routing protocol (WDFAD-DBR) that takes into account the depth difference between two hops to overcome void nodes. A Reuleaux triangle is introduced in

WDFAD-DBR such that each node overhears the transmission of high priority node to avoid redundant transmission. The priority is based on its depth from its sonobuoy. If a high priority node starts its data transmission, the nodes with lower priority suppress their transmission. This scheme achieves high PDR in sparse case, less energy consumption and minimum delay level. However, the scheme fails to improve network performance in dense area network due to robustness. The work presented in [60] and [61] adjusts depth of sensor nodes to eliminate void hole problem in static USN architecture. The proposed centralized and distributed topology control mechanism determines isolated and void nodes to adjust depth of nodes to a new location.

#### 2.4.4 Location Based Routing

In RDBF, an efficient route search towards destination is performed using location information. For finding suitable node for forwarding process, a fitness function is defined based on distance with respect to sink. Hence, nodes closer to the sink have higher priority to get selected as forwarder nodes. In order to avoid redundant transmissions and collisions, if a node overhears same packet transmission from another node, it simply drops the packet. Residual energy threshold is maintained for efficient energy consumption. However, accurate position information is required for each node for successful communication, which is hard to obtain in underwater environment [62]. The RMTG geocast routing protocol relies on multiple pieces of information, such as location information of nodes and their neighbors, route discovery for selection of node closest to the destination and route maintenance. This protocol has addressed problems like void hole and link breakage. A multicast shortest path is formed for packet transmission within the intended geographic region [63]. Vector based forwarding (VBF) has been proposed in [53]. VBF considers node location information and forwards packets through all the intermediate nodes that lie in the virtual pipeline between source and destination node pairs. When a node receives a packet from the downstream node, it first checks whether it is within the virtual pipeline or not. If a node is



within the virtual pipeline, then it computes holding time using the *desirableness factor* of the forwarder,  $\alpha$ , maximum predefined delay, and the propagation delay towards the edge of the transmission range of the sender node. Desirableness factor includes the ratio of the node's distance from the center of virtual pipe and width of the virtual pipeline plus the distance from the sender node. Every time when the same sender forwards the packet, the specific number of node(s) at around closer to the center of the virtual pipeline depleted earlier. It has been observed from the simulations that when network become more dense then the delays between the neighbor nodes decreases and therefore the balance between holding time differences degrade the network performance. Therefore, enormous loss of energy seen and packet delivery ratio suffered. The radius of the pipeline is not fixed in the VBF. Finally, in a sparse network scenario, it is really hard to find nodes within the virtual pipeline between sender and the sink node pairs. In other words, there must exist a single path inside the virtual pipeline between sender and sink to successfully forward packet towards the sink, which is hard in the sparse network scenario.

Instead of using a single virtual pipeline between sender and the Sink node, authors proposed hop-by-hop VBF (HH-VBF) [64] that forms a separate pipeline between the Sink and each forwarding or relaying hop. The authors assume that is better to form a hop-by-hop relative pipeline to find more suitable packet forwarders. The radius of the pipeline is similar to the transmission range of the node. The holding time computation in HH-VBF is not different than the VBF. HH-VBF fairly improves the packet delivery ratio compared to VBF because it increases the chance of finding more suitable forwarder within the hop-by-hop virtual pipeline. As VBF, HH-VBF fails to provide energy fairness within the network.

The authors in [65], proposed Adaptive HH-VBF (AHH-VBF). It is claimed that AHH-VBF adaptively adjusts forwarding distance and the transmission power. The forwarding distance regulated base on the 1-hop neighbor density at each hop and the transmission power is computed to the maximum distant forwarder in the range. The radius of the hop-by-hop pipeline is controlled to reduce the packet forwarding by many nodes in the forwarding region. In order to achieve

transmission power and forwarding area adaptiveness, AHH-VBF sends multiple *Request* messages at different power levels and maintains the neighborhood table when it receives *Acknowledgement* packets in response to the *Request*. If the number of neighbors found during this process is less than  $\tau$ , then transmission power is set to the maximum power; otherwise, it is adjusted accordingly. The energy efficiency is achieved through the transmission power adjustment and pipeline radius. However, several data packet transmissions from the same source node will always select the same set of forwarders, which violates the energy fairness in the network as in HH-VBF. Additionally, the power adaptiveness does not guarantee that avoidance of packet duplication and as well as the potential forwarder selection. Following is the discussion about the location based routing protocols for underwater networks that do not consider any holding time.

The concept of directional power adaptiveness to overcome the packet flooding in underwater networks is also proposed in the Focused Beam Routing (FBR) [66]. Power and flooding angle are gradually increased according to the predefined gradients before forwarding data packets. A node requires to send many Request to Send (RTS) packets and waits for the Clear to Send (CTS) packets from neighbors in the beam direction. In sparse networks, RTS control overhead at each hop can consume more energy as well as increase the end-to-end delay for the data packet. FBR faces RTS and CTS delay, which is reduced by scheme name Layer by Layer Angle Based Flooding (L2-ABF) [67]. In L2-ABF, the flooding angle of the data packet in a cone shape towards the upper layer (towards the direction of Sink node). The power and angle (the length and width of the cone) depend on the layer distance and relative node speed between sender and the receiving nodes, respectively. There may be many attempts to send data packets in a sparse networks and multiple copies may be forwarded in the dense and random network deployment scenario.

In [68], authors have proposed the state-less, location- and receiver-based routing protocol named Directional Flooding-based Routing (DFR). All nodes in DFR knows their own location, location of sink node, and the location their immediate neighbors. DFR does not employ any holding time, which means that all the nodes

that receive the copy of a data message will further forward towards upstream. However, it controls the flooding direction of the data packets within the certain zone in the direction of Sink node. Size of the flooding zone is adapted with the upstream link quality. As link quality fluctuates in the underwater environment, hence the flooding zone may be unnecessarily become wider, consume more energy and reduce delivery ratio.

A modified Dynamic Source Routing based Location-aware source routing (LASR) has been proposed in [69]. It uses link quality e.g., expected transmission count (ETX) and location awareness as a routing metric to forward packets towards Sink node. As it uses the source routing, therefore, the packet size is directly proportional to the number of hops that packet has been relayed. Furthermore, it requires to flood the route request in the entire network to find the suitable route towards the destination, which drastically reduces the network performance and consumes network resources.

#### 2.4.5 Energy Based Routing

In ARP, data packets are assigned different delivery priorities that depend on application requirement. Higher priority packets are sensitive to delay. So, there is a fair trade off between delay and packet delivery in ARP. It uses location information and it is an energy efficient protocol however, it incurs high communication overhead [70]. To avoid horizontal communication between same depth sensor nodes, DVPR opts triangular inequality theorem. According to that, same depth nodes are avoided using coordinate information of participating nodes in communication. However, accurate position information is a challenging task itself [71]. Authors in [72], propose EEDBR using both the depth and the residual energy of nodes to find the next hop forwarder node. The selection of next hop forwarder node is based on the greedy approach. The source node searches neighbor nodes within its transmission range. It selects a node having lowest depth and high energy among others. The packet is delivered to nodes having low depth and high energy. EEDBR achieves high energy efficiency and throughput, however it fails

to cope with void node in sparse case which results in high energy consumption and end to end delay.

In [73], authors present a layered approach for reliable and energy efficient data transmission in USNs. A binary tree is established from source to destination and controls propagation power at each hop. The network area is divided into multiple vertical layers for efficient data transmissions. However, due to multi-path communication, redundant packets are high in number which results in rapid energy depletion of sensor nodes. Geographic routing introduces location errors as discussed in [74] and [75]. The protocols proposed in these papers present location error robust routing protocols to minimize energy consumption in geographic routing techniques. The work in [74] selects node with minimum expectation value while [75] calculates MSE to estimate location errors. The authors in the literature, worked for the void hole avoidance, however, none of the void hole avoiding algorithm implemented location error avoidance scheme. Also, the depth adjustment based routing protocols like [60], [61] and [18] consumes abundance of energy during depth adjustment of sensor nodes. However, this excessive energy consumption issue has not been addressed in these papers. Therefore, the USN's lifetime is compromised. On the other hand, most of the location error robust protocols in literature, like [74], [75], and [76] do not consider void hole problem. In these papers, the forwarder node discards data packet if it contains no neighbor in its range. In [77], Scalable Localization scheme with Mobility Prediction (SLMP) protocol is proposed. In this work, mobility patterns for sensor nodes are predicted in order to minimize localization errors in the network. SLMP divides localization process into ordinary node localization and anchor node localization.

#### 2.4.6 Pressure Based Routing

Hydrocast pressure routing protocol [45] exploits pressure information of sensor nodes to route data packets towards surface sinks. The priority of next hop neighbor node is set via a parameter which is calculated using packet advancement towards sink and the packet delivery link cost. Hydrocast determines a cluster of

forwarders within the communication range of each other to avoid hidden terminal problem. A mechanism to deal with the void nodes is also defined in this work. Whenever, a node finds itself in a communication void area, it searches for a lower depth node using controlled flooding. Anycast routing is implemented to forward data to one of the sink nodes.

### 2.4.7 Sink Mobility Assisted Routing

Cayirpunar, O. et al. [78] proposed a sink mobility based routing strategy for WSNs in order to prolong network lifetime. This work presents optimal patterns to mobilize sink. However, high delay may be encountered due to single sink roaming in whole network field. In another work by S. Chen and W. Lin [79], a geo-cast technique has been proposed to minimize energy consumption and void hole problem. The Autonomous Underwater Vehicle (AUV) moves in the network field according to user defined pattern and collects data from sensor nodes. This protocol also works for awaking sensor nodes in the next-to-visit region by AUV. This helps to achieve energy efficiency in the network field. In [80], authors considered three different scenarios: network field division into zero, two and four logical regions. The sensor nodes transmit their sensed data to AUV and Courier Nodes (CNs). Each node transmits data directly to MS when it comes within direct transmission range of node. Sensor nodes can transmit their sensed values to CNs as well where they further transmit that data to MS.

The authors in [81] introduced AUV-aided Underwater Routing Protocol (AURP) to minimize energy consumption in USNs. Multiple AUVs are introduced in this paper for data gathering. In AURP, the nodes relay/forward packets to gateway nodes where the gateway nodes transmit data to AUVs. All the AUVs are responsible to gather data from gateway nodes forwarded towards the surface station. This sufficiently reduces the number of hops towards surface station, and therefore energy is preserve from excessive wastage. This Chapter, present a novel location error aware transmission range and depth adjustment-based routing protocol to cope with both the void hole problem and localization errors in mobile

USNs. Another objective of proposed work is to achieve maximum coverage over the monitoring network region. The proposed work have performed multiple sink positioning in the way to attain objective up to the maximal extent. As sinks are mechanically driven devices and a specific cost is associated with them thus, the sink movement arrangement is such a way that to minimize the total travelled distance of sinks deployed in three dimensional field. Such distance constrained problem is addressed in [82], in which sink time profile is monitored. Additionally, time profiles of all the deployed sinks are monitored and based on that scheduling is performed. Sink selection and its location are decided based on monitored time profiles of all the sinks.

In another contribution, authors presented the technique to optimize the network lifetime. In this technique routing tracks are found prior to transmit the packet by keeping variable pause time. This differs from proposed approach as the research have jointly considered routing and sink mobility [83]. In [84], controlled sink mobility for network lifetime maximization is proposed. Sink moves to balance energy consumption in the network. In this work, sink mobility is concerned with optimal sink route finding and then sink moves towards the regions of high residual energy nodes. Similarly, sink mobility is introduced in [85], focusing on minimization of energy expenditure. Periodic sink mobility is introduced in this work to maximize coverage on network field.

In GEographic and opportunistic routing with Depth Adjustment-based topology control for communication Recovery over void regions (GEDAR) [18], a depth adjustment based geographic and opportunistic routing protocol is proposed. To select a set of neighbor nodes for forwarding data towards sink, location information of known sinks and sensor nodes is used. Each forwarder node is assigned a priority using advancement and packet delivery probability. GEDAR avoids redundant transmissions; only higher priority nodes transmit data while other nodes overhear and suppress their transmission. If a node fails to find any forwarder node within its vicinity, it displaces to a new location using depth adjustment procedure. According to depth adjustment, void node moves down towards predecessor node. If the predecessor node is not a void node, displaced node transmits its

TABLE 2.2: Comparison of the State of the Art Work in UWSNs

Protocol	Features	Achievements	Limitations
GEDAR [21]	Geographic and Opportunistic Routing	Void hole avoidance	High energy consumption, high end to end delay
DBR [57]	Depth Based Routing	Improved PDR in dense area network	Performance degraded in sparse area
EEDBR [72]	Depth and Energy Based Routing	Network lifetime is maximized via energy balancing	Redundant packets, more energy consumption
AVN-AHH-VBF [44]	Location Information Based Routing	Network performance is improved	More redundant packets, high end to end delay
GBPR [86]	Grid Based Routing	Reduced APD	Less efficient for void hole avoidance
LCAD [87]	Cluster Based Routing	Increased network lifetime	High end to end delay
HMR-LEACH [88]	Cluster Based Routing	Prolonged lifetime	High end to end delay
VBVA [89]	Vector Based Routing	Improved PDR, Less void holes	High energy consumption, end to end delay
Hydrocast [45]	Pressure Based Routing	Decreases void node probability	Increase in overhead
WDFAD-DBR[59]	Depth Based Routing	Improved network lifetime, Less energy consumption	End to end delay is increased
H2-DARP-PM [51]	Hop Count Based	Improved PDR	High energy consumption
Multimodel Communication [50]	Multimodel Communication Approach	Energy fairness, improved PDR	High end to end delay
H2-DAB [55]	Depth Based Routing	Energy efficient	Computationally complex
VBF [53]	Location Information Based Routing	Increase in PDR	High energy consumption in dense network
VAPR[56]	Depth based routing	Void hole avoidance	High energy consumption

Continuation of Table 2.2

<b>Protocol</b>	<b>Features</b>	<b>Achievements</b>	<b>Limitations</b>
Movement Assisted [61]	Depth based routing	Void hole elimination in static USN	Computationally complex algorithm
RMTG [63]	Location Information Based Routing	Increased end-to-end delay	Reduced void hole and link breakage
HH-VBF [64]	Vector Based Routing	Improved throughput	Reduced energy fairness
FBR [66]	Flooding based routing	Reduced unnecessary flooding	Increase end-to-end delay due to RTS and CTS
L2-ABF [67]	Angle Based Routing	Improved PDR and Reduced E2ED	Multiple copies of data transmitted in network
ARP [70]	Location Information Based Routing	Energy efficient	High communication overhead
DFR [68]	Flooding Based Routing	Limit the energy consumption	No strategy for void hole in sparse network
LASR [69]	Link state MANET Routing	Higher PDR	High computation by tracking system
Energy Efficient Tree Based [73]	Binary Tree Based Routing	Efficient data transmission with improved PDR	High redundant packets, high energy consumption
SLMP [77]	Location Error Based Routing	Minimized location error	High end to end delay, computationally complex
AUV-PN [90]	AUV Based Data Gathering	Increased lifetime, minimum overhead	AUV not visit all the network
Sink based statoin [78]	Sink Mobililty Based Routing	Improved network lifetime	High delay due to sink mobility
Bandwidth efficient data gathering [80]	Sink Mobililty Based Routing	Improved network lifetime and PDR	High delay due to sink mobility
ESDR [91]	Event Segregation Based Packet Forwarding	Low end to end delay	High computation by event segregation



data through this node otherwise predecessor also adjusts its depth.

In the realm of UASNs, there is a plethora of research to achieve efficient routing in the network [92–94]. However, here this research only focus on the specific domain of routing protocols that are related to proposed scheme. Thus, the previous works that suppress the packet broadcast in underwater acoustic sensor networks using node location information [95] and the holding time [57], are discussed in this section.

In [96], the authors proposed an AUV (which acts as a mobile sink) based distributed data-gathering scheme to efficiently collect data from the selected nodes, called path-nodes, instead of traversing the whole network. The path nodes are the data collection points and are optimally selected to shorten the AUV trajectory as well as achieve network energy efficiency. A mobile geocast or mobicast in the three-dimensional (3D) AUSN with mobile sink has been investigate in [81]. The main objective of the mobicast is to minimize energy consumption and avoid energy hole problem during data collection. The whole 3D UASN is divided into multiple 3D geographic zones that are also called zone of reference (ZOR). The AUV collects data from the sensor within the ZOR and moves through the user-defined path. The sensors within the ZOR conserve their energy by only waking up at the AUV's visit time.

From the above mobile sink based literature review, it is observed that the sink mobility improves the network efficiency in terms of end-to-end delay, battery power, packet delivery ratio, and so on. Hence, any scheme proposed for the UASN must be tested with and without sink mobility to verify its effectiveness.

## 2.5 Conclusion

This chapter is about the deep insight to the research in designing the WSNs and UWSNs routing protocols. The basic knowledge to achieve the objectives of the research is explored. Initially, this chapter provides the background study of the terrestrial wireless sensor networks. The requirements and applications of the

terrestrial and underwater sensors has been presented in detail. Along with applications, the routing protocols performance dependency on the evaluation metrics has been investigated. The comparison tables for both terrestrial and underwater routing protocols has been presented. Moreover, the underwater channel characteristics are discussed in detail.

## Chapter 3

# DOW-PR DOLphin and Whale Pods Routing protocol for UWSNs

### 3.1 Summary of the Chapter

The existing WDFAD-DBR protocol considers the weighting depth of the two hops in order to select the next Potential Forwarding Node (PFN). To improve the performance of WDFAD-DBR, DOLphin and Whale Pod Routing protocol (DOW-PR) has been proposed. In this scheme, the transmission range is divided into a number of transmission power levels and at the same time select the next PFNs from forwarding and suppressed zones. In contrast to WDFAD-DBR, the proposed scheme not only considers the packet upward advancement, but also takes into account the number of suppressed nodes and number of PFNs at the first and second hops. Consequently, reasonable energy reduction is observed while receiving and transmitting packets. Moreover, the proposed scheme also considers the hops count of the PFNs from the sink. In the absence of PFNs, the proposed scheme will select the node from the suppressed region for broadcasting and thus ensures minimum loss of data. This research also come up with another routing scheme (whale pod) in which multiple sinks are placed at water surface, but one sink is embedded inside the water and is physically connected with the surface sink

through high bandwidth connection. Simulation results show that the proposed scheme has high Packet Delivery Ratio (PDR), low energy tax, reduced Accumulated Propagation Distance (APD) and increased the network lifetime.

## 3.2 Introduction

DBR [57] uses the depth information of the sensor node for flooding the data packets towards the centralized station. The depth can be found with the help of depth sensor, which is integrated within every sensor node. The flooding is omni-directional so any node that is in the range of a sensor receives the packet. The sensor node adds its depth information to the packet. This depth information is compared by the receiving node with its own depth. In case the current node is shallower than the depth information appended in the packet, the receiving node is a PFN. The PFN holds the packet and sets the timer based on the holding time computation. In case PFN does not receive any duplicate copy of the packet until the expiration of the timer, it will forward the packet. On the contrary, if the node receives a duplicate copy of the packet before the expiry of the timer, then it will simply drop the packet. In case the receiving node is deeper than the sender node, it will drop the packet if and only if there are PFN available to source. WDFAD-DBR) [59] will choose the forwarder node by calculating the weighting sum of the difference in the depth at two hops. The DBR only considers depth of first hop PFNs for data forwarding but on the other hand WDFAD-DBR uses the accumulative depth at two hops nodes. The proposed scheme, DOW-PR protocol considers the number of PFNs, number of suppressed nodes and the hop count to select the node for forwarding the packet generated/forwarded by the source node. Nonetheless, the proposed scheme will select the shallowest suppressed node for forwarding the packet if the source node suffers from void region towards the sinks. The proposed scheme will divide the transmission range into different energy levels, so that the node (if selected as forwarder) that is closer to the source node will require less amount of transmission energy compared to the node that is far away. Therefore, the transmission energy will not remain constant through the

transmission range; rather, it will vary in different energy levels. Furthermore, another proposed scheme called whale-pod comprised of multiple sinks placed at the water surface with an additional sink deployed underwater at the depth of 700 m. A high bandwidth physical connection exists between the embedded sink and the surface sinks. When the packet is received by the embedded sink, it is considered as a successful delivery of a packet to the destination.

### **3.2.1 Contributions:**

The contributions of the research work have been summarized in the itemized text below: (1) The optimal set of mapped values for number of potential forwarding nodes and number of suppressed nodes has been investigated; (2) Significant energy is saved due to optimal route discovery mechanism; (3) Additional energy conservation achieved by dividing forwarder region into transmission power levels; (4) An optimal solution provided to cater for the problem of voids and energy holes; (5) Performance parameters included in formulating the holding time i.e., number of potential forwarder, number of suppressed nodes, hop count; (6) Significant improvement in end-to-end delay achieved by readjusting the position of sink nodes; (7) Traffic congestion sorted out by averaging potential forwarding nodes which forms the basis of item 2. To implement the above mentioned contributions, the following steps has been taken:

- Selection of forwarder by computing the optimal average number of PFNs of the forwarding nodes,
- Calculating optimal transmission power adjustment based upon more distant node from the source node in potential forwarding region,
- Finding the alternate node from the suppressed region for the case if source node is in a void,
- Carrying out packet holding time calculations to assign priorities,
- Finding the nearest sink for the case if one of the sink is embedded underwater.

In this chapter, the proposed protocol DOW-PR focuses on selecting the optimal forwarder. This is very similar to the WDFAD-DBR. Much like WDFAD-DBR, DOW-PR also considers the weighting sum of depth of the current and the next expected hops' sensor nodes. The novelties of the proposed protocol that differentiate themselves from counterpart WDFAD-DBR is mentioned in itemized text as follows:

- To improve the performance of WDFAD-DBR, a state-of-the-art DOW-PR routing protocol has been proposed in which transmission range divided into different transmission power levels while selecting the next forwarding node. The source node searches for the optimal power level for packet transmission.
- The proposed work consider the additional parameters i.e., number of PFNs and number of suppressed nodes. WDFAD-DBR does not consider the above-mentioned parameters due to which a network consumes a significant amount of receiving energy, especially in dense networks.
- Along with other parameters, the proposed scheme also considers the number of hops traversed by the packet initiated from the source node. Consequently, DOW-PR optimizes the shortest possible path and thereby improves the end-to-end delays.
- WDFAD-DBR does not provide any mechanism for void hole occurrences at the second hop forwarder. The proposed protocol DOW-PR will select the node for broadcasting from the suppressed nodes when there is no PFN available.
- In DOW-PR, the extended version (Whale pod) is proposed in which one of the sink drown into the water and it is bridged through the physical guided medium and have no constraint of energy and bandwidth.

The rest of the chapter has been structured as follows. Section 3.3 is about the identification of the problem and present the problem statement. The system model is explained in Section 3.4. The experimental setup and simulation outcome approaches are described in Section 3.5. Performance comparison and analysis discussed in Section 3.6. Finally, a brief conclusion is proposed in Section 3.7.

### 3.3 Problem Statement

The WDFAD-DBR protocol abbreviates the priorities of PFNs in designing the holding time of the received packets by considering the accumulative depth differences of the potential forwarding nodes at hops 1 and 2 [59]. WDFAD-DBR does not only consider the depth of the current node, but also the depth of the node at the next expected hop. Therefore, weighting sum of the depth difference i.e.,  $H$  is the combination of depth difference  $h$  between the source node and next PFN and the depth difference  $h1$  between the PFN at hop 1 to the next expecting PFN at hop 2. However, WDFAD-DBR does not consider the number of suppressed nodes and number of PFNs of a source node, which consumes a significant amount of receiving energy. The reason behind it arises from the fact that a large number of PFNs result in receiving the packet as well as the high probability of duplicate packets generated at the first hop and hence excessive transmission energy wasted. The second important reason is that WDFAD-DBR does not consider the hops number for a packet to travel through. In case of a void hole i.e., when the forwarding node does not exist or the existing forwarding node does not have enough energy to communicate, WDFAD-DBR will drop the packet straight away and therefore Packet PDR degraded. The proposed protocol considered the number of suppressed nodes, number of PFNs, and hop count of each potential forwarder as well as the weighting sum of the two hops neighbors. For instance, if considering node S as the source node and nodes A and B are the next hop potential forwarding nodes, as shown in Figure 3.1. WDFAD-DBR will select node A as a forwarding node, as weighting sum of heights for two hops is greater than any other path. However, node A having a large number of PFNs will suffer from a large amount of receiving and transmitting energy due to the chance of initiating duplicate packets. The causes of duplicate packets has been discussed in Section 3.3.2. The proposed dolphin-pods routing will give preference to node B for forwarding in order to overcome the above-mentioned problems. When considering the number of PFNs and number of suppressed nodes, a reasonable amount of receiving energy will be conserved. Moreover, WDFAD-DBR considers the fixed

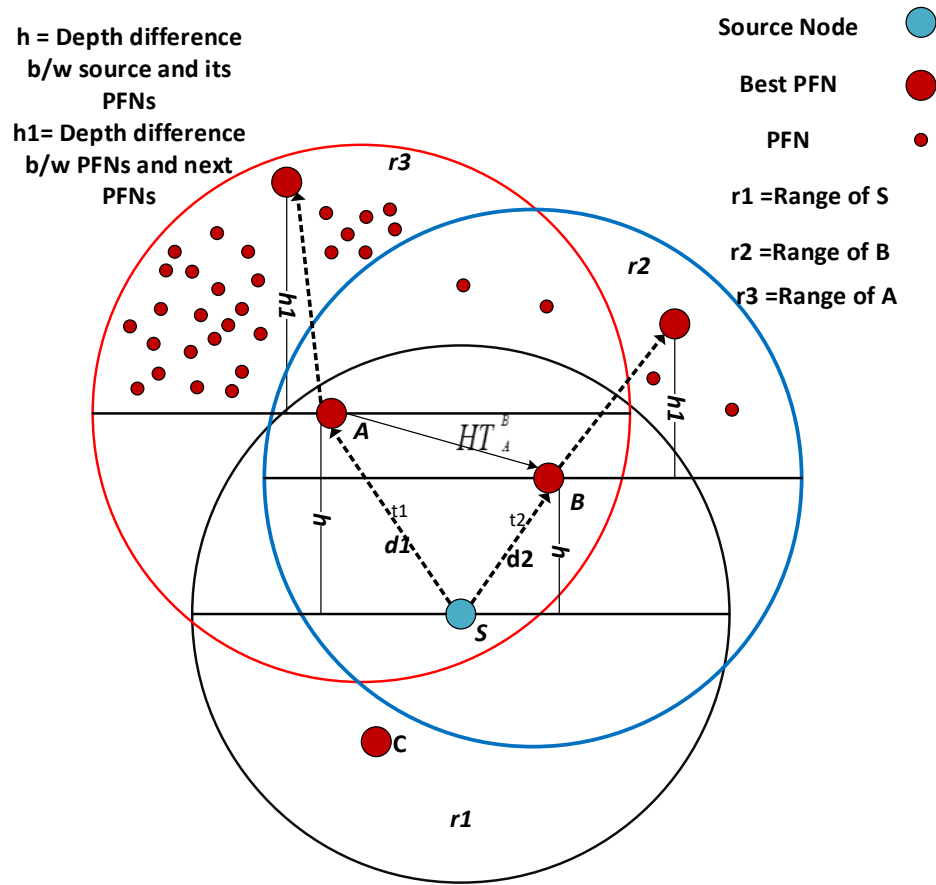


FIGURE 3.1: Forwarder node selection scenario

transmission power level for all nodes in the range of a source node, whereas the proposed scheme divides the transmission range into different transmission power levels such that the appropriate transmission energy level is used by the source node to conserve the energy.

### 3.3.1 Preliminaries

The following notations are used in the proposed DOW-PR scheme:

- *Sink Node D*: A UWSN sink node (also called destination node) is a type of node that is placed at the ocean surface or embedded inside water. Primarily, its function is to collect data from the sensor node and forward it to the base station through high speed radio link. These sinks or destination nodes can



be static or mobile. Let  $D$  be a set of network sinks, then:

$$D = (D_1, D_2, D_3, D_4, \dots, D_8, D_{EM}). \quad (3.1)$$

- *Transmission Range ( $T_r^S$ ) of Node S*: Transmission range of node S is an omnidirectional distance from source node  $S(x_s, y_s, z_s)$  that currently forwarded the packet  $p$  until where it can transmit the packet  $p$ .
- *Eligible Neighbors ( $EN_i$ ) of Node i*: Nodes that are in transmission range of a node  $i$ . Let  $N$  be a set of nodes in a network

$$N = \{n_1, n_2, n_3, n_4, \dots, n_k\}. \quad (3.2)$$

Then, Eligible Neighbors of Node  $i$  can be expressed as  $EN_i \subseteq N$

$$EN_i = \{j \in N \quad \wedge \quad DIST_j^i \leq T_r^i\}, \quad (3.3)$$

where  $DIST_j^i$  is the Euclidean distance between node  $i (x_i, y_i, z_i)$  and node  $j (x_j, y_j, z_j)$  in three-dimensional Euclidean space:

$$DIST_j^i = \sqrt{(x_i - x_j)^2 + (y_i - y_j)^2 + (z_i - z_j)^2}. \quad (3.4)$$

- *Potential Forwarders ( $PF_i$ ) of Node i*: Potential Forwarders of node  $i$  are those nodes that are in transmission range  $T_r^i$  and their depth ( $d_j$ ) is less than depth ( $d_i$ ):

$$PF_i \subseteq EN_i, \text{ where}$$

$$PF_i = \{j \in EN_i \quad \wedge \quad d_j \leq d_i\}. \quad (3.5)$$

- *Potential Forwarding Zone (PFZ)*: Potential Forwarding Zone (PFZ) is the hemispherical region whose radius is equal to  $T_r^S$  and each point in PFZ has lesser distance to the sink as compared to source node. PFZ is the subregion of  $T_r^S$  of node S and the nodes in the region are called potential forwarder nodes

(PFNs), which are next forwarders of packet  $p$ . Any point in 3D Euclidean space  $q(x_q, y_q, z_q)$  is considered to be in the PFZ of  $S$ , if it satisfies the following conditions:

$$DIST_D^q < DIST_D^S, DIST_S^q < T_r^S, \text{ where}$$

- a**  $DIST_D^q$  is the Euclidean distance between point  $q(x_q, y_q, z_q)$  and Sink  $D(x_D, y_D, z_D)$  in three-dimensional Euclidean space:

$$DIST_D^q = \sqrt{(x_q - x_D)^2 + (y_q - y_D)^2 + (z_q - z_D)^2}. \quad (3.6)$$

- b**  $DIST_S^q$  is the Euclidean distance between point  $q(x_q, y_q, z_q)$  and Source  $S(x_s, y_s, z_s)$  in three-dimensional Euclidean space:

$$DIST_S^q = \sqrt{(x_s - x_q)^2 + (y_s - y_q)^2 + (z_s - z_q)^2}, \quad (3.7)$$

$$Z_q \leq Z_s.$$

Neighbors of node  $i$  that are in PFZ of  $S$  :

$$X_i = \{n_i \in PF_i \mid DIST_{n_i}^i \leq T_r^i \wedge Z_{n_i} \leq Z_s\}. \quad (3.8)$$

### 3.3.2 Causes of Duplicate Packets

Primarily, the duplicate packets are generated due to the following facts:

- Firstly, the holding time of packet  $p$  at node  $i$   $HT_i^p$  is computed by a node  $i$  and the timer is started upon successful reception of packet  $p$  (refer to figure 1). Node  $i$  does not forward the packet when  $HT_i^p$  is on, however, data packets from neighboring nodes can be received by it, which may be duplicates of  $p$  or other data packets. Before the expiry of  $HT_i^p$ , if node  $i$  receives additional copies of  $p$  (a single or multiple copies), it abandons the transmission of  $p$ . However, for the case that no copies of packet  $p$  are received before  $HT_i^p$  expiry, packet  $p$  is forwarded by  $i$ . Hence, simply by duplicating broadcast overhead is minimized, which is essential when bandwidth and energy are

scarcely available resources as in UASN scenario. However, if in case, the holding time difference between any two nodes A and B ( $HT_A^p - HT_B^p$ ) is smaller than the propagation delay of a packet p from node A to B, the duplicate packets will be generated.

- The second reason for generating the duplicate packet is the hidden terminal problem. In a hidden terminal problem, the source node broadcasts and the potential forwarding nodes receive the packet. The problem occurs when the highest priority node broadcasts the packet while some of the potential forwarding nodes of the source node are not in the range and thus do not receive the duplicate packet, which causes these packets to be generated.
- Thirdly, relaying packets over multiple hops might result in a failed delivery of the packet to its destination because of high error rate of the acoustic channel, path losses and channel impairments. Duplicate packet generation and transmission become imperative because of the above-mentioned scenarios.

## 3.4 Proposed Scheme

This section, describes the network architecture, division of transmission range in different transmission power levels, and selection of suppressed node in the absence of potential forwarding nodes.

### 3.4.1 Network Architecture

The network architecture of DOW-PR protocol is composed of sink nodes, relay nodes and anchored node as shown in Figure 3.2. Sink stations are situated at the sea roof and consists of radio and acoustic modem in order to communicate with each other through radio link and with the sensor networks through acoustic signals. These nodes are centralized stations, which can receive and transmit signals to the external networks. Anchored nodes are fixed at the seabed and their task is to collect data from the environment. Anchored nodes are fixed with

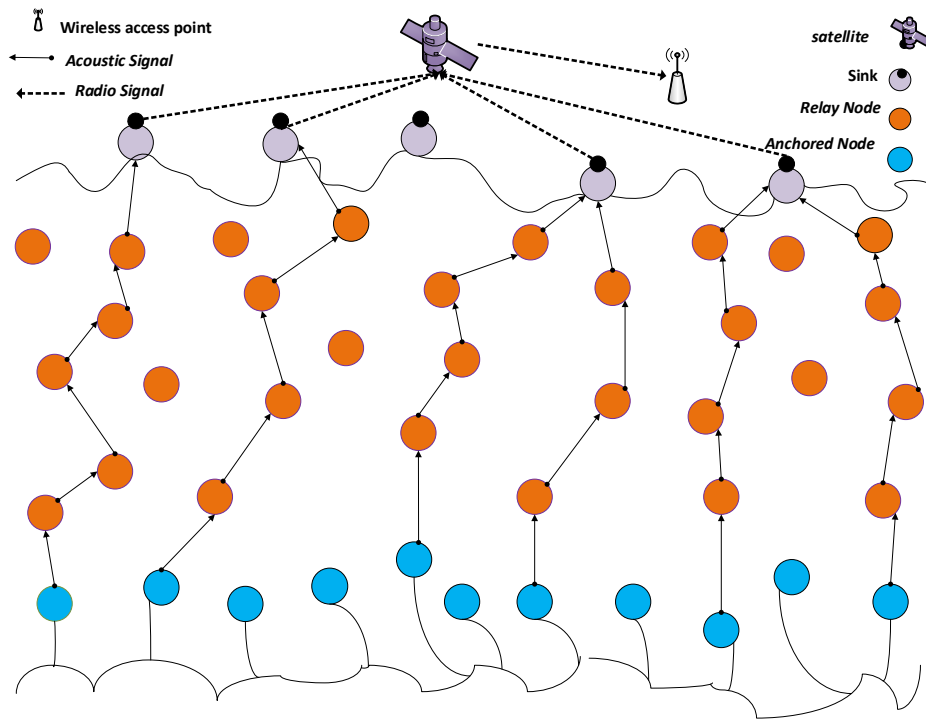


FIGURE 3.2: Network architecture

the tether [97] and movable with water current or any other disturbance in the environment. Relay nodes are deployed at different depths, which forward the received data. Sink nodes can communicate within water through acoustic links and communicate with the external network through radio links. Basically, sink nodes are the centralized stations. Since sink nodes can communicate with each other, the data packet received by any sink nodes will be considered a successful delivery to the destination. Typical applications of this network include monitoring of underwater plates in tectonics or environmental monitoring [98].

### 3.4.2 Packet Types in the Dolphin and Whale Pods Routing

There are three various types of packets in DOW-PR routing protocol, which are NEIGHBOR REQUEST, ACK and DATA. The source node uses packet *NEIGHBOR REQUEST* to search its qualified forwarding nodes. Its format is shown as an NR (TID, SID, DP, VA). TID field is a two-bit number that differentiates between the packets. The TID for NR is “00”. SID abbreviated as ID of the source

and it is broadcast in the neighbor request message. DP represents the depth of source node and VA is a one bit number represents the void hole announcement. The value of VA will be true if the source found a void hole. *ACK* packet is sent in reply to neighbor request means the neighbor node send its information. The format of ACK is ACK (TID, SID, DP). The TID for ACK packet is “01”, SID presents the identification ID of the current neighbor sensor and DP is the depth of node sending *ACK* packet. *DATA* is the real data and it has header and payload. The format of DATA is (TID, SID, DID, DP, PID). The TID value for DATA packet type is “10”, SID is the source ID, DID represents the destination address, DP represents source depth and PID representing packet sequence number. The neighbor request and Acknowledgment packet has smaller size than the DATA packet.

### 3.4.3 Division of Transmission Range into Different Transmission Power Levels

The proposed protocol divides the transmission range into six different transmission energy levels as shown in Figure 3.3. For example, the next forwarder is close to the source node i.e., in transmission zone TZ1, then it will require less transmission energy. On the other hand, if the next potential forwarding node is far away in transmission range from the source node i.e., in TZ6, then higher transmission energy will be required. To increase the network lifetime, the proposed scheme uses different transmission power levels, which range from P1 to PN for broadcasting a DATA packet. The sender node floods a neighbor request message using power intensity level of PN. All the neighboring nodes receive the neighbor request message and reply with an acknowledgment packet. According to the acknowledgment packets received from different neighboring nodes from different transmission levels, the source node sets the transmission power. For example, from Figure 3.3, the source node S broadcast a neighbor request with a power level PN. The node A in transmission zone TZ1, node B in TZ3 and node C in TZ4 level received the neighbor request. The nodes A, B, and C reply with the

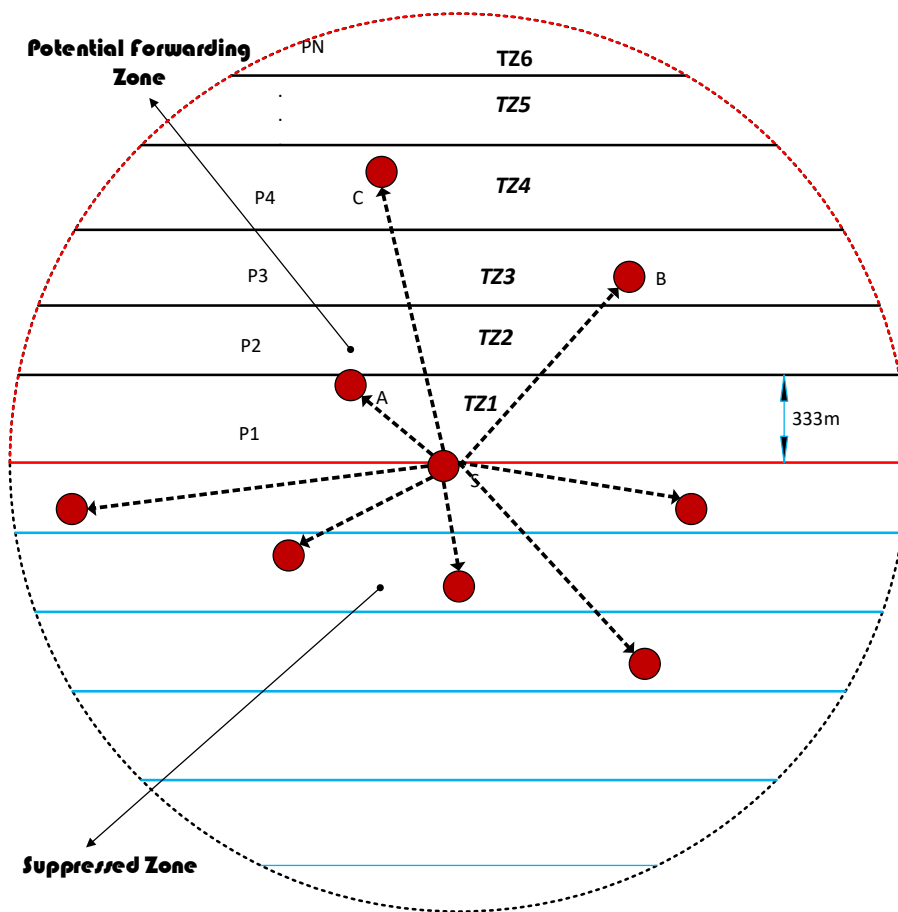


FIGURE 3.3: Division of transmission zones (TZ1–TZ6)

acknowledgment. The acknowledgment packet contains the depth field pertaining to the depth of the sender. According to the DP field in the acknowledgment packet, the source node found the nodes in different transmission levels. The node A is lying in transmission portion TZ1, node B placed transmission zone TZ3, while node C is in transmission zone TZ4. Thus, the node C has a smaller depth than all the other nodes. The source node sets the transmission power level to P4 for broadcasting the DATA packet and with this power level all the three nodes received the packet successfully. The nodes then calculate the holding time and set the timer according to their holding time.

### 3.4.4 Selection of a Forwarding Node among Suppressed Nodes

WDFAD-DBR selects the route based upon the weighting sum of depth difference between first and second hop PFNs. WDFAD-DBR drops the packet when there is no PFN(s) found and that means the data is lost. The source node S finds PFNs by sending a neighbor request packet. However, if the source node does not have any PFN, then the node for forwarding the packet will be selected from the suppressed nodes (refer to Figure 3.4). The selection of suppressed node will be based on the depth and having PFN(s) other than the source node. The source node S will select node A for forwarding, which has smaller depth in suppressed nodes and also has a PFN D, which then continues broadcasting, ensuring minimum lost data. For the case if source node S have node i as only PFN and that too is a void node then two conditions can further occur i.e.:

1. Node  $i$  doesnot have suppressed neighbors
2. Node  $i$  have suppressed neighbors

In the former scenario node  $i$  simply drops packet. In the latter case node  $i$  forwards packet towards its suppressed node which has lesser depth than depth of source node.

### 3.4.5 Holding Time Estimation

When neighbors of a source node receive data packets, it decodes and extracts the depth information of a source node and compares it with its own depth field DP. If DP value of the receiver is lesser than DP value of the source node, and also the void announcement VA field has a value of 0, then it will forward the packet after necessary holding time calculation when no other PFN is available to source. For the case, if PFNs are available, then each PFN will calculate the holding time according to the Fitness Function (HH) value, which is described below. The proposed scheme not only considers the sum of depth difference of

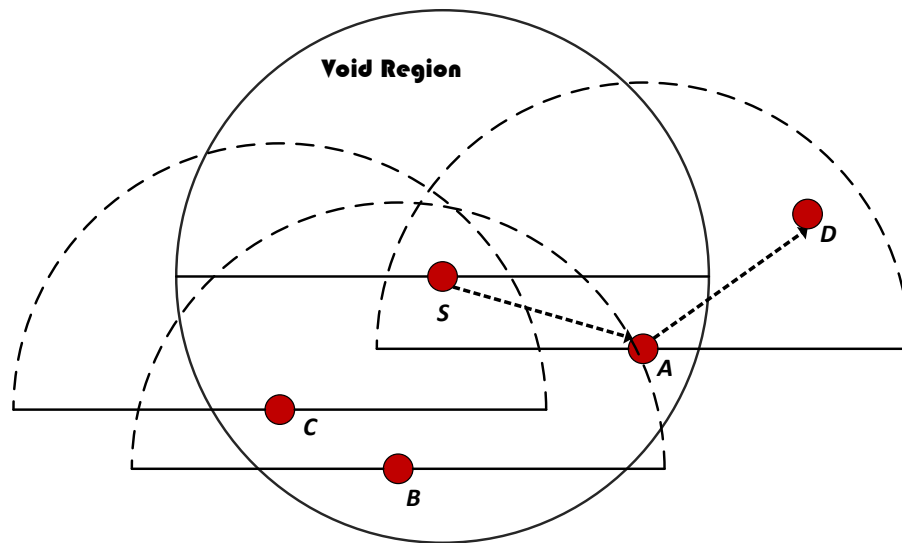


FIGURE 3.4: Forwarder selection from the suppressed nodes

the two hops ( $H$ ), but also considers the number of PFNs ( $PFN_{num}$ ), number of suppressed nodes ( $SUP_{num}$ ), and the hop count from PFN to sink, which is best in favor of performance metrics. Thus, the proposed scheme will consider all of the above-mentioned factors in selecting the next forwarding node.

To find the Fitness Function (HH) value; mapped the  $PFN_{num}$ ,  $SUP_{num}$  into arbitrary values called as division factors represented by  $DIV_{PFN}$  and  $DIV_{SUP}$ , respectively. This is further elaborated in the simulation analysis section:

$$H = \alpha h + (1 - \alpha)h1, \quad (3.9)$$

where  $h$  is the depth difference of the source node to its PFN and  $h1$  is the depth difference of the PFN to the next expected hop and  $\alpha$  is weighting coefficient and its value is between 0 and 1. For node A,  $h$  is the depth difference of the source node S and itself A and  $h1$  is the depth difference of node A and E as shown in Figure 3.5. The Fitness Function is then calculated as:

$$HH = \frac{H}{((DIV_{PFN} + DIV_{SUP}) \times HOP_{tosink})}. \quad (3.10)$$



The holding time is a function of the fitness value:

$$T(HH) = k * (HH) + \beta, \quad (3.11)$$

$$T(HH) = k \frac{H}{((DIV_{PFN} + DIV_{SUP}) \times HOP_{tosink})} + \beta. \quad (3.12)$$

Let Figure 3.5 nodes A (transmission range specified by red circle), B and C have the same number of suppressed nodes.

For Node A :  $H = 8$ ,  $PFN_{num} = 8$ ,  $HOP_{tosink} = 4$  so  $DIV_{PFN} = 1$ .

For Node B :  $H = 16$ ,  $PFN_{num} = 90$ ,  $HOP_{tosink} = 4$  so  $DIV_{PFN} = 15$ .

For Node C :  $H = 12$ ,  $PFN_{num} = 40$ ,  $HOP_{tosink} = 4$  so  $DIV_{PFN} = 7$ .

According to WDFAD-DBR, node B will be selected as a next forwarder, but it has a large number of PFNs, which will consume a lot of receiving energy and generate a large number of duplicate packets. In DOW-PR protocol, the node having highest Fitness Function (HH) value will be selected as the next forwarder. Thus, Fitness Function (HH) calculates for Nodes A,B and C as follows:

Node A:

$$HH = \frac{8}{1 \times 4} = 2,$$

Node B :

$$HH = \frac{16}{15 \times 4} = \frac{16}{60},$$

Node C :

$$HH = \frac{12}{7 \times 4} = \frac{12}{28}.$$

If source node S broadcasts a packet, then all the neighbor nodes i.e., A, B, C, M and N shown in Figure 3.5 acquire this packet. The suppressed nodes M and N will temporarily hold or drop the packet depending on the presence or absence of node(s) in Potential Forwarding Zone (PFZ). Nodes A, B and C are PFNs of source S and will compute the holding time and start timers. If a duplicate packet

is not encountered until expiry of the timer, then this specific PFN will be selected and readily forward the packet. On the other hand, if it receive the duplicate, then it simply drops it. For the scenario, in which node A and B receives the packet at  $t_1$  and  $t_2$ , respectively, and the duration of the packet propagated from A to B is  $t_{12}$ . As fitness value (HH) for node A is greater than node B, then the following condition is satisfied:

$$T[HH_A] < T[HH_B]. \quad (3.13)$$

The holding time between two neighboring nodes should be different in such a way that the forwarder node that has a greater fitness function (HH) value transmits the packet before the transmission of the same packet from other nodes. For instance, if node A has the highest fitness function value, then it will transmit prior to node B. Upon the receiving duplicate packet from node A, it simply drops the packet. The following equation must be satisfied to avoid duplicate packets:

$$t_1 + T[HH_A] < t_2 + T[HH_B] - t_{12}. \quad (3.14)$$

Substituting Equation (3.11) in Equation (3.14) results in:

$$k \leq \frac{(t_2 - t_1) - t_{12}}{HH_A - HH_B}. \quad (3.15)$$

According to the triangle inequality theorem, the sizes of each vector in the triangle is lesser than the addition of the other two vectors length, thus  $(t_2 - t_1) - t_{12}$  is always less than 0, and, as  $HH_A > HH_B$ , thus  $k$  is always a negative number. The above two inequalities will be satisfied if:

$$|k| \geq \frac{(t_2 - t_1) - t_{12}}{HH_A - HH_B}. \quad (3.16)$$

For the worst case, the value of  $k$  will be :

$$k = \frac{\frac{2R}{V_0}}{HH_A - HH_B}, \quad (3.17)$$

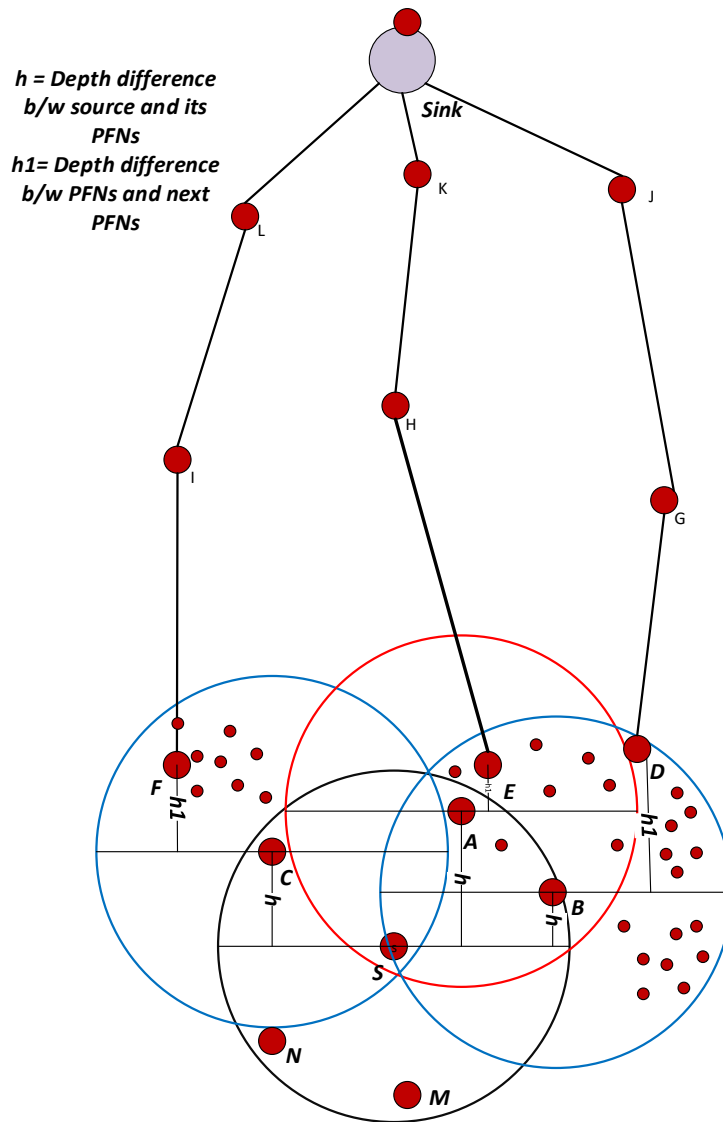


FIGURE 3.5: Holding time scenario

where  $V_0$  is the propagation speed of acoustic signal and  $R$  is the maximum transmission range. The value of  $k$  varies between 0 and  $R$ , as it depends on  $(HH_A - HH_B)$  and  $HH_A \in [0 R]$ .  $k$  cannot always satisfy the above inequality in Equation (3.14) as  $k \rightarrow -\infty$  when  $(HH_A - HH_B) \rightarrow 0$ . If replace the  $(HH_A - HH_B)$  by a global variable  $\delta$  such that  $(HH_A - HH_B) \geq \delta$ , then it guarantees that node A will forward the packet before node B. Hence,

$$k = \frac{-2R}{\delta}. \tag{3.18}$$

To find  $\beta$ , considering the node having the maximum Fitness Function (HH) value will have the holding time approximately zero; therefore, from Equation (3.11),

$$\frac{-2R}{\frac{V_0}{\delta}} + \beta = 0. \quad (3.19)$$

By solving the equation and putting the values in (3.11):

$$T(HH) = \frac{2R}{\frac{V_0}{\delta}}(R - HH). \quad (3.20)$$

The node having the highest fitness function (HH) value will be selected as a next forwarder. For instance, node A will calculate the holding time and start timer. When the timer is expired, then node A will forward the packet. If the other nodes in the range of A, i.e., B receives the duplicate packet during the holding time, it will drop both the packets because it means the original packet is already transmitted. The holding time is inversely proportional to  $\delta$ , if select larger  $\delta$ , then the holding time will decrease and therefore end-to-end delay will also reduce. Along with this improvement, there is also reduction in energy consumption that has been noticed and this is due to optimal forwarder selection at each hop.

### 3.4.6 Whale Pods Routing Protocol

The proposed work DOW-PR divides the whole transmission region into two levels of nodes distribution. One level in which the nodes are in closest proximity to the surface sinks and the other is the nodes that are in closest proximity to the sink deployed underwater. There are nine sinks that are placed at the sea surface, while one is placed inside the water. The anchored nodes are fixed at the bottom that can generate and transmit a packet towards PFZ. The relay nodes are transportable with the water current in horizontal direction. These nodes are capable of generating, forwarding and receiving a packet from other nodes. Whenever the node transmits or receives a packet, the first and foremost step followed by the forwarder is to calculate its distance with the sink set D. The node compares the

distance between itself and the rest of the sinks from the set  $D$  sequentially and finds PFNs lying in the hemisphere in the direction of the minimal distinct sink. The direction of data packet flow will be towards the sink lying at its closest proximity. If the separation between forwarding node and sink deployed on the sea surface is less than the sink deployed underwater, then the holding time computation will be carried out for the nodes present in the hemisphere in the direction of the surface sink  $D$ . On the other hand, if the source node is in closest proximity to the embedded sink  $D_{EM}$ , then the holding time computation will be carried out for the nodes present in the hemisphere in the direction of the embedded sink  $D_{EM}$ .

The above-mentioned phenomena can be further elaborated by a scenario shown in Figure 3.6. For example, in the network initialization phase, node N1 will first lookup for a sink in its closest proximity. For instance, after necessary computation in the initialization phase, it finds embedded sink  $D_{EM}$  is the nearest sink i.e.,  $d2 < d1$ . Node N1 will identify the PFNs in the hemisphere centered on the virtual vector connecting it with sink  $D_{EM}$ . The best forwarder node will be selected using the same holding time computation described earlier in the dolphin pod technique. Likewise, if node A in Figure 3.6 has  $d4 < d3$ , then it will find PFNs in the direction of the surface sink  $D$ . Algorithm 1 described the best forwarder selection technique i.e., valid for both dolphin pods routing and whale pods routing protocol.

### 3.5 Simulation Analysis

In this section, the detailed simulation analysis of the proposed dolphin pod scheme in contrast to WDFAD-DBR is presented in addition to the simulation results in the enhanced version (whale pods routing scheme) compared with dolphin pods routing protocol. DOW-PR has been developed in MATLAB (Version: R2015a,

**Algorithm 1:** Algorithm for selecting the forwarder among PFNs

---

```

1 for  $i \leftarrow 1$  to Nodes by 1 do
2    $broadcastID = S(i).id$ 
3    $PFNs = S(S(i).id).PFN$ 
4    $Flag = 1$ 
5   while Flag do
6     for  $j \leftarrow 1$  to SinkNodes by 1 do
7       find distance  $D_j^i$  with sink(j)
8       if  $D_j^i < t_{(range)}$  then
9         Packet successfully delivered
10         $Flag = 0$ 
11        Break
12    if  $PFNs == 0$  then
13       $broadcastID = broadcastID - TrEnergy$ 
14       $SUPs = S(S(i).id).SUPs$ 
15      if  $SUPs \neq 0$  then
16         $Chk\_FSUP = 0$ 
17        for  $k \leftarrow 1$  to  $SUPs$  by 1 do
18          Caculte Fitness Function ( $HH_k^i$ ) value for  $k_{th}$  suppressed node
19           $Chk\_FSUP = HH_k^i$ 
20          if  $Chk\_FSUP < HH_k^i$  then
21             $Chk\_FSUP = HH_k^i$ 
22             $broadcastID = S(S(i).ID)SUP(k)$ 
23             $Flag = 0$ 
24            Break
25        else
26          Drop the packet,  $Flag = 0$  , Break
27    if  $PFNs == 1$  then
28       $broadcastID = broadcastID - TrEnergy$ 
29       $broadcastID = PFN\_ID$ 
30    if  $PFNs > 1$  then
31      for  $j \leftarrow 1$  to SinkNodes by 1 do
32        find distance  $D_j^i$  with sink(j)
33        if  $D_j^i < t_{(range)}$  then
34          Packet successfully delivered,  $Flag = 0$  , Break
35       $SuitableHH = \infty$ 
36      for  $s \leftarrow 1$  to  $PFNs$  by 1 do
37        Caculte Fitness Function ( $HH_s^i$ ) value for  $s_{th}$  PFN node
38         $broadcastID = broadcastID - TrEnergy$ 
39        if  $HH_s^i < SuitableHH$  then
40           $SelectedID = S(S(S(i).ID).PFN(s)).ID$ 
41           $SuitableHH = HH_s^i$ 
42      if Check  $== 1$  then
43         $broadcastID = SelectedID$ 
44        Caculate Holding time according to SuitableHH

```

---

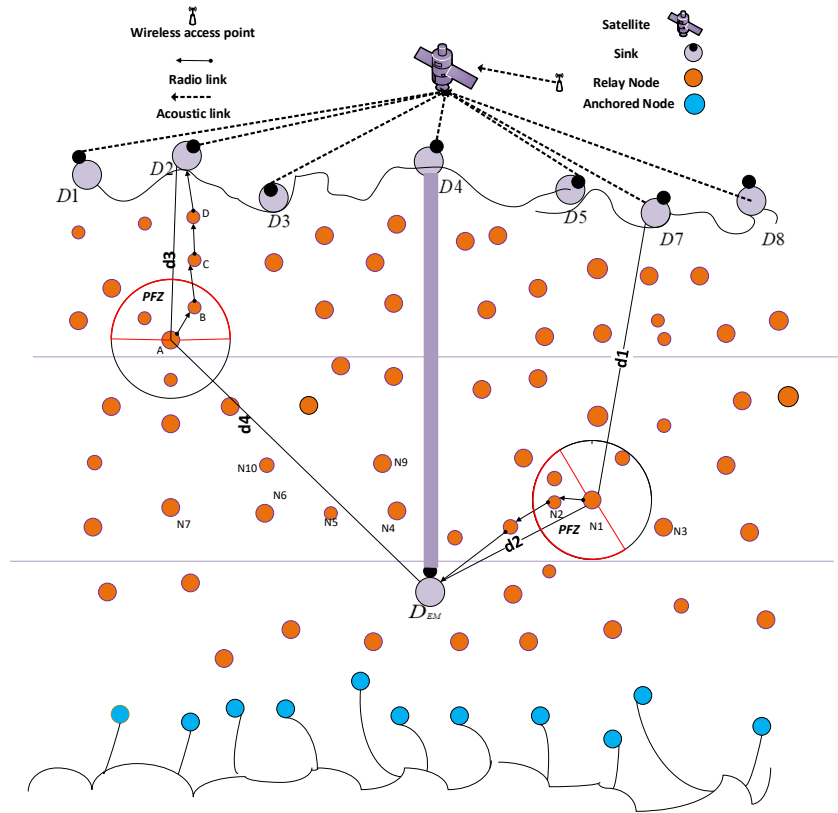


FIGURE 3.6: Network architecture for whale pods routing

Product of MathWorks, Inc.) and simulations are carried out to test the performance compared to WDFAD-DBR. The simulations have used all the underwater environment settings as in WDFAD-DBR.

### 3.5.1 Simulation Setup

In the simulation setup there are deployment of 100–500 network nodes in the three-dimensional volumetric space of  $10 \text{ Km} \times 10 \text{ Km} \times 10 \text{ Km}$  (length, width, height), as shown in Figure 3.7. The average volumetric region covered by the individual node varies from  $2 \text{ Km}^3$  to  $10 \text{ Km}^3$  for dense to sparse networks respectively and if uniform network distribution is considered too. There are nine sinks deployed and these are fixed on the water surface. The data packet consists of header of 11 bytes while the payload size is 72 bytes with a data rate of 16 kbps. The neighbor request and acknowledgment packets length is 50 bits each. Computed the expression in Equation (3.20) to find the optimal forwarder among the PFNs.

The parameters used in fitness function are potential forwarding nodes number  $PFN_{num}$  and the suppressed nodes number  $SUP_{num}$ .  $PFN_{num}$  and  $SUP_{num}$  may have larger values in the denominator of the fitness function HH and subsequently reduces holding time difference between the PFNs and therefore may cause duplicate copies of data packet generated. To cope with the larger values of  $PFN_{num}$  and  $SUP_{num}$ , mapped  $PFN_{num}$  and  $SUP_{num}$  into arbitrary values called division factors i.e.,  $DIV_{PFN}$  and  $DIV_{SUP}$ , respectively. The main concept of these prediction arbitrary values based on the rule of thumb. These mapped values (SET1, SET2 and SET3) have been shown in Tables 3.1 and 3.2. For instance, if considering the 1st entry in SET3 i.e., for  $1 < PFN_{num} < 10$  and  $1 < SUP_{num} < 10$ , the mapped values are  $DIV_{PFN} = 1$  and  $DIV_{SUP} = 2$ , respectively. The simulations have been carried out for all the three sets individually and investigated the appropriate set that achieves best performance of the network. After extensive simulations, it is found that SET3 gives best results. All the simulation parameters are listed in Table 3.3.



TABLE 3.1: Actual number of PFNs mapped into arbitrary values

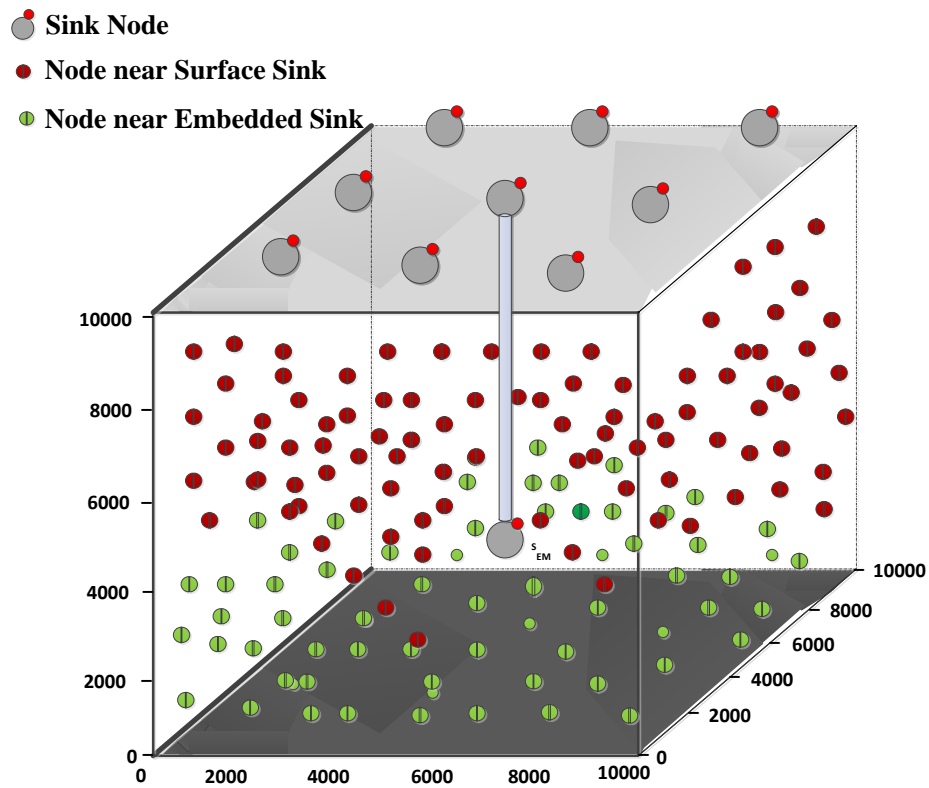
SET1		SET2		SET3	
Actual Range	Arbitrary Value	Actual Range	Arbitrary Value	Actual Range	Arbitrary Value
$1 \leq PFN_{num} \leq 100$	$DIV_{PFN} = 1$	$1 \leq PFN_{num} \leq 50$	$DIV_{PFN} = 1$	$1 \leq PFN_{num} \leq 10$	$DIV_{PFN} = 1$
$100 \leq PFN_{num} \leq 200$	$DIV_{PFN} = 2$	$50 \leq PFN_{num} \leq 100$	$DIV_{PFN} = 2$	$10 \leq PFN_{num} \leq 25$	$DIV_{PFN} = 3$
$200 \leq PFN_{num} \leq 300$	$DIV_{PFN} = 3$	$100 \leq PFN_{num} \leq 200$	$DIV_{PFN} = 4$	$25 \leq PFN_{num} \leq 50$	$DIV_{PFN} = 7$
$300 \leq PFN_{num} \leq 400$	$DIV_{PFN} = 4$	$200 \leq PFN_{num} \leq 450$	$DIV_{PFN} = 7$	$50 \leq PFN_{num} \leq 100$	$DIV_{PFN} = 15$
$400 \leq PFN_{num} \leq 500$	$DIV_{PFN} = 14$	$450 \leq PFN_{num} \leq 500$	$DIV_{PFN} = 11$	$100 \leq PFN_{num} \leq 200$	$DIV_{PFN} = 25$
-	-	-	-	$200 \leq PFN_{num} \leq 350$	$DIV_{PFN} = 39$
-	-	-	-	$350 \leq PFN_{num} \leq 500$	$DIV_{PFN} = 75$

TABLE 3.2: Actual number of SUPs mapped into Arbitrary Values

SET1		SET2		SET3	
Actual Range	Arbitrary Value	Actual Range	Arbitrary Value	Actual Range	Arbitrary Value
$1 \leq SUP_{num} \leq 100$	$DIV_{SUP} = 5$	$1 \leq SUP_{num} \leq 50$	$DIV_{SUP} = 2$	$1 \leq SUP_{num} \leq 10$	$DIV_{SUP} = 2$
$100 \leq SUP_{num} \leq 200$	$DIV_{SUP} = 8$	$50 \leq SUP_{num} \leq 100$	$DIV_{SUP} = 5$	$10 \leq SUP_{num} \leq 25$	$DIV_{SUP} = 5$
$200 \leq SUP_{num} \leq 300$	$DIV_{SUP} = 9$	$100 \leq SUP_{num} \leq 200$	$DIV_{SUP} = 11$	$25 \leq SUP_{num} \leq 50$	$DIV_{SUP} = 11$
$300 \leq SUP_{num} \leq 400$	$DIV_{SUP} = 11$	$200 \leq SUP_{num} \leq 350$	$DIV_{SUP} = 15$	$50 \leq SUP_{num} \leq 100$	$DIV_{SUP} = 22$
$400 \leq SUP_{num} \leq 500$	$DIV_{SUP} = 14$	$450 \leq SUP_{num} \leq 500$	$DIV_{SUP} = 21$	$100 \leq SUP_{num} \leq 200$	$DIV_{SUP} = 41$
-	-	-	-	$200 \leq SUP_{num} \leq 300$	$DIV_{SUP} = 65$
-	-	-	-	$300 \leq SUP_{num} \leq 350$	$DIV_{SUP} = 75$
-	-	-	-	$350 \leq SUP_{num} \leq 500$	$DIV_{SUP} = 87$

TABLE 3.3: Parameters' settings

<b>Parameters</b>	<b>Values</b>
Number of nodes	100:50:500
Number of sinks	9
Maximum transmission range of each node	2 km
Deployment region: 3D Region of 10 Km	Length: 10 km
-	Height: 10 km
-	Width: 10 km
Header size of DATA	11 Bytes
Payload size OF DATA	72 Bytes
Size of ACK Packet	50 bits
Size of Neighbor Request	50 bits
Data rate	16 Kbps
Initial Energy of each node	100 J
Maximum transmission power	90 dB re <i>micro</i> Pa
Power threshold for receiving	10 dB re <i>micro</i> Pa
Sending Energy	50 W
Receiving Energy	158 mW
Idle Energy	158 mW
Center Frequency	12 KHz
Acoustic Propagation	1500 m/s
$\delta$	2 Km
Bandwidth	4 KHz
Random Walk	2 m/s
Probability of moving left	0.5
Probability of moving right	0.5
Alive node threshold energy	5 W

FIGURE 3.7: Network deployment with embedded sink  $D_{EM}$ 

### 3.5.2 Hop Count Mechanism

Hop count mechanism gives a hops number to each node according to the sequence/serial numbers of depth levels between the node and the sink. The PFNs of the source node are those nodes that have a smaller depth than the source node and lies in the range of the source node. Similarly, the nodes that are in the range of the source node but have a larger depth than the source node are called suppressed nodes. All those nodes having a sink in its range have a hop number equal to (hp1) and the nodes having depth greater than maximum transmission range PN and lesser than twice of the maximum transmission range will lie at hop 2 (hp2). Similarly, the mechanism continued until the sea bed reached. For example, from Figure 3.8, node A has a sink node in its range S1, so the hop number of node A is set to (hp1) . The node B and C will lie at hop 2 (hp2) if and only if these are suppressed nodes of node A and sink S1 is not in range. The node D and E will lie at hop 3 if and only if these are suppressed nodes of C and having

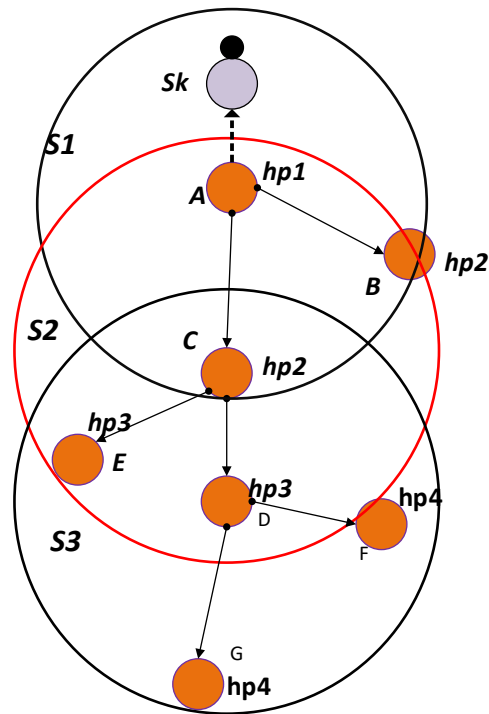


FIGURE 3.8: Hop count mechanism

a depth greater than twice the maximum transmission range and lesser than three of the transmission range.

### 3.5.3 Data Delivery Mechanism

Data delivery mechanism is used to forward the generated or received packets to its destination. Every node can generate a packet. If the closest proximity sink is present in predefined maximum transmission power range of the source node, then it relays the packet to the sink and it is therefore successfully delivered to the destination. All the sinks are communicated/connected via high speed radio links. If the sink is not in the range, then the Algorithm 1 selects the best node for forwarding according to the fitness function (HH). The fitness function is set in such a way that the forwarding node has a higher weighting sum of depth difference of the two hops, average PFNs number, least suppressed node numbers and having a lower hops count value.

Each node is assigned a unique HH value calculated through a fitness function in Equation (3.10). When the HH value is set differently for each node, then, according to that, value holding time from Equation (3.20) for each node is calculated. The holding time is set to a very low value pertaining to the node having the highest (HH) value among all the nodes. Thus, the node having the lowest holding time will bear highest priority and be selected for retransmitting the packet. All other nodes in its vicinity (range) will simply drop the packet by over hearing and therefore considerably reduce the energy consumption and the collision probability. Data delivery mechanism for Whale Pods is almost the same as Dolphin Pods, but only direction of data flow is different and it is based upon the minimum distance either from the surface sinks or embedded sink  $D_{EM}$ . For instance, any node live in the region closer to the embedded sink (Figure 3.6) as compared to the surface sink will find next forwarder in the direction of the embedded sink. Consequently, Potential Forwarding Nodes (PFNs) will also be selected that lie in the hemisphere in the direction of the embedded sink  $D_{EM}$ .

### 3.6 Performance Comparison and Analysis

We evaluate DOW-PR against WDFAD-DBR and DBR in term of APD, energy tax, end-to-end delay, packets dropped number and alive nodes number for different ranges of  $PFN_{num}$  and  $SUP_{num}$ . The proposed work defined the measurement sets (SET1, SET2, SET3) of three different ranges for  $PFN_{num}$  and  $SUP_{num}$  as shown in Tables 3.1 and 3.2, respectively. The simulation results for SET3 gives optimal results in comparison to the other two in terms of all metrics. Therefore, SET3 is found to be the best selection for simulation (refer to Figure 3.9).

*Performance Metrics:* The proposed system will define a new metric called Alive Nodes Number (ANN) besides the common performance metrics, i.e., APD, End-to-End Delay (E2ED), Energy Tax (ET) and PDR.

- *Alive Nodes Number (ANN):* A node having enough energy that it can receive, process and forward the packet is called alive node. To categorize the alive

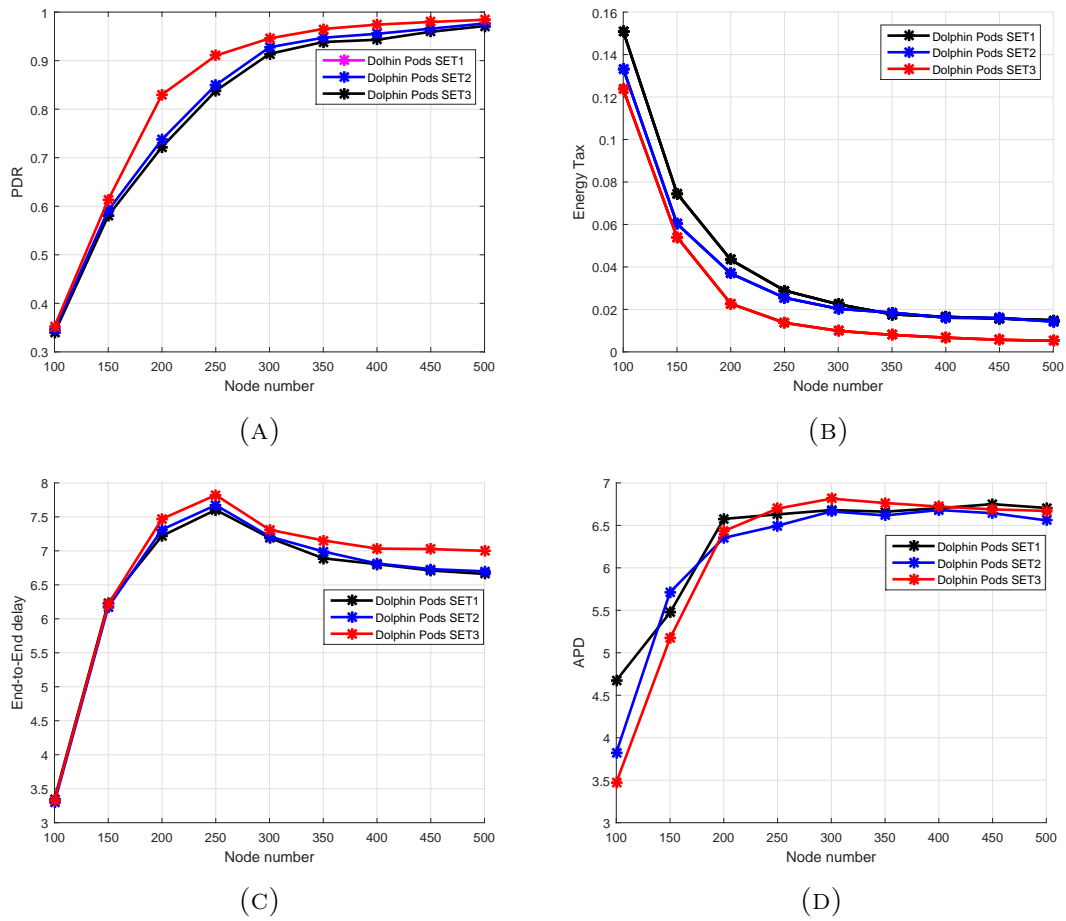


FIGURE 3.9: (a) PDR vs. number of nodes; (b) energy tax vs. number of nodes; (c) end-to-end delay vs. number of nodes; (d) APD vs. number of nodes. Comparison in Dolphin Pods using SET1, SET2, SET3.

nodes, the threshold  $E_{TH}$  is defined i.e., the minimum energy required for the node to receive  $E_{RCV}$ , process  $E_{PROC}$  and forward  $E_{FOR}$ . Threshold energy may be defined mathematically as:  $E_{TH} > E_{RCV} + E_{PROC} + E_{FOR}$

- *Packet Delivery Ratio (PDR):* PDR is the ratio of the packets received by the sink to the total packets generated by the network. The packets may be received multiple times, so this redundant packet is considered to be a one distinct packet:

$$PDR = \frac{\text{Packets received}}{\text{Packet Sent}}. \quad (3.21)$$

- *End-To-End Delay (E2ED):* The E2ED is defined as the average time taken for a packets transmission from the instant the source node started transmission

to the instant it is delivered to the destination. E2ED consists of transmission delay, propagation delay, processing time and holding time. Due to the multiple-sink nature of the network, a packet may be received by more than one sink, so the shortest time will be considered as end-to-end delay.

- *Energy Tax (ET)*: The energy tax is defined as the average energy expenditure per node when a packet is successfully delivered to its destination. It includes the energy for sending packet, receiving packet, computational energy, and the idle state energy shown in the equation below:

$$EnergyTax = \frac{E_{total}}{nodes \times packets}, \quad (3.22)$$

where  $E_{total}$  defined the total energy consumption,  $nodes$  define the total number of nodes in the network and  $packets$  define the total packets successfully received by the sink. The duplicate packet received by the sink is removed from the total number of packets because energy tax is the amount of energy per packet per node in the network.

- *Average Accumulated Propagation Distance (APD)*: APD is defined as the average accumulated distance of each hop of all the packets that are successfully delivered to the sinks. There is a multi-sink network environment in which more than one sink can receive a packet, so the shortest accumulated propagation distance is considered as a final accumulated propagation distance.

The APD can be found by the following mathematical equation:

$$APD = \frac{1}{n_p} \sum_{j=1}^{n_p} \sum_{i=1}^h dist_j^i, \quad (3.23)$$

where  $n_p$  is the number of packets,  $h$  is the hop number of packet from source node to sink and  $dist_j^i$  is the distance of the  $i$ th hop of the  $j$ th packet.



### 3.6.1 Simulation Results in the Dolphin Pods Routing Scenario

In this section, the simulations are performed upon the dolphin pod routing in which all the sinks are placed on the water surface without any sink embedded  $D_{SM}$  underwater. It can be seen from Figure 3.10 that the similar trend of increasing PDR for DBR, WDFAD-DBR and DOW-PR protocol when network density increases. The reason behind the common trend is the fact that, if density of the network increases, there will be more probability of occurrence of active node(s) at the next hop and therefore a reduction of void holes. DOW-PR outperformed in terms of PDR in comparison to WDFAD-DBR and DBR. In DBR, the node having the lowest depth among the potential forwarding nodes will be selected as a next forwarder and will not consider the depth of the expecting hop, which results in increasing the chance of a void hole. However, WDFAD-DBR selects the next expecting hop on the basis of weighting sum of depth difference of the two hops, which reduces the chance of a void hole happening. The PDR of DBR and WDFAD is almost the same from node numbers 270–500, i.e., in a dense network. The reason is the presence of enough PFNs in the range of a source node, which reduces the probability of void hole. PDR of a dolphin pod is higher than WDFAD-DBR, primarily because WDFAD-DBR selects the next expecting hop on the basis of weighting sum of depth difference between the two hops. Nonetheless, a dolphin pod considers all the factors including weighting sum of depth difference of the two hops, the number of PFNs, suppressed nodes number, and the hop count value to sink. The difference between the PDR of dolphin pod and WDFAD is higher for a sparse network and reduces due to the dense network. Secondly, WDFAD-DBR drops the packet in the absence of PFN, but dolphin pods select a node for forwarding from the suppressed nodes and therefore prevent the loss of the data. The PDR of dolphin pods is higher than WDFAD-DBR in both sparse and dense networks. However, in a sparse network, WDFAD-DBR more often drops the packet due to high probability of void holes and therefore a more proportional gain of PDR in dolphin pods resulted. On the other hand,

as node number increases and void hole probability decreases, the fraction gap in PDR results. Moreover, there are two types of void holes occurring in routing protocols. One is due to lack of a potential forwarder in the range of a source node and the other is due to the lack of energy in a potential forwarding node [97]. This means that there is a forwarding node of the source node but it doesn't have a sufficient threshold energy. The dolphin pod is trying to avoid both the void and energy holes. When the void holes occurred due to no PFN in the range of the source node, it selects a forwarding node from the suppressed nodes as shown in Figure 3.4. Subsequently, it reduces the re-transmissions and reduces the energy consumption due to redundant packets' avoidance. When the energy consumption is reduced, then the energy tax or an average energy expenditure per packet of each node is decreased as it is clear from Equation (3.22). Consequently, energy is conserved and therefore the occurrence of energy holes is also reduced. As a result, by overcoming both the void and energy hole, the PDR of the dolphin pods' routing scheme increases. The PDR statistics are shown in Table 3.4, in which it can be easily notice the PDR improvement by 11.89%, 6.085% and 3.365% in the scenario where node densities are 200, 300 and 400, respectively.

Moreover, dolphin pod routing assigns weight both to the packet advancement as well as to the network traffic density in such a way that priority is given to the less denser traffic path at the cost of packet advancement. The fitness function (HH) value will be less for the more dense path in which the probability of traffic density is high. Therefore, the dolphin pods scheme selects the path where the forwarder of the source node has a higher value of weighting sum of depth difference of the hops (H) [59], average number of forwarding nodes, very small number of suppressed nodes and is close to the sink, which means that the fitness function (HH) for that path is greater, which reduces the collision probability at the receiver. As a result, the PDR value is increased.

Next, this work investigates the energy tax comparison of a proposed dolphin pod with WDFAD-DBR protocol. When compared to idle listening, packet reception, sensing and processing of operations, in underwater acoustic networks, transmission of a packets is the most energy consuming operation. Transmission of data

packets accounts for most of the energy consumed due to their large size when compared to control packets. The above argument is already validated through experimental measurement by the authors in [99]. Energy cost for transmitting a single data bit is roughly equal to the energy consumption for processing thousands of operations [24]; however, complexity of the algorithm may increase energy cost. The proposed algorithm considers all of the above-mentioned energy usage parameters. However, only considering the receiving and transmitting energies will also not affect the general trend. DBR and WDFAD-DBR do not exploit certain energy efficient parameters, due to which the proposed scheme (DOW-PR) outperformed the two in terms of energy conservation. The simulation results are drawn for energy tax against the nodes number in the network (refer to Figure 3.9 for mapping into arbitrary values in SET3). The similar trend found for energy tax in all protocols DBR, WDFAD-DBR, and dolphin pod i.e., energy consumption reduces when the nodes number increases. This is due to the fact that increasing nodes in the network causes the increase of energy resource and also the probability of successful packet delivery being improved. Therefore, it reduces the retransmissions of the packets as nodes number increases and will significantly reduce the energy wastage.

Secondly, DOW-PR scheme exploited the adaptive nature of data transmission power, which depends upon the maximum displaced node within the transmission range (refer to Figure 3.3). Consequently, a significant amount of energy saving resulted, in contrast to WDFAD-DBR in which a fixed amount of energy was utilized at each hop regardless of the node displacement. In sparse networks, the transmission power adjustment is not very effective due to the nodes being widely dispersed, and there will be low probability of a nearby potential forwarder for lesser transmission energy usage. On the other hand, in dense networks, there will more likely be the presence of nodes in the maximum transmission range and therefore more options of ranges can be investigated. Generally, source nodes need to transmit with maximum power in case there is a forwarding node in its farthest transmission zone. Consequently, a greater number of nodes will receive the packet due to maximum transmission, but this is a rare occurrence. However,

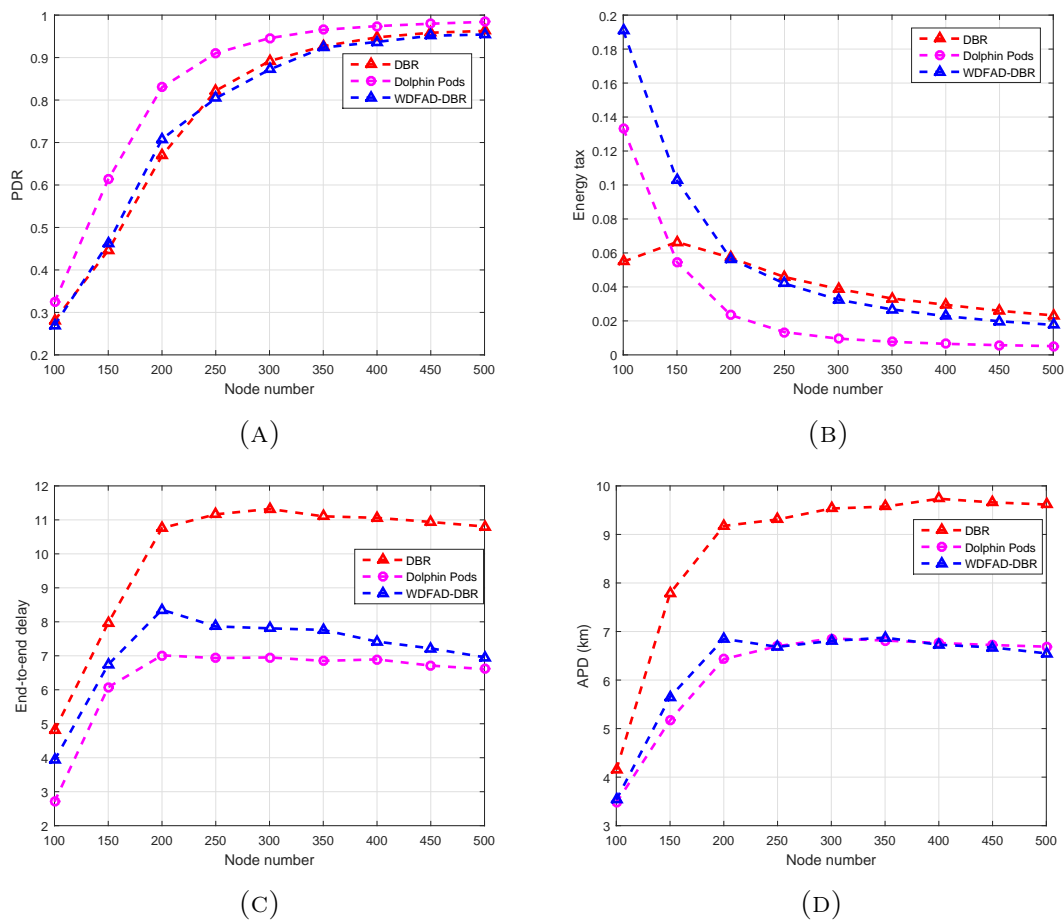


FIGURE 3.10: (a) PDR vs. number of nodes; (b) energy tax vs. number of nodes; (c) end-to-end delay vs. number of nodes; (d) APD vs. number of nodes. Simulation results using arbitrary values in SET3.

in WDFAD-DBR, the source node will transmit with a fixed maximum power level, no matter if the farthest forwarding node is even lying in a close proximity transmission zone. The above procedure adopted in the proposed scheme significantly reduces the energy consumption without compromising other performance parameters. Therefore, either being sparse or dense, the proposed protocol (DOW-PR) convincingly beat both DBR and WDFAD-DBR in terms of efficient energy utilization.

Moreover, the proposed scheme in this paper selects the next expecting hop by considering the weighting sum of the depth difference of the two hops, the PFN number, suppressed nodes number and the hop number of the expected next forwarding node, which reduces the total energy to a very low level. Energy tax is directly proportional to the total energy consumption, and inversely related to nodes

number and number of packets generated (refer to Equation (3.21)). WDFAD-DBR selects the next forwarding node by taking the accumulative advancement between the two hops, but it does not consider the receiving energy consumption due to available PFNs number and suppressed nodes number. Dolphin pod considers the energy efficient forwarder/path based upon the receiving energy consumption in potential forwarding nodes number and suppressed nodes number associated with the source node. Dolphin pod gives weight to both parameters by setting the division factors  $DIV_{PFN}$  and  $DIV_{SUP}$ . If the number of PFNs and SUPs nodes are less, then the division factors ( $DIV_{PFN}$  and  $DIV_{SUP}$ ) are set to very low values and, therefore, the receiving energy consumption in this case is negligible. Consequently, the forwarder selection criteria will then only be based on the weighting sum of depth difference of the hops (H) value as from Equation (3.10). For the case, if number of PFNs and number of suppressed nodes of a source is greater, dolphin pods set the division factors to a high value and will then be based on number of PFNs and suppressed nodes number means the receiving energy is consumed in larger amounts, so the forwarder/path, which has a low value of fitness function, will be selected.

It can also be easily judged through Figure 3.10b in which there is huge reduction in energy tax. However, the percentage improvement in energy tax reduces as nodes number increases. This is due to the fact that the collision probability increases at the receiver, and the number of retransmissions will consume quite a lot more energy. The analysis shows that there are 37.07%, 30.81%, 29.11% and 25% more energy conserved for 200, 300, 400 and 500 nodes, respectively (refer to Table 3.5).

Primarily, end-to-end delay increases for both dolphin pod routing and WDFAD-DBR protocol by increasing the nodes density i.e., from 100 to 250 nodes. For any further increase in node density, the end-to-end delay appears to be reduced, and this is due to number of reasons that included reducing hops count, increasing collision probability and better successful packets delivery at the destination. In a dense network scenario, there are enough nodes readily available at the edge of the transmission range for selecting the next hop forwarding node. Dolphin pod

considers the hop number of each node in fitness function, which reduces the APD as well as end-to-end delay. The analysis shows that there are 37.07%, 30.81%, 29.11% and 29.00% average improvement in end-to-end delay for 200, 300, 400 and 500 nodes, respectively (refer to Table 3.6).

Along with the above-mentioned improvements in the performance metrics, also investigate the other important metric, the average number of packets dropped in the network. Referring to Figure 3.11, it can be easily noticed that there is a significant reduction of packet drop in the proposed DOW-PR scheme as compared to WDFAD-DBR.

The reasoning behind this improvement is that, this mechanism ensures better life span of the individual local nodes and the network as well. The logical arguments are somehow similar to energy tax improvement described earlier.

WDFAD-DBR does not take into account the void hole occurrence probability; instead, it only considered the packet upward distance advancement at the two hops. On the other hand, the proposed DOW-PR scheme considered the potential forwarder nodes number at both one and two hops. Moreover, if the source node does not find the forwarder in the forwarding direction, then it could select a node from the suppressed region and therefore the scheme came up with utmost reduction of average packets dropped by a node in the network (refer to Figure 3.11c). The logic not only causes the reduction of the packets dropped number, but it also significantly improved the energy consumption. The result shown in the Figure 3.11a,b for alive nodes number against the number of simulation rounds. It has been noticed that, as number of rounds increases, the number of alive nodes reduces.

This study further elaborates the above-mentioned trend in Figure 3.11c that the number of packets drop reduces with the increase in network density. This is due to the fact that there are more numbers of alternative forwarders readily available in the dense networks compared to sparse networks. Consequently, the number of packets dropped reduces. The other strong reason is that, in a sparse network, the packets may not reach the distinct neighbors due to high bit error rate or degraded

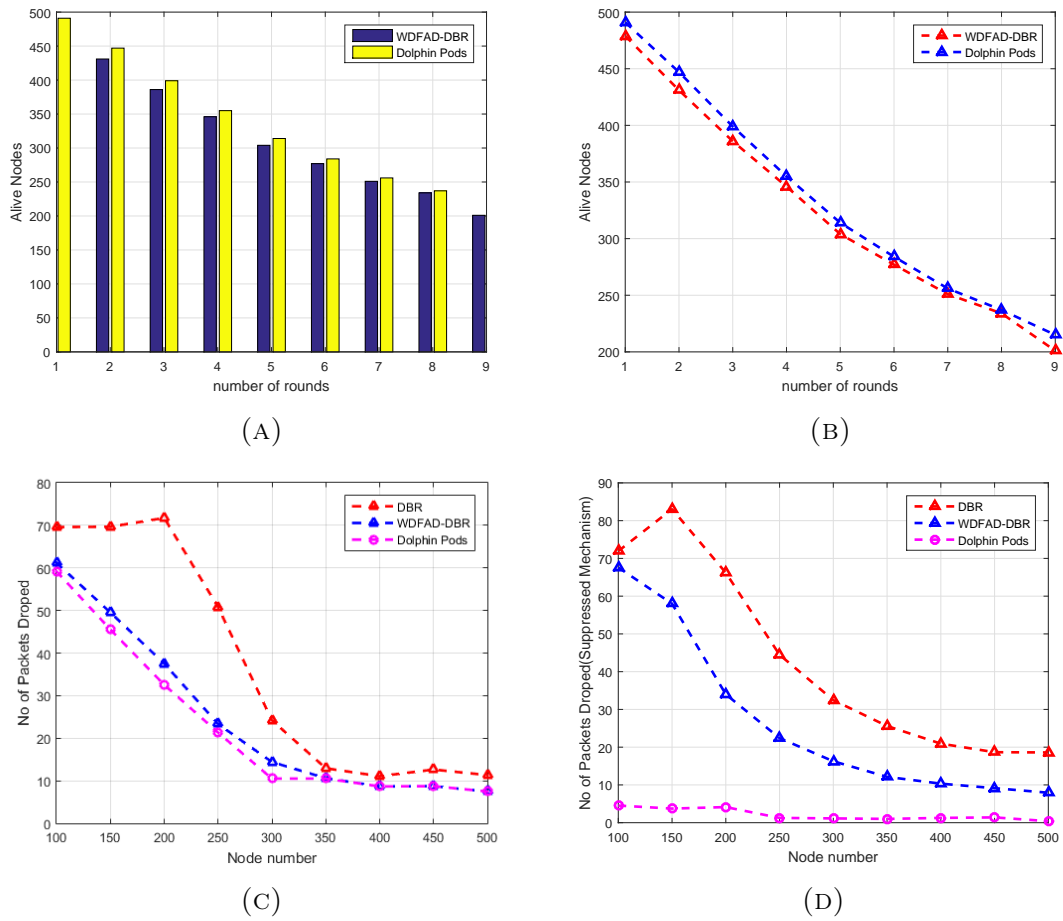


FIGURE 3.11: (a) number of alive nodes vs. rounds; (b) number of alive nodes vs. rounds; (c) number of packets dropped with suppressed vs. number of nodes; (d) number of packets dropped without suppressed vs. number of nodes.

Simulation results using arbitrary values in SET3.

link quality, and hence the packets dropped. Conversely, in dense networks, enough nodes are placed in close vicinity of the source node, which causes reduction of packets being dropped. However, the hops count value to reach the destination increased and may degrade end-to-end delay.

### 3.6.2 Simulation Results in the Whale Pods Routing Scenario

The simulations have been repeated for the whale pod routing version of the proposed DOW-PR protocol. It has been shown in the results that there is a great deal of improvement compared to its predecessor dolphin pod routing in all

the prescribed performance metrics. Referring to Figure 3.12b, it can be observed that the energy tax of the whale pod DOW-PR protocol is reduced throughout the density of the network (i.e., from 200 to 500 nodes). The reasons behind this is that the packet(s) generated/forwarded from the nodes in the vicinity of the embedded sink does not have to travel a long distance.

TABLE 3.4: Overall PDR improvement in dolphin pods routing compared to WDFAD-DBR

Node Number	200	300	400	500
Improvement with Tr = 1000 m	14.61%	7.12%	4.23%	3.56%
Tr = 2000 m	9.17%	5.05%	2.5%	1.5%
Average Improvement	11.89%	6.085%	3.365%	2.53%

TABLE 3.5: Overall Energy saved in dolphin pods routing compared to WDFAD-DBR

Node Number	200	300	400	500
Improvement with Tr = 1000 m	38.46%	30.12%	28.32%	28.49%
Tr = 2000 m	35.68%	31.50%	29.90%	29.51%
Average Improvement	37.07%	30.81%	29.11%	29.00%

TABLE 3.6: Overall End-to-End delay improvement of dolphin pods with WDFAD-DBR

Node Number	200	300	400	500
Improvement with Tr = 1000 m	24.76%	24.11%	22.50%	20.12%
Tr = 2000 m	31.17%	26.89%	24.62%	23.17%
Average Improvement	27.96%	25.5%	23.56%	21.64%

Instead, it is collected locally. This means that the few forwarders involved have a lesser amount of energy consumed. It can also be easily judged through Figure 3.12d in which there is huge reduction in average APD and therefore reduces the number of hops propagated. However, the percentage improvement in energy tax reduces as nodes number increases. This is due to the fact that the collision



probability increases at the receiver and number of retransmissions will consume quite a lot more energy.

Moreover, it is further analyzed that there are more number of copies generated or forwarded as the messages pass through more hops. Next, the deployment of an additional sink in the whale pod scenario causes a significant improvement in the PDR (refer to Figure 3.12a). It can be seen that presented updated scheme i.e., whale pod routing protocol beats the dolphin pod routing regardless of any number of nodes in the network. Behind this improvement, there are multiple reasons that include the high probability of finding the sink in the range of nodes, less number of hops count, less propagation distance and so on. The closest proximity nodes to the embedded sink either directly communicate with the sink or through a fewer number of hops and therefore the probability of packets drop reduces.

Last but not least is the important metric end-to-end delay that needs to be optimized especially when there is run-time data needed in the network. The end-to-end delay has been investigated for both DOW-PR scenarios. The simulation results show the obvious improvement in end-to-end delay and this is because of the same argument described repeatedly in the above text i.e., the locally available embedded sink reduces the propagation distance. For instance, if the node at the seabed generated a packet, then it has to propagate at least the full  $z$ -coordinate (i.e., 10 km) to be collected by the sink at the sea surface. On the other hand, in the whale pod scenario, the same packet will be received at the embedded sink and propagated through the distance of 2.5 km at the most.

Although the proposed protocol outperforms the aforementioned performance metrics, it has been observed some limitations and constraints in certain specific scenarios as discussed below:

In sparse networks, there are probably fewer PFNs present at each node in the network due to which overall improvement seems to be negligible; however, the computational cost still becomes greater. The abovementioned constraint in DOW-PR will become even more pressing when transmission range is also low. WDFAD-DBR focuses on the packet advancement at the first and second hop. It works

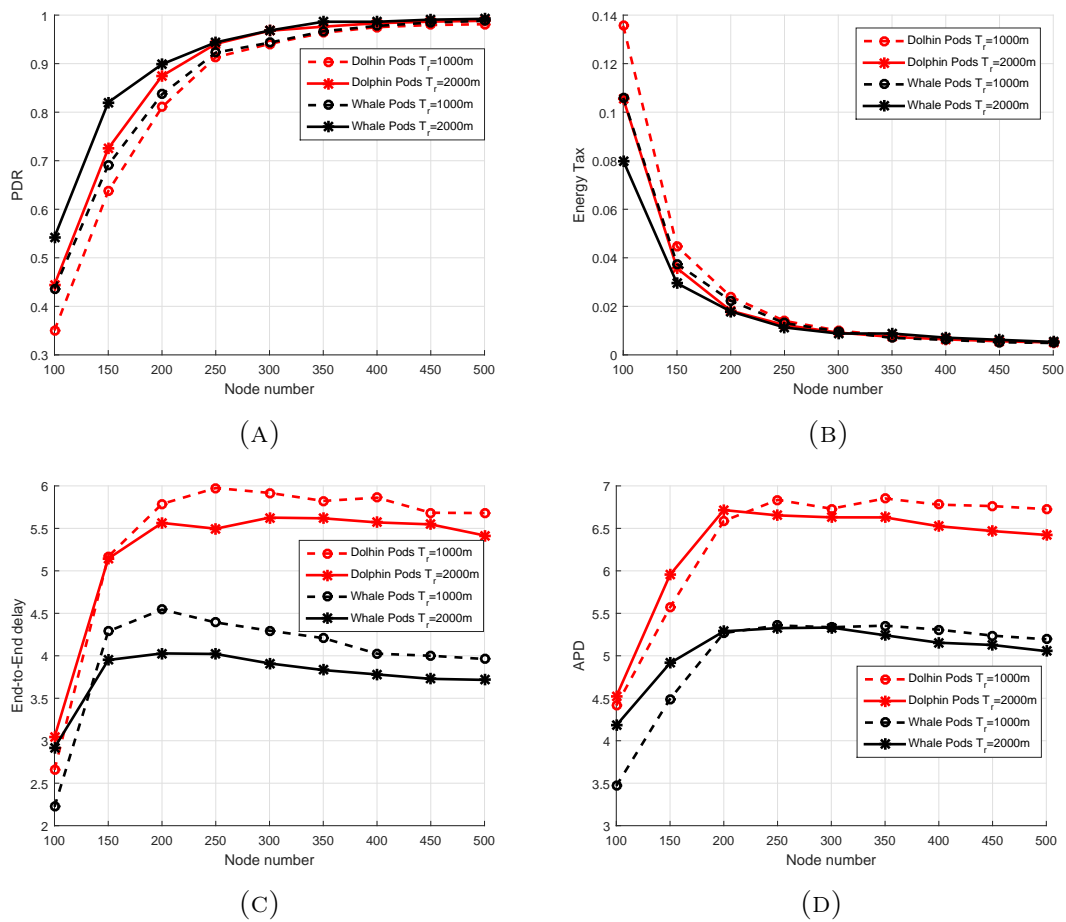


FIGURE 3.12: (a) PDR vs. number of nodes; (b) energy tax vs. number of nodes; (c) end-to-end delay vs. number of nodes; (d) APD vs. number of nodes. Comparison of dolphin pods with whale pods/routing.

well compared to DOW-PR in delay intolerant ad hoc underwater networks, where prolonged network lifetime is not required. DOW-PR has other limitations in the scenario where the source node is in a void and its predecessors also donot have PFNs other than the source node. In this case, the node will drop the packet or have progressive backward transmissions. In sparse networks with low average data packet generation, a low number of duplicate packets occurs due to which energy losses reduce in both DOW-PR and WDFAD-DBR, but DOW-PR will carry out more complex computational algorithms. In sparse networks, the probability of the void hole occurrence is high due to which DOW-PR will produce a huge number of void announcement messages, which will be disseminated in the entire network. It has been observed that, contrary to WDFAD-DBR, DOW-PR undergoes additional energy loss in transmitting void announcement control packets

and thereby collision probability is also increased. In the future, the authors plan to undertake research that will overcome the above-mentioned constraints.

Features	Achievements	Price to pay
Forwarder selection from SUPs	PDR improvement Figure 3.10a	End-to-end delay Figure 3.10c
Prioritizing forwarder through Holding time	Energy consumption reduction Figure 3.10b	Upward packet advancement
	Duplicate packets reduction Collision avoidance	
Embedded Sink	Prolong network lifetime Figure 3.11c, end-to-end delay reduction Figure 3.12c, Reliability Figure 3.12a	Deployment and physical connection maintenance cost
Transmission zones	Energy tax reduction Figure 3.10b	Computationally complex
Hop Count Mechanism	APD Improvement Figure 3.10d	Computationally complex
	end-to-end delay Figure 3.10c	

TABLE 3.7: Performance trade-offs

### 3.7 Conclusions

A dolphin and whale pods routing protocol (DOW-PR) has been proposed in this chapter. There are two versions of the proposed protocols i.e., dolphin pods and the whale pods. Whale pods routing protocol is the further enhancement of the dolphin pods routing. Basically, the proposed scheme enhanced the performance of the metrics simulated in its state-of-the-art counterpart routing protocol i.e., Weighting Depth Forwarding Area Division Depth Based Routing (WDFAD-DBR) protocol. DOW-PR provides a reduction in energy consumption, increasing PDR, and minimizing end-to-end delay. In the proposed scheme, it explores the role of the parameters like potential forwarding nodes number, suppressed nodes numbers and hops count value in designing the holding time equation. Moreover, the values of the above-mentioned parameters have been mapped (SET1, SET2 and SET3) into arbitrary values and that are also tested for simulations. The investigations through simulations showed that dolphin pods routing beats the WDFAD-DBR, on average improving by 31.5% of energy tax, 6% of PDR, and 24.6% of E2ED. Furthermore, the whale pods routing protocol outperformed the dolphin pod version and therefore improvement is seen in energy tax, PDR and E2ED. However,

certain performance trade-offs have been observed and listed in Table 3.7. The implementation of holding time mechanism is computationally complex due to the fact that it included the extra parameters like number of PFNs, number of suppressed nodes and HOP count. Moreover, computational complexity has also been seen in adjusting the transmission power levels adaptively at the run time.

DOW-PR was designed to select forwarder from the upper hemisphere of transmission range in the direction of a nearest sink node. The advantage of spatial division was ignored in forwarder selection. It could be more beneficial if the larger forwarding zone be spatially divided in small logical units in order to mitigate the effects of duplication and excessive energy consumption. Moreover, the performance of DOW-PR could be improved if it included time variant parameters of the harsh acoustic channel. Packet collision rate and probability of successful packet transmission are necessary ingredients that contribute towards reliability of the network. Therefore, the next chapter exploits the above mentioned parameters. Geo-spatial division is the main focus of the next chapter, in which geo-opportunistic paradigm implemented and tested . The research work proposed in DOW-PR has been extended through the above mentioned parameters in Geo-spatial Division Geo-Opportunistic Routing with Interference Avoidance (GDGOR-IA). The communication range is spatially divided in logical cube and incorporated in GDGOR-IA.

## Chapter 4

# Mobile Sinks assisted Geographic and Opportunistic Routing based Interference Avoidance for UWSN

### 4.1 Summary of the Chapter

The distinctive features of acoustic communication channel-like high propagation delay, multi-path fading, quick attenuation of acoustic signal, etc. limit the utilization of UWSNs. The immutable selection of forwarder node leads to dramatic death of node resulting in imbalanced energy depletion and void hole creation. To reduce the probability of void occurrence and imbalance energy dissipation, this chapter, propose mobility assisted geo-opportunistic routing paradigm based on interference avoidance for UWSNs. The network volume is divided into logical small cubes to reduce the interference and to make more informed routing decisions for efficient energy consumption. Additionally, an optimal number of forwarder nodes is elected from each cube based on its proximity with respect to the destination to avoid void occurrence. The selection of number of nodes is based upon the error probability and collision rate probability. The effect of this selection with minimum number of neighbors helps in reduction of interference because

minimum number of neighbors access the wireless channel. However, the threshold is set to maintained the reliability of the network. Moreover, the data packets are recovered from void regions with the help of mobile sinks which also reduce the data traffic on intermediate nodes. Extensive simulations are performed to verify that the proposed work maximizes the network lifetime and packet delivery ratio.

## 4.2 Introduction

A group of interconnected sensor nodes through acoustic channel form a UWSN. The collaborative behavior of sensing devices in the network enables: monitoring of remote locations, physical environment, temperature, humidity, battlefield, oceans, volcanoes and many more [24, 100], whereas sensors are the key component of UWSN, which are randomly deployed over the specified network volume, to monitor, sense, gather and transmit the information of interest. In UWSN, sensor nodes have limited battery, which is key consideration while designing a routing strategy. Also the sustainable deployment of sensor system is required to reduce the deployment and operational cost to prolong the network operational time [101].

In order to ensure successful communication among the nodes in acoustic network, the necessary factors are required to be considered in the design of a routing algorithm. For instance, the major factors associated with underwater channel need to be analyzed e.g., high delay of acoustic signal propagation because sound can propagate in acoustic environment with speed of 1500 m/s [102], high bit error rate because of noise and dynamic nature of acoustic medium, limited bandwidth, multi-path fading, etc. [21]. Therefore, an efficient routing strategy for acoustic channel is desired which balances energy dissipation to optimize the network lifespan [103]. For minimal energy consumption, geographic routing is widely accepted because of its scalable and simple implementation methodology [18, 103]. Moreover, the stateless nature of geographic routing allows it to communicate without establishing entire path from source to destination. This algorithm only computes

one eligible neighbor which acts as a potential forwarder to relay the data packet. Additionally, this routing mechanism is highly effective when node density is high because it follows greedy forwarding mechanism to transmit the data in multi-hop manner [21]. While in sparse deployment, due to the greedy approach, nodes select an optimal route in terms of distance which results in immutable selection of the same node resulting in sudden depletion of the node battery [104]. This death of the node creates energy hole which results in the breakage of the data route because of which downstream nodes cannot deliver their sensed information to the base station.

The aforementioned limitation is avoided through Opportunistic Routing (OR) paradigm, in which the selection of the forwarder set ensures successful data delivery towards the destination node even if one node from the set fails, still, the data is delivered [105]. However, the delivery of redundant packets at base station degrade the performance of OR. To avoid the transmission of duplicate packets, control message exchange or holding time mechanism is used in opportunistic routing strategy. In the former approach, node with minimum distance and shorter route from the destination compared to nominated neighbors of the sender, is elected to deliver the data by acknowledging with control message that data is delivered successfully. In the later one, holding time is computed for each neighbor node to assign the priority in order to communicate on the acoustic channel. In case of high priority node failure, node with second high priority in the set, transmits the data packet after its holding time expires. Still, in receiver based communication, duplicate packets from the hidden terminal regions are not suppressed. The hidden terminal is a region, where nodes lie in the transmission range of source node, but these nodes are unable to receive transmission or failure acknowledgement from the high priority node and ultimately transmit data packet towards the destination.

Due to duplicate transmissions from the hidden terminal volume, unnecessary energy dissipates resulting in short network lifespan. To mitigate the aforementioned constraint, a paradigm known as geo-opportunistic routing emerges, in which geographic routing is adopted for greedy forwarding by using geographic location of

the set of forwarder nodes [105, 106]. However, in multi-hop data delivery, nodes positioned nearby base station are overburden with traffic which dissipates the node energy very quickly. Due to the quick dissipation of node battery near the sink, nodes placed away from destination are unable to transmit data due to the unavailability of forwarders.

To reduce the data load at intermediate nodes and recover data from the void regions, mobile sinks are mounted over the ships, vehicle, etc. to gather the information of interest from the region of interest. The availability of mobile sinks enables new horizon of applications including but not limited to seabed survey, the detection of minerals from the oceans which are humanly not possible to monitor [107]. Hence, the mobility provided ease to directly retrieve the information from the communication void. With the incorporation of sink mobility, the network topology and delay in the network increases with the passage of time. To reduce the aforementioned constraints in geo-graphic, opportunistic, geo-opportunistic and mobility of sinks, this research have made the following contributions:

#### 4.2.1 Contributions:

Two routing algorithms have been proposed; geo-spatial division based opportunistic routing scheme for interference avoidance (GDGOR-IA) and geographic routing for maximum coverage with sink mobility (GRMC-SM). The distinctive features of proposed work are list as follows:

- The distribution of the network field into small cubes is performed to make local routing decisions for efficient energy consumption.
- The distributive geo-opportunistic routing in geo-spatial network field avoids the interference by restricting number of nodes.
- In order to minimize traffic load on intermediate nodes, mobile sinks gather data directly from underwater nodes and also use to recover data from void hole.



- An optimal holding time is formulated to ensure that successful transmission acknowledgement receives before the time expires of an individual node.

This chapter is organized as: Section 4.3 presents the pre-requisites of the network which are network model, energy model and control messages. Geo-opportunistic routing without sink mobility is discussed in Section 4.4 and Section 4.5 illustrates geo-opportunistic routing with sink mobility. In Section 4.6, a detailed linear programming based mathematical problem formulation subjected to attain optimal network lifetime and PDR. Section 4.7 presents a detailed discussion of simulation results regarding network lifetime, PDR and data traffic load. Finally, Section 4.8 concludes proposed work based on the analysis made in Section 4.7 with compared existing literature. The symbols and notations used in the manuscript are listed in table. 1.

## 4.3 Preliminaries

### 4.3.1 Network Architecture

All nodes are deployed randomly in three dimensional network field also shown through Figure 4.1. The volume of the network is divided logically into small cubes to perform distributive routing in each cube. The number of cubes are represented as  $C_n = \{c_1, c_2, c_3, \dots, c_n\}$  where each cube nodes are connected to its adjacent neighbor cube nodes through acoustic link. The sensor nodes operate in two modes: the first one is, sensing mode where node predicts the environmental effects and the second one is transmitting mode in which sensed data is delivered to the destination through acoustic data link. The network is homogeneous and consists of  $N_n = \{N_1, N_2, N_3, \dots, N_n\}$  nodes deployed inside the water along with set of sonobuoys  $S_s = \{s_1, s_2, s_3, \dots, s_n\}$  which are positioned at the water surface. Also, an assumption is made that each node is capable to transmit data successfully within its communication range. All the sensing devices are provided with limited memory, modem for acoustic communication, transceiver and battery. While sonobuoys have both acoustic and radio modems. The former is used to

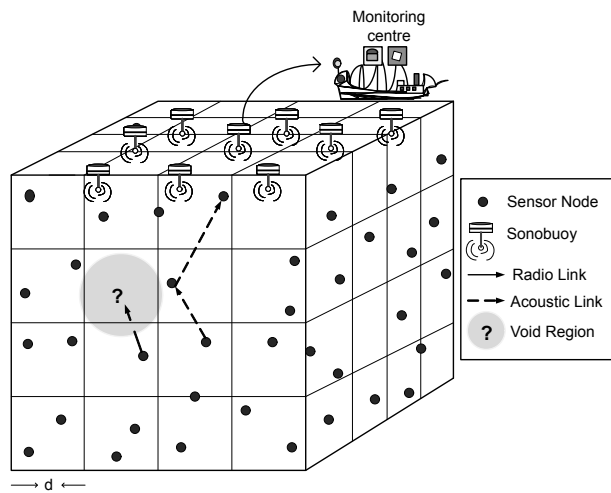


FIGURE 4.1: Network Architecture

retrieve information of interest from the underwater sensors, and latter to deliver data for further processing to the offshore data center. Further, an assumption is made that every node knows its location in advance. Whereas, the depth of void node also adjusted through the same mechanism as discussed in [108, 109]. The cost associated with depth adjustment is similar as provided in [110]. Simulations consider the unit disk graph model in which data packet always received successfully within the transmission range [111].

### 4.3.2 Beacon Message Types

Beacon message contains identifiers to establish connections among the network nodes. Each node uses beacon identifiers for performing transmission of data packet, sensing along with reception of data packet [18]. From the beacon identifiers, each node maintains a neighbor table which consists of cube number, unique ID and  $X$ ,  $Y$ ,  $Z$  coordinates. The ultimate objective to broadcast beacon messages among the network nodes is to acquire information of neighbor nodes and closest sonobuoy [103]. To acquire coordinates of each node in the acoustic environment, this research have used the same mechanism as discussed in [112]. The periodic broadcast of the beacon message increase the overhead resulting in low network performance. Therefore, the beacon message only transmit the changed identifier to keep neighbor table fresh and avoid the data packet loss. Due to

the transmission of updated identifier, unnecessary flooding of broadcast message is avoided and the purpose of neighbor information also fulfilled. Similarly, any sonobuoy belonging to the set  $\mathcal{S}_s$  has quintuple of information that includes ID of the sonobuoy,  $\mathbf{X}$ ,  $\mathbf{Y}$ ,  $\mathbf{Z}$  coordinates, sequence number of the beacon message and  $\Lambda$  as a flag to indicate that latest neighbor information is propagated among the neighbor nodes. With the help of neighbor information, every node transmits its sensed data to reach its nearest sonobuoy through its neighbor nodes.

### 4.3.3 Potential Neighbor Set Selection

After the dissemination of beacon message, every node has its neighbor table. However, still it is required to nominate potential forwarder node because every neighbor is not the potential forwarder for relaying data packets. The potential neighbor is defined as the node which has shorter route than the source node. In both proposed schemes, this research adopt the greedy approach to transmit data towards the destination node. Neighbor nodes which satisfies the criteria of greedy forwarding are computed using Equation (4.1). The ultimate goal of greedy forwarding is to advance the data packet through shortest and energy optimal path to reach the destination.

$$\mathbf{F}_{set}(\mathbf{k}) = \mathbf{n}_i \in \mathbf{N}_k(\mathbf{t}) : \exists \mathbf{S}_n \in \mathcal{S}_s(\mathbf{t}) | D(\mathbf{n}_k, \mathbf{s}_{n^*}) - D(\mathbf{n}_i, \mathbf{s}_n) > 0 \quad (4.1)$$

The potential neighbor set selection follows  $\mathbf{n}_k(\mathbf{t})$  steps to include  $\mathbf{N}_k(\mathbf{t})$  and  $\mathcal{S}_k(\mathbf{t})$  neighbors and sonobuoys at time  $\mathbf{t}$  in the neighbor table [65]. In Equation (4.1),  $\mathbf{F}_{set}(\mathbf{k})$  provides potential neighbor set of a source node  $\mathbf{k}$ .

### 4.3.4 Geospatial Division Model

As discussed earlier, in proposed schemes network filed is logically divided into  $\mathbf{C}_n$  cubes through geospatial division method. The following relationships between two cubes are:

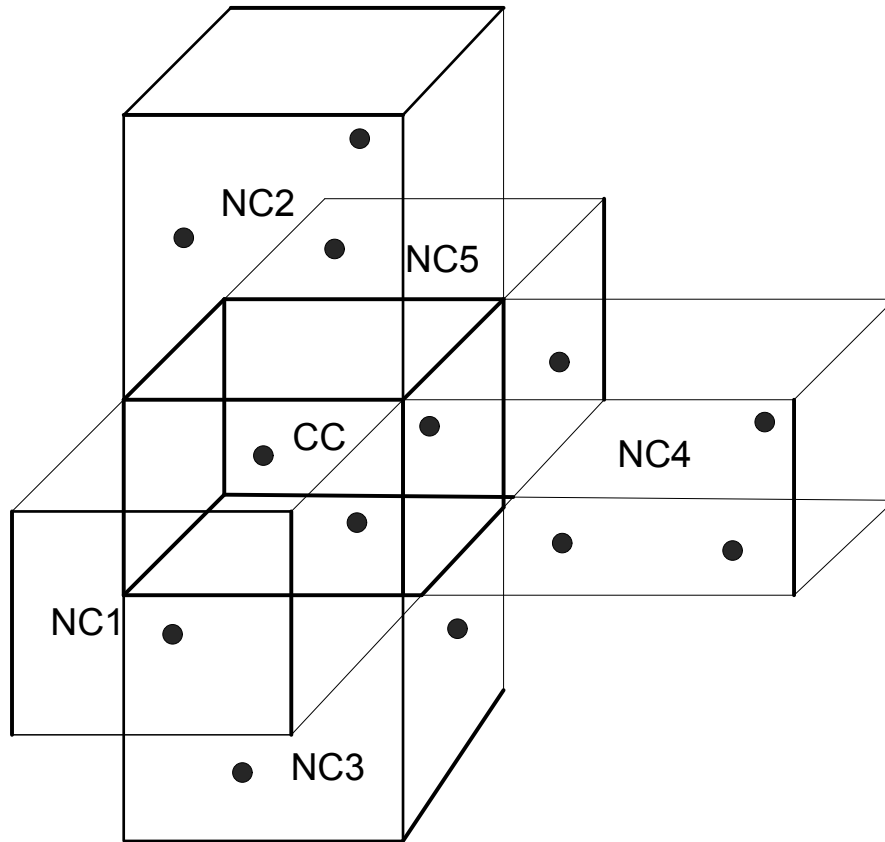


FIGURE 4.2: Cubical representation of target cube

- Two cubes are adjacent to each other at common vertex, that is vertex adjacent.
- Two cubes are neighbor with common one edge, that is edge adjacent.
- If two cubes have adjacent surface to one another, that is surface adjacent.
- Otherwise, cubes are completely disjoint.

The first three; cubes have adjacent vertex, edges and surfaces. Moreover, each cube has 8 adjacent neighbor vertex, 12 edges and 6 surfaces. Figure 4.2 denotes a current cube (CC) with its neighbor cubes (NCs), NC1, NC2 up to NC5. The selection of cubes is discussed in Section 4.4.

## 4.4 GDGOR-IA

This section, discusses the selection of the target cube in detail as follows:

#### 4.4.1 Target Cube Selection

GDGOR-IA works in two phases: in phase I, the Algorithm 2 runs for the selection of target cube. For that purpose, a source node is considered to be lying at the center of CC acquires its coordinates and source cube ID. A set of nodes in respective NCs of CC calculates Euclidean distance with respect to their nearby sink node. After the computation of Euclidean distance, every neighbor node from NCs calculates its physical distance to satisfy the greedy forwarding criteria to become the potential forwarder node to relay the data packet. The NC with smallest Euclidean distance is selected as Target Cube (TC) for the CC. All the cubes are priorities based on the computed distance, which are used as backup to transmit data incase of high priority neighbor cube failure. This is the where actually opportunistic routing really helps to find out an alternate route to proceed with the greedy data forwarding. It is to be noted that whenever Euclidian distance is measured with the sonobuoy, the distance is measured from the centre of the cube. In case, two NCs are meeting the selection criterion, choose any one of them randomly.

---

#### Algorithm 2: Target cube selection

---

```

1 begin
2   Node A acquires its coordinates ( $A_x, A_y, A_z$ ) and its CC'ID
3   Calculate  $D_{CC}$  of CC with the nearest sonobyouy
4   Calculate  $NCs = \{NC1, NC2, NC3, \dots NCi, ..\}$  of a SC
5   Calculate  $D_{NC}$  for the set of NCs with their respective sonobuoy
6   Select NC with lowest  $D_{NC}$  from the destination
7   Prioritize all NCs according to distance with their respective nearest
   sonobuoys
8   if  $D_{NC} < D_{CC}$  then
9     Check whether nodes exist in NC
10    Mark NC as target cube for forwarding phase
11    else
12      Select other NC with lowest  $D_{NC}$  from the sets
13
14    Endif
15 End procedure

```

---

#### 4.4.2 Next-Hop Forwarder Set Selection Criterion

In geographic routing single forwarder node is nominated to transmit data towards the destination. The primary disadvantage associated with the single forwarder selection is packet loss in case of bad link quality or void hole. Therefore, the proposed scheme has incorporated the geo-opportunistic routing paradigm to utilize the broadcast nature of wireless channel to nominate multiple forwarder node. This forwarding enables the selection of the potential forwarder set to ensure the reliable data delivery with minimal retransmissions in worst scenarios. However, it incurs more delay because all neighbor nodes wait till packet reaches the farthest node. To overcome this problem, the algorithm instead to select TC with less number of nodes but within a threshold set after considering link quality in Equation (4.2). This shows the error probability  $P_{BER}$  and collision rate probability  $P_{CR}$  where  $L$  is the size of packet [113]. The selection of TC with minimum number of neighbors helps in reduction of interference because minimum number of neighbors access the wireless channel. Moreover, the delay is reduced up to significant amount due to the participation of few nodes from the NC. Furthermore, within the TC, election of next-hop forwarder set is done through advancement towards the destination (ADV). The ADV is calculated for the set of nodes  $N_k = \{N_1, N_2, N_3, \dots\}$  in the TC. The nodes are prioritized on the basis of highest advancement towards the destination.

$$\alpha = \frac{1}{P_{CR}} \times (1 - P_{BER})^L \quad (4.2)$$

$$ADV(n_i) = D(n_k, s_n^*) - D(n_i, s_i^*) \quad (4.3)$$

$ADV(n_i)$  shows the advancement of  $n_i$ , and neighbor of the source node is represented with  $n_k$  towards its closest sonobuoy in Equation (4.3). For node  $n_i$  belonging to the potential neighbor set  $F_{set}(k)$  taken from Equation (4.1), normalized advancement towards the destination is calculated according to Equation (4.4) [21].

$$NADV(n_i) = ADV(n_i) \times P(d_k^i, L) \quad (4.4)$$

Algorithm 3 illustrates the selection of next hop forwarder in GDGOR-IA. Firstly, source node acquires the information about the neighbor nodes which is performed as discussed in Algorithm 2. Once neighbor information acquired, source node proceeds to the next step for the nomination of potential forwarder node to execute the network operations. Let's assume that source node  $\mathbf{n}_a$  deployed in downstream current cube which has neighbor cubes consists of numerous set of neighbor nodes  $\mathbf{PF}_{set}(\mathbf{n}_a)$  named as potential forwarders of  $\mathbf{n}_a$ . This set is a subset of  $\mathbf{F}_{set}(\mathbf{n}_a)$  in all nodes meet the selection conditions imposed through Equation (4.4). If  $\mathbf{PF}_{set}(\mathbf{n}_a)$  is an empty set, then take help from the information of Algorithm 2 providing the set of available NCs which can be used as target cubes. Each node differentiates itself from the other based on the cube ID. In case of multiple available target cubes, then obtain multiple forwarder sets  $\mathbf{F}_{set}(\mathbf{n}_a)$  for  $\mathbf{n}_a$ . In such conditions, the comparison of the accumulated NADV of all sets to select the cubes which has less node number for avoiding the interference and minimizing the delay.

---

**Algorithm 3:** Next-hop forwarder selection
 

---

```

1 begin
2   Procedure: select next-hop forwarder
3   for  $\mathbf{n}_b \in \mathbf{F}_{set}(\mathbf{n}_a)$  do
4     Select nodes residing in TC from  $\mathbf{F}_{set}(\mathbf{n}_a)$ 
5   Endfor
6   Put selected nodes in  $\mathbf{PF}_{set}(\mathbf{n}_a)$ 
7   if  $\mathbf{PF}_{set}(\mathbf{n}_a) \leq \mathbf{F}_{set}(\mathbf{n}_a)$  then
8     if  $\mathbf{PF}_{set}(\mathbf{n}_a) = \{\}$  then
9       Run phase I of the algorithm
10      Select cube placed at second priority in  $\mathbf{NCs}(\mathbf{n}_a)$ 
11     else
12       Calculate NADV for  $\mathbf{PF}_{set}(\mathbf{n}_a)$  according to Equation (4.4)
13       Order all the nodes in  $\mathbf{PF}_{set}(\mathbf{n}_a)$  according to their NADV
14       Select node with highest NADV as next hop forwarder
15       Calculate  $\mathbf{T}_{hold}$  according to Equation (4.5) for  $\mathbf{PF}_{set}(\mathbf{n}_a)$ 
16     Endif
17   Endif
18 End procedure

```

---

As the final step, the nodes in the set are ordered according to their NADV. Next

hop forwarder node is selected based on highest normalized advancement and rest of the nodes are prioritized accordingly. The next hop forwarder node holding time is calculated using Equation (4.5).

$$\mathbf{T}_h^i = \mathbf{T}_p + \sum_{j=1}^i \frac{D(\mathbf{n}_j, \mathbf{n}_{j+1})}{s} + i \times \mathbf{T}_{proc}. \quad (4.5)$$

$\mathbf{T}_p$  depicts the propagation delay incase of one hop away sender from the destination. The second part of the expressions contains the propagation delay of all the member nodes where  $s$  is the speed of sound in the acoustic medium. The third expression  $\mathbf{T}_{proc}$  depicts the processing time of each node  $i$  at each hop.

All nodes belonging to the same cube can overhear each others transmission that handles the hidden terminal problem effectively. All other nodes gather packets from neighbor nodes to acquire information about cube ID. This process caters problem of hidden terminal along with the interference among potential neighbor nodes residing in the same cube, thus the packet loss is reduced.

## 4.5 GRMC-SM

In system architecture there are deployment of mobile sinks  $\mathbf{MS}_n = \mathbf{ms}_1, \mathbf{ms}_2, \dots, \mathbf{ms}_n$  to retrieve information directly from nodes. Figure 4.1 illustrates multi-sink architecture which is also discussed in Section 4.3.1,  $\mathbf{S}_n$  sinks are replaced with mobile sinks  $\mathbf{MS}_n$ . The updated network model is depicted is Figure 4.3. As illustrated in Figure 4.3, all sinks are deployed uniformly within the network region, where nodes communicate with the nodes of neighbor cube in their transmission range to handover the data packet to the closest  $\mathbf{MS}_n$ . In case of coverage hole, sinks change their coordinates in order to gather data packet from the node directly. The sink movement is governed with the intent to minimize the total travelled distance which directly minimize the delay. Though, there is a particular cost associated with the mechanical movement of sinks but mobile sinks come to the



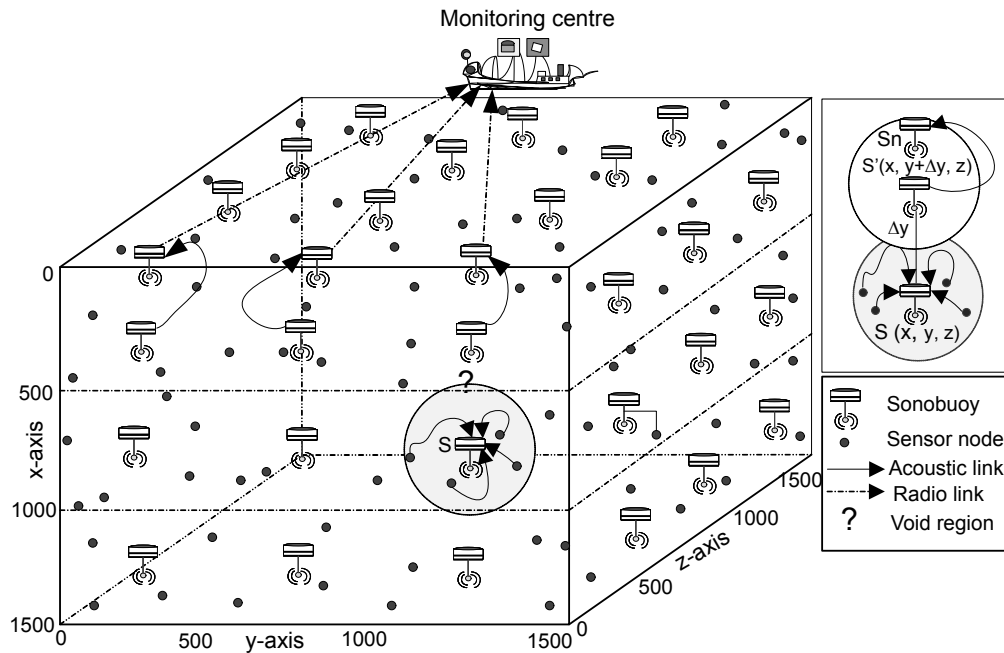


FIGURE 4.3: Schematic diagram of GRMC-SM

water surface to deliver data and also get recharged, thus, sinks have no constraint of energy to perform network operations.

#### 4.5.1 Data Forwarding and Routing in GRMC-SM

In GRMC-SM, all nodes forward their packets to one-hop neighbors or in-range sinks placed at shorter the distance from the surface than the node itself. The deployment of mobile sinks is uniform in the field to cover maximum volume of the network. If, a node is unable to find sink(s) in its transmission range then nodes relay data packet via multi-hop mechanism towards the destination by following the greedy approach. Algorithm 4 presents the data forwarding (DFM) and routing mechanisms in GRMC-SM.

In case, a node is trapped in a coverage hole and does not find a potential neighbor node or nearby sink. This node broadcasts a void-node-declaration message to its neighbors in the CC and to the NCs to avoid the data loss and transmission trap. This declaration saves node battery and allows the network nodes to operate for maximal time period. This information is further spread to the nearby mobile sink, which aid the void node to deliver its sensed and received information to the base

station for further processing. Once  $MS_n$  receives the void-declaration message, the movement of the closest mobile sink is triggered to change its course to provide to the void node at top priority. When mobile sink  $S'(x, \Delta y, z)$  disseminates the changed co-ordinates in its transmission range, the void node forwards its data to  $S'$ . From there onward, mobile sink relays composite data to the sinks placed at the surface. As a last step, a set of surface sinks transmits data via radio link to monitoring centre on the surface.

#### 4.5.2 Recovery Mode via Sink Mobility

Several methods of void hole recovery have been proposed e.g., physically replacing the dead nodes or recharging the sensor node battery; mechanical movement of the sensor nodes to adjust the depth [21] and usage of relay nodes to perform particular function of relaying data in case of void occurrence.

System architecture incorporated the sink mobility in GDGOR-IA scheme to analyze the effect of controlled sink mobility when void hole occurs. During the operation of forwarding, when a node traps in the void region and finds no alternate route to proceed the network communication even after examining its neighbor information. To resume the greedy forwarding, void node recovery mechanism operates. To inform the low depth neighbors, void-node-declaration packet is disseminated to inform the mobile sink. If neighbor node receives this declaration message and is not a void node itself, it replies the void-node-declaration-reply message with its location and neighbor information. This step is basically a message-based recovery for sender void node.

In other case, if the downstream node is also in the void node, then scenario leads towards local maxima trap with couple of void nodes in it. Thus, all data packets will be dropped because potential forwarders are not available to relay the transmitted data packet. To overcome earlier said scenario, uniform mobile sink deployment is performed in GDGOR-IA scheme and evaluated the performance of the proposed GDGOR-SM. Deployment of sinks in three dimensional network

**Algorithm 4:** Data forwarding mechanism (DFM)

---

```

1 begin
2   Procedure Directional forwarding(Node, Data)
3     Initially,  $F_s = \phi$ 
4     For Node ' $a$ ',
5     for  $Neighbors(a)$  do
6       Greedy forwarding
7       if  $s \in Neighbors(a)$  then
8         if  $D_a^{rs} < D_s^{rs} || D_s^a \leq R_c$ 
9           Send packet
10          EndIf
11       if  $n \in Neighbors(a)$  then
12         if  $D_n^{rs} < D_a^{rs}$  then
13            $F_s \leftarrow F_s \cup n$ 
14           Compute ADV using Equation (3)
15           Arrange nodes based on ADV
16           Select first priority node from  $F_s$ 
17         Endif
18       Endif
19     Endif
20   Endfor
21   Forwarding between sinks
22   Sinks forward data based on advancement
23   Either directly or using intermediate sinks
24   if  $Neighbors(s) = \phi$  then
25      $s(x, y, z) \leftarrow s'(x, y + \nabla y, z)$ 
26     if  $Neighbors(s')$  exist then
27       for  $s_i \in Neighbors(s')$  do
28         Calculate  $D_{s_i}^{rs}$ 
29         if  $D_{s_i}^{rs} < D_{s'}^{rs}$  then
30           Choose  $D_{min}^{rs}$  as a forwarder,
31           Forward data
32         Endif
33       Endfor
34     Endif
35   Endif
36 End procedure

```

---

field is intended to reduce and recover data from the void regions. In mountain like trapped region, nodes look for nearby sink using two hop information. When a sink receives void-node-declaration message disseminated by node having coordinates  $(\mathbf{X}, \mathbf{Y}, \mathbf{Z})$ , it calculates its new depth based on location information of the void node. In worst scenarios, depth adjustment of sink node is not progressive towards the destination. However, data discarded due to communication void is forwarded to the sink.

## 4.6 Mathematical Formulation Using Linear Programming

Linear programming is a common mathematical strategy which gives an optimal outcome for a linear problem. Here, discussed how linear programming helps in optimizing throughput and balancing energy consumption.

### 4.6.1 Energy Consumption Minimization

The imbalanced energy depletion among the network nodes degrade the network performance. In this regard, various routing algorithms are proposed to address this problem. Thus, energy minimization is performed based on objective function by following linear constraints. In both proposed schemes, energy consumption caused during transmission and reception of data packet. The formulation of the objective function to optimize energy consumption is proposed in (Equation (4.6)).

$$\text{Minimize } \sum_{i=1}^N E_{consumed}(i) \quad \forall i \in N \quad (4.6)$$

where  $E_{consumed}$  is the energy consumed per packet per node in the network.

Initially, the energy depletion is because of packets transmission and reception which is counted as shown in Equation (4.7).

$$\mathbf{E}_{consumed}(ij) = (\mathbf{E}_{TX} + \mathbf{E}_{RX}) \quad (4.7)$$

In Equation (4.7),  $\mathbf{E}_{consumed}$  between node  $i$  and node  $j$  is mainly due to the transmission of data  $\mathbf{E}_{TX}$  over the distance ( $\mathbf{D}_{(ij)}$ ). The receiving energy ( $\mathbf{E}_{RX}$ ) depends on number of bits received in the data packet from sender node according to Equation (4.8).

$$\mathbf{E}_{TX}^{max} = \mathbf{P}_{TX} \times (\mathbf{HS} + \mathbf{L})/\mathbf{DR} \quad (4.8)$$

$$\mathbf{E}_{RX}^{max} = \mathbf{P}_{RX} \times (\mathbf{HS} + \mathbf{L})/\mathbf{DR}, \quad (4.9)$$

Equations (4.8) and (4.9) show optimal values of  $\mathbf{E}_{TX}$  and  $\mathbf{E}_{RX}$  and depend on transmission  $\mathbf{P}_{TX}$  and receiving  $\mathbf{P}_{RX}$  powers, respectively. Whereas, packet size is (HS+L) and DR depicts data rate.

$$E_{total} = E_{initial} \times N \quad (4.10)$$

$E_{total}$  depicts the summation of network nodes energy as initial energy ( $E_{initial}$ ) given in Equation (4.10). The  $E_{consumed}$  in each round ( $r$ ) is stated in Equation (4.11) as,

$$E_{consumed} = \sum_{r=1}^{r_{max}} (E_{consumed}(r)). \quad (4.11)$$

For GDGOR-IA scheme, energy consumption due to depth adjustment of void nodes shown in Equation (4.12),

$$E'_{consumed} = \sum_{r=1}^{r_{max}} (E_{consumed}(r) + E_{DA}(r)), \quad (4.12)$$

where  $E_{DA}(r)$  depicts the amount of energy dissipated in depth adjustment during each round which is added till maximum round  $r_{max}$  reaches.

$$E_{DA} = N_{vn} \times (E_{DA}(n_{vn})). \quad (4.13)$$

$N_{vn}$  represents the number of void node.

Objective function in Equation (4.6) is defined under following linear constraints:

$$E_{(TX,RX)} \leq E_i^r \quad \forall i \in N \quad (4.14)$$

$$D_{(i,j)} \leq R_c \quad \forall i, j \in N \quad (4.15)$$

$D_{i,j}$  represents the distance between nodes  $i$  and  $j$  which must be less or equal to the  $R_c$  communication range.

$$E_{DA}(n_{vn}) \leq E_i^r \quad \forall i \in N \quad (4.16)$$

In GRMC-SM,  $E_{consumed}$  is mainly due to single or multi-hop communication in the network. Therefore,  $E_{consumed}$  associated with this scheme can be computed by Equation (4.11).

$$E_{(TX,RX)} \leq E_i^r \quad \forall i \in N \quad (4.17)$$

The summation of transmission and reception energies  $E_{(TX,RX)}$  should remain less for successful transmission. While,  $E_{(TX,RX)}$  restricts receiving energy through Equation (4.18).

$$E_{(TX,RX)} \leq E_i^r \quad \forall i \in N \quad (4.18)$$

To limit the communication of the transmitter node within the transmission vicinity  $R_{TX}^{max}$ , Equation (4.19) is used. Moreover, the distance should be greater than zero as given  $R_{TX}^{min}$  in Equation (4.20),

$$D_i^j \leq R_{TX}^{max} \quad \forall i, j \in N \quad (4.19)$$

$$D_i^j \geq R_{TX}^{min} \quad \forall i, j \in N. \quad (4.20)$$

$$E_{TX}^{min} = E_{TX}/L_s \quad (4.21)$$

$$E_{RX}^{min} = E_{RX}/L_s \quad (4.22)$$

**Graphical Analysis:** Let consider a scenario where 250 m be the transmission range and  $L_s$  levels i.e.,  $L_s = [1-5]$ . The intention to make transmission  $L_s$  is to note down the pattern of energy dissipation based on  $L_s$  expressed in Equations (4.21) and (4.22). Where  $(HS + L) = 888$  bits,  $DR = 50$  kbps,  $N = 450$ ,  $P_{TX} = 2$  W, and  $P_{RX} = 0.0158$  W. Based on earlier given parameters,  $E_{TX}$  is  $35mJ$  J computed via Equation (4.21) at  $L_s = 1$  and  $7mJ$  J via Equation (4.21) when  $L_s = 5$ . By Equation (4.22),  $E_{RX}$  is  $0.56$  mJ computed at  $L_s = 1$  and  $2.8$  mJ computed when  $L_s = 5$ .

$$7.56 \leq E_{TX} + E_{RX} \leq 37.8 \quad (4.23)$$

$$0.56 \leq E_{RX} \leq 2.8 \quad (4.24)$$

$$7 \leq E_{TX} \leq 35 \quad (4.25)$$

Figure 4.4 depicts the feasible region in which energy consumption always results in optimal network lifespan. Thus, points from given region yield minimal energy consumption with valid solution.

The solution is tested on the following vertex which are computed in Figure 4.4a.

$$\text{at } P_1 : 0.56 + 7 = 7.56 \text{ mJ}$$

$$\text{at } P_2 : 0.56 + 35 = 35.56 \text{ mJ}$$

$$\text{at } P_3 : 2.8 + 7 = 9.8 \text{ mJ}$$

$$\text{at } P_4 : 2.8 + 35 = 37.8 \text{ mJ.}$$

For GRMC-SM, following vertex are used which are depicted in Figure 4.4b.

$$\text{at } P_1 : 0.027 + 0.25 = 0.27 \text{ mJ}$$

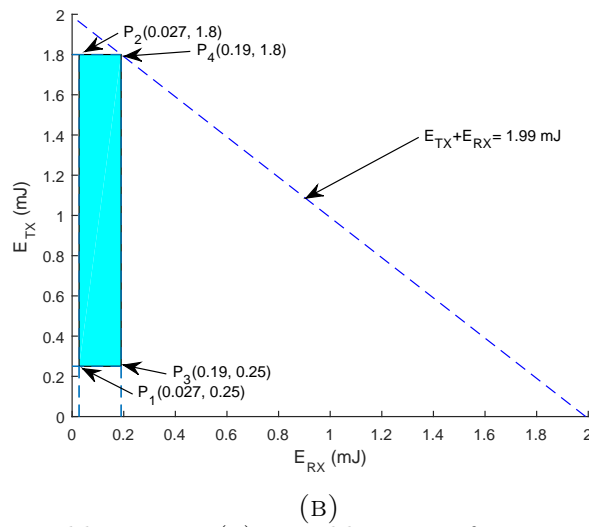
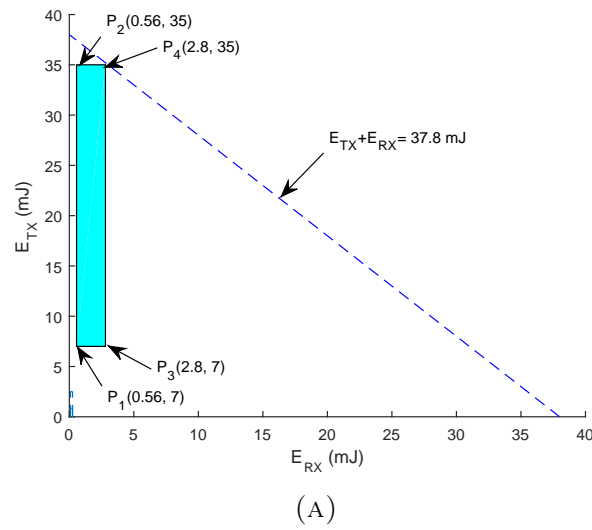


FIGURE 4.4: Feasible regions (a) Feasible region for energy tax minimization (GDGOR-IA); (b) Feasible region for energy tax minimization (GRSM-MC).

at  $P_2$  :  $0.027 + 1.8 = 1.827$  mJ

at  $P_3$  :  $0.19 + 0.25 = 0.44$  mJ

at  $P_4$  :  $0.19 + 1.8 = 1.99$  mJ.

Hence, the energy consumption within the bounded region is minimal resulting in optimal network lifespan, which is further verified through simulations in Section 4.7.



### 4.6.2 PDR Maximization

In order to enhance network throughput by consuming minimum energy, packets are transmitted through multiple hops. Throughput is number of packets successfully reached the sink. Link quality is taken into consideration by defining threshold value  $\delta$  for selecting optimal neighbor nodes at each hop. Additionally, it ensures successful packet delivery. Moreover, energy needed to transmit the packet must be fulfilled during forwarding according to C1. All aforesaid constraints are considered during the formulation of the objective function given in Equation (4.26).

$$NT(p) = \text{Maximize} \sum_{i=1}^N T_p(i); \quad \forall i \in N, \quad (4.26)$$

where  $NT_p(i)$  is network throughput,  $T_p(i)$  represents the number of successful packets reached to destination which are generated by node  $i$ . mathematically in can be expressed by Equation (4.27).

$$\text{Maximize} \sum_{r=1}^{r_{max}} NT_p(r); \quad \forall 1 \leq r \leq r_{max}, \quad (4.27)$$

such that:

$$\text{C1: } E_{TX,RX} \leq E_r$$

$$\text{C2: } P_{link} \geq \delta$$

$$\text{C3: } E_{TX,RX} \geq E_{th},$$

where  $E_{th}$  is the threshold for transmission and reception energies.

$$\text{C4: } 0 < D_{ij} \leq D_{ij}^{max}.$$

C1, C2, C3 and C4. C1 and C3 restrictions on  $E_{TX}$  and  $E_{RX}$  are set to avoid unnecessary energy consumption. In GRMC-SM, all nodes report their sensed data to the nearest sink. PDR of the network is accumulated packets successfully

received at all the sinks. Equation (4.27) shows the summation of all the data packets in  $r$  rounds. Feasible region for GDGOR-IA lies within these following vertex points as shown in Figure 4.5a.

at  $P_1(0.34, 150)$

at  $P_2(0.55, 200)$

at  $P_3(0.60, 250)$

at  $P_4(0.83, 550)$ .

Similarly, for GRMC-SM, feasible region lies within following vertex points illustrated in Figure 4.5b:

at  $P_1(0.45, 150)$

at  $P_2(0.6, 200)$

at  $P_3(0.65, 250)$

at  $P_4(0.89, 550)$ .

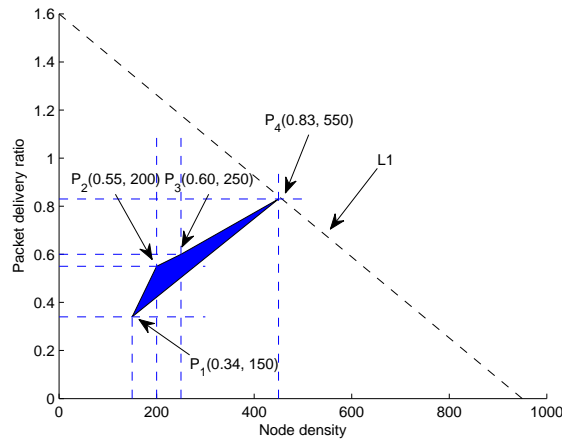
### 4.6.3 Minimization of Average Delay

During the operation of forwarding in the network, sender nodes transmit packets directly or via multi-hops. The proposed work defines average delay incurred due to direct and multi-hop transmission in  $r$  rounds for  $N$  number of nodes in the network as in Equation (4.28). In multi-hop transmission, node waits for  $T_w$  time as shown in Equation (4.29),

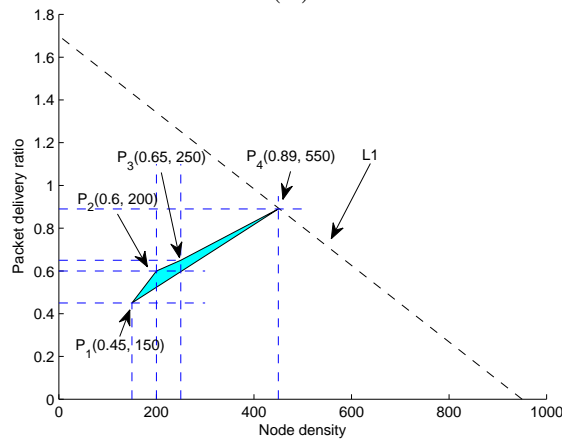
$$D_{ave} = \left( \sum_{i=1}^N D_{tot}(i) \right) / P_{succ} \quad \forall i \in N. \quad (4.28)$$

$$T_w = D_{Proc} + D_{Prop} + T_{hold}, \quad (4.29)$$

$$D_{Prop} = (R_c - D(ij)) / s, \quad (4.30)$$



(A)



(B)

FIGURE 4.5: Feasible regions. (a) Feasible region for throughput maximization (GDGOR-IA); (b) Feasible region for throughput maximization (GRMC-SM).

$$T_{hold} = \sum_{i=1}^j D(n_i, n_{i+1})/s. \quad (4.31)$$

Total delay incurred comprises of delay due to direct transmission and multi-hop transmission as in Equation (4.32),

$$D_{tot}(i) = D_{DT}(i) + D_{MHT}(i) \quad (4.32)$$

$D_{tot}(i)$  is the delay occur in transmitting  $P$  number of packets successfully towards destination by any node  $i$ . For direct transmission to in range sinks, time taken is accumulation of propagation time and processing time.

$$D_{DT-min} = T_w \times H_n; \quad (4.33)$$

where  $H_n = 1$  for direct transmission scenario when the sink is in transmission range of source node.

$$D_{MHT-min} = H_{n-min} \times T_w; \quad (4.34)$$

$$D_{MHT-max} = H_{n-max} \times T_w; \quad (4.35)$$

The objective function in Equation (4.28) is formulated under following constraints C1, C2, C3:

$$\text{at C1: } 0 < D_{max}^{ij} \leq R_c$$

$$\text{at C2: } 0 < T_w$$

$$\text{at C3: } H_{n-min} \leq H_{n-max}$$

**Graphical analysis:** Let's consider, if source node be in the transmission range of sink and it relays data directly. During this, delay caused is represented via  $D_{DT}$ . On the other hand, when sink cannot be accessed directly by the sender node, then packet is transmitted through multiple hops. By assuming that minimum delay is caused on one-hop transmission and maximum delay occurs when data is delivered through multiple hops. The computation of maximum and minimum delays caused in both direct transmission scenario and multi-hop scenario; as, shown in Fig. 7.

$$1.35 \leq D_{DT} + D_{MHT} \leq 3.45$$

$$0.45 \leq D_{DT} \leq 0.6$$

$$0.9 \leq D_{MHT} \leq 2.85$$

Each vertex of the region is shown as:

$$\text{at } P1 : 0.45 + 0.9 = 1.35 \text{ s}$$

$$\text{at } P2 : 0.45 + 2.85 = 3.30 \text{ s}$$

$$\text{at } P3 : 0.6 + 0.9 = 1.5 \text{ s}$$

at  $P4 : 0.6 + 0.285 = 0.885$  s

Each vertex of the region is shown as:

$$1.72 \leq D_{DT} + D_{MHT} \leq 3.71$$

$$0.50 \leq D_{DT} \leq 0.65$$

$$1.22 \leq D_{MHT} \leq 3.06$$

Each vertex of the region is shown as:

$$\text{at } P1 : 0.5 + 1.22 = 1.72 \text{ s}$$

$$\text{at } P2 : 0.5 + 3.06 = 3.56 \text{ s}$$

$$\text{at } P3 : 0.65 + 1.22 = 1.87 \text{ s}$$

$$\text{at } P4 : 0.65 + 3.06 = 3.71 \text{ s}$$

## 4.7 Simulation Results and Discussions

Simulation results of proposed work are presented against three existing state of the art schemes; GEDAR

[21], EnOR [104], RE-PBR [114] and AUV-CH [96]. The performance is evaluated based on PDR, fraction of local maximum nodes, energy consumption per packet per node, end-to-end delay and depth adjustment. Further the analysis of proposed methodologies is done by varying traffic load as well. The detailed discussion is presented as follows:

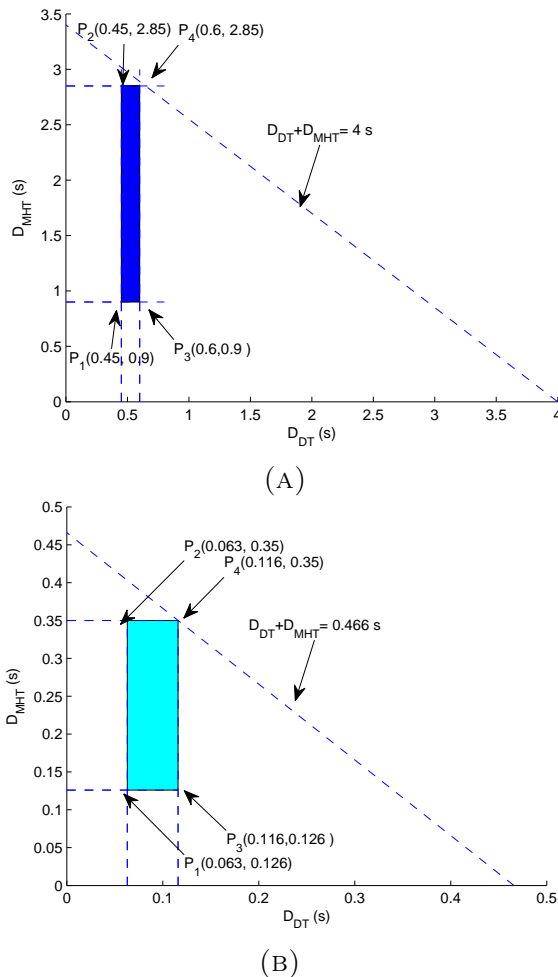


FIGURE 4.6: Feasible regions. (a) End to end delay: feasible region for GDGOR-IA; (b) End to end delay: feasible region for GRMC-SM.

### 4.7.1 Simulation Settings

To perform simulations, nodes are varied from 150–450 with 45 sonobuoys positioned at the water surface to gather data from underwater nodes. The network dimensions are  $1500 \text{ m} \times 1500 \text{ m} \times 1500 \text{ m}$ . Moreover, the transmission range is  $R_c = 250 \text{ m}$  and  $DR = 50 \text{ Kbps}$ . Also, it considers a payload of 150 bytes in each data packet including 20 bytes of beacon message. The energy dissipation associated with transmission, reception, idle state and depth adjustment is  $P_t = 2 \text{ W}$ ,  $P_r = 0.1 \text{ W}$ ,  $P_i = 10 \text{ mW}$  and  $E_m = 1500 \text{ mJ/m}$ , respectively, [21]. The average of 50 distinctive simulation runs is taken for getting near optimal results against each value plotted in the graphs.

## Performance Metrics

In this section, basic performance parameters are defined as:

- PDR: The ratio of packets successfully received at surface sonobuoys over number of packets transmitted from each network node during the network operational time. The mathematical expression is given as follows:

$$PDR = \frac{P_{sonobuoys}}{P_{total\_gen}}. \quad (4.36)$$

where,  $P_{sonobuoys}$  shows the quantity of packets delivered at the destination, while  $P_{total\_gen}$  depicts the summation of packets generated from each network node.

- Fraction of void nodes: It is the amount of network nodes fail to deliver the data packet over the acoustic communication channel because of unavailability of further forwarder nodes in thier transmission range.
- Energy consumption: It is defined as, the energy utilized in transmitting and receiving a data packet by a node within its transmission range. It is measured in joules (J).
- End-to-end delay: Time required for transmitting and propagating data from source to destination is called end-to-end delay and its unit is seconds (s).
- Depth adjustment: Net distance covered by a void node to find a forwarder node for resuming network operations is called depth adjustment and it is measured in meters (m).

### 4.7.2 Analysis of proposed Scheme Results against Existing State of the Art

The simulation results of proposed schemes; GDGOR-IA, GRMC-SM, and GDGOR-SM against existing methodologies GEDAR, AUV-CH, and EnOR are proposed in

this section. The discussion is divided into different subsections; fraction of void nodes, depth adjustment, PDR, energy consumption, and end-to-end delay.

#### 4.7.2.1 Fraction of Void Nodes

Figure 4.7 depicts the fraction of failure in proposed and baseline schemes. The behaviour of GDGOR-SM shows that when node density is varied from 100–150, the fraction of node failure is decreasing gradually, however, as the quantity of nodes increased to 200, then sudden down fall is observed in the results of Figure 4.7. Further, after deploying more number of nodes up to 200–500, the trend shows continuous decrease. This scheme has less failure because of mobile sonobuoys which dive into the water from the surface to retrieve data directly and return data to specified destination. Similarly, in GRMC-SM, the trends of decreasing node failure at various node densities are almost similar to GDGOR-SM, however, the failure rate is higher due to the consideration of multihop transmission when mobile sonobuoy is not in range of a node.

Whereas, AUV-CH and EnOR performance starts declining because in opportunistic routing multiple sensor nodes participate in communication, and the reliability of delivering data is although high but the chances of communication failure are also high in both schemes. On the other hand, EnOR is focusing on rotating the forwarder node and has no mechanism for void avoidance, therefore it has high fraction of void nodes. The GEDAR utilizes sonobuoys which are positioned at the surface of water, whereas, lack of sonobuoys mobility exposes GEDAR scheme to communication failure. Thus, it is evident that 30% nodes lie in the category of void nodes in sparse network in both GEDAR and GDGOR-IA. Thus, the fraction of node failure is high when less number of nodes are deployed in the network and after increasing the number of nodes, it tends to reduce significantly in all the schemes. Fraction of void nodes is reduced in GEDAR and GDGOR-IA by opting depth adjustment mechanism. Whereas, the fraction of void occurrence is more in RE-PBR when the network is sparse because, it is hard to find forwarder node with high link quality along with the highest remaining battery and lower depth



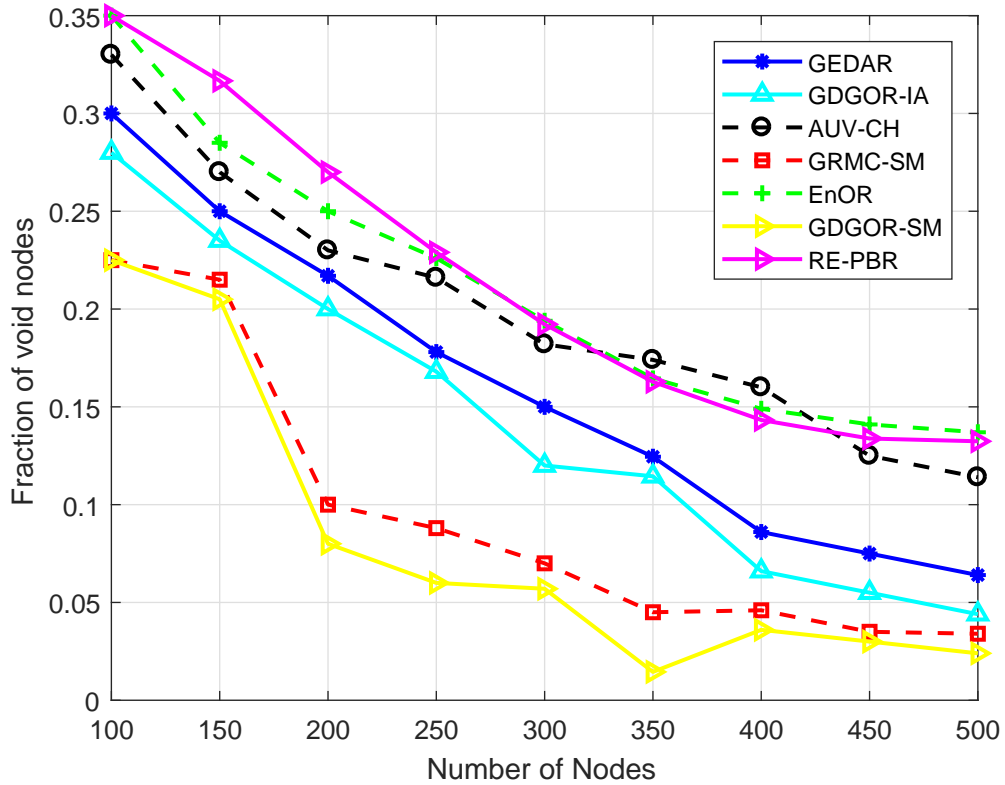


FIGURE 4.7: Fraction of void nodes plots

node. Moreover, the quantity decreases significantly as the density increases from 150–450. The reason of sudden decrease was the availability of more nodes in the transmission range of source node. As it is illustrated in Figure 4.7, RE-PBR only beats EnOR, while in other schemes, the mechanism of recovery is available which makes them more effective and efficient in terms of handling energy consumption.

#### 4.7.2.2 Depth Adjustment

At low network density, distance between void nodes is high. Figure 4.8 depicts the displacement of void nodes in GDGOR-IA and GEDAR. It can be seen that at node number 200, 15% of network nodes are void nodes. As node number in the network field increases, the displacement of void nodes decreases. This is because of increase in node density, the fraction of void nodes decreases as shown in Figure 4.7.

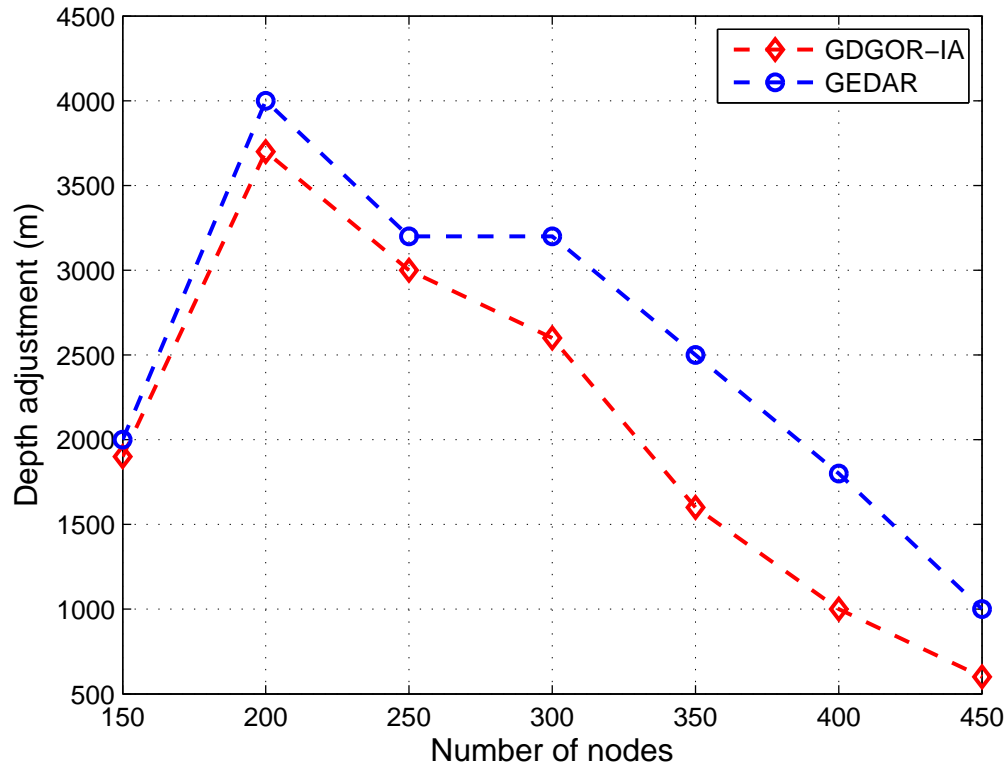


FIGURE 4.8: Depth adjustment plots

#### 4.7.2.3 PDR

The PDR of all schemes is monotonically increasing as depicted in Figure 4.9. However, the proposed work supersedes all the existing compared schemes because of the incorporation of sonobuoys mobility. Although all the three proposed schemes have opted void node recovery mechanism, cost associated with each scheme is different. At the beginning, GDGOR-IA performs same as GEDAR but the interference avoidance mechanism reduces the chance of data loss resulting in high PDR.

Initially, the PDR is very high of RE-PBR because of the consideration of link quality during the selection of forwarder node. The inclusion of link quality metric, enables reliable delivery of data packets at the destination as illustrated in Figure 4.9. The increase in PDR is gradual with the increase in node number because of consistent rotation of forwarder node, which avoids dramatic death of node. However, when node density reaches 350, the proposed schemes GDGOR-SM and

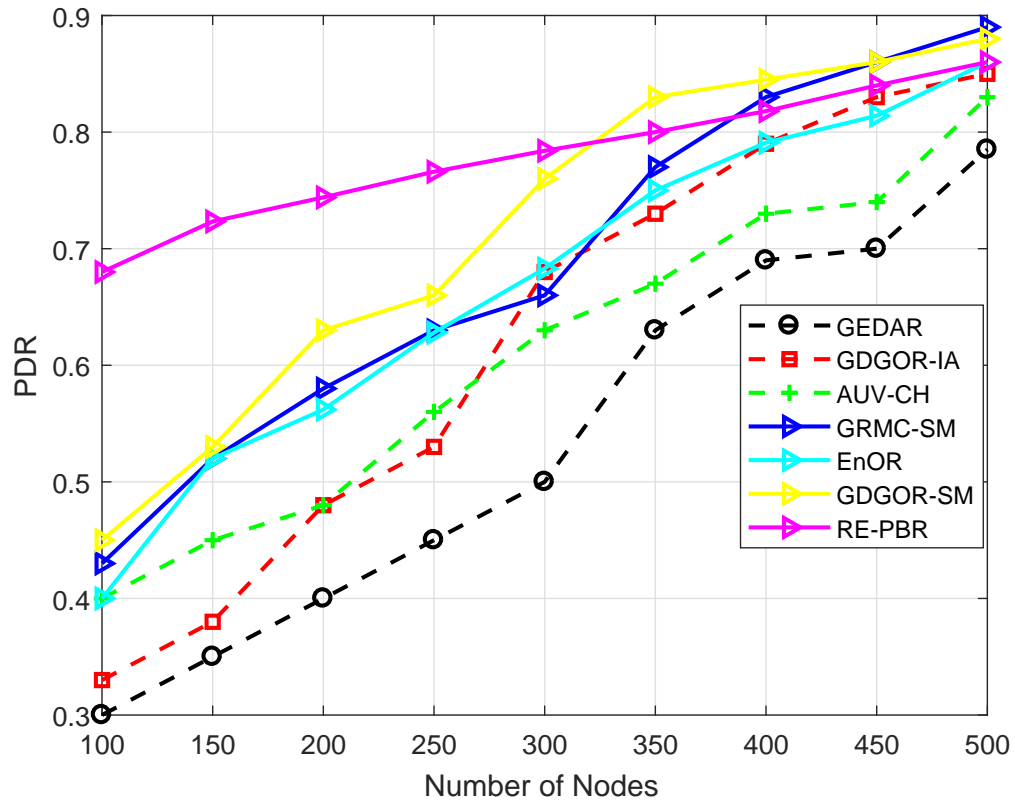


FIGURE 4.9: PDR plots

GRMC-SM outperform RE-PBR because mobile sinks collect data directly from sensor nodes.

PDR in EnOR is very much high as compared to AUV-CH and even from proposed scheme, GDGOR-IA because of its ability to assign priorities to each node which ensures imbalance energy dissipation throughout the network operational time. However, the major reason of not beating all schemes is the absence of mobile sonobuoys due to which only data is delivered via multi-hopping. If void node occurs, then no mechanism is defined to recover data packet which results in data loss. While AUV-CH performs not well because of its ability to gather data from every node which takes time and gathers less data as compared to the proposed schemes.

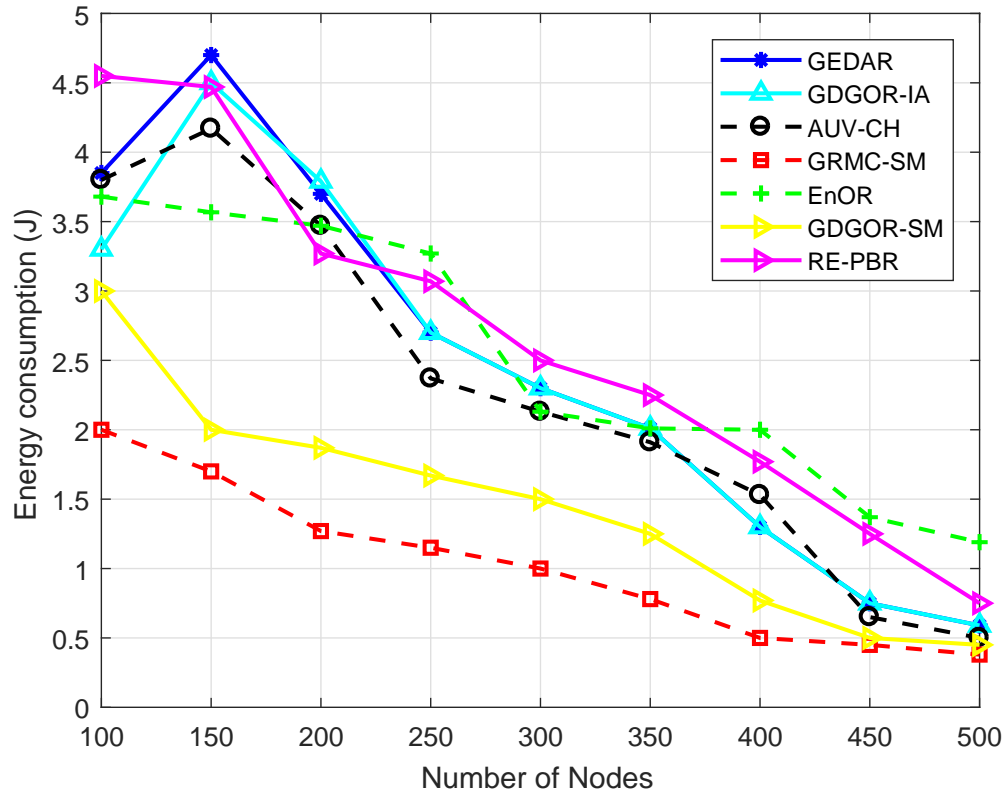


FIGURE 4.10: Energy consumption comparative plots

#### 4.7.2.4 Energy Consumption

The depletion of node battery is directly proportional to distance between transmitter node and receiver node. The energy utilization is presented in Figure 4.10 which clearly states that GRMC-SM outperforms rest of the compared schemes in the plot. Initially, the energy is 2 J at 100 nodes while as the density increases it goes down gradually to less than 0.5 J at 500 node number. The reason of this continuous fall down is that nodes start finding plenty of neighbors within the communication vicinity. As stated earlier discussion, energy consumption is directly related to distance, thus, when nodes find neighbors in the transmission range quite often and mobile sonobuoys continuously patrolling the acoustic environment than energy is significantly reduced by deploying more number of nodes. The pattern of energy dissipation in GDGOR-IA is the same, however, because of the consideration of interference, it needs to choose next hop with utmost care.

While, GDGOR-IA has more energy dissipation at node 100 however, it reduces as the node density increases but still has more energy than AUV-CH. In GEDAR

and GDGOR-IA, energy consumption is mainly due to the depth adjustment for recovery purpose. At the beginning, fraction of void node is high in sparse network as shown in Figure 4.7. Hence, more energy consumption occurs due to large displacement of nodes on average to recover communication voids. The trend of energy consumption follows the same behaviour for GEDAR and GDGOR-IA when node number is below 250.

The AUV-CH and EnOR show moderate energy consumption from beginning till the node density 500. While, GEDAR has high energy consumption initially, but, it reduces suddenly after the node density increases from 150. The EnOR has minimum energy consumption 1.25 J when number of nodes are 500. Whereas, AUV-CH has slightly higher energy dissipation than GDGOR-IA as clearly depicted in Figure 4.10. Whereas, the dissipation of node battery is high in RE-PBR due to consistent rotation of relay node which helps in balancing energy, however, the involvement of more hops results in high energy consumption as compared to proposed schemes.

#### 4.7.2.5 End-To-End Delay

In Figure 4.11, the end-to-end delay is consistently because of more number of nodes participate in communication when node density increases. Highest delay is experienced by AUV-CH due to data gathering from every node in its communication range, and the delay is 2.5 s at 500 node number. This delay is occurring because of high traffic load that results in to more number of transmissions. Whereas, EnOR has higher delay due to opportunistic forwarding in which time consumed at assigning priorities to each node in the forwarder set for avoiding immutable selection of each node towards the destination. This incorporates more delay in EnOR, however, lower than AUV-CH. While, delay in RE-PBR is less than all schemes throughout the network lifetime except GDGOR-IA. The reason of less delay than other schemes is, the selection of high quality link which mitigates the chances of retransmissions.

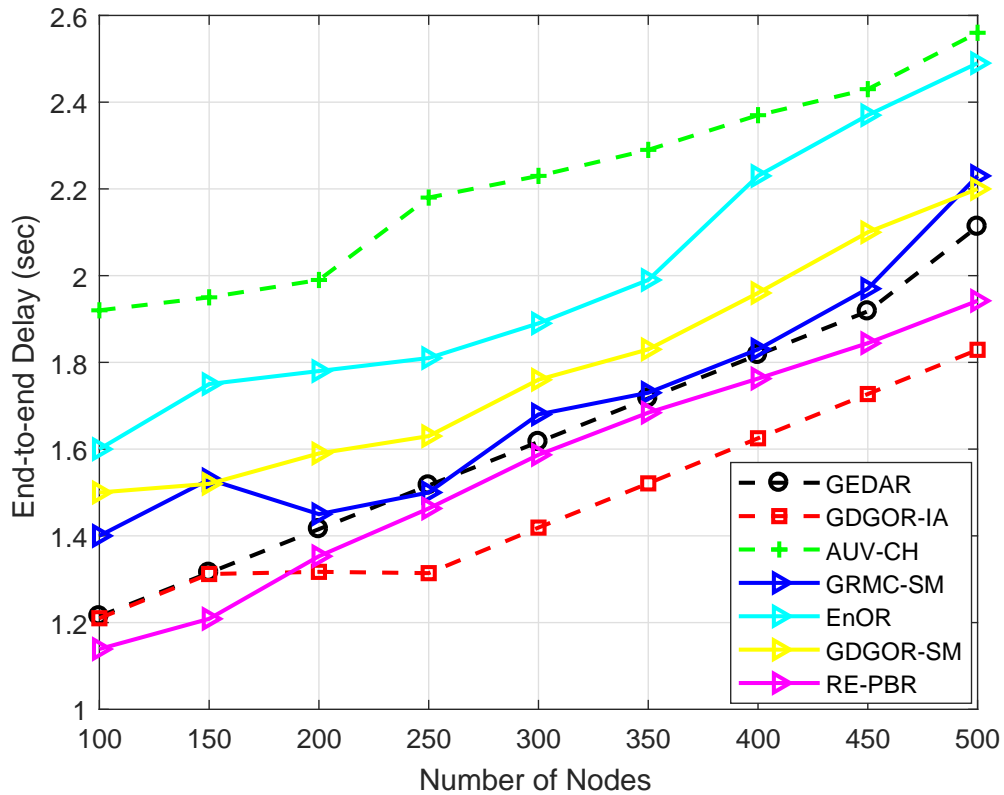


FIGURE 4.11: End to end delay plots

Whereas, GDGOR-IA bears the same delay as GEDAR in Figure 4.11. However, GDGOR-IA opts void hole avoidance mechanism along with interference avoidance in order to avoid communication voids and data loss. This incurs more delay due to several number of hops taken to bypass void holes. In GRMC-SM scheme, number of hops taken to deliver data to sinks is less while compared with other schemes because of mobile sonobuoys involvement for data gathering from acoustic nodes directly. Thus, reduced end to end delay is experienced in GRMC-SM and GDGOR-SM as shown in Figure 4.11. Performance analysis of GEDAR against proposed technique is given in Table. 3.

#### 4.7.2.6 Performance Trade-Offs

From the simulation results, it can be concluded that there is trade-off between performance parameters. In GEDAR. GDGOR-IA scheme, achieves slightly better PDR is slightly high with 14% less delay in the network. This is due to the interference avoidance mechanism opted in the scheme that minimizes the delay

caused due to the opportunistic routing opted in GDGOR-IA. GRMC-SM secures high PDR at low energy cost as compared with GRGOR-IA and GEDAR. While incorporating sink mobility in GDGOR-IA, energy cost associated with depth adjustment is diminished due to sink deployment in three dimensional volume for maximum coverage.

### 4.7.3 Observations of the Research

TABLE 4.1: Analysis of performance parameters against GEDAR

Parameter	GDGOR-IA	GRMC-SM	GDGOR-SM
PDR (%)	4	7	3
Energy tax (%)	10	51	12
Latency (%)	16	-48	15

#### 4.7.3.1 Performance Analysis Based on Varying Traffic Loads

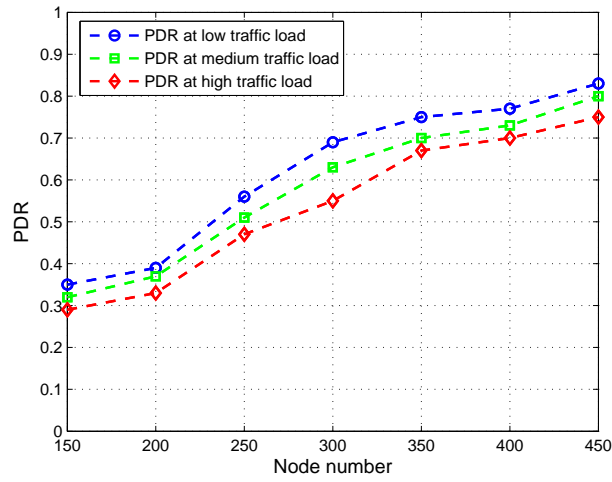
To analyze the effect of traffic load in the network, this research carried out an analysis for GRGOR-IA routing scheme. At three different values of traffic load, the proposed scheme is evaluated performance parameters. In Figure 4.12a, PDR is high at medium packet size at 50 kbps data rate. PDR increases when node density is high, after the deployment of 350 nodes, it remains constant due to availability of node in the transmission range increases, however, few become potential forwarders. This research considered latency in Figure 4.12b that is high at high data packet size while considering same data rate for three data packet sizes. It is because, high traffic load incurs more delay overall in the transmission process. Whereas, latency incurred due to medium traffic load is less comparatively. Trend for energy consumption in Figure 4.12c follows same pattern for all three traffic loads. However, at high traffic load, energy consumption is high that is because of more energy consumption for high packet rate. Initially, energy consumption is more for medium traffic load while compared with low traffic load scenario. Later

on, with the increase in node number, energy consumption stays same for medium and low traffic loads.

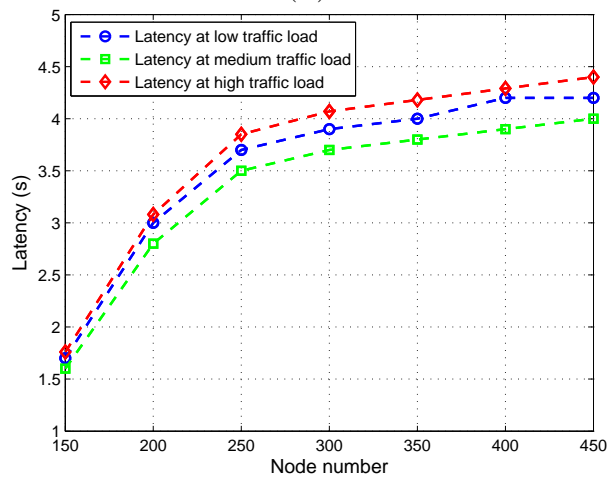
#### 4.7.3.2 Performance Analysis of GRMC-SM by Varying Number of Sinks

To investigate the fraction of isolated nodes and their effect on PDR, the analysis have been conducted by varying sonobuoys from 9–64 sonobuoys. Void regions in the network are significantly reduced in GRMC-SM due to three dimensional deployment of sinks in the network region. Worst scenario is when number of sonobuoys are 9 and performance gets better with the increased number of sonobuoys. Because of increase in sonobuoys number, the void regions and connectivity holes in the network are avoided. Hence, other performance parameters improve along with fraction of void nodes as shown in Figure 4.13. Considering the fact that only 5% nodes are in void region in case of 64 sonobuoys deployed in the network, observe PDR gets higher in this scenario while compared with other scenarios. Average delay reduces due to more direct transmissions in 64 sonobuoys in the network. Anyhow, there are few costs associated with multi-sink architecture, specifically, when sinks are deployed in three dimensional field.

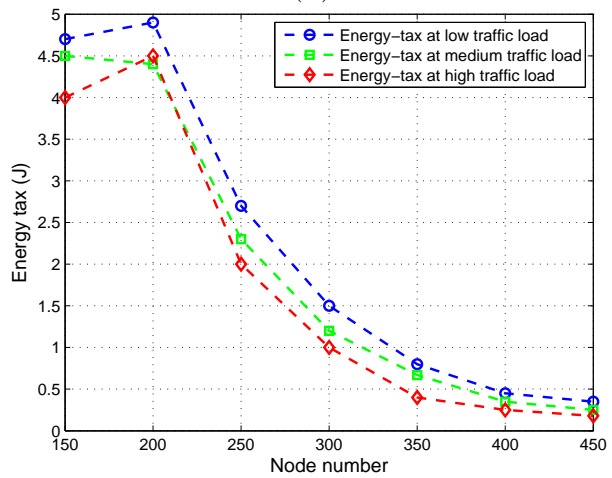




(A)

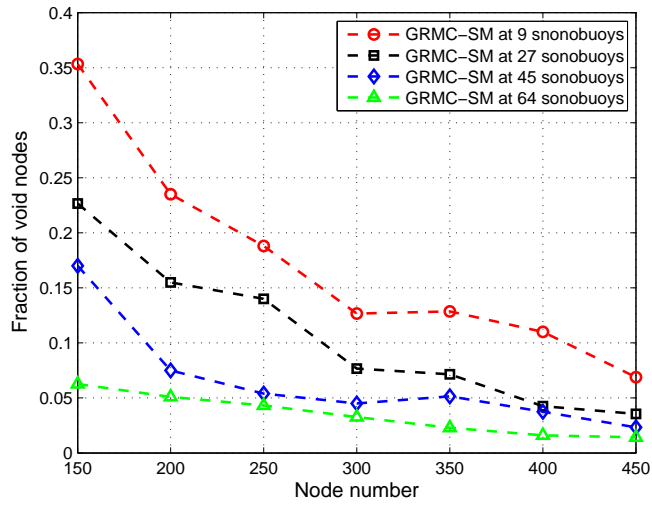


(B)

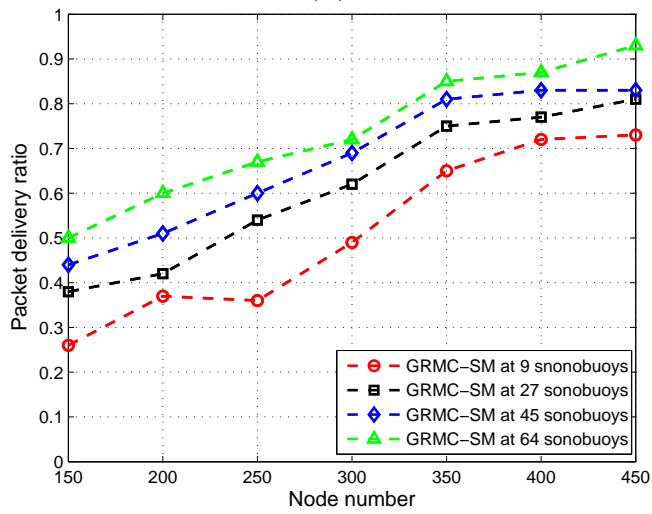


(C)

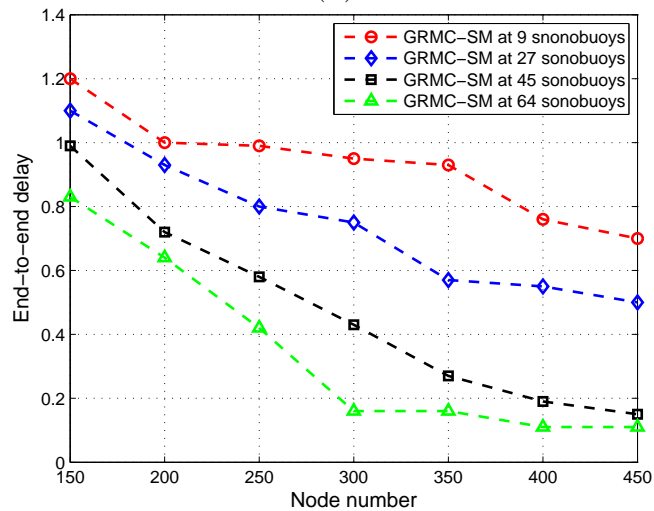
FIGURE 4.12: Performance parameters for GDGOR-IA. (a) PDR for GDGOR-IA; (b) Latency for GDGOR-IA; (c) Energy tax for GDGOR-IA.



(A)



(B)



(C)

FIGURE 4.13: Performance parameters for GRMC-SM. (a) Fraction of void nodes under different number of sonobuoys; (b) PDR under different number of sonobuoys; (c) End to end delay under different number of sonobuoys.

## 4.8 Conclusions

In this chapter, the proposed schemes have performed collaborative tasks of routing data towards the destination while coping with communication voids. The proposed schemes exploit geographic information to route data greedily towards the sonobuoys. Three dimensional division has made network scalable and forwarding is directional because of selection of upstream nodes from the neighbor cube. In this way, hops taken to execute a complete transmission from sender node to sonobuoy has reduced significantly. Moreover, interference avoidance in GDGOR-IA helps in reduction of packet loss, thus it improves PDR. In GRMC-SM, controlled sink mobility considerably enhances network performance as compared to baseline schemes. Energy cost is significantly improved due to coping with communication voids by reducing fraction of void nodes. Consequently, these schemes provide efficient solution for reliable communication among the network nodes. Mathematical problem formulation using linear programming provides feasible solution for minimizing the consumption of energy, reducing average end-to-end delay and maximizing PDR. This chapter proves the role of sink mobility in network for lifetime improvement, linear optimization is effective in term of minimizing the energy consumption of nodes, geographic routing seems promising choice and reduced tradeoff gap between energy consumption and other important parameters. This Chapter covers research questions 3,5,6 and 10 mentioned in chapter 1.

Transmission range adjustment and geo-spatial division are individually implemented in DOW-PR and GDGOR-IA respectively. In order to get benefit of both these researches, the hybrid version of these two i.e. LETR were incorporated. The novelty of location error prediction was also included while selecting the forwarder. GDGOR-IA incorporates the division of forwarding zone into small logical cubes in transmission range of the sender node. The geo-spatial division reduced the probability of finding nodes in small cubic region especially in sparse network scenario . This research further investigated the other methods of forwarding region division. The next chapter is the extended work of GDGOR-IA i.e. Location

Error Resilient Transmission Range based routing protocol (LETR). Moreover, LETR also considered the transmission range adjustment technology proposed in DOW-PR routing protocol.

# Chapter 5

## Position adjustment based location error resilient geo-opportunistic routing for void hole avoidance in UWSN

### 5.1 Summary of the Chapter

This chapter presents four routing protocols for Underwater Sensor Networks (USNs): Location Error resilient Transmission Range adjustment based protocol (LETR), Mobile Sink based GEographic and Opportunistic Routing (MSGER), Mobile Sink based LETR (MSLETR) and Modified MSLETR (MMS-LETR). LETR considers transmission range levels for finding neighbor nodes. If a node fails to find any neighbor node within its defined maximum transmission range level, it recovers from communication void regions using depth adjustment technology. MSGER and MSLETR avoid depth and transmission range adjustment and overcome the problem of communication void regions using MSs. Whereas, MMS-LETR takes into account: noise attenuation at various depth levels, elimination of retransmissions using multi-path communication and load balancing.

The performance of proposed protocols is evaluated through simulations using different parameters. The simulation results show that MMS-LETR supersedes all counterpart schemes in terms of packet loss ratio. LETR significantly improves network performance in terms of energy consumption, packet loss ratio, fraction of void nodes and the total amount of depth adjustment.

## 5.2 Introduction

USNs recently came up with hundreds of applications like harbor monitoring, oceanographic data collection, seaquakes monitoring, submarine tracking, etc. [18]. In traditional USNs, a number of tethered sensor nodes are dropped in the targeted network area for monitoring. However, the inherent challenges like high bit error rate, limited bandwidth and large end-to-end delay have very bad impact on deployment and in design of USNs. Nevertheless, high end-to-end delay is observed in USNs due to speed of sound in water i.e. 1500 m/s [18]; the acoustic signals are the most preferred way of communication in acoustic environment because radio waves get absorbed in water due to high frequency range, whereas, optical waves are applicable only to short range transmissions and face heavy scattering.

Besides sensing, many sensor nodes have the capability to locate themselves using positioning system. Global positioning system provide an expensive and power consuming solution to the localization problem. Therefore, local positioning system is the most feasible and cost effective technique for localization in underwater. However, erroneous nature of local positioning system effects communication between network nodes. Besides localization errors, one of the major challenge is the efficient utilization of limited node battery which directly effects the network performance. Further, it is quite difficult to replace sensor node's battery in harsh aquatic environment. Thus, need of efficient and reliable routing mechanism emerges which can ensure error resilient and energy efficient communication between sensor nodes.

Geographic routing is considered as the most promising data transmission technique to address the key USN's issues because it is simple and scalable [45]. Moreover, complete route establishment and maintenance towards sink is not required. Whereas, locally optimal routes are selected at each hop till the packet reaches its destination. Geo-opportunistic routing add more benefits for data transmission in terms of high packet delivery ratio and reduced energy consumption. In opportunistic routing, only a highest priority node transmits data where multiple neighbor nodes keep the same copy of the packet. The neighbor nodes hear and suppress their transmissions to avoid interference. A second priority node transmits data when the highest priority node fails to transmit [18].

Although, geo-opportunistic techniques provide simple and energy efficient solution though, void hole problem severely impacts performance of these protocols. If a node is unable to locate any neighbor node in its vicinity, it is considered as a void node. The deployment strategy of sensors and the imbalanced energy consumption result in void holes creation. In this situation, the routing protocols either route the data packets using some recovery mechanism or simply discards packet.

In this chapter, four routing protocols have been proposed: Location Error resilient Transmission Range adjustment based protocol (LETR), Mobile Sink based GEographic and Opportunistic Routing (MSGER), Mobile Sink based LETR (MSLETR) and Modified MSLETR (MMS-LETR) for USNs. The proposed protocols provide solution to localization problems as well as for the recovery of void regions. LETR uses location information of sensor and sink nodes to locate a set of neighbor nodes. An angle between sender and receiver is calculated and the node is considered as an eligible neighbor only when the calculated angle lies between defined thresholds. Each sensor node calculates its advancement while the node with minimum advancement is selected as a neighbor node. To successfully deliver data packets and maximize network throughput along with energy efficiency, LETR calculates Mean Square Error (MSE). This helps to cope with the inefficiency introduced by geographic routing (without considering location inaccuracy) in terms of energy consumption and network throughput. The packet

delivery probability, packet advancement and MSE are used altogether in the selection of optimal forwarder node. One of the most important feature of LETR is transmission range adjustment for void area recovery. Instead of message based void area recovery, the system prefer to use transmission range adjustment and depth adjustment technology to recover communication void regions. The transmission range of each sensor node is divided into  $k$  levels where the search of neighbor nodes search initially starts at  $k_o$  and the value of  $k$  increments if no neighbor found at that level. If a node is unable to locate any neighbor within maximum transmission range, it adjusts its depth towards surface sinks. Sensor nodes displace to new position during depth adjustment. To the best of our knowledge, this work is the first that considers both localization errors and void node recovery in geographic routing and provides an amalgamate solution using LETR. Simulation results prove that the LETR reduces packet drop ratio by considering location errors and packet delivery ratio.

Whereas, in order to avoid packet loss and imbalanced energy consumption due to dynamic underwater environment, MSGER works to avoid depth adjustment by adjusting the position of multiple MSs to gather data from the network nodes. MSLETR works like the same way as LETR, the only difference is the incorporation of MSs which replaces the step of power adjustment with MSs position adjustment. MMS-LETR increases the network lifetime by minimizing the energy consumption and reducing the data packet loss. The proposed solution also reduces the fraction of void nodes and energy consumption in the network using transmission range and depth adjustment technology.

The rest of the chapter is organized as follows: In Section 5.3, problem statement is defined while Section 5.1 explains system model in detail. Section 5.5 illustrates the functioning of proposed schemes. The performance of proposed protocol is evaluated in Section 5.6 over defined parameters. Section 5.7, conclude this research work.



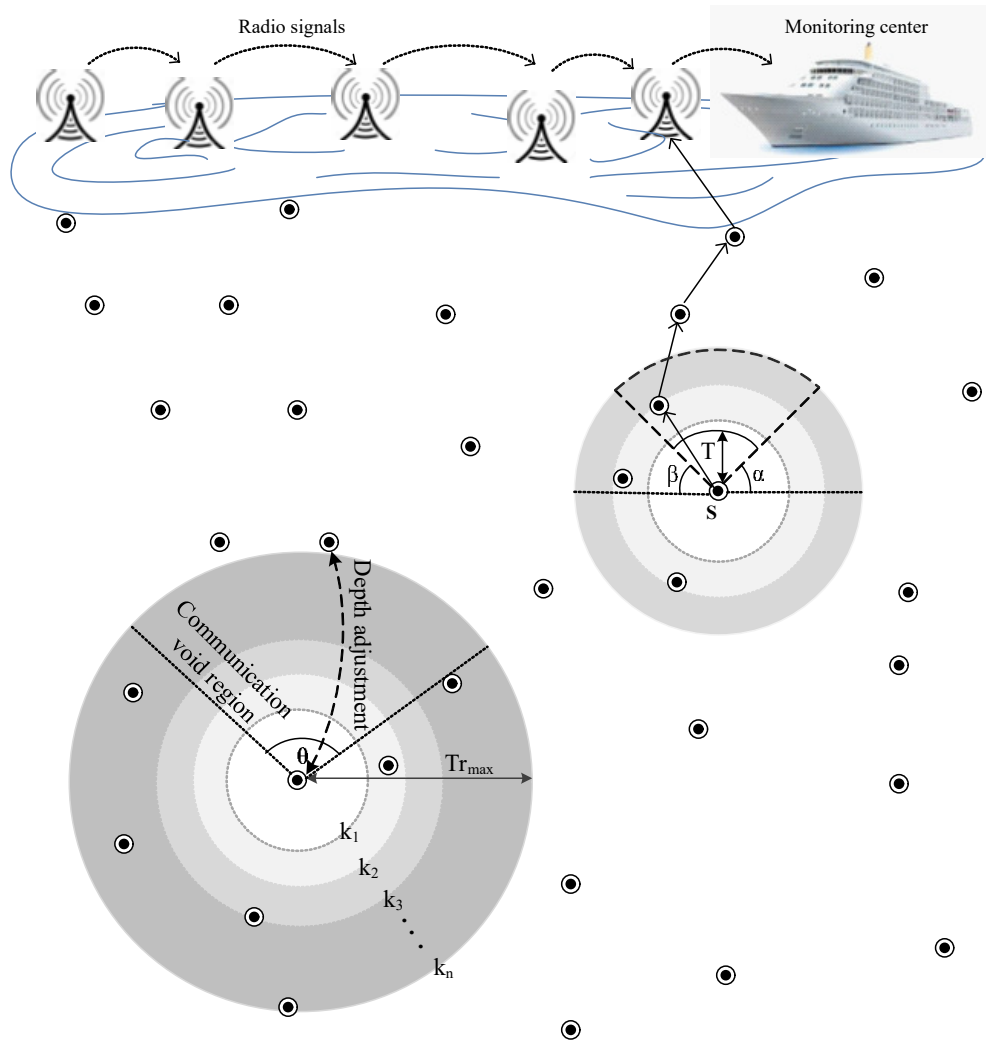


FIGURE 5.1: Network model for LETR

### 5.3 Problem Statement

Geographic routing proves to be the best option where establishment and maintenance of complete route between the sender and the receiver is not required. The routes are established via disseminating location information to neighbor nodes, which reduces the control overhead resulting in energy efficiency and high packet delivery ratio. However, the dynamic acoustic environment still have inaccuracy in location information. Due to inaccurate location information, the number of retransmissions and communication overhead increases, which degrades the network performance. Geographic routing boils down to location errors nevertheless, geographic routing combined with opportunistic routing leads to void regions.

GEDAR [18] proposed geo-opportunistic routing protocol for void recovery. However, the depth adjustment procedure in GEDAR negatively impacts the network performance in terms of lifetime, energy consumption and topology configuration. Whenever a sensor node discovers itself to be in a communication void region, it calls depth adjustment procedure and moves to a new depth. According to GEDAR, node always displace towards bottom in order to forward its data through predecessor node. In case of more than one predecessor nodes, a sensor node is unable to decide its ultimate destination, towards which it needs to move. If the predecessor node is also a void node, the same depth adjustment procedure applies to predecessor nodes. This high amount of energy consumption during displacement ultimately shortens network lifespan. Also, after certain amount of time during network operation, the areas nearer to sink become sparse due to node movement towards bottom. Thus, the reception of data packets at sink is no more possible. On the other hand, if a node has no other node in its vicinity, it can neither move to a new location nor it has choice to forward its data towards sink. Thus, the node becomes a spare node in the network.

In deep water, noise attenuation is low as deep sea is more quite than surface. Therefore, single path communication should be preferred in high depth while the communication in the area near surface highly affects due to various types of noises. GEDAR selects forwarder set at each hop where highest priority node among them is eligible to transmit data. However, at medium and lower depths multi-path communication should be preferred to avoid packet drop ratio. To successfully deliver data at sink, localization accuracy requirements should also be highlighted. Many location error resilient protocols proposed to tackle localization issue. Authors in [74] provide location error aware protocol to handle energy consumption and increase packet delivery probability in sensor networks. However, most of the protocols dealing with location errors do not implement mechanisms for void hole recovery [53], [75]. GEDAR implements geographic routing with no mechanism to cope with the erroneous location information. Such limitations severely affect network communication and throughput. Underwater channel noise

also play a key role in high energy consumption and packet drop ratio in the network. The aforementioned limitations need to be addressed through novel routing protocols. Therefore, this research presents LETR, MSLETR and MMS-LETR which are discussed in detail in section 5 and 6.

## 5.4 System Model

This system consider a homogeneous and hierarchical network architecture as depicted in Fig. 5.1. It is evident from the depicted proposed model that the sensor nodes are randomly deployed along with the multiple sinks placed at the surface of water. In multi-sink architecture, it is assumed that a data packet received at one sink will be considered received successfully at the destination. Sink nodes are equipped with both radio and acoustic modems. These nodes are also provided with GPS facility to determine their location. Sensor nodes use acoustic signals for data transmission while sinks mutually communicate through radio waves. The sensor nodes sense and transmit data periodically. Sensor nodes exploits depth adjustment technology (winch based apparatus or inflatable buoys). The velocity for sensor's vertical movement is 2.4 m/min at an energy cost of 1500 mJ/m. The sensor nodes compute their location using an existing localization method, Time of Arrival (ToA) as in [115] and MoteTrack location identification scheme [116]. The network topology is denoted as an undirected graph  $G(t) = (V, E(t))$  where  $V$  correspond to sensor nodes and  $E(t) = e_{uv}(t)$  denote the links between any pair of sensor nodes  $u$  and  $v$  at time  $t$ .

### 5.4.1 Packet Delivery Estimation Model

Many factors like low bandwidth, high bit error rate and delay severely degrade the performance of underwater communication channel. The attenuation on an unobstructed path, over  $d$  distance for a  $f$  frequency signal due to large scale fading, is stated as follow [117]:

$$A(d, f) = d^k \alpha(f)^d, \quad (5.1)$$

where  $k$  and  $\alpha(f)$  specify the spreading factor and absorption coefficient, respectively. Spreading factor  $k$  determines the signal's propagation geometry and its values are  $k = 2$ ,  $k = 1$  and  $k = 1.5$  for spherical, cylindrical spreading and practical scenario, respectively. Equation 5.2 calculates the absorption coefficient using Throp's formula [118] as:

$$\alpha(f) = \frac{0.11f^2}{1+f^2} + \frac{44f^2}{4100} + f^2 + 2.75 \times 10^{-4} f^2 + 0.003 \quad (5.2)$$

Equation 5.3 provides the average Signal-to-Noise Ratio (SNR)[119]

$$\chi = \frac{E_b}{N_o A(d, f)} \quad (5.3)$$

where  $E_b$  is the per bit transmission energy and  $N_o$  represents the noise power density in a non-fading Additive White Gaussian Noise (AWGN) channel.  $E_b$  and  $E_o$  are the constant values. The probability distribution of  $SNR$ , defined in [119] is given as:

$$\rho_d(X) = \int_0^\infty \frac{1}{\Gamma(d) e^{\frac{-X}{\Gamma(d)}}} \quad (5.4)$$

Equation 5.5 provides the probability of error:

$$\rho_e(d) = \int_0^\infty \rho_e(X) \rho_d(X) dX \quad (5.5)$$

where  $\rho_e(X)$  is the probability of error at a specific SNR  $X$ . It is preferred to use the Binary Phase Shift Keying (BPSK) modulation which is widely used in literature for acoustic modems [45]. To calculate bit error probability [120] using Equation 5.6 as:

$$\rho_e(d) = \frac{1}{2} \left( 1 - \sqrt{\frac{\Gamma(d)}{1 + \Gamma(d)}} \right) \quad (5.6)$$

The delivery probability of  $m$  sized packet over  $d$  can be expressed as:

$$\rho(d, m) = (1 - \rho_e(d))^m \quad (5.7)$$

## 5.5 Proposed Protocols

This section discusses the routing algorithms LETR, MSGER, MSLETR, and MMS-LETR in detail. In order to differentiate, LETR is proposed in separate section because of no sink mobility. Secondly, under the section of sink mobility based routing protocols; MSGER, MSLETR and MMS-LETR are given in a separate subsection.

### 5.5.1 LETR

This section provides detailed functioning of proposed protocol. LETR amalgamates geographic and opportunistic routing by incorporating transmission range and depth adjustment capability while coping with location errors.

#### 5.5.1.1 Controlled Beaconing Algorithm

Beaconing is a crucial process for network convergence [18]. For this purpose, LETR incorporates the controlled beaconing algorithm. To conserve energy, keep the size of beacon message as short as possible. During network initialization phase, each sensor node and sink broadcasts beacon messages. Due to localization errors and node mobility (due to water currents) the information within beacon message becomes ineffective. Therefore, the sensor nodes broadcast periodic beacons to get updated information as illustrated in algorithm 5. Also, the depth

adjustment negatively impacts network convergence.

The proposed scheme implement controlled beaconing algorithm. The transmission power of each sensor node is divided into  $k$  levels. Dividing transmission power into levels help sensor nodes in void region recovery. Each sensor node accordingly adjusts its transmission power within its maximum transmission range after detecting itself as a void node.

After network initialization, each sensor node and sink broadcasts beacon message as shown in lines 4 - 7 in algorithm 5. As a result, each sensor node gets to know about all the nodes in its vicinity. If a node receive no beacon, it declares itself as a void node. Each sink broadcasts beacon only once while sensor node broadcasts beacon periodically or when it adjust depth and transmission level. Initially, each node embeds its location information and Current Clock Time (CCT) (helps to identify recent beacon from a node) in beacon message and broadcasts it. When a node identify itself as a void node, it adjusts its transmission range. While the void node adjust its transmission level, it broadcasts a beacon to inform its neighbors about its existence. If there exists any node at that level, the node will send back an acknowledgment packet containing the location information of the node. Sensor node adjust its depth when no forwarder node is found within maximum transmission level. However, the probability of being void node with maximum transmission range is very small, therefore, beaconing happens rarely. The proposed scheme conserve extra energy utilized during depth adjustment in

GEDAR.

---

**Algorithm 5:** :Controlled Beaoning Algorithm

---

```

1 Initial depth(node) ← DP(i)
2 Adjusted depth(node) ← DP(a)
3 procedure: INITIALIZATION
4 procedure: BroadcastBeacon(sink)
5 Beacon·Loc ← Location.coordinates(sink)
6 BroadcastBeacon()
7 procedure: BroadcastPeriodicBeacon(node)
8 Beacon·Loc ← Location.coordinates(node)
9 Beacon·Time ← CCT
10 BroadcastBeacon()
11 if depth(node) ← β then
12   | Beacon·Loc ← Location.newcoordinates(node) repeat steps 9 - 10

```

---

### 5.5.1.2 Neighbor Set Selection

This section, discuss in detail the mechanism for the selection of neighbor nodes. After network convergence, each node selects a set of neighbor nodes in order to choose a suitable forwarder for data transmission.

**Angle based neighbor selection** A sensor node select its neighbors by calculating its angle with all the nodes in its transmission range. However, the upper and lower bounds ( $\alpha$  and  $\beta$  respectively) for defining angle  $\theta$  as provided in equation 5.8.

$$\alpha < \theta \leq \beta \quad (5.8)$$

To confined neighbor selection area to overcome excessive energy consumption due to opportunistic routing. Also, overhearing probability decreases as the number

of neighbor nodes increases [121]. Thus, more redundant packets and high energy consumption will affect network performance. Ultimately, network lifetime shortens. Equations in 5.9, 5.10, 5.11 and 5.12 are used in calculation of  $\theta$ :

$$\begin{aligned}x_d &= x_i - x_j, \\y_d &= y_i - y_j, \\z_d &= z_i - z_j\end{aligned}\tag{5.9}$$

where  $z_d = \zeta$

Equation 5.9 calculates  $x$ ,  $y$  and  $z$  dimension differences between sender  $i$  and neighbor node  $j$

$$\vartheta = \sqrt{(x_d)^2 + (y_d)^2}\tag{5.10}$$

$$S_n = \frac{\zeta}{\vartheta}\tag{5.11}$$

where,  $S_n$  calculates the slope of the line between two points (nodes)

$$\theta = \tan^{-1}(S_n)\tag{5.12}$$

$$d_{p,q} = \sqrt{\sum_{i=1}^N (q_i - p_i)^2},\tag{5.13}$$

Equation 5.13 calculates the distance between sender  $p$  and neighbor node  $q$ , where,  $i$  specifies the dimensions of a node, therefore,  $N = 3$

$$T \leq d_{p,q}\tag{5.14}$$



This research also define a threshold  $T$  (predefined constant value) provided that its value is less than or equal to  $d_{s,n}$  as shown in equation 5.14, where,  $d_{s,n}$  defines the distance between sender and neighbor node. Fig. 5.2 illustrates neighbor selection, forwarder selection and data transmission process in LETR. As shown in this figure, the transmission range of each sensor node is divided into  $k$  levels. Initially, a node checks its forwarder within first transmission level. If no eligible forwarder found within first level, the node adjusts its transmission power and continues the process within second transmission level and so on till it finds neighbors within range.

One of the reason behind angle based neighbor node selection is to overcome hidden terminal problem which is achieved using equation 5.8. Minimum distance between sensor nodes assures overhearing, which leads to fewer chances of hidden terminal problem.

### 5.5.1.3 Forwarder Set Selection

LETR implements opportunistic routing for forwarder selection using packet advancement and node priority value. The packet advancement based forwarder selection criteria is applied using equation 5.15 on the set of neighbor nodes,

$$P_{adv} = d_{s,sink} - d_{n,sink} \quad (5.15)$$

where  $d_{s,sink}$  is the distance between source node  $s$  and sink. The term  $d(n, sink)$  shows the distance between neighbor  $n$  and the sink node. As discussed previously, The proposed work select all the nodes within the angle defined by equation 5.8 as the neighbor nodes. However, to find eligible neighbors the neighbor set is confined only to the nodes fulfilling the criteria defined by equation 5.8. The list of neighbors are sorted on the basis of maximum  $P_{adv}$  value such that only nodes having minimum distance with sink become eligible to transmit data. Such a selection also helps to overcome collisions and extra energy consumption.

Due to low energy cost and overhead, geographic routing seems to be an attractive

option for wireless sensor networks. However, dynamic nature of acoustic channel, quantifiable inaccuracy in location still exists, no matter; which technique or routing strategy is implemented. In an unpredictable environment such as underwater, the probability of location errors is very high. Sensor nodes slightly drift with water currents which leads to packet drop and energy wastage in location based routing. Fig. 5.2 illustrates localization error due to node mobility. To minimize the mobility assisted localization errors, in prior to sending data packets, estimated and actual location of nodes are computed. This will directly increase packet delivery ratio with minimal energy consumption. Using equation 5.13 and the following estimated distance  $\hat{d}_{p,q}$  formula, calculate  $MSE$  in equation 5.17 in [75]:

$$\hat{d}_{p,q} = \sqrt{\sum_{i=1}^N (\hat{q}_i - \hat{p}_i)^2} \quad (5.16)$$

$$MSE_{p,q} = E(\hat{d}_{p,q} - d_{p,q})^2 \quad (5.17)$$

where equation 5.18 computes the estimated distance  $\hat{d}$  as given below.

$$E(\hat{d}_{p,q}) = \sigma_{p,q} \sqrt{\frac{\pi}{2}} L_{\frac{1}{2}}\left(-\frac{d_{p,q}^2}{2\sigma_{p,q}^2}\right) \quad (5.18)$$

where  $\sigma_{p,q}^2 = \sigma_p^2 + \sigma_q^2$ ,  $\sigma_p$  and  $\sigma_q$  are the standard deviation. The Laguerre polynomial denoted by  $L_{\frac{1}{2}}(x)$  is provided in equation 5.19

$$L_{\frac{1}{2}}(x) = \exp\left(\frac{x}{2}\right) \left[ (1-x)I_0\left(-\frac{x}{2}\right) - xI_1\left(-\frac{x}{2}\right) \right] \quad (5.19)$$

LETR finds appropriate forwarder on the basis of equation 5.20 as given below:

$$NPV = \frac{P_{adv} \times \rho(d, m)}{MSE_{p,q}} \quad (5.20)$$

where  $NPV$  denotes the Node Priority Value. Equation 5.20 helps to select a node with minimum  $MSE$  in order to minimize packet loss ratio, energy consumption in retransmissions and the number of collisions. At this stage each node already knows about its neighbors, therefore, every node calculates itself, its best suitable forwarder using equation 5.20. Whereas, a node selects forwarder with highest  $NPV$ .

**Transmission range adjustment** Void hole being an inherent problem in USNs, significantly degrades network performance in terms of network lifetime and throughput. The proposed scheme, implement a novel hybrid adjustment based technique i.e. transmission range adjustment and depth adjustment to overcome void hole problem.

The transmission range of each node is divided into  $k$  levels, where ( $k = k_1, k_2, \dots, k_n$ ). The neighbor selection process based on the transmission range adjustment helps to avoid void holes and balance energy consumption in the network. The sensor nodes adaptively selects transmission range, thus the probability of void holes minimizes. Initially, every node search for forwarder node within  $k_1$ , if no eligible forwarder is found within the specified range, it adjusts its power accordingly to transmit data to some node within  $k_2$ . The process continues up to  $k_m$  i.e. the maximum transmission level. The power adjustment of sensor nodes consume more energy, however, message based void hole recovery procedure incorporates high overhead. In Fig. 5.2, one can see that a sensor node  $S$  initially search for a forwarder node within  $k_1$ . It successfully finds a forwarder  $u$  and transmit data from  $s$  to  $u$  and then node  $u$  to node  $v$ , where node  $v$  is unable to find any forwarder within  $k_1$ , thus transmits data to some node  $w$  by adjusting transmit power. The system declare a node as a void node if it is unable to find any forwarder within  $k_m$ .

**Algorithm 6:** Forwarder Set Selection

---

```

1  $k \leftarrow k_o$ 
2 Broadcast beacon()
3 if response received then
4    $d_{p,q} \leftarrow \sqrt{\sum_{i=1}^N (q_i - p_i)^2}$ 
5   Calculate  $x_d, y_d, z_d$  using equation 5.9
6    $\vartheta \leftarrow \sqrt{(x_d)^2 + (y_d)^2}$ 
7    $S_n \leftarrow \frac{z_d}{\vartheta}$ 
8    $\theta \leftarrow \tan^{-1}(S_n)$ 
9   if  $\alpha < \theta \leq \beta$  then
10     $L \leftarrow$  store ID and coordinated of node
11    Node.status  $\leftarrow$  neighbor found
12  else
13    Discard node ID
14    node.status  $\leftarrow$  no neighbor found
15     $k \leftarrow k_o + 1$ 
16    while  $k \leq k_m$  do
17      repeat step 2 - 16
18 if  $k = k_m$  then
19   if  $k = k_m$  and node.status  $\leftarrow$  no neighbor found then
20     node.status  $\leftarrow$  void
21     procedure: Displacement()
22     Send node.status announcement
23     procedure: CalculateNewDepth(time)
24     Move towards shallower depth  $D_n$ 
25     Adjusted depth  $\leftarrow k_o$ 
26     if node.status  $\leftarrow$  neighbor found then
27       procedure: ForwarderSearch()
28     else
29       Move towards shallower depth  $D_n$ 
30       Adjusted depth  $\leftarrow k_o + 1$ 
31       continue till  $k_m$ 
32   else
33      $\hat{d}_{p,q} \leftarrow \sqrt{\sum_{j=1}^N (\hat{q}_i - \hat{p}_i)^2}$ 
34      $MSE_{p,q} \leftarrow E(\hat{d}_{p,q} - d_{p,q})^2$ 
35      $P_{adv} \leftarrow \omega(R - d_{s,n}) + d_{n,sink}(1 - \omega)$ 
36      $\rho(d, m) \leftarrow (1 - \rho_e(d))^m$ 
37      $NPV \leftarrow \frac{P_{adv} \times \rho(d, m)}{MSE_{(p, q)}}$ 
38      $v \leftarrow \max(NPV)$ 
39     if  $NPV(\text{node}) = v$  then
40       node  $\leftarrow$  Forwarder

```

---

#### 5.5.1.4 Controlled Depth Adjustment

LETR involves controlled depth adjustment besides transmit power adjustment to further maximize data delivery and network lifetime. This research also optimizes traditional depth adjustment procedure defined by GEDAR. The system prefers to use transmission level adjustment technique over depth adjustment in case of void nodes. However, depth adjustment is used only when a sensor node fails to find a forwarder within maximum transmission range; hence, controlled depth adjustment. Algorithm 6 provides depth adjustment procedure in lines 24 - 35. Displacement procedure initiates when a node is designated as a void node. Each void node broadcasts its status as provided in line 25 of algorithm 6. The predecessor of void nodes transmits data through any other node in its vicinity. The amount of displacement is set according to the transmit power level of node i.e. initially a node moves upward and covers distance equal to the initial transmission range as shown in algorithm 6. It checks for forwarder node using range adjustment procedure, upon failing to find any forwarder till  $k_m$ , the void node again adjusts depth. The same process is repeated until a node finds a forwarder. The proposed scheme avoids node displacement towards bottom to avoid topology dynamics occurring due to the depth adjustment of predecessor nodes of sender. Also, due to high energy consumption during network operation, number of void nodes are greater, thus, all the sensor nodes sit in the bottom of water. Ultimately, no data reception at sink is possible.

#### 5.5.2 Sink Mobility based Routing Protocols

Hierarchical routing always remains prone to hot problem due to overburden of data traffic to intermediate nodes. To avoid the hot problem and high energy consumption over long distances, mobility assisted protocols are well suited. To evaluate the outcome, the simulations have incorporated the mobility in GEDAR and LETR. A number of Mobile Sinks (MSs) are deployed in the network field to gather sensed data. The MS nodes act as a data mule which roams in the network field to gather data from sensor nodes. It is a more energy efficient solution than

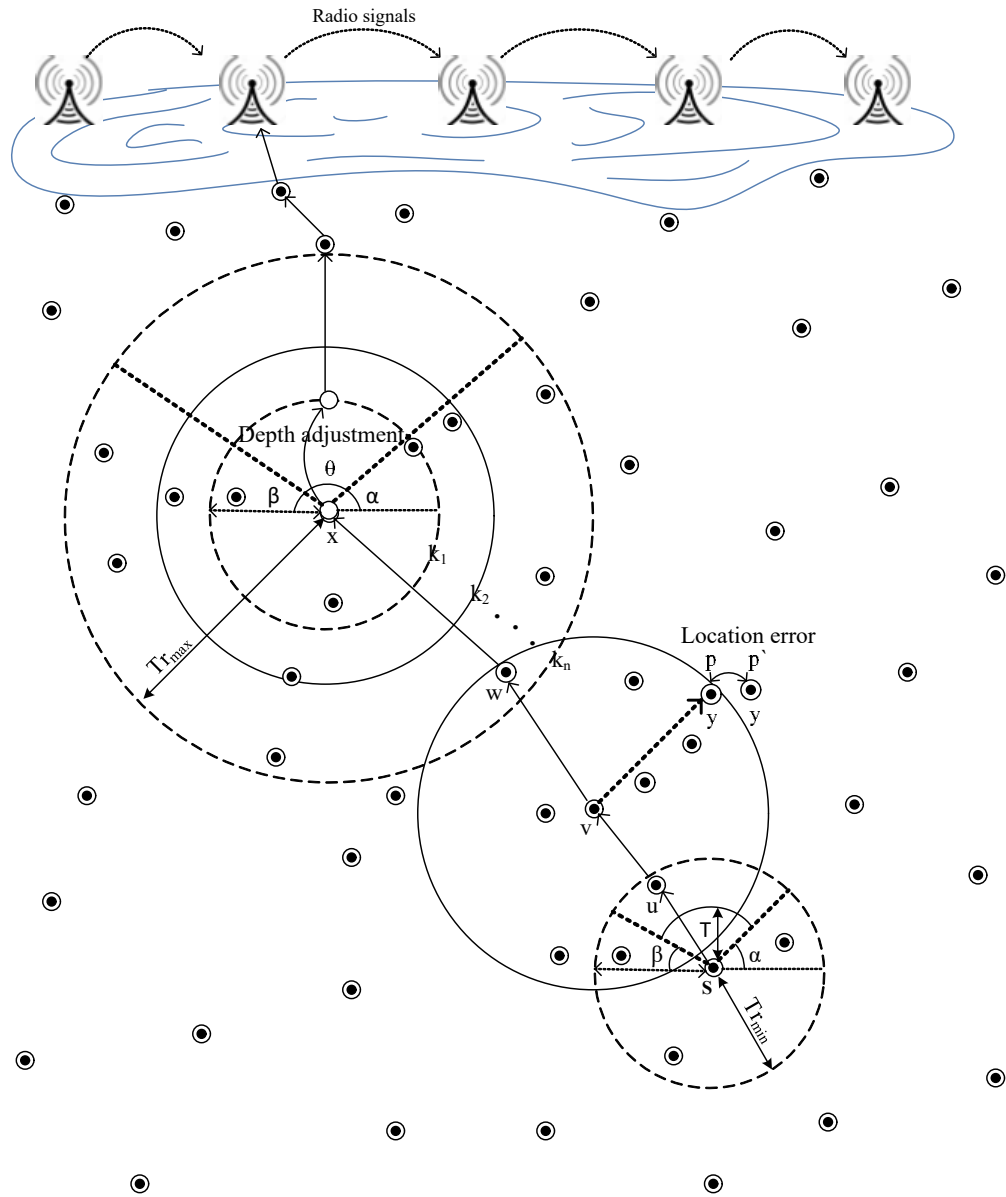


FIGURE 5.2: Operation of LETR

the static sink schemes.

In all the MS based protocols, there are deployment of 50 percent of total network sinks at the surface and declare them static. While the other 50 percent sinks are mobile and are dispersed in the communication region. The MSs helps to overcome communication void region problem as well. If a node encounters no neighbor in its vicinity, it just waits for MS and continuously check for neighbor as well as sink node. A node can have no eligible forwarder at the beginning but after sink displaces to a new position, current void node become successful to find its forwarder or to reach MS directly. The details of MS based protocols are

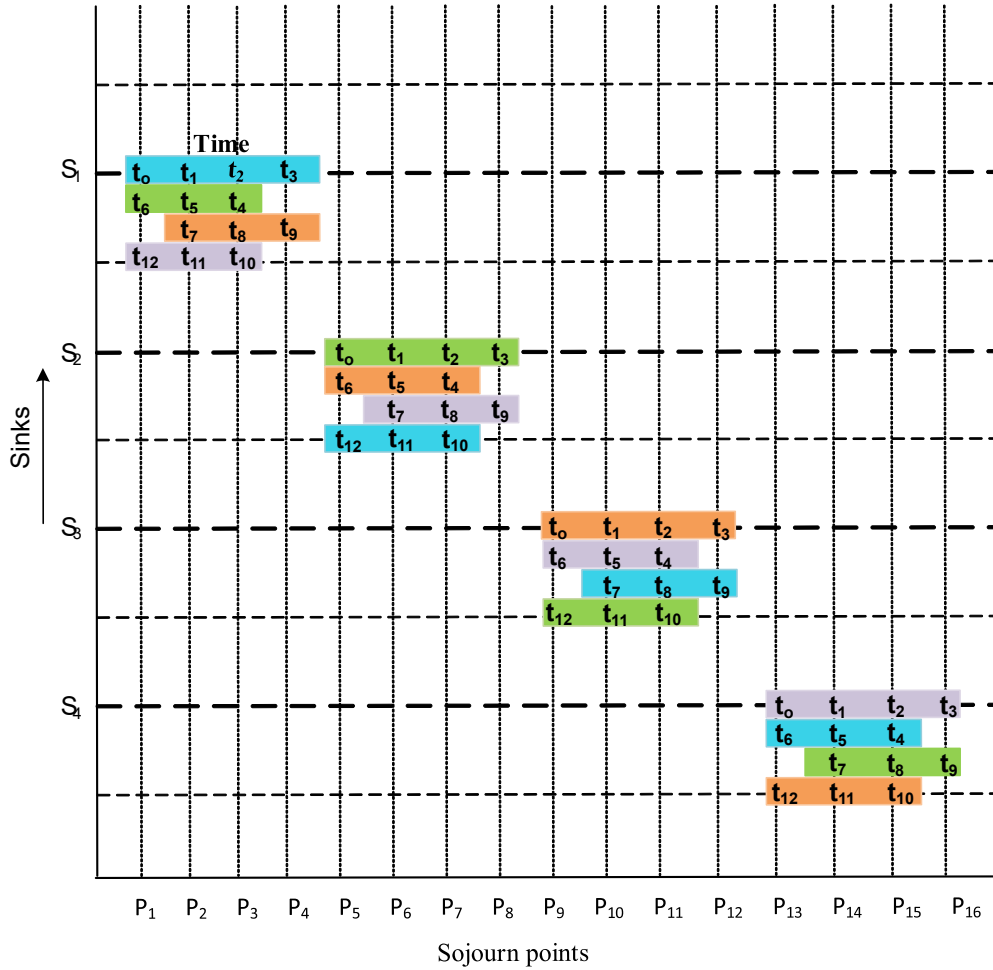


FIGURE 5.3: Sink mobility pattern of MSGER and MSLETR

proposed in the following subsection.

### 5.5.2.1 MSGER

MSGER works to avoid depth adjustment and introduces multiple MSs to gather data from the network nodes. For simplicity, the network field is divided into three logical layers. The axis of network field is divided into three layers, such that each sensor node gets direct access to MS in its vicinity via its maximum transmission range. Equal number of mobile and static sinks are deployed in the network. therefore, the network equally divide the total number of MSs in all layers. The proposed archetecture deploy four Ms at each layer where sinks at layer 1 move along x-axis, layer 2 sinks move along y-axis and the layer 3 sinks move up and down along z-axis. The sojourn period is uniform for all the MSs.

Fig. 5.3 illustrates the mobility pattern of MS in layer 1. Out of many, only show mobility pattern of four sinks in Fig. 5.3, however, all other sinks in layer 2 and 3 follow the same pattern, whereas, the sojourn points for the sinks at layer 2 and 3 are different. These sinks move and collect data from sensor nodes. All the nodes transmit data directly to MS when it comes in their transmission range. If the node is unable to transmit data directly, it transmits data through forwarder node. The forwarder selection mechanism in MSGER is the same as in GEDAR. Introducing MS instead of depth adjustment increases energy efficiency and throughput in the network.

### 5.5.2.2 MSLETR

This section introduce MSLETR protocol to check the impact of sink mobility on different performance parameters of LETR. The MSLETR protocol works like LETR. However, this proposed work omit depth and transmission range adjustment in this protocol. Just like MSGER, there are division of network field logically into layers and deploy sinks in the same pattern as in MSGER. The criteria for the selection of forwarder set is the same as that of LETR. In case of void node, it do not displace that node or adjust its transmission power, this system control void regions using sink mobility. The sensor nodes transmit data directly to their in range mobile or static sink, whereas, a distant node transmits data using forwarder node.

### 5.5.2.3 MMS-LETR

This section, present another MS based protocol which is an enhancement of MSLETR. This protocol, take into account: balanced and efficient energy consumption, noise attenuation in deep water areas and communication reliability. This system also cope with retransmissions due to channel impairments.



**System Model** System model divide the network field into four layers for efficient data transmission i.e. L1, L2, L3 and L4 where L1, L4 and L2, L3 are of equal sizes respectively. The area under L2 plus L3 is subdivided into three sub-layers of equal size ( $0.5 \text{ km}^3$ ) as shown in Fig. 5.4. The sensor nodes contains only acoustic modem while the sinks have both acoustic and radio modems. The MSs are deployed at the upper boundary of each layer. There are deployment of three MS at each layer; L1 and L3 where six MSs are deployed at L2. The trajectory of these MSs is shown in Fig. 5.4. The deployment of all the sinks at equal distance along x-axis from each other. Initially, sink A, C and E are at the boundary of L1. All these sinks collect data from nodes within defined sojourn time and moves to their respective places. As it is clear from the figure, sink A has to move upward while sink B moves downward. After arriving at the layer boundary both sinks A and B change their positions along x-axis as well. So after certain amount of time, sink A moves at the position of sink B whereas, sink B replaces sink A at that particular moment. The same trajectory is followed for all the MSs. The nodes within vicinity of sink transmits data directly while other nodes transmit through multi-hop mode. After collecting data from sensor nodes, each MS transmits data using multi-hop mode to its in range sink, i.e. bottom layer sinks transmit data to upper layer sinks till it reaches surface sinks. All the sinks at the surface transmit the sensed data to onshore data center through radio waves communication.

**Working of MMS-LETR** This section discuss in detail the working of MMS-LETR protocol. The selection of forwarder nodes carried for multi-hop communication while nodes having sink in their transmission range transmit data directly to sink. Each MS stops at every defined location for the same amount of time. In MMS-LETR, sensor nodes select their next hop forwarder in the same way like LETR as discussed in section 6.5.1. Therefore, it is not discuss again the forwarder selection process here.

**Data Transmission** At higher depths, signal transmission is much more smoother than in shallow water. This is because the amount of noise at water surface is always relatively high. Thus, the chances of packet loss are high in regions near the surface. Therefore, there are implementation of multi-path communication in sub-layers nearer to surface.

After selecting a set of forwarders for each node, the system transmit data to highest *NPV* node in the list. The data transmission and sink mobility patterns are described in MMS-LETR algorithm provided in 7. One of the key features of MMS-LETR is load balancing in the network. In order to balance energy consumption in the network, there is shift the load of data transmission to different nodes in the forwarder list. The proposed work select first three nodes (sorted in descending order) according to *NPV* from the list and transmit data to each node periodically. In case of single forwarder node in the list, a new forwarder node is selected periodically according to the same procedure defined above for forwarder selection. However, this is not required frequently due to sink mobility. If the sensor node has sink in its direct transmission range, it just transmits data to sink instead of any other forwarder node. As there are deployment of multiple sinks in the network, each node find its distance with all the sinks and transmit data to the nearest one.

As mentioned earlier, transmissions at higher depth are less affected by noise therefore, single path transmissions are preferred. Whereas, high packet loss ratio due to more noise at surface demands multi-path communication. In MMS-LETR, the nodes at the boundary of each sub-layer generates binary tree by transmitting data to two neighbor nodes. Multiple copies of the same packet are transmitted along different paths. All these copies are combined at the surface sinks and the original packet is generated. The nodes within the layer transmit data to only one node. This helps to avoid excessive energy consumption, multiple redundant packets and congestion in the network.

As shown in Fig. 5.4, node *S* at the boundary of sub-layer 1 performs multi-path routing while the receiver nodes perform single-path routing as they do not lie on the boundary layer.

**Algorithm 7:** Data Transmission and Sink Mobility

---

```

1 Locationofboundarynode  $\leftarrow \Lambda$ 
2 Distancecovered  $\leftarrow \xi$ 
3 Sojournntime  $\leftarrow \tau$ 
4 Transthresholdtime  $\leftarrow \sigma$ 
5 Each sensor calculate distance with all sinks
6 Search forwarder using Eq. 5.20
7 for  $i = 1:Nodes$  do
8   if sink is within R then
9     | Set sink id as forwarder
10  else
11  | Set sensor node id as forwarder
12 procedure: DataTransmission()
13 while  $\sigma$  not expired do
14   | Transmit data to first forwarder node in the list
15   if  $\sigma$  expired then
16   | Set second highest NPV node as forwarder
17   | Repeat step 17 and transmit data to third highest NPV node
18   | Continue till  $\sigma$ 
19 if single forwarder exists then
20   | Transmit data to that node till MS is in R
21 if  $\tau$  expired then
22   | L1 sinks displace upwards and covers distance  $\xi$ 
23   | L2 and L3 sinks displace downwards and covers distance  $\xi$ 
24 Repeat steps 26 - 29 till sinks reaches opposite boundaries of layers
25 if sink arrived at opposite boundaries then
26   | Update their x-axis position accordingly
27 if senor node position  $== \Lambda$  then
28   | Perform multi-path routing

```

---

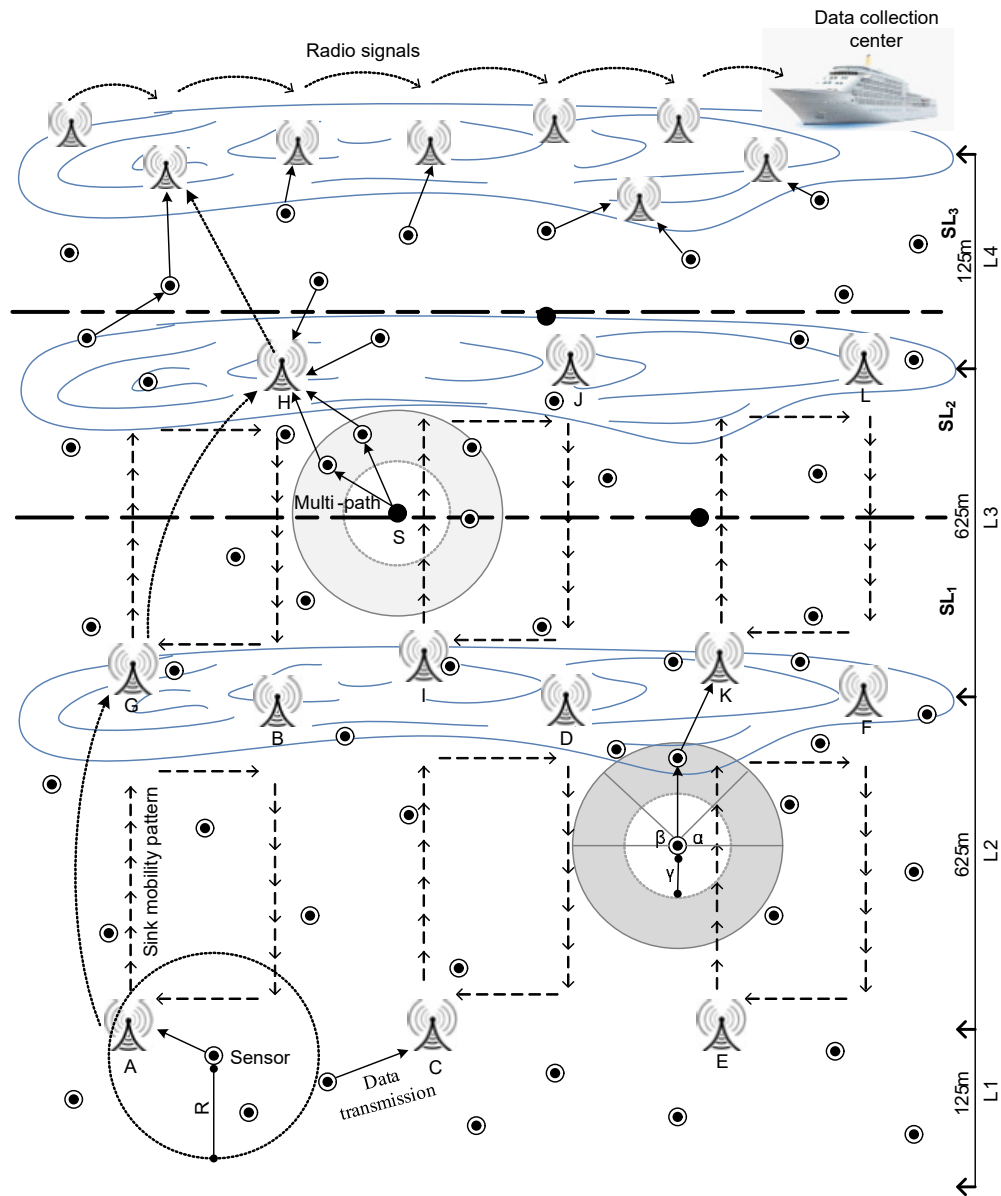


FIGURE 5.4: System model for MMS-LETR

## 5.6 Performance Evaluation

To evaluate the performance of LETR, MSGER, MSLETR and MMS-LETR against GEDAR, extensive simulations are carried out to measure the performance in terms of energy cost, total depth adjustment, packet loss ratio and the number of void nodes. The MS based protocols avoid depth adjustment therefore, it compare performance of MSGER, MSLETR and MMS-LETR against GEDAR and LETR through packet loss ratio and energy consumption. The setting of the key simulation parameters follows the related study [18] and are listed in Table 5.1. In

TABLE 5.1: Network Simulation Parameters

Option	Value
Area	1500m $\times$ 1500m $\times$ 1500m
Transmit power	2W
Reception power	0.1W
Idle state power	10mW
Transmission range	250m
Number of nodes	150 - 450
Number of sonobuoys	25
Energy for depth adjustment	1500mJ/m

simulations, the sensor nodes range from 150 to 450 and are deployed randomly in 1500m  $\times$  1500m  $\times$  1500m network field. The number of on-surface sonobuoys are 25. For fair comparison, there are deployment of same number of sonobuoys (i.e. 25) in all schemes including GEDAR. The simulation setup sets the same maximal transmission range for all nodes as 500 *m* which is divided into six levels [122] while the minimum transmission range is 250 *m*. Data rate is 50kbps. Each node generates 200 bits packet having 50 bits of control field and 150 bits of data field. For fair analysis, the simulation parameters mentioned in table 5.1 are setup for both proposed and counterpart routing protocols. Moreover, the simulation parameters are well taken to evaluate the performance metrics. For instance the range of selected number of nodes is deployed from 150 to 450 to judge the impact of node density in performance at region of interest. For transmitting packets (channel access), the sensor nodes use Carrier Sense Multiple Access with Collision Avoidance (CSMA/CA) under the non-beacon enabled mode of IEEE 802.15.4 [123]. The value of  $\alpha$  and  $\beta$  in equation 5.8 is 45 and 135 respectively.

### 5.6.1 Impact of varying node density on packet loss ratio

In Fig. 5.5, the simulations for packet loss ratio of GEDAR, LETR, MSGER, MSLETR and MMS-LETR is carried out by increasing node density. It is clear from the provided figure that the MS based schemes have only few packet losses while GEDAR has highest packet loss ratio than all the counterpart schemes.

GEDAR incorporates high packet loss ratio due to its long hop paths formed during depth adjustments in order to circumvent void regions. When the number of hops increases, acoustic channel becomes more overloaded hence packet loss ratio increases. The node displacement leads to reconfiguration of routes between the source and the destination, which degrades the network throughput. During the depth adjustment, void node and all of its predecessor nodes discard their generated packets and regenerates the packet after finding a new forwarder node. Also, if a node fails to locate any forwarder after depth adjustment, it just discards the packet. GEDAR provides no mechanism to alleviate location errors, thus, localization problem leads to packet losses. Proposed scheme LETR, dilute depth adjustment procedure with transmission range adjustment. We set an optimum range for data transmission; besides energy conservation is achieved by limiting node displacement. Another major reason behind minimum packet loss ratio in LETR is the consideration of location errors. Packet is transmitted to the node with minimum MSE, thus, the probability of packet loss decreases. In case of depth adjustment in LETR, void node displaced towards sink rather than towards bottom, this actually minimizes the node distance with sink. Therefore, node transmits its data packet through minimum hops avoiding interference and congestion. The node displacement towards sink may cause disconnection between the network nodes. However, due to transmission level adjustment, the probability of such a problem is very small as compared to the disconnectivity problem arising in GEDAR due to depth adjustment. MSGER and MSLETR protocols include the MSs, where sensor nodes transmit data directly to the MS when it is in range of the sensor node. Therefore, long hop routes and depth adjustments are not required. Hence, packet loss ratio in MS based schemes is improved than the static sink based schemes. The Fig. 5.5 clearly illustrates that the MMS-LETR provides best throughput among all the counterpart schemes by minimizing packet loss ratio. As the MMS-LETR considers noise attenuation at different depth levels and performs multi-path routing to avoid retransmissions. This diminishes the probability of packet loss ratio, thus, the throughput of network maximizes. Also, the pattern of sink mobility in MMS-LETR plays a key to improve its results.

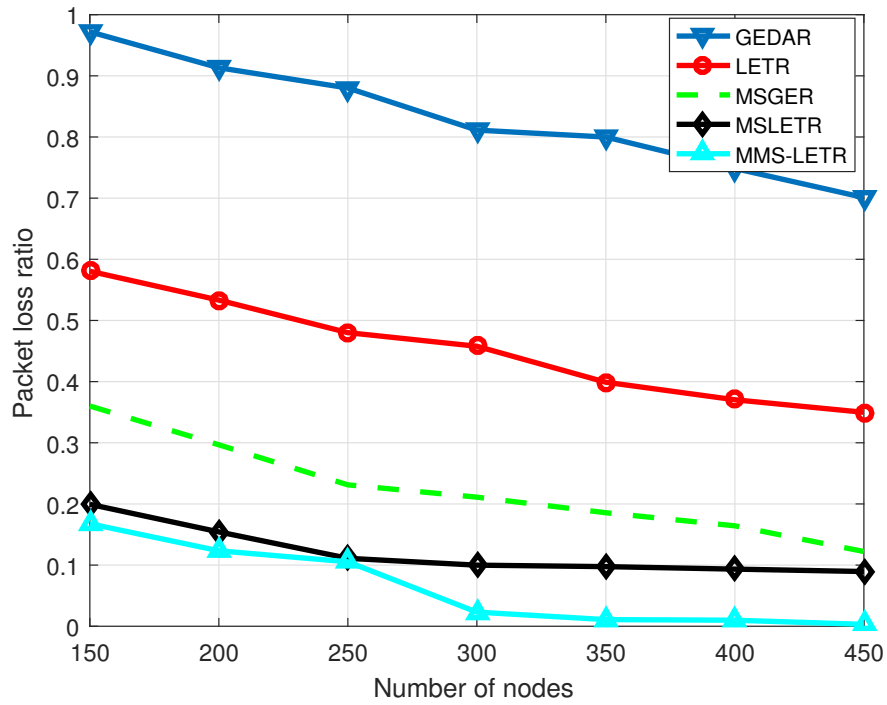


FIGURE 5.5: The ratio of packets lost during simulation

### 5.6.2 Impact of sink mobility on energy consumption

Fig 5.6 illustrates the total amount of energy consumed by sensor nodes at particular amount of time during network simulation. Provided in the Fig. 5.6, total energy consumption is highest in the network implementing GEDAR. The reason behind this behaviour is the node's displacement in case of being void node. LETR has more energy consumption than the MS based protocols because it involves multi-hop data transmission towards static surface sinks. The total amount of energy consumed by the sensor nodes in MSGER and MSLETR protocols is less than the GEDAR and LETR. However, both of the MS based protocols have almost similar amount of energy consumption. This is due to the sink movement to collect data directly from the network nodes by avoiding long distance communication. Therefore, the amount of energy consumed by all sensor nodes in the network is less against static sink based protocols.

It is evident from Fig. 5.6, MMS-LETR consumes relatively high energy than the MS based protocols like MSGER and MSLETR. The reason behind this result is the amount of energy consumed during multi-path routing. All the nodes at the

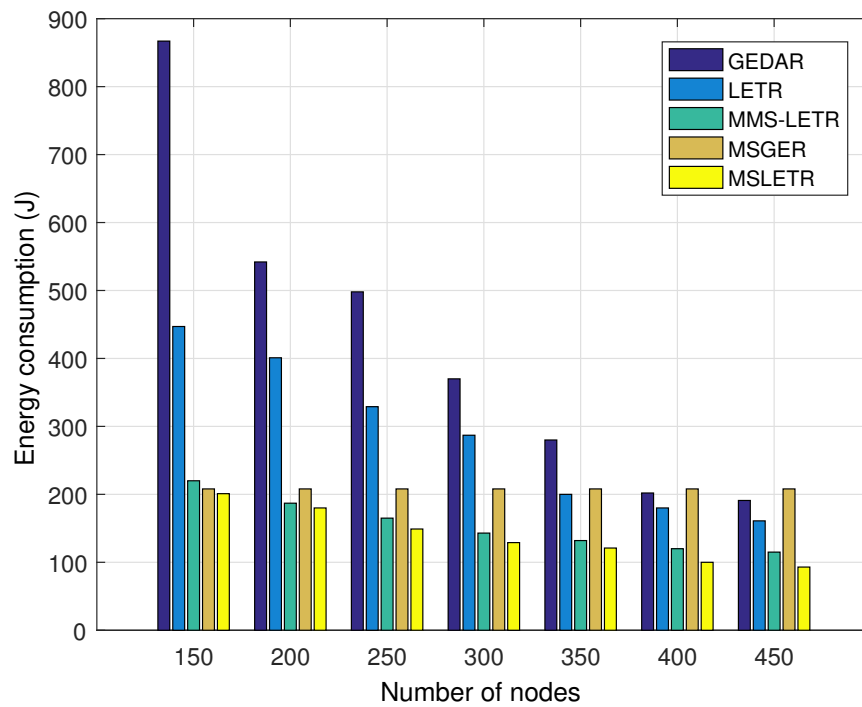


FIGURE 5.6: Energy consumption in the network field

boundary of sub-layers transmit data at two different paths in order to successfully deliver data at sink and avoid retransmissions. However, the MMS-LETR incorporates sink mobility to gather data at various intervals from numerous regions of the network. This enhances the delay, however, energy consumption is minimized and the packet delivery ratio is optimized.

### 5.6.3 Impact of depth adjustment on energy consumption

Figs. 5.7 and 5.8 illustrates the percentage of energy consumption in physical actuation and acoustic communication by the sensor nodes in both GEDAR and LETR. Energy consumption due to physical activity of sensor nodes decreases while increasing node density as shown in the Fig. 5.7. Sparse networks amalgamate more communication void regions relative to denser network fields. Therefore, more energy is consumed in depth adjustment based technique like GEDAR. When node density is 150, approximately 80 percent of total network energy is consumed in depth adjustment activity as shown in Fig. 5.7, while the graph has decreasing



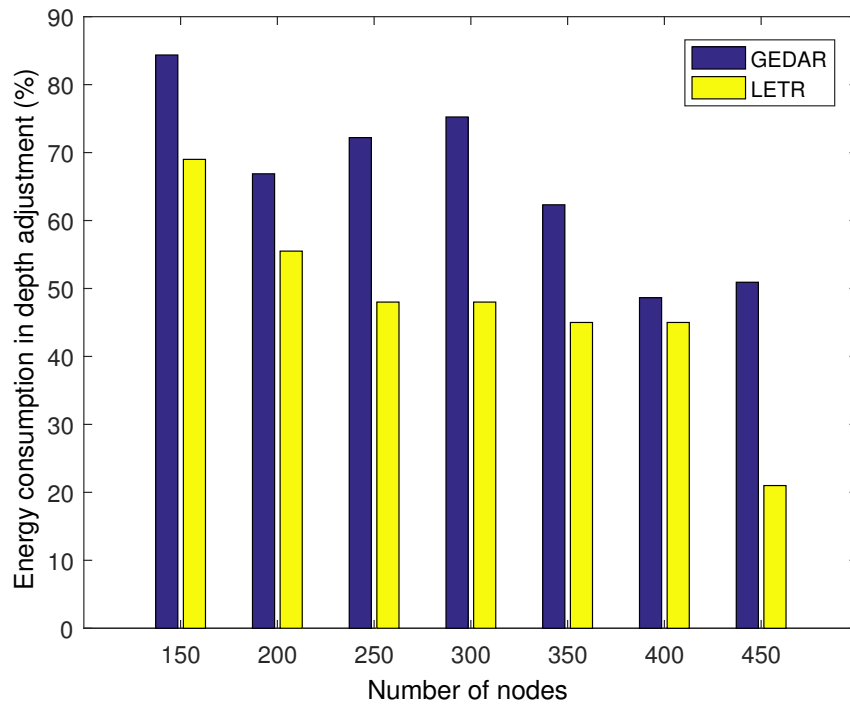


FIGURE 5.7: Percent energy consumed in depth adjustment

behaviour at higher node densities. As the node density increases, the probability of void regions decreases which ultimately leads to fewer depth adjustments. Each sensor node consumes 1.5 mJ/m during depth adjustment. Therefore, high energy is consumed in lower densities due to high depth adjustments.

In LETR, the total amount of depth adjustments in the network is very small, therefore, the energy consumption due to depth adjustment is also minimum. LETR recovers void holes using transmission range adjustment. The sensor node only displaces to a new position when it fails to find any neighbor node within its maximum transmission range. Therefore, fewer displacements are performed, leading to less energy consumption during the physical activity.

#### 5.6.4 Impact of data transmission on energy consumption

In Fig. 5.8 the proposed scheme provide comparison of energy consumption due to acoustic communication of sensor nodes in both proposed and counterpart techniques. GEDAR consumes high amount of energy in depth adjustment while fewer transmissions are possible with residual energy. Therefore, a small amount of energy is consumed in transmissions. On the other hand, if node density increases, energy consumption due to data communication also increases. The reason behind this result is the fewer displacements required at high node density. The probability of void holes is very small in denser network fields, hence, fewer depth adjustments. The maximum part of the total network energy (sum of energies of all the sensor nodes in the network) is consumed in acoustic communication. Therefore, it is observed increasing behavior of energy consumption in Fig. 5.8 at higher node densities.

On the other hand, LETR consumes a large part of network energy in useful activity i.e. acoustic communication as opposed to GEDAR. There is consideration of the energy consumed during depth adjustment as the wasted energy. The proposed scheme conserves energy by avoiding excessive energy hungry depth adjustments. Therefore, network energy is utilized in transmissions instead of just depth adjustments. As it is clear from Fig. 5.8, the energy consumption is approximately 60 percent at 150 nodes while it is more than 90 percent at 450 nodes. These results clearly show that the LETR avoid excessive depth adjustments and conserves sufficient amount of network energy for data gathering tasks. This leads to high network throughput.

#### 5.6.5 Impact of varying node density on fraction of void nodes

Fig. 5.9 plots the fraction of void nodes against total number of nodes deployed in the network field. As shown in this figure, the number of void nodes decrease with the increase in network density. LETR achieves best results due to transmission

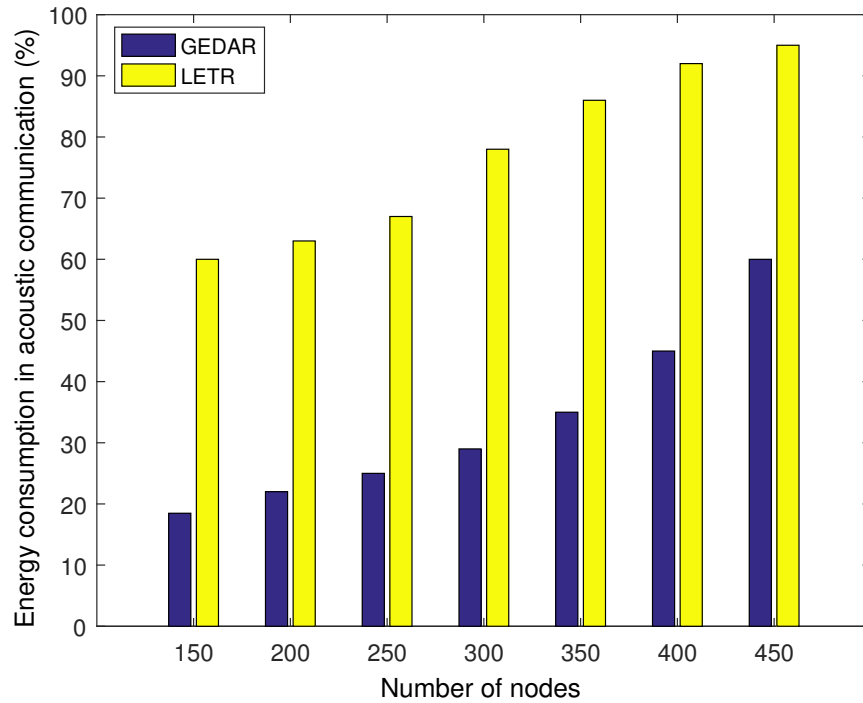


FIGURE 5.8: Percent energy consumed in communication

range adjustment and controlled depth adjustment of sensor nodes. In GEDAR, node adjusts its depth whenever it finds itself as a void node. However, each void node moves downward in order to transmit its data either through its predecessor node or any other in range node. Such displacement of nodes disturbs whole network topology and increases the probability of void nodes in the network. Also, nodes always adjust their depth down towards bottom which increases its distance with surface, hence long hop paths and high energy consumption of sensor nodes further leads to high fraction of void nodes in GEDAR. On the other hand, when LETR is applied, the proposed transmission range adjustment along with depth adjustment mechanism reduces 85 percent the fraction of void holes at medium and high node densities. Each sensor node checks for its forwarder by adjusting its transmission range level within its maximum transmission range which lends to energy conservation. The proposed scheme incorporates controlled depth adjustment when a sensor node fails to locate any forwarder within its maximum transmission range level. As opposed to GEDAR, the proposed scheme perform depth adjustment in bottom up fashion to increase the chances of finding forwarder

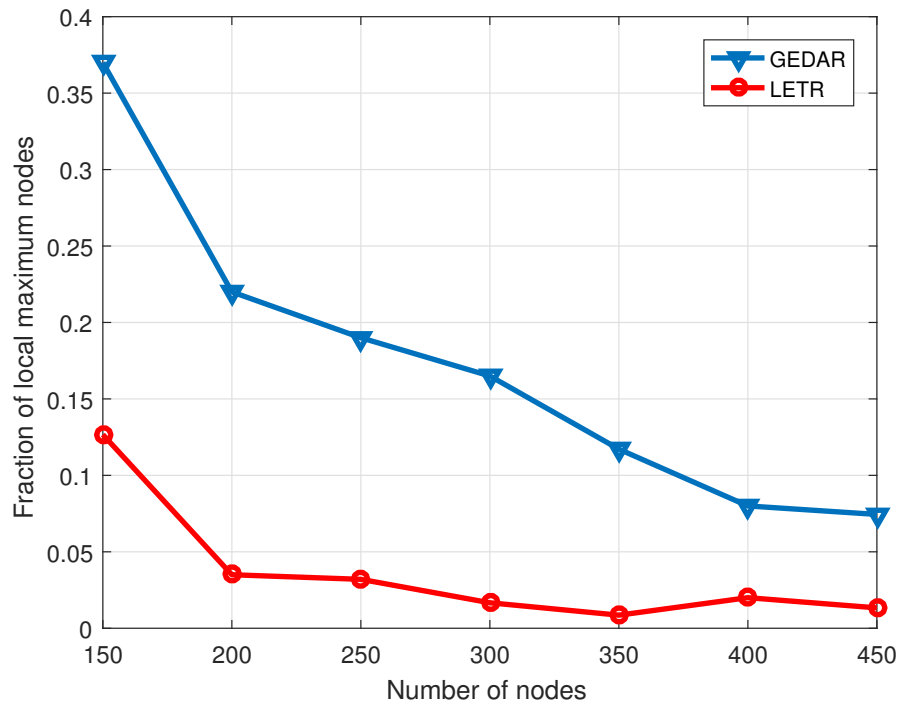


FIGURE 5.9: Fraction of void nodes

nodes. This may increase a node's probability to be in sink vicinity. Thus, fraction of void nodes decreases in proposed scheme.

### 5.6.6 Impact of varying node density on node displacement

Fig. 5.10 provides the total depth adjusted by the network nodes. As corroborated by Fig. 5.10, the amount of displacement decreases while increasing node density. In sparse scenarios, more void areas exist whereas in dense networks the probability of occurrence of void regions decreases due to less distance between nodes. Fig. 5.9 supplements results and discussion in this section. The difference between amount of depth adjusted by GEDAR and LETR is quiet large. The reason behind such a difference is the depth adjustment as the second priority in case of void nodes. Most of the times, sensor nodes find their neighbors by adapting various transmission range levels, therefore, the necessity of depth adjustment reduces in LETR.

In GEDAR, the total depth adjustment is very high as compared to LETR. Each

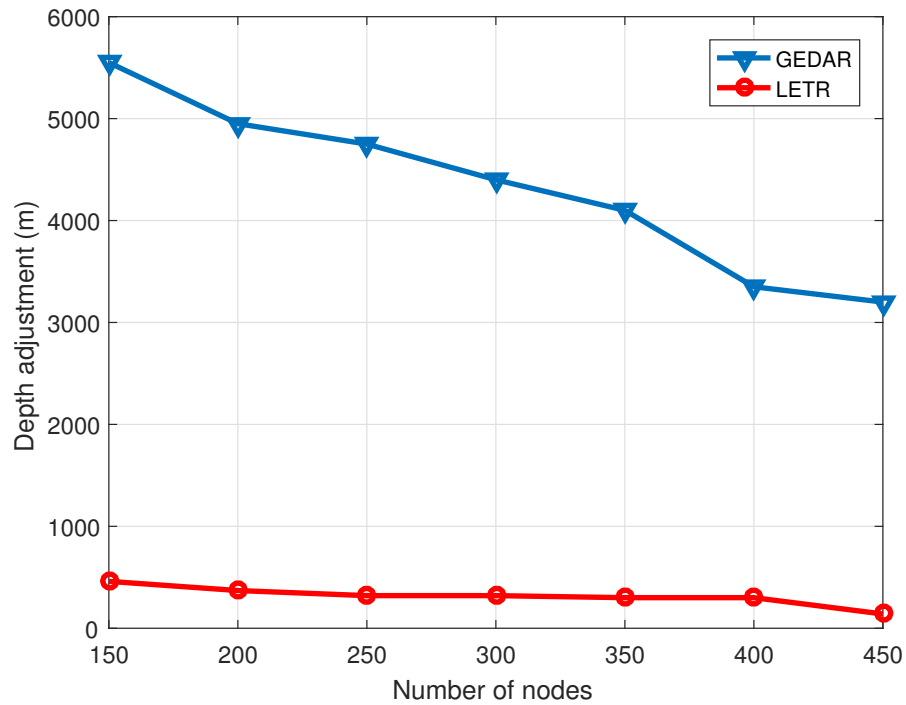


FIGURE 5.10: Depth adjustments in the network

node moves to a new location whenever it locates itself in a communication void region. Also, every void node adjusts its depth until it finds a forwarder node or it has no space for further displacement. This sufficiently increases the amount of displacement of sensor nodes in the network. LETR implements transmission range adjustment in order to avoid long displacements of sensor nodes in the network. The proposed scheme implements depth adjustment technique only when a node is unable to find any forwarder node within its defined maximum vicinity. Thus, sensor nodes become successful to find their suitable forwarder within their maximum transmission range. However, when the nodes start dying due to their energy depletion, network becomes sparse hence finding forwarder within maximum transmission range becomes difficult, consequently, node adjusts its depth. Therefore, the proposed scheme requires fewer depth adjustments to conserve energy, increase throughput and prolong network functioning time.

## 5.7 Conclusion

In order to make geographic routing protocols more energy efficient and suitable for large scale networks, it is necessary to cope with location errors. Consideration of noise attenuation is also another major factor to improve the performance of routing protocols. This chapter presents geo-opportunistic routing algorithms for void hole avoidance using transmission range and depth adjustment technology. The transmission range adjustment technique helps to avoid void holes while depth adjustment is only applied in extreme scenarios where a sensor node fails to find any neighbor within its maximum transmission range. This helps to reduce the packet drop rate. A major contribution of this work is to tackle location errors in traditional geographic routing along with void hole avoidance. The proposed scheme calculate MSE to mitigate the effects of localization errors on forwarder selection and data transmission. The controlled depth adjustment significantly conserves energy consumption and contributes to more data transmissions in the network. Instead of node displacement towards bottom of water, this system adjust node depth towards sinks at the surface. It reduces the distance of node with sink and the chances of frequent network topology readjustments, thus energy consumption is reduced and network lifetime prolongs. Another major contribution of this work is the MMS-LETR protocol which considers noise attenuation to eliminate retransmissions. The defined sink mobility patterns provides maximum network coverage, which minimizes packet loss ratio. The proposed scheme introduced sink mobility in both GEDAR and LETR to reduce packet loss ratio and improve energy efficiency. The simulation results prove that the location error resilient void hole avoidance technique increases network throughput and conserves energy as compared to traditional geographic routing techniques. The proposed technique cope with localization errors, thus packet drop rate is reduced. Consequently, LETR improves the network performance against a depth adjustment based geographic routing protocol, GEDAR at varying node densities. On the other hand, MS based protocols further improve the performance in terms of packet loss ratio and energy consumption.

All routing protocols explained in previous chapters were developed to achieve better lifespan of the network. It is however ignored to realize the residual energy of the forwarding node. Along with this there are no mechanisms incorporated to cope with the imbalance between the holding time difference and propagation delay of packet between nodes. For this reason, an Energy Scaled and Expanded Vector Based Forwarding (ESEVBF) scheme is proposed.

## Chapter 6

# An Energy Scaled and Expanded Vector-Based Forwarding Scheme for Underwater Acoustic Sensor Networks with Sink Mobility

### 6.1 Summary of the Chapter

Underwater Acoustic Sensor Networks (UASNs) come with intrinsic challenges like long propagation delay, small bandwidth, large energy consumption, three-dimensional deployment, high deployment and battery replacement cost. Any routing strategy proposed for UASN must take into account these constraints. The vector based forwarding schemes in literature forward data packets to sink using holding time and location information of the sender, forwarder and sink nodes. Holding time suppresses data broadcasts; however, it fails to keep energy and delay fairness in the network. To achieve this, the research propose an Energy Scaled and Expanded Vector-Based Forwarding (ESEVBF) scheme. ESEVBF uses the residual energy of the node to scale and vector pipeline distance ratio to expand the holding time. Resulting scaled and expanded holding time of all



forwarding nodes has a significant difference to avoid multiple forwarding, which reduces energy consumption and energy balancing in the network. If a node has a minimum holding time among its neighbors, it shrinks the holding time and quickly forwards the data packets upstream. The performance of ESEVBF is analyzed through in network scenario with and without node mobility to ensure its effectiveness. Simulation results show that ESEVBF has low energy consumption, reduces forwarded data copies, and less end-to-end delay.

## 6.2 Introduction

Most of the vector based routing schemes proposed for the UASN employ holding time that is distributively computed by each node using the local node or network parameters, e.g., distance to sink, proximity to the center of the virtual pipeline between the sender and sink, distance to the previous hop sender and the receiving node, etc. First, nodes check either they are within the virtual pipeline or not. Once a node ensures that it is located within the virtual pipeline, then it estimates the holding time. Holding time is estimated every time when a node receives the first copy of the packet from downstream nodes. The timer is triggered and its duration is set to the estimated holding time period. Once the timer expires and if that node does not receive any other copy from its neighbors, it will forward the packet and all the other nodes will suppress the packet forwarding. A preferable forwarder must have the smallest holding time compared to its immediate neighbors and is desirable to forward the packet.

For example, to avoid long propagation delays, vector based routing schemes consider node's proximity information between the sender and the sink node, and nearness to the pipeline center in the holding time. It is projected that the packet forwarding through these nodes reduces the end-to-end delay. However, all communication through these nodes will deplete their energy and result in a void energy hole problem. Therefore, the energy fairness should be achieved among all the nodes within the vector as well as in the network. Hence, the energy factor

must be considered in the holding time computation to increase network lifetime. Nevertheless, the nodes with sufficient energy do not guarantee the shortest path (with small end-to-end delay) between sender and sink. On the other hand, better forwarding decisions or precise holding time estimation can be attained if an updated network state (complete or partial network) information is available at each node in the network. This network state information availability is possible through the exchange of control packets, which again impacts the bandwidth, energy, and inflates the error rate. Hence, any forwarding scheme for UASN must consider the constraints and provide the mediated solution. Additionally, the difference between holding times estimated by all the immediate neighbors should be larger than the propagation delay between them to properly suppress the unnecessary packet forwarding. Otherwise, many copies of the same packet will be forwarded in the network.

It is a well established fact that the acoustic signal consumes more energy and experiences a very long propagation delay and channel error in the aquatic environment [124]. The propagation delay and energy consumption increases drastically if the farthest acoustic node in the network needs to communicate data towards the sink that placed at the fixed location. In order to efficiently collect data, different schemes in literature adopt sink mobility. Mobile sink, also called mobile station, can be any node that moves in the aquatic environment either autonomously, e.g., autonomous underwater vehicle (AUV) [125], over the anchored rope, vessel, etc. The mobile sink is considered to have sufficient available resources to roam in the network (frequent refuelling and/or recharging). Hence, any routing scheme proposed for the UASN must also be analyzed in the mobile sink UASN scenario to verify its effectiveness.

### **6.2.1 Contributions**

Inspired from the above discussion, this research proposed a novel energy scaled and expanded vector based forwarding (ESEVBF) for UASNs. ESEVBF estimates

holding time of the potential forwarders by keeping the following points under consideration.

1. The holding time of all the potential forwarders is scaled using the neighboring nodes' energy information. It increases the holding time *difference* between them even for a small variation in the energy level of neighbors.
2. The expanded proximity closeness ratio of the forwarding candidate nodes towards the virtual pipeline between sender and sink is added in holding time computation to signify the node preference<sup>1</sup>.
3. Each candidate forwarder uses its neighboring node information to find suitability to abbreviate its holding time duration to curtail the end-to-end delay.
4. Energy efficiency and energy balancing are achieved by employing the normalized residual energy information of the neighboring nodes in the holding time and suppressing more number of packets.
5. No constant parameters in the holding time estimation are used.
6. The proposed scheme is analyzed in the network scenarios with and without sink mobility.

The simulation results show that ESEVBF improves energy efficiency and reduces end-to-end delay without compromising the reliability compared to its counterpart, AHH-VBF.

The organization of the remaining chapter is as follows: In Section 6.3, holding time and the working principle of ESEVBF is described. Simulation analysis in terms of energy consumption, end-to-end delay, the number of copies of data packets, packet delivery ratio, and average hop count, in the underwater network without and with sink mobility, is performed in Section 6.4. Finally, the discussion is concluded in Section 6.5.

---

<sup>1</sup>Both 1) and 2) scale and signify the holding time difference between the candidate forwarders for small parameter variance. This ensures that all nodes in the transmission range of the suitable forwarder (with minimum holding time) must receive copy of the packet before their holding time expiration.

## 6.3 Proposed Scheme

This section, present the detailed discussion of proposed scheme. The proposed scheme is compared with the AHH-VBF that uses the holding time  $HT_p^i$  of node  $i$  to forward packet  $p$  towards the Sink  $D$ . The  $HT_p^i$  suppresses extra copies of  $p$  by selecting the potential forwarder  $i$  using its projection distance from the center of the virtual cylinder or pipeline<sup>1</sup>, distance towards  $D$ , and distance from the node  $S$  (a node from which  $i$  received a copy of  $p$ ). AHH-VBF adaptively adjusts the transmission power and radius of the virtual cylinder to its maximum distance mobile neighbor. In contrast to AHH-VBF, the proposed scheme estimates  $HT_p^i$  based on the normalized residual energy scaled distance from  $S$ , expanded distance from the virtual cylinder's centerline, and distance towards  $D$ . The resultant  $HT_p^i$  prioritize the nodes that have large residual energy, near the center of the virtual cylinder, and least distant to  $D$ . In addition to that, it also increases the difference between holding times of all nodes in the potential forwarding zone to suppress more copies of  $p$ . In result, the packet collision at next hops can be avoided and network energy can be conserved to maximize the network lifetime.

### 6.3.1 Problem Statement

When a node  $S$  transmits the data packet (either that data packet is generated by that node or received from the downstream sensor nodes.), all the neighboring nodes within its  $T_r^S$  and in the  $PFZ$ , receive that packet. Now, the question arises that which node(s) has(ve) to further transmit or relay the packet in upstream direction? The answer to this question is the holding time,  $HT$ . Upon successful reception of packet  $p$ , a node  $i$  computes the  $HT_p^i$  and starts the timer. During  $HT_p^i$  is on,  $i$  does not forward the packet. However, node  $i$  can receive data packets from its neighboring nodes, which may be copies of  $p$  or other data packets. When node  $i$  receives additional one or more than one copies of  $p$  while  $HT_p^i$  did not expire, then it suppresses the transmission of  $p$ . On the contrary, if  $HT_p^i$  expires and no

<sup>1</sup>The terms virtual pipeline or virtual cylinder are interchangeably used in the context of this chapter.

copies of packet  $p$  have been received during the  $HT_p^i$  period, then  $i$  forwards the packet  $p$ . This simple phenomenon alleviates the extra broadcast overhead, which is necessary for the UASN scenario where energy and bandwidth are the scarce resources. However, UASN has an added feature that must be considered while designing the holding time, which is the long propagation delay.

Consider a scenario where multiple nodes in the  $PFZ$  receive  $p$ , then all nodes in  $PFZ$  will calculate their respective holding time  $HT_p^i$ . If the number of nodes in  $PFZ > 1$ , then the difference between their holding times must be greater than the propagation delay between them. Let, holding time of nodes 1 and 2 in  $PFZ$  for data packet  $p$  is  $HT_p^1 = 1.2s$  and  $HT_p^2 = 1.3s$ , refer Fig. 6.1. And let the propagation delay between both the nodes 1 and 2 is  $\frac{D_2^1}{v_s} = 0.2s$ , where  $v_s$  is the acoustic signal speed in the aquatic environment. In this scenario, node 1 will forward the packet after  $1.2s$ , however, due to a long propagation delay and the short holding time difference, 2 will not receive the copy of  $p$  from node 1 and its  $HT_p^2$  will expire. Hence, 2 will also forward the packet  $p$ . Similarly, any other node(s) in the  $PFZ$  that has/ve holding time difference less than the propagation delay between them, will also forward(s) the packet  $p$ . Therefore, even by applying the holding time, multiple copies of the same packet will be forwarded by the nodes in the  $PFZ$  that will impact the energy consumption as well as the packet collision at the next hop receiving nodes, e.g.,  $n_i$  in the network scenario shown in Fig. 6.1.

From the above discussion, it is observed that there is a close relationship between the holding time difference between the close proximity neighbors, especially in the underwater communication scenario. This relationship is shown Fig. 6.2. A well-established fact about the underwater acoustic networks is its long propagation delay that is one of its limitations to be considered by any packet forward scheme. The figure also shows that the propagation delay between node  $i$  and  $j$ ,  $\tau_{(i,j)}$ , that is directly proportional to the distance between them. It is obvious that if the difference between the holding time of node  $i$  and  $j$  for packet  $p$ ,  $HT_p^i - HT_p^j$ , is greater than the  $\tau_{(i,j)}$ , then the packet suppression can be achieved. Otherwise, if the  $HT_p^i - HT_p^j < \tau_{(i,j)}$ , then multiple copies of  $p$  will be broadcasted in the network. The shaded area in the figure is the duplication zone. This can easily be avoided

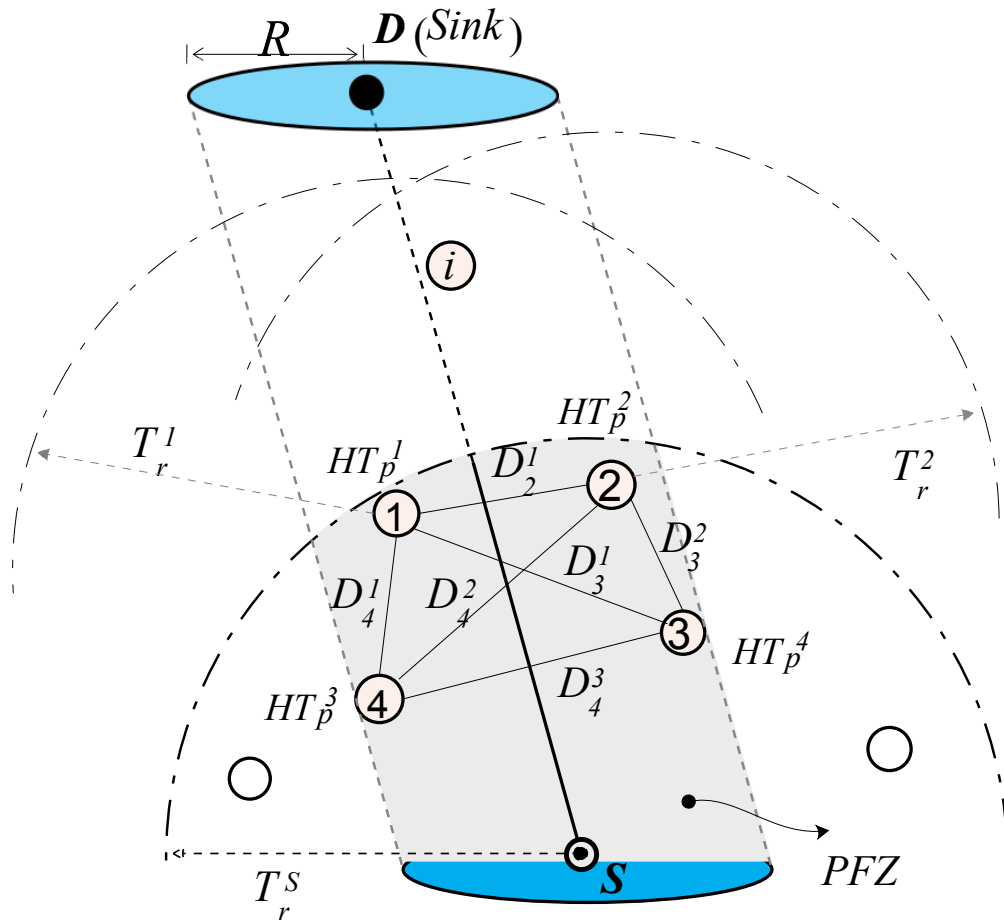


FIGURE 6.1: Holding Time and PFZ scenario

when the holding time difference is larger than the propagation delay. One of the drawbacks of the larger holding time is the long end-to-end delay that should be avoided in holding time-based forwarding schemes.

Based on the above discussion, this research presents the new packet forwarding scheme that suppresses the data packet broadcast storm by adapting the novel energy scaled and expanded holding time estimation and neighbor information based data forwarding in the underwater acoustic networks. A detailed discussion about the proposed holding time computation and the forwarding schemes is discussed below.

### 6.3.2 Preliminaries

Following is the brief description of the notations that have been used in the proposed forwarder selection scheme.

- *Neighbors of node  $i$ , ( $\xi_i$ ):* All the nodes that are in  $T_r^i$  form which  $i$ .

$$\xi_i = \{j \in \mathcal{N} \mid D_j^i \leq T_r^i\} \quad (6.1)$$

where  $\mathcal{N}$  is the set of nodes in the network and  $D_j^i$  is the Euclidean distance between  $i$  and  $j$  in three-dimensional Euclidean space:

$$D_j^i = \sqrt{(x_i - x_j)^2 + (y_i - y_j)^2 + (z_i - z_j)^2} \quad (6.2)$$

- *Potential Forwarding Zone (PFZ):* PFZ is the region of between node  $S(x_S, y_S, z_S)$  (that currently forwarded the packet  $p$ ) and Sink  $D(x_D, y_D, z_D)$ . PFZ is the subregion of  $T_r^S$  of node  $S$  and the nodes in the region are called potential forwarder nodes (PFNs), which are preferable to further relay  $p$ . Any point in 3D euclidean space  $f(x_f, y_f, z_f)$  is considered to be in the PFZ of  $S$ , if it satisfies the following conditions:

$$\begin{aligned} D_D^f &< D_D^S, \\ D_S^f &< T_r^S, \text{ and} \\ z_f &\leq z_S. \end{aligned}$$

Neighbors of node  $i$  that are in PFZ of  $S$ :

$$\chi_i = \{n_i \in \xi_i \mid D_{n_i}^i \leq T_r^i \wedge D_S^{n_i} \leq T_r^S \wedge z_{n_i} \leq z_S\} \quad (6.3)$$

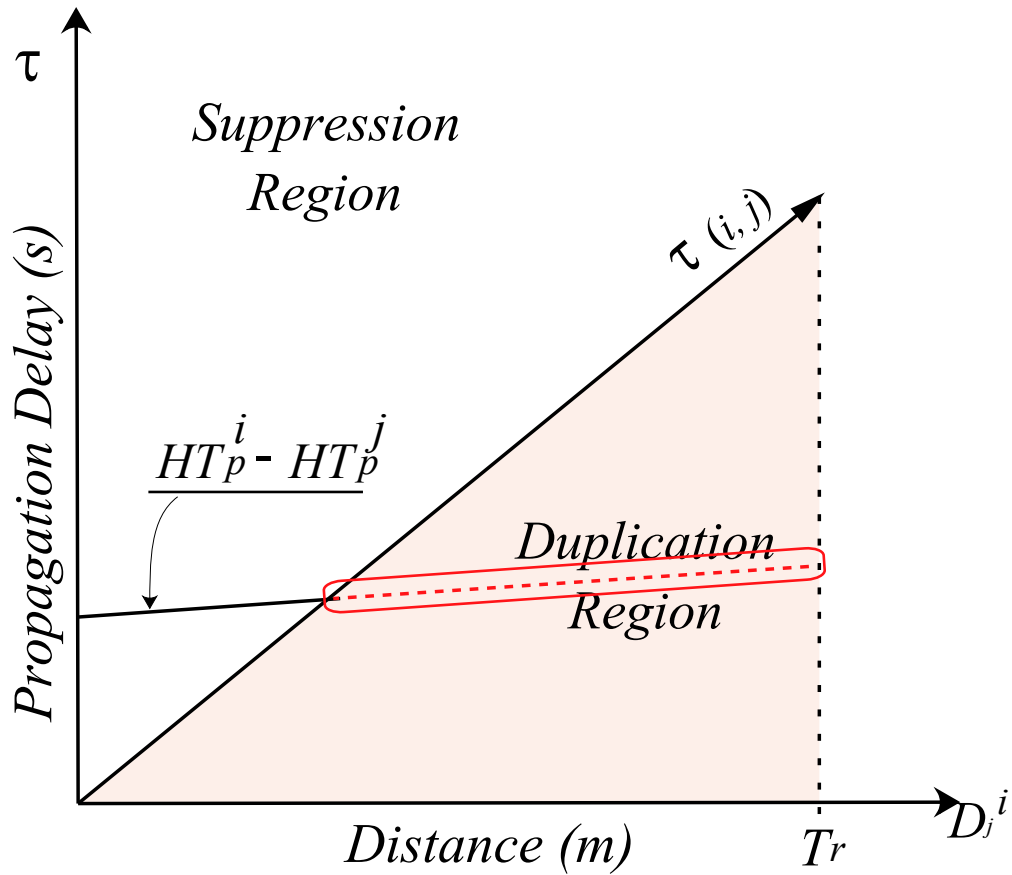


FIGURE 6.2: Relationship between holding time difference and broadcast suppression in the underwater networks

### 6.3.3 Estimation of $HT_p^i$

Every node  $i$  that is within the  $PFZ$  first computes its holding time  $HT_p^i$ , when it receives the packet  $p$  from  $S$  as follows:

$$HT_p^i = \alpha + \beta + 1 - \overbrace{\left( \frac{D_D^S - D_D^i \cos(\theta_i)}{T_r^S} \right)}^{\gamma} \quad (6.4)$$

The first factor of  $HT$  expression,  $\alpha$ , considers the distance of potential forwarder from the edge of the  $T_r^S$  that is scaled with the inverse normalized residual energy of the node. Any node that is closest to the edge of the  $T_r^S$  and has the maximum residual energy will be logically preferable forwarder and  $\alpha$  is computed as:



$$\alpha = e^{(-E_i)} \left( \frac{T_r^S - D_S^i}{v_s} \right) \quad (6.5)$$

where

$$E_i = \frac{e_i - e_{min}}{e_{max} - e_{min}}$$

$$e_{min} = \min(e_j | \forall j \in \chi_i)$$

$$e_{max} = \max(e_j | \forall j \in \chi_i)$$

$$E_i \in [0, 1]$$

The energy of a node is relatively normalized to all the neighboring nodes' residual energy in that are neighbors of  $i$  and in PFZ. The node with maximum residual energy within the neighborhood, including the current forwarding node, will have the  $E_i = 1$  and vice versa. In AHH-VBF, this factor increases the chances of node  $i$  to become potential forwarder if it is at the edge of the of  $T_r^S$ . On the contrary, the proposed scheme scales this parameter using the scaled residual energy of node  $i$ . The  $e^{(-E_i)}$  element in  $\alpha$  decreases overall  $HT_p^i$  of node  $i$  with larger residual energy and makes it more suitable candidate to forward  $p$ .

The next factor of the  $HT$ ,  $\beta$ , is the ratio of the projection distance  $P_i$  of the potential forwarding node  $i$  from the centerline of the virtual cylinder with radius  $R$ . This centerline connects nodes  $S$  and  $D$  that are at the center of the lower and upper faces of the cylinder. Nodes that are furthest from this centerline are not desirable as forwarders and their  $HT$  must be larger than the one that are closer the centerline. To achieve this, AHH-VBF just takes the ratio of  $P_i$  and  $R$ ,  $\beta = \frac{P_i}{R}$ , which returns the value of  $\beta$  within the closed interval  $[0, 1]$ . However, the value of  $\beta$  should be expanded to widen this value to easily avoid multiple data transmissions as:

$$\beta = \tan \left( \frac{P_i}{R} \right) \quad (6.6)$$

where  $P_i$  is estimated as:

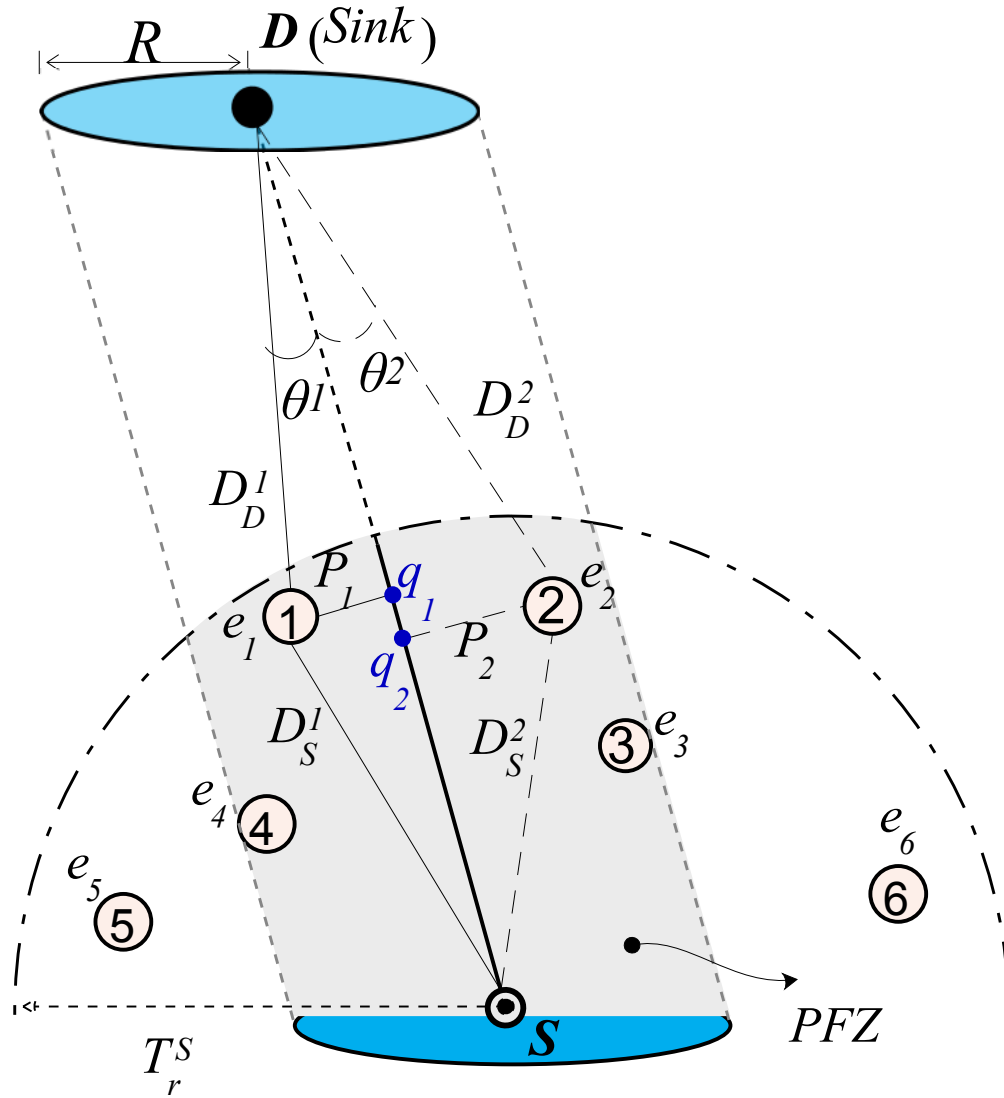


FIGURE 6.3: Holding time estimation parameters and scenario

$$P_i = (2 \times A) / D_D^S,$$

$$A = \sqrt{\rho \times (\rho - D_D^S) \times (\rho - D_D^i) \times (\rho - D_S^i)}, \text{ and}$$

$$\rho = \left( \frac{D_D^S + D_D^i + D_S^i}{2} \right).$$

The last factor of the  $HT$ ,  $\gamma$ , projects the distance of the potential forwarder towards the sink. Any node in  $PFZ$  that is closer to the sink is a suitable to be the next potential forwarder. The  $\gamma$  of all the nodes in  $PFZ$  is between  $[0,1]$ .

In this factor, the element  $D_D^i \cos(\theta_i)$  results the distance between the projection point  $q_i$  on the centerline and the Sink node. Here,  $\theta_i$  is calculated as:

$$\theta_i = \cos^{-1} \left( \frac{D_D^{S^2} + D_D^{i^2} + D_S^{i^2}}{2 \times D_D^{S^2} \times D_D^i} \right) \quad (6.7)$$

The ratio of the difference between  $D_D^S$  and  $D_D^i \cos(\theta_i)$  and  $T_r^S$  will be high when node  $i$  is closer to the sink and vice versa. Subtraction of that ratio from 1 will have a very small increment in the holding time of node  $i$  if it is closer to the sink node, enables node  $i$  to be more suitable forwarding candidate. On the hand, the holding time of node  $i$  will be sufficiently increased when it is far from the sink and closer to  $S$ . In order to efficiently forward the data packet, multiple packets are exchanged between nodes to maintain 1-hop neighboring state at each node. These packets include neighbor request (**NEIGH\_REQ**), neighbor acknowledgment (**NEIGH\_ACK**), and **data** packet. The structure, header format, and the purpose of all those packets is similar to the one that is used in [65]. Similarly, the same set of steps are followed by proposed scheme when it receives **NEIGH\_REQ** and **NEIGH\_ACK**. Because the prime objective of this research is to select more suitable data packet forwarders, hence, a new set of steps proposed when **data** packet is received by node  $i$ . Detailed working principle of proposed **data** packet forwarding algorithm is shown in Algorithm 1.

When node  $i$  receives data packet  $p$ , it first checks, whether the packet is already in the Packet Queue ( $PQ$ ), waiting to be forwarded or not. In case of no packet found in  $PQ$ , timer for that packet is not active, and  $D$  is in  $T_r^S$ , then  $i$  checks its position that either  $i$  is PFZ or not. Accordingly, node  $i$  computes its  $HT_p^i$  and initiates the timer  $Timer_p$ . During the  $Timer_p$  is active, node may receive multiple copies of  $p$  form other nodes and records the number of copies received. Once the  $Timer_p$  expires, node  $i$  forwards the **data** packet if it received only single copy of the packet, otherwise, it drops and removes the packet from  $PQ$ .

To conclude this subsection, this research have proposed the holding time that uses an energy scaled closeness to the edge of the  $T_r^S$ , expanded proximity to

**Algorithm 8:** Algorithm 1: Proposed data Packet Forwarding Algorithm

---

```

1 Output: Forward or Drop  $p$ 
2 Input: Node  $i$  receives  $p\{ID_p, S(x_S, y_S, z_S), T_r^S, e_S, DATA\}$ 
3  $PQ(m, c) =$  Packet Queue //  $m$  : Packet,  $c =$  Copies of  $m$ 
4
5  $\xi_i =$  Neighbor List of  $i$ 
6  $\chi_i =$  Neighbor List of  $i$ 
7  $Timer_m =$  Timer for packet  $m$ 

8 if  $\{p$  is not in  $PQ\}$  then
9   Add  $p$  in  $PQ$  and Set  $c = 1$ 
10  if  $Timer_p$  is OFF then
11    get  $T_r^S$  from  $p$ 
12    get Loc( $S$ ) from  $p$ 
13
14    if  $D_D^S > T_r^S$  then // Sink  $D$  is not in  $T_r^S$  of  $S$  */
15      Compute  $P_i$  using Loc( $S$ ), Loc( $D$ ) and Loc( $i$ )
16      if  $P_i < W$  then
17        Compute normalized  $E_i$ 
18        Calculate  $HT_p^i$ 
19        if  $HT_p^i < \min\{HT_p^j | \forall j \in \chi_i\}$  then
20          Set  $Timer_p = HT_p^i / 2$ 
21        else
22          Set  $Timer_p = HT_p^i$ 
23        Start  $Timer_p$ 
24        Call TimerExpire
25
26  Drop  $p$ 
27  Remove  $p$  from  $PQ$ :  $PQ = PQ \setminus p$ 
28  Exit
29 else
30   Drop ( $p$ )
31   Increment  $c$ 
32   Update  $\xi_i$ 
33   Exit

1 Procedure TimerExpire( $p, PQ$ )
2 if  $p$  in  $PQ$  and  $c > 1$  then
3   Remove  $p$  from  $PQ$ :  $PQ = PQ \setminus p$ 
4   Exit
5 else
6   Update  $(x_i, y_i, z_i), T_r^i$ , and  $e_i$  in  $p$ 
7   Forward  $p$ 
8   Remove  $p$  from  $PQ$ :  $PQ = PQ \setminus p$ 
9 return

```

---

the centerline of the cylinder between  $S$  and  $D$ , and adjacency towards the sink node. Collective, all those factors are necessary for the selection of the appropriate forwarder.

## 6.4 Results and Analysis

In this section, the detailed simulation analysis of the proposed scheme in contrast to the conventional AHH-VBR scheme is proposed. To fairly evaluate the performance of both the schemes, we simulated an underwater 3D network of  $2km \times 2km \times 4km$  area, where  $X_{max} = Y_{max} = 2km$  and depth of  $Z_{max} = 4km$ . The network size of 200 to 450 nodes has been simulated with the varying transmission ranges, ranging from 500m to 900m to demonstrate the sparse and dense network scenarios. In each simulation trial, the nodes are deployed randomly in the said network area and every individual sensor node acts as a data source (generates data packets) as well as a forwarder node. The position of the Sink node is static during the whole simulation course. Sink node is positioned at the water surface and at the center of the network area with coordinates  $(X_{max}/2, Y_{max}/2, 0)$ . All nodes are homogeneous in terms of transmission range in every trial and are assigned initial energy  $E_0$  as  $E_{min} + rand(E_{rand})$ , where  $E_{min} = 50j$  and  $E_{rand} = 30j$ . A single network scenario for a given transmission range and network size is simulated 100 times. Therefore, all distinct points in the graphs of the simulation results are an average of 100 simulation trials.

The payload size of the data packet, neighbor request, and acknowledgment packets are  $70 \times 8$  bits, 64 bits, and 112 bits, respectively. The common header of 88 bits is used for all packet types in simulation. In addition to that, the data rate of  $16 \times 10^3$  bits per second and the underwater acoustic delay propagation delay of 1500m has been set in the simulations. Network is static during the complete simulation period. In last, the pure ALOHA is used at MAC layer because it is not susceptible to delays and does not use any collision detection and the avoidance mechanism.

As stated earlier in a brief discussion about the conventional AHH-VBF, it ensures the packet forwarding reliability by setting the minimum forwarder threshold,  $\tau$ , which depends upon the error probability, the packet collision rate, and the size of the packet. However, in simulations, AHH-VBF considered  $\tau \geq 2$ , which indicates that there should be at least two or more than two forwarders in the forwarding region. This ensures the reliability as well as the collision probability at the next hop forwarder(s). Additionally, it consumes more energy and utilizes more bandwidth, which is the scarce resource of the UASN. This situation can easily arise when the holding time difference between two or more than two forwarders is very negligible or smaller than the propagation delay between them. On the contrary, proposed scheme intends to avoid multiple transmissions of the data message towards the upstream direction, to save energy and avoid collision at upstream receivers. In short, the proposed scheme not only selects the spatially suitable but also the energy-rich acoustic node among the forwarders pool. Hence, the fair performance comparison is achieved by setting  $\tau = 1$  and analyzing the packet suppression count or the number of forwarders count and energy consumption. During all simulation scenarios, there are 200 data sources that generate data packets destined to Sink node. The same number of data sources is used for the large network size scenarios with the intention to find the impact of identical data traffic on network performance.

The simulation results are analyzed for two underwater network scenarios: One with the static Sink, which is placed on the sea surface at the fixed location and the other where the Sink is mobile. In the static Sink scenario, the Sink is placed at  $(X_{max}/2, Y_{max}/2, Z = 0)$  coordinates. On the contrary, in the mobile Sink network scenario, the sink moves vertically from the sea surface towards the seabed with a constant speed,  $sp = 5m/s$ . However, its  $X$  and  $Y$  coordinates remain constant. Once the sink reaches the seabed, it floats upward towards the sea surface with the same speed. Example sink mobility scenario is shown in Fig. 6.4, where sink moves vertically through the cable holding the anchored surface buoy. The primary objective of considering the Sink mobility scenario is the test performance of the proposed scheme in diversified network paradigms.

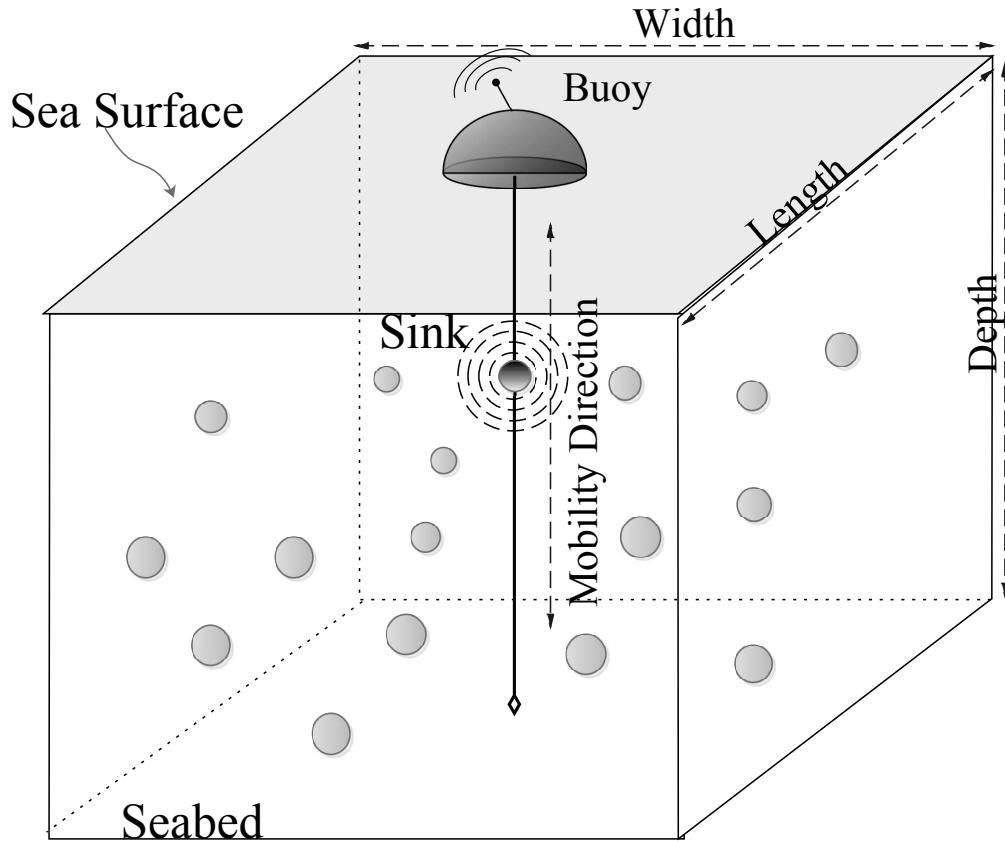


FIGURE 6.4: Mobile sink network scenario

### 6.4.1 Performance Metrics

Following is the brief description of the performance metrics that are analyzed through simulations.

- *Total forwarded copies of data*: represents the number of copies forwarded in the network for all data packet transmissions initiated by the source nodes.
- *Number of dead nodes*: is the total number of nodes that could not participate in the data forwarding process because they have residual energy less than the transmission energy.
- *End-to-end delay*: is the cumulative delay experienced by the data packet between its source and the sink node.
- *PDR (Packet Delivery Ratio)*: is the ratio of successfully received data packets by sink over the total number of generated data packets.

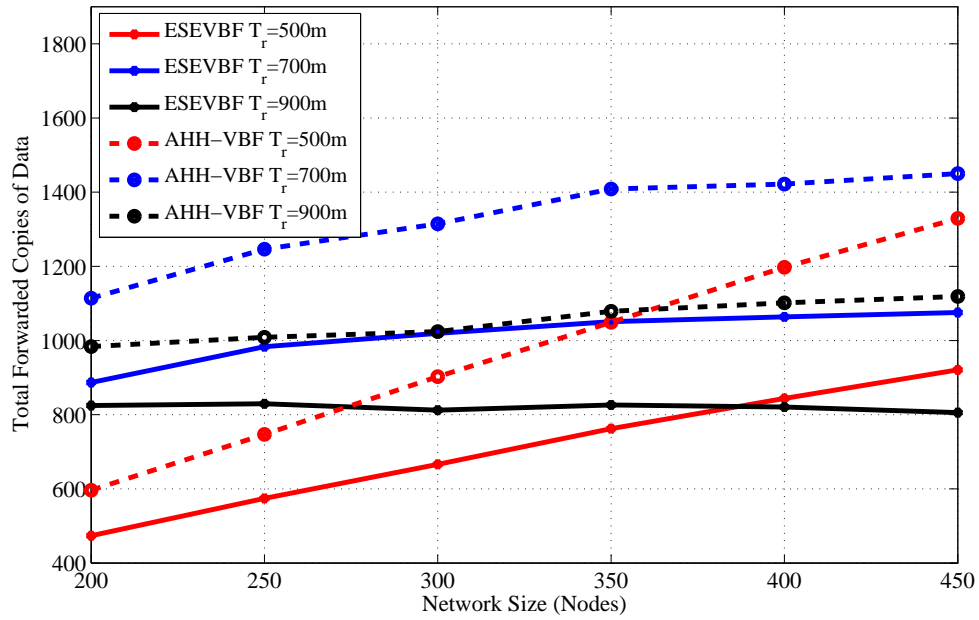


FIGURE 6.5: Number of data message copies forwarded in the network for different network size

- *Energy consumption*: total energy consumption in the network during the whole simulation time.
- *Hop count*: represents the average number of hops that the data packets have traversed between source and sink node.

Following is the brief discussion about each performance metric that is estimated through simulations in the static Sink network scenario.

#### 6.4.2 Simulation Results in the Static Sink Scenario

In this section, all the results are estimated for the network scenario with static sink. In this case, the Sink is placed at sea surface and the center of the network deployment region.

Figures 6.5 and 6.6 show the total number of copies of the data message forwarded in the network versus varying network size and transmission range, respectively. It can be seen in Fig.6.5 that in a sparse network scenario,  $T_r = 500$  and network size, the total copies of data packet forwarded in the network is smaller than the



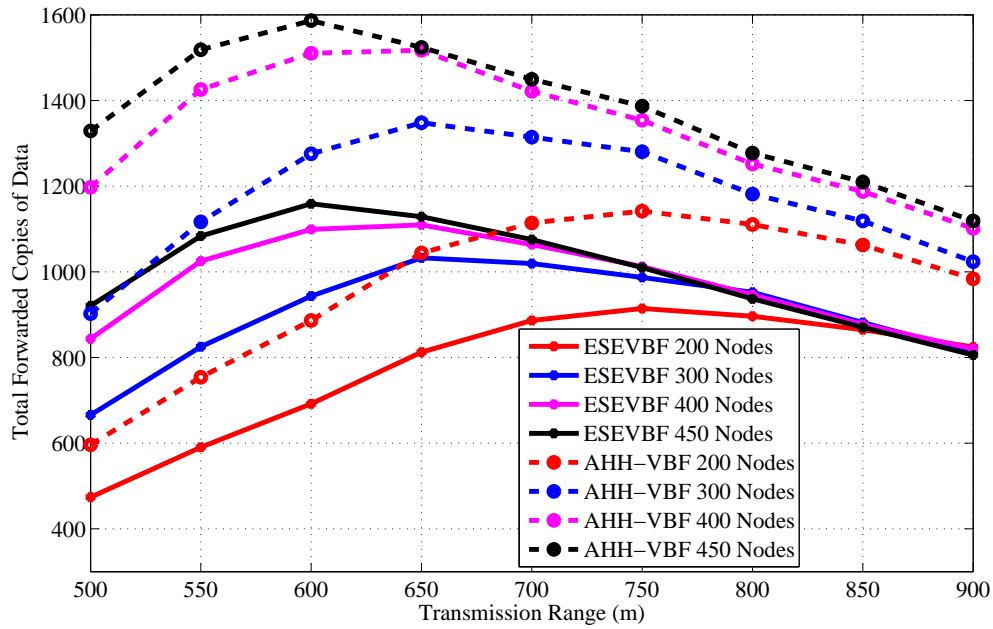


FIGURE 6.6: Number of data message copies forwarded in the network for different transmission range

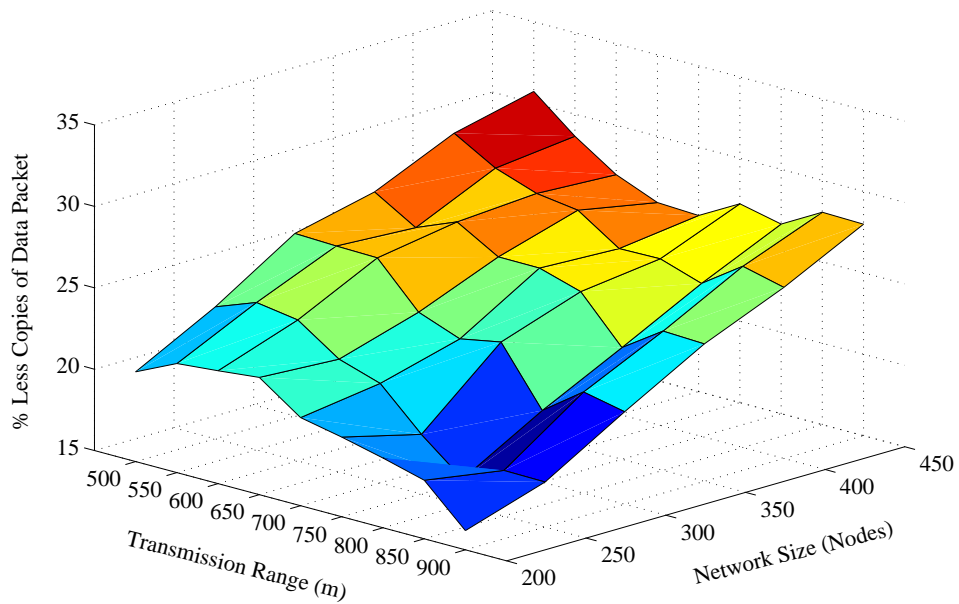


FIGURE 6.7: % reduced data packets by the proposed scheme for different  $T_r$  and network size

dense network scenario. The reason behind this phenomenon is that most of the copies of the data packet fail to reach the next hop forwarders. As the network size increases, more copies of the data message are successfully propagated in the network. On the contrary, for large transmission range and small network

size, more data packets are successfully forwarded in the network, but when the network size increases, most of the packets are dropped in the network due to a large collision probability. Increase in data packet copies due to large transmission range plus network size is due to two factors; a) increase in the pipeline radius directly surges in the number of forwarding candidates in PFZ, b) the propagation delay between potential forwarders in PFZ will be longer and could be more than the holding time difference between them.

The next interesting trend that has been observed in the graphs is the difference between total copies of the data packet that are forwarded by AHH-VBF is larger than the proposed scheme. It shows that the holding time difference between the potential forwarders is less than the propagation delay between those nodes. Hence, multiple nodes from the PFZ send copy of the same data packet, which results in more energy consumption that is discussed later in this section. In contrast, the proposed scheme computes holding time and exponentially scales the holding time using normalized energy factor to increase the holding time difference between potential forwarders. Consequently, it minimizes the data packet duplication and saves energy in the proposed scheme. The same performance metric has been investigated for different transmission ranges and fixed network size and a similar trend has been observed in Fig. 6.6. On average, the proposed scheme generates 27.55% less copies of the data packet for all  $T_r$  and network size of 450 nodes. Similarly, in  $T_r = 900m$  and all network size scenarios, the proposed scheme disseminates about 21.93% fewer copies of the data packet in the network. A detailed performance gain achieved by the proposed scheme in this regard is shown in Fig. 6.7. The maximum performance gain achieved by the ESEVBF in contrast to the AHH-VBF is 30.72% for the network size of 450 nodes and  $T_r = 500m$ .

Next, investigate the end-to-end delay experienced by the successful data packets between the source  $S$  and sink node  $D$  for varying network size and transmission range as shown in Fig. 6.8 and 6.9, respectively. The overall delay experienced by a data packet includes processing, propagation, and the holding time delay at each forwarding stage in the network. The impact of network sparseness and

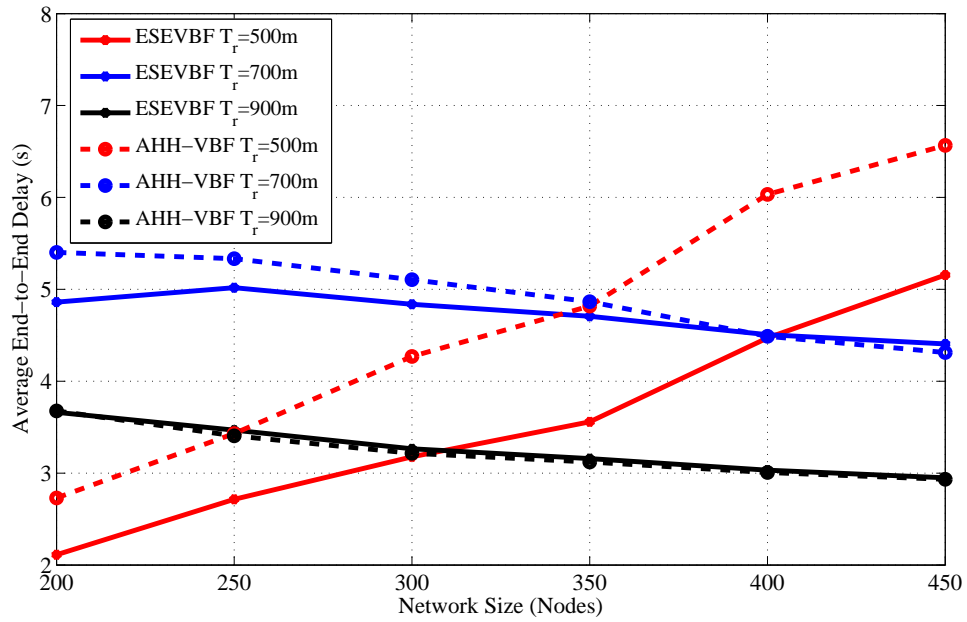


FIGURE 6.8: End-to-End delay between Source node that generated data message and Sink node versus the network size

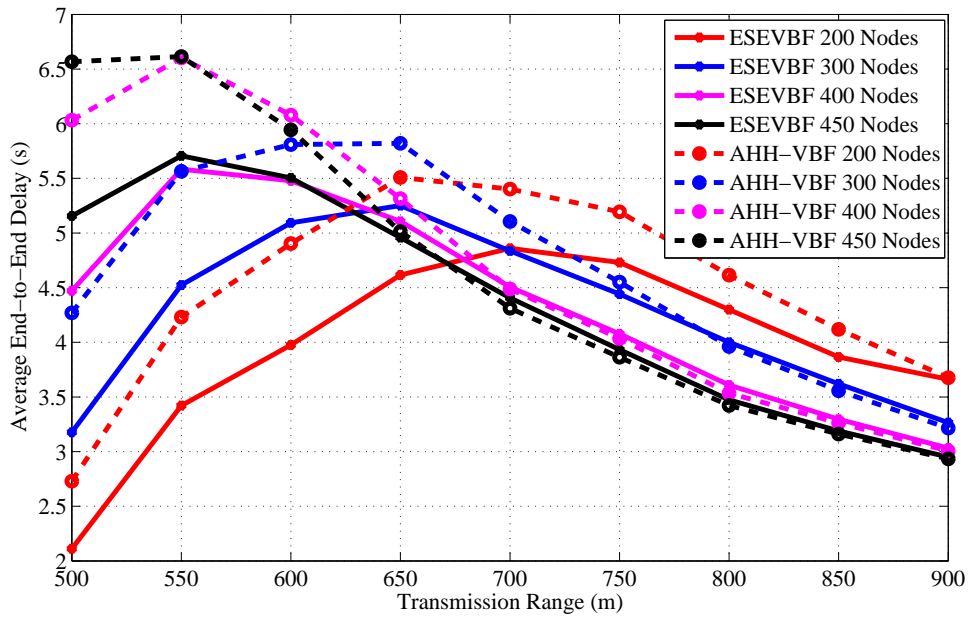


FIGURE 6.9: End-to-End delay between the source node that generated data message and Sink node versus transmission range

denseness can be seen in those graphs. It is evident from the graphs that the end-to-end delay experienced by the AHH-VBF is larger than the proposed scheme. The main reason behind this behavior is proposed in potential forwarder selection algorithm. As stated earlier in the proposed forwarder selection algorithm section,

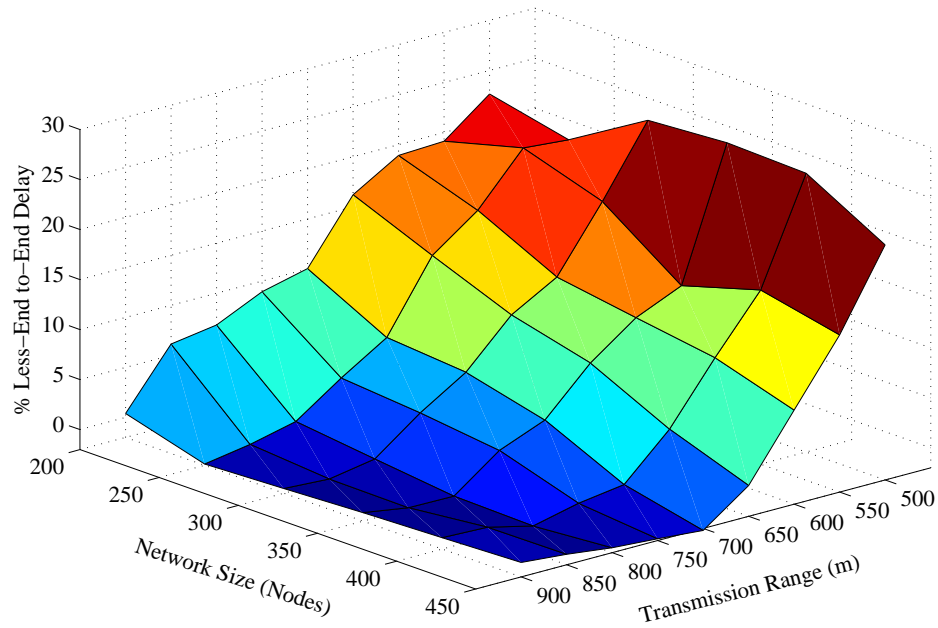


FIGURE 6.10: The overall percentage less End-to-End delay achieved by the proposed scheme for different  $T_r$  and network size

all the nodes share their location and residual energy information with their 1-hop neighbors. When a node receives data packet from any one of its neighbors, it computes its own holding time. As recall from previous discussion that the holding time computation only requires the location plus depth information of sender node  $S$ , Sink node  $D$ , node's own location, and the residual energy information. However, the same information of the neighboring nodes is also available in the neighborhood table of each node. Hence, the node can easily estimate the packet holding time of all common neighbors of  $S$  and node itself, which also fall in the *PFZ*.

It is also a well-established fact that computation energy cost is very small compared to communication and other operations of the node. Once the node estimates the holding time of its own as well as its neighbors, it checks whether its own holding time is smaller than the neighbors or not. If the receiving node's holding time is smaller than its common neighbors, then instead of waiting for a long holding time duration, it forwards the packet after  $\frac{HT_p^i}{2}$ . However, the AHH-VBF does not exploit the neighborhood information available at the node and each node has to wait for a holding time duration before further relaying the data packet. This is

the reason that despite the energy scaling and expansion of the proposed holding time, its end-to-end delay is smaller than the AHH-VBF. Subsequently, the same behavior can be observed for any network scenario, refer Fig. 6.8 and 6.9.

In Fig. 6.8, the trend of the end-to-end delay for a small transmission range (e.g.,  $T_r = 500m$ ) is increasing with respect to the network size in contrast to the end-to-end delay behavior resulted by large transmission ranges. The main arguments behind this behavior are: (a) in case of a small  $T_r$ , the packet fails to reach  $D$  if it is relayed over multiple hops, due to channel impairments, path losses, high error rate of the acoustic channel, and so forth. (b) because of the network sparsity, end-to-end connectivity could not be established. Therefore, in a sparse network scenario, only the short hop-distant packets can reach  $D$  and experience a small end-to-end delay. On the contrary, in a dense network environment, the packet has to traverse a large number of hops, which causes a very long end-to-end delay. The similar trend is also observed in Fig. 6.8. Furthermore, it is also noticed in Fig. 6.8 that as  $T_r$  increases, the end-to-end delay descends, which is due to the collision that leads to a large data packet loss. This collision happens when different potential forwarders relay the same data packet because of the small holding time difference and the large propagation delay between these forwarders, refer the theory related to Fig. 6.2. Data packets in the proposed ESEVBF scheme experience about 23.77%, 12.6%, and 3.65% less end-to-end delay compared to AHH-VBF in any network size scenario with  $T_r = 500m$ ,  $T_r = 600m$  and  $T_r = 700m$ , respectively. As the  $T_r$  increases, the end-to-end delay of both the schemes becomes identical because the Data packet is forwarded through less number of hops and directly reaches the sink node. The overall performance gain (percent improvement in end-to-end delay) achieved by the proposed ESEVBF is shown in Fig. 6.10.

After the data packet broadcast and end-to-end delay analysis, investigate the overall energy consumption in the network. Figure 6.11 and 6.12 show the total energy consumption in the network during the whole simulation duration for different network size and transmission range, respectively. In underwater acoustic networks, transmission of a packet is the most energy consuming operation in the

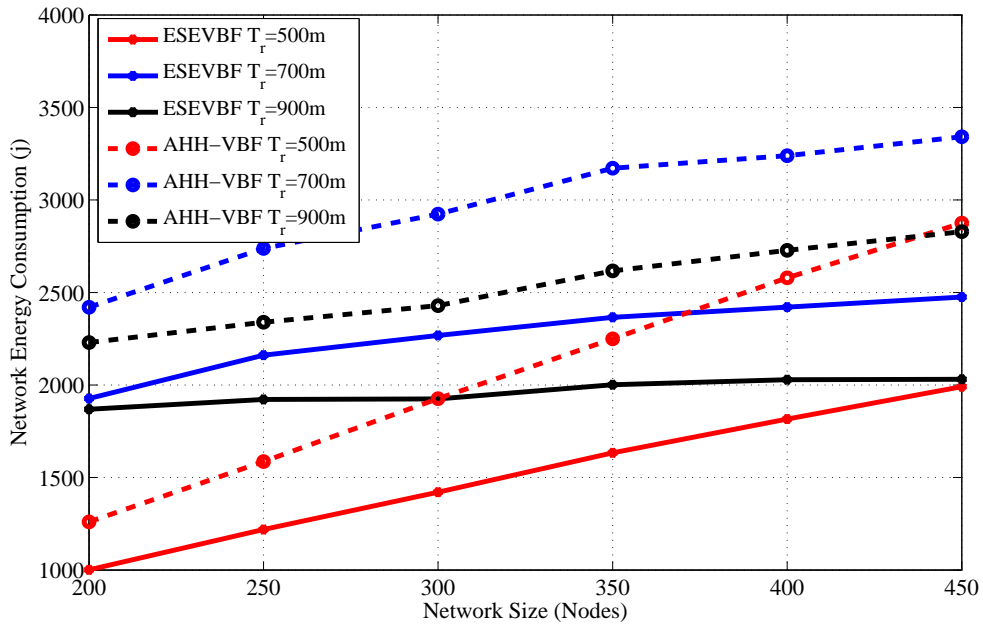


FIGURE 6.11: Overall network energy consumption versus the network size

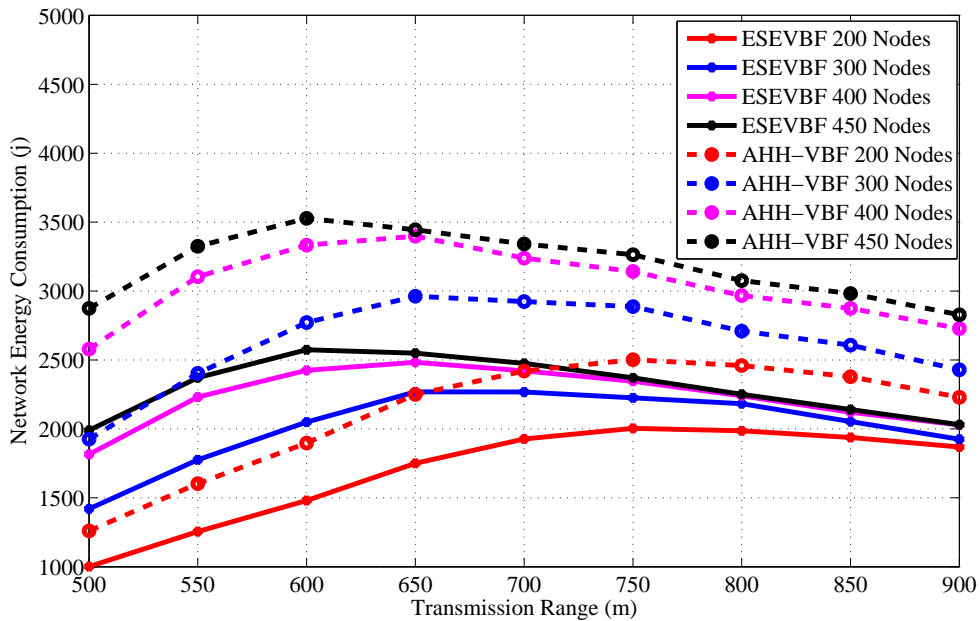


FIGURE 6.12: Overall network energy consumption versus the transmission range

network compared to the packet reception, idle listening, sensing, and the processing operations. As data packets are large in size compared to the control packets, therefore, their contribution to the energy consumption dominates the energy consumed by the transmission of other packets or network operations. Therefore, the trends of the overall network energy consumption graphs are comparatively similar

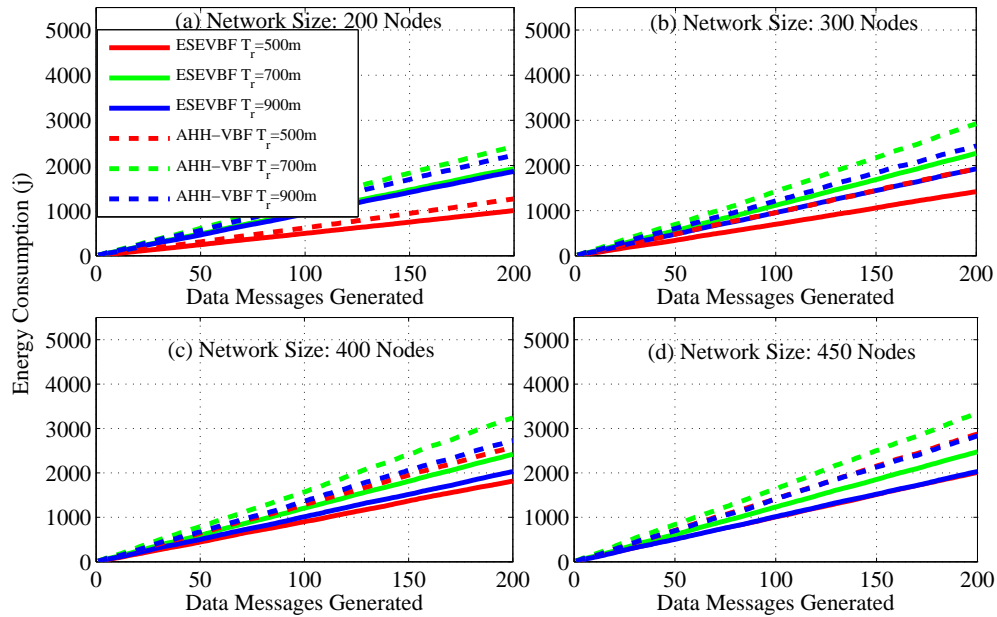


FIGURE 6.13: Overall network energy consumption for varying number of data packets generated by the source nodes in the network

to the results that depict the total number of forwarded copies of the data packets in the network. Hence, the main reasons and arguments related to energy saving are similar to the one that avoids broadcast of more copies of the data packet. As a result, the overall energy consumption of the proposed scheme is less than the AHH-VBF.

The simulation results show that the energy consumption in the sparse network is very small because most of the data packets could not be forwarded further in the upstream direction towards the Sink. Similarly, the number of forwarders, as well as the data packet receiving nodes (receiving energy consumption), are very few, which is one of the reasons for this small network energy consumption. Conversely, the opposite is the case for a dense network scenario where the successful communication of data packets increase energy consumption in the network. As the number of data sources are fixed in all the simulation scenarios, hence, we also recorded the overall network energy consumption after the individual broadcast of the packet by each source, refer Fig. 6.13. The results show that maximum energy maximum energy saved by the proposed scheme is approximately 30.8%. The average percentage less energy consumed by the proposed scheme in comparison to

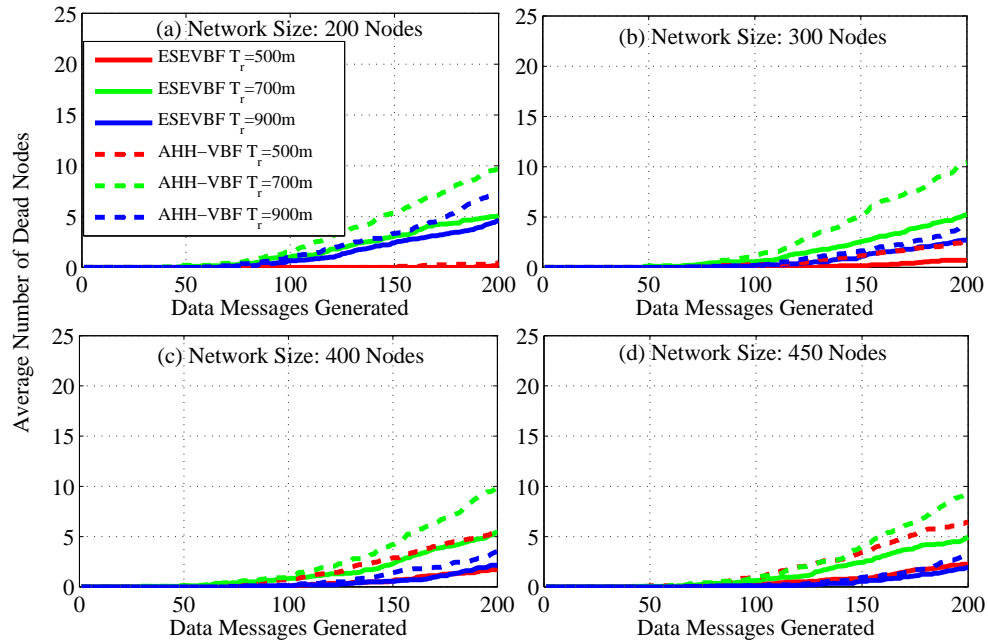


FIGURE 6.14: Number of dead nodes for varying number of data packets generated by the source nodes in the network

AHH-VBF is summarized in Table.6.1.

TABLE 6.1: Overall energy saved by the proposed scheme compared to AHH-VBF

<i>Network Size</i>	<b>200</b>	<b>250</b>	<b>300</b>	<b>350</b>	<b>400</b>	<b>450</b>
$T_r = 500m$	20.6	23.1	26.3	27.4	29.6	<b>30.8</b>
550m	21.7	24.1	26.1	25.9	28.1	28.7
600m	21.9	23.6	26.0	26.9	27.2	27.0
650m	22.2	21.9	23.4	25.4	26.9	26.0
700m	20.4	21.1	22.4	25.4	25.3	25.9
750m	19.9	18.7	22.9	24.7	25.3	27.4
800m	19.3	16.6	19.5	21.9	24.5	26.8
850m	18.6	17.9	21.3	23.6	26.2	28.2
900m	16.2	17.8	20.8	23.5	25.6	28.2
<b>Energy Saved</b>	<b>20.1%</b>	<b>20.5%</b>	<b>23.2%</b>	<b>25.0%</b>	<b>26.5%</b>	<b>27.7%</b>

As already discussed that more energy is consumed by the underwater acoustic networks, which can deplete the battery power of some nodes (dead nodes) during the simulation duration. Therefore, we also studied the number of dead nodes during the simulation period, as shown in Fig. 6.14. It is evident from the figure that the battery power of few nodes is completely consumed in the network scenario of 200 nodes and  $T_r = 500m$ , Fig. 6.14(a), because a small number of data traffic is handled by the network. In the similar network scenario but for the large  $T_r$ , more network nodes die out, because more data packets are communicated



in the network. The battery power of more number of nodes deplete when the network becomes denser. However, it can easily be seen from the results that for  $T_R = 700m$ , the number of dead nodes is larger than the  $T=900$  and  $500m$ , refer Fig. 6.14(a). The obvious phenomenon behind this is that in an extremely dense network scenario, a large number of potential forwarders get the chance to forward data messages because of a very small difference between their holding time. Therefore, the collision probability at the next hop increases and the next hop nodes fail to further communicate the data packet. Hence, the data packet communication is restricted only to a few hops in the network. On the other hand, in  $T_r = 700m$ , more data packets are successfully propagated in the network, which consumes more network energy and results in a large number of dead nodes in the network, refer Fig. 6.14(c) and (d) for further details. Similarly, in the dense network scenario, e.g., Fig. 6.14(d), the small transmission range (e.g.,  $T_r = 500m$ ) consumes more energy due to the fact that most of the nodes participate in the Data packet forwarding. Hence, large number of nodes die out for small  $T_r = 500m$  compared to the large  $T_r = 900m$ . From the results, it can easily be seen that the battery power of a very small number of nodes is depleted during the simulation of ESEVBF. Resultantly, it increases the underwater monitoring duration and the network with ESEVBF can survive for a longer duration that the one using AHH-VBF.

From the above analysis, it is clear that the proposed scheme saves energy, reduces broadcast storm, and communicates data packets with less delay. In addition to these performance gains, the average number of hops that each data packet traverse from  $S$  to  $D$  is also analyzed for different network sizes and  $T_r$ , refer Fig. 6.15 and 6.16, respectively. The hop count data coincides with previous analysis that for a small  $T_r = 500$  and network of 200 nodes, the average number of hops is smaller than the large  $T_r$ s. The rationale for this behavior is that the data messages from sources that are at distant location, fail to reach  $D$  due to unavailability of the path(s). However, when the network becomes dense, the data packet has to traverse many hops to reach  $D$  for  $T_r = 500$ . On the other hand, it can easily be noticed from the results that the average number of hop counts of the proposed

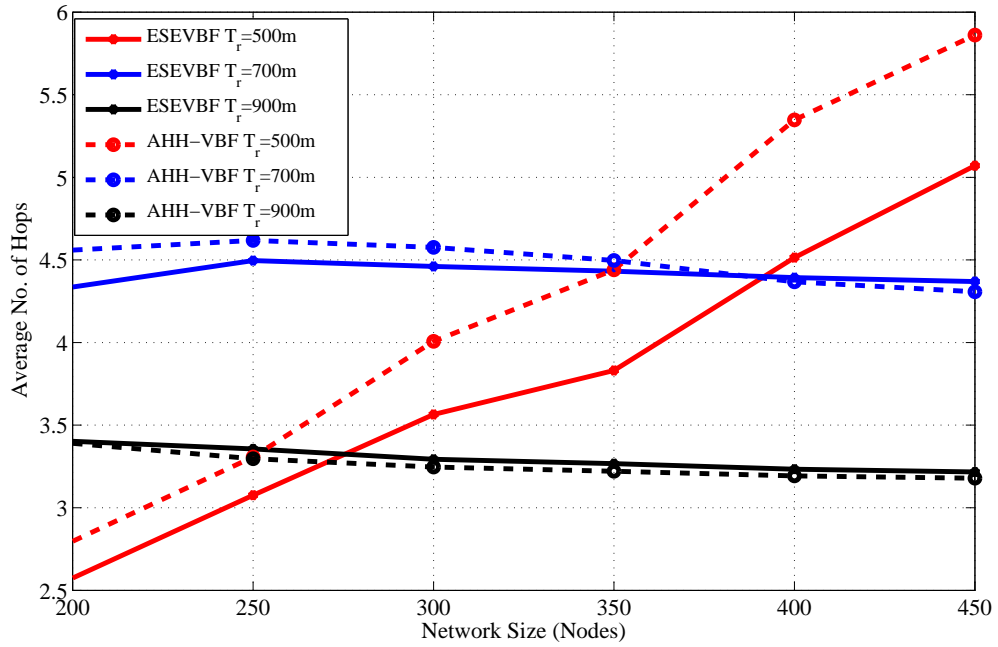


FIGURE 6.15: Average No. of Hops data messages traversed versus the network size

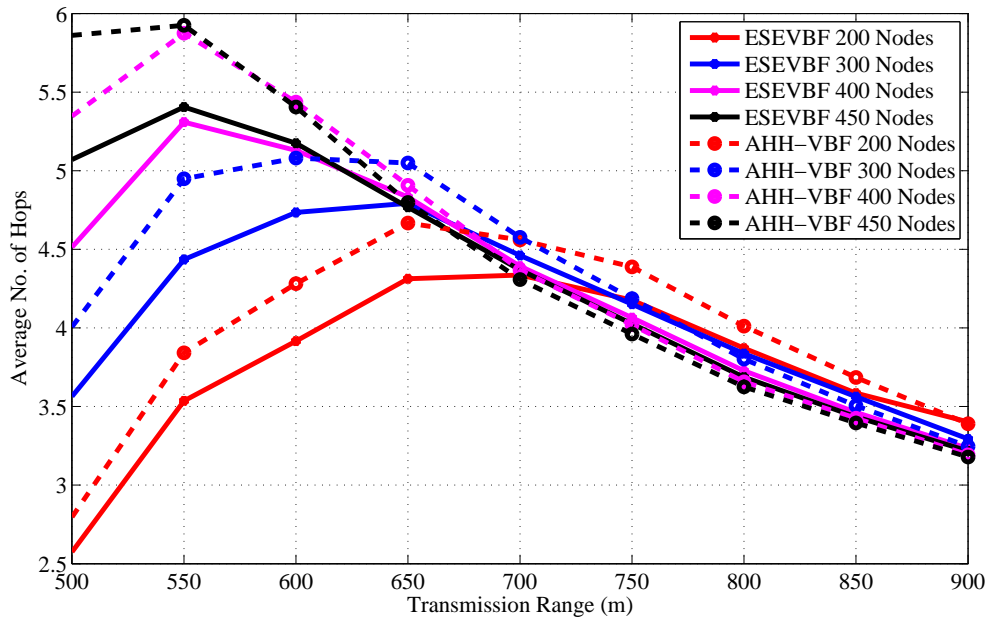


FIGURE 6.16: Average no. of hops data messages traversed versus transmission range

scheme is smaller than the AHH-VBF because the forwarder selection criteria mostly considers the node's closeness towards the center of the virtual cylinder and the Sink node. Notwithstanding, the proposed scheme scales the holding time with residual energy factor plus the expanded ratio of the closeness towards the

center of the virtual cylinder. This may increase the chances of other nodes to serve as potential forwarders that have large residual energy and slightly different virtual cylinder distance ratio. This is the reason that for large  $T_r$ , the average number of hops traversed by the Data packet in ESEVBF is slightly larger or almost identical to the AHH-VBF. The impact of this slightly larger hop count is reduced by taking the advantage of utilizing the neighborhood information in holding time calculation and reducing the holding time of the potential forwarder that has a smallest holding time among neighbors. Therefore, this marginally high hop count factor has not much impact in presence of the other significant performance gains achieved by the proposed scheme.

Along with those performance gains, finally, the simulations carried for the packet delivery ratio or PDR =  $\left( \frac{\text{Successfully received data at } D}{\text{total generated data by } S} \right)$ . PDR is one of the fundamental performance measures of every routing strategy is also analyzed. Figure 6.17 and 6.18 show the PDR comparison of the proposed and the AHH-VBF scheme for different network size and transmission range, respectively. Figures show that the proposed scheme has almost similar PDR as the AHH-VBF as the network size or  $T_r$  is very large. On the other hand, the ESEVBF has slightly less PDR because ESEVBF selects the potential forwarders in the in PFZ that have closeness to the center of the cylinder and have larger residual energy. However, due to small number of nodes in the PFZ due to network sparseness, it is quite difficult to find suitable forwarders. Hence, the PDR of the ESEVBF is lower in those network scenarios. Conversely, in the dense network scenario, the chances of finding the suitable forwarder from the PFZ becomes very high that increases the PDR. The above results show that the proposed scheme achieves energy efficiency, broadcast less number of Data packets, and has lower end-to-end delay at the cost of slightly lower or almost identical PDR in different network scenarios.

In the next subsection, briefly analyze and contrast the impact of Sink mobility on the performance gain of both ESEVBF and the AHH-VBF schemes.

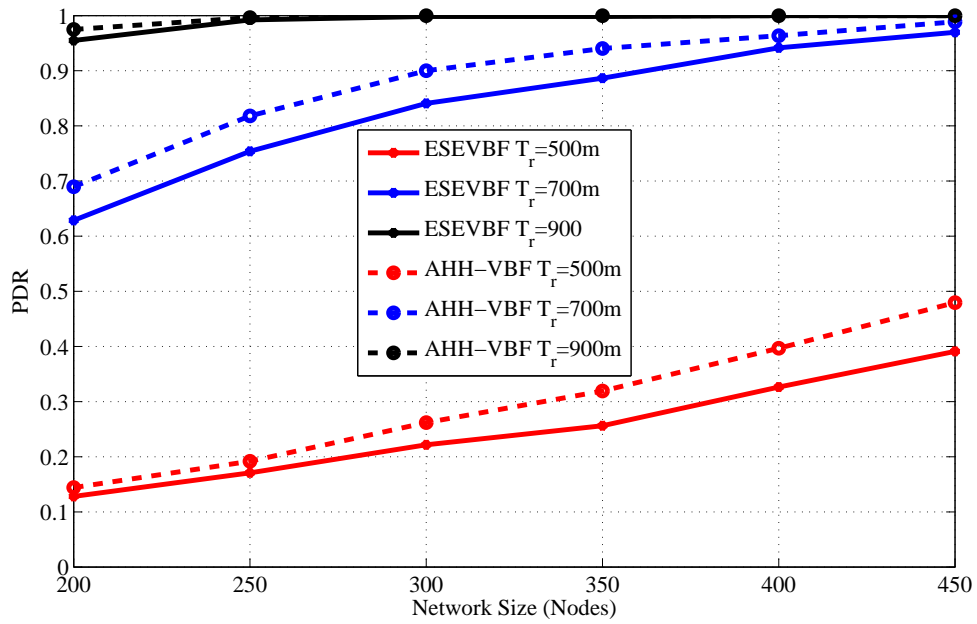


FIGURE 6.17: Average packet delivery ratio versus the network size

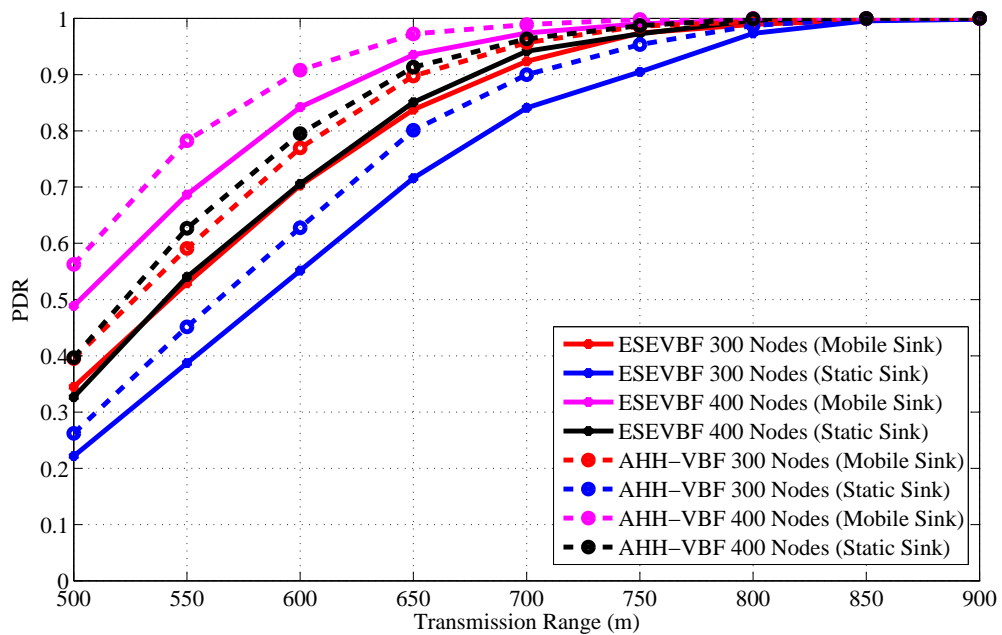


FIGURE 6.18: Average packet delivery ratio versus the transmission range

### 6.4.3 Simulation Results in the Mobile Sink Scenario

In previous section, the critical analysis and reasoning proposed about the performance gain of the ESEVBF in the network scenario with the static Sink. However, the literature suggests that introduction of the Sink mobility enhances the network performance in terms of small end-to-end delay, reduces the broadcast of the

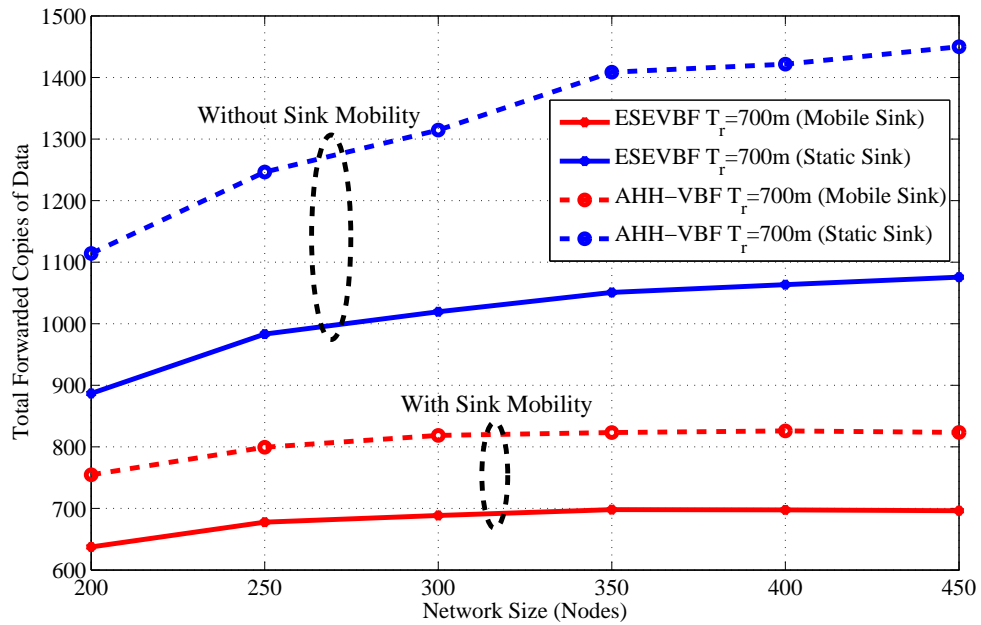


FIGURE 6.19: Total copies of data message forwarded in the network with and without Sink mobility for different (network size)

number of Data packets, minimizes energy consumption and increases the network lifetime, and so on. Although, the AHH-VBF has not been tested in the mobile Sink network scenario, however, there are extensive simulations of AHH-VBF as well as presented ESEVBF in the mobile Sink paradigm and the results are discussed below.

Figure 6.19 shows the total number of copies processed within the network of varying size and transmission range Figure 6.20. It is evident from the figure that the Sink mobility minimizes the broadcast of the number of data packet copies in the network. The reason behind this phenomenon is that Sink moves within the network and passes near the data generating and forwarding nodes. Hence, these nodes just have to forward data packet at fewer hops to reach the Sink that is within the close proximity of these nodes, refer Fig. 6.21 and 6.22 that shows average number of hops the data packet traverses in the network to reach the Sink. Figures 6.19 and 6.20 explicitly show that the ESEVBF and AHH-VBF forward far more less copies of data packet in the mobile Sink scenario as compared to the one with static Sink. The analysis shows that ESEVBF for any network size in a mobile Sink scenario processes 12.6%, 24.4%, 32.5%, ..., and 34.0% less

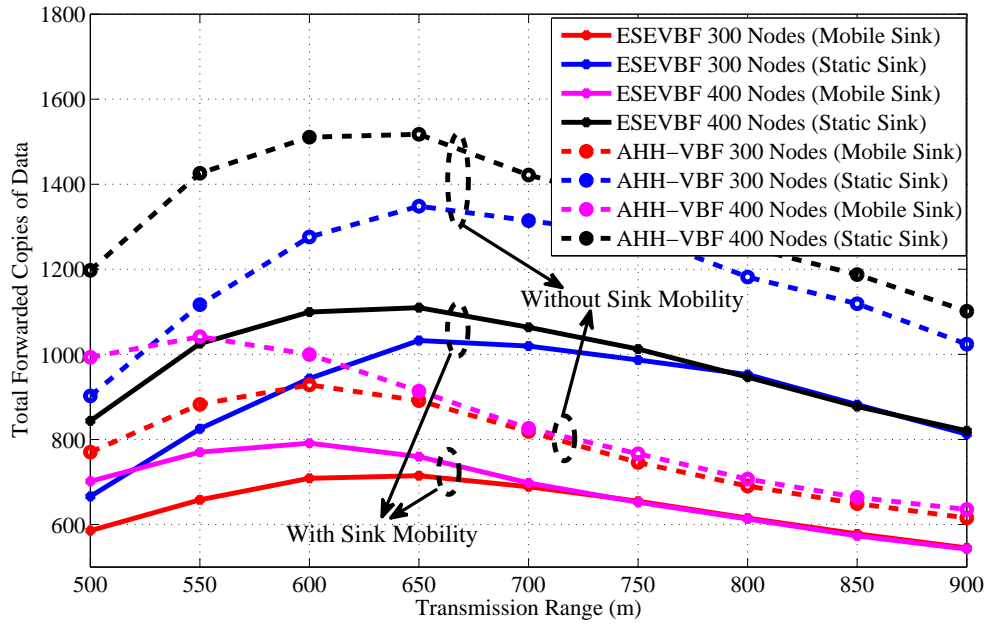


FIGURE 6.20: Total copies of data message forwarded in the network with and without Sink mobility for different (transmission range)

number of data messages in the network compared to static Sink scenario for  $T_r$  of  $500m$ ,  $600m$ ,  $700m$ ,  $\dots$ , and  $900m$ , respectively. Similar data packet gain is also achieved by the AHH-VBF in the network with Sink mobility. Additionally, it is also obvious from the figure that ESEVBF outperforms the AHH-VBF in any network scenario. The mobility enables the Sink to vary its proximity respective to the data packet source and the forwarder nodes. Hence, the number of hops traversed by the data packet is far more less in the mobile Sink network than the static Sink network scenario, refer Fig. 6.21 and 6.22.

Above analysis shows that the Sink mobility in the underwater network scenario significantly reduces the number of data message copies and the number hops the message traverses in the network. In result, it can easily be predicted that the end-to-end delay must also be alleviated in this network setting. Figure 6.23 shows the end-to-end delay experienced by the data message in a network with static and mobile Sink for varying network size and transmission range Figure 6.24. A notable difference in the end-to-end delay can be observed in the figure. On average, the ESEVBF lessens about 28.5%, 31.0%, 31.4%,  $\dots$ , and 34.0% of end-to-end delay in the network with mobile sink than the network without sink mobility for the size

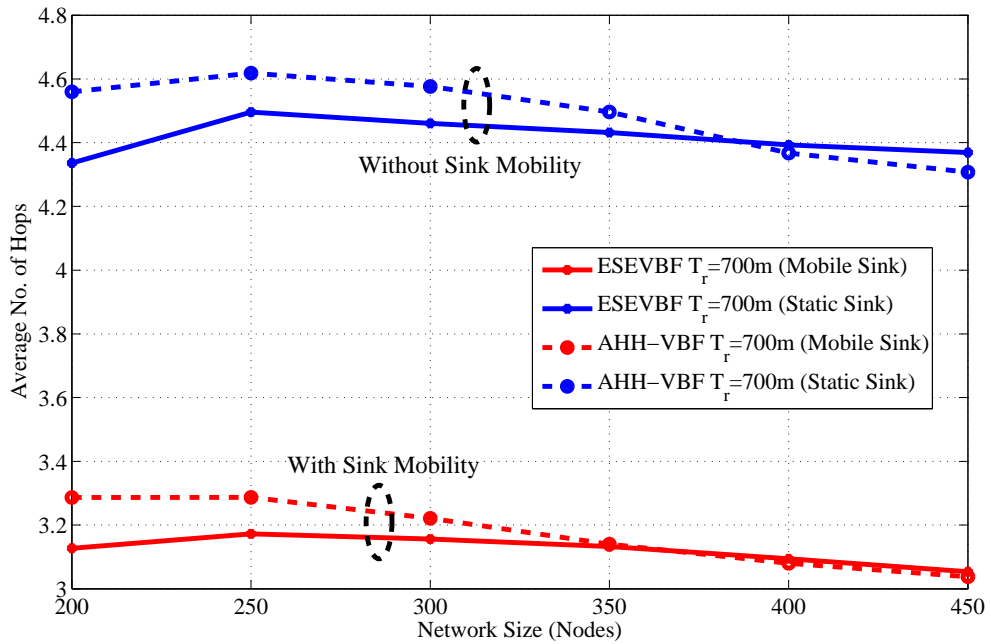


FIGURE 6.21: Average number of hops the data message needs to traverse in network to reach static and mobile Sink (Network with varying size)

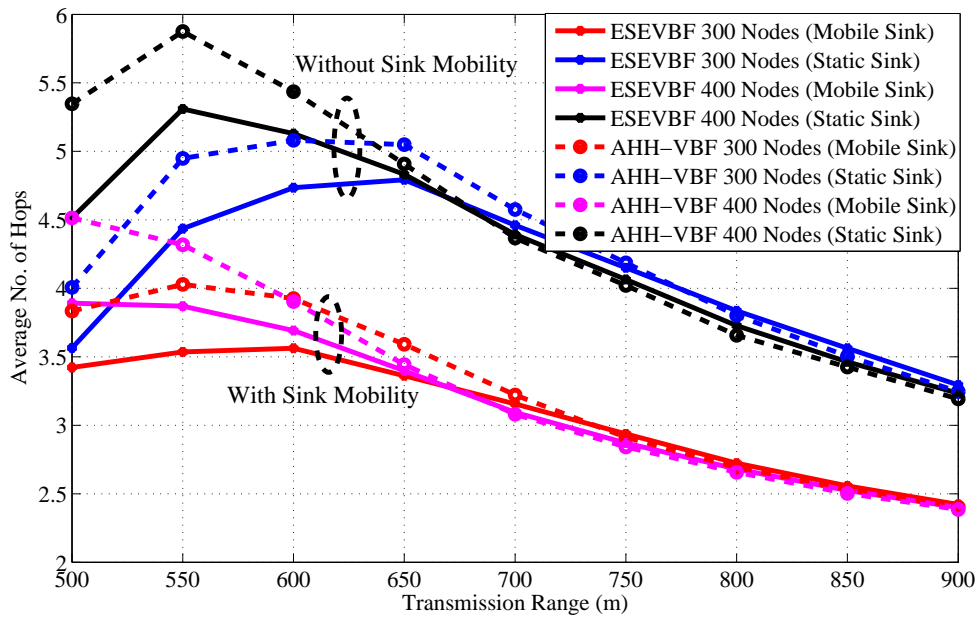


FIGURE 6.22: Average number of hops the data message needs to traverse in network to reach static and mobile Sink (Network with varying transmission range)

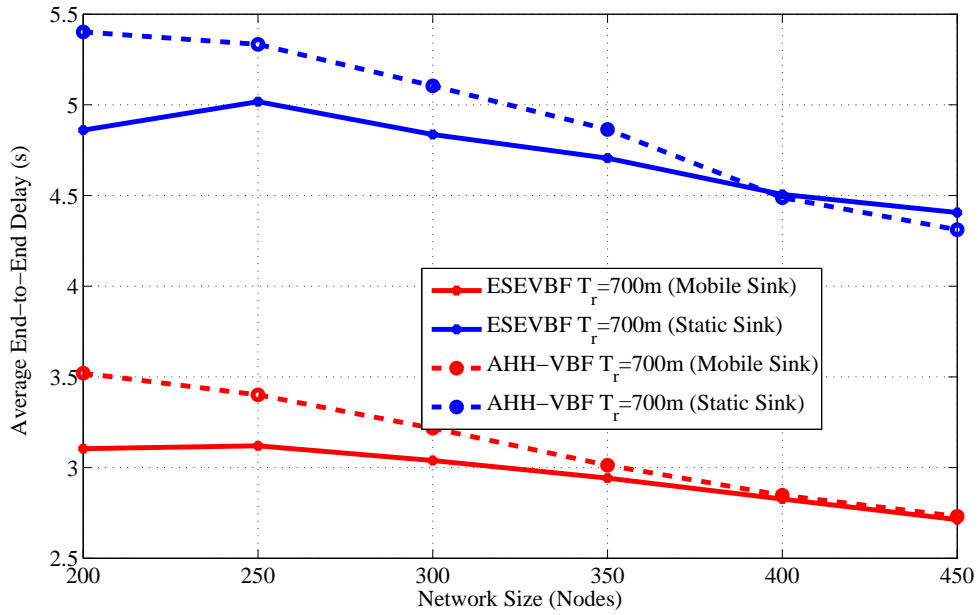


FIGURE 6.23: End-to-end delay experienced by the data message in a network with static and mobile Sink for varying network size

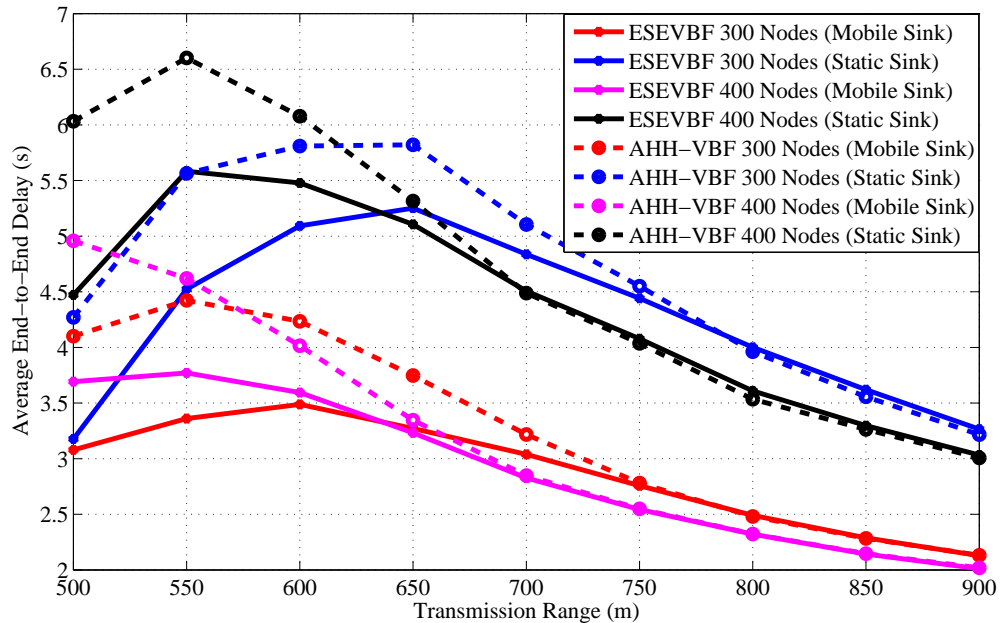


FIGURE 6.24: End-to-end delay experienced by the data message in a network with static and mobile Sink for varying transmission range



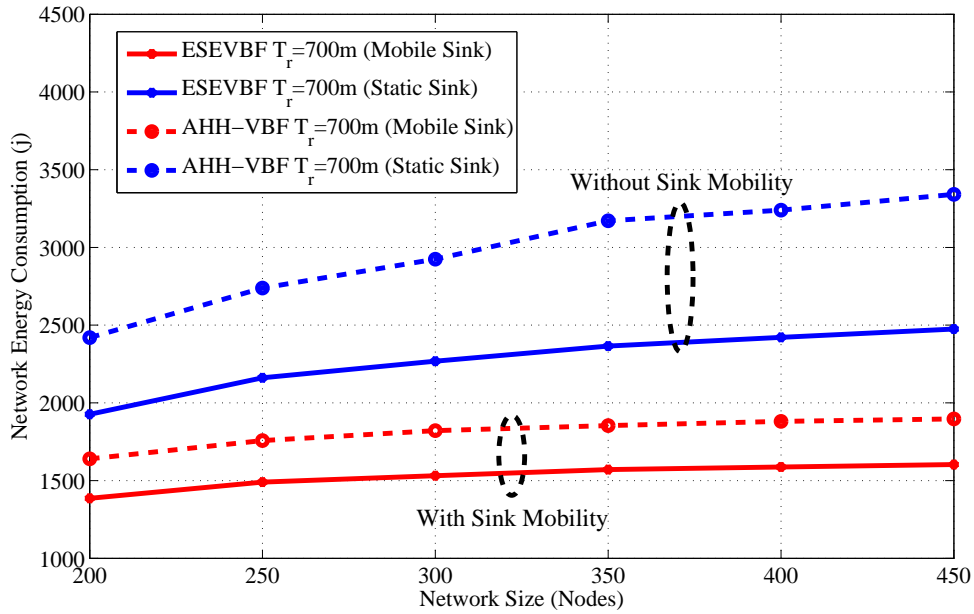


FIGURE 6.25: Network energy consumption in the static and mobile Sink network scenario for varying network size

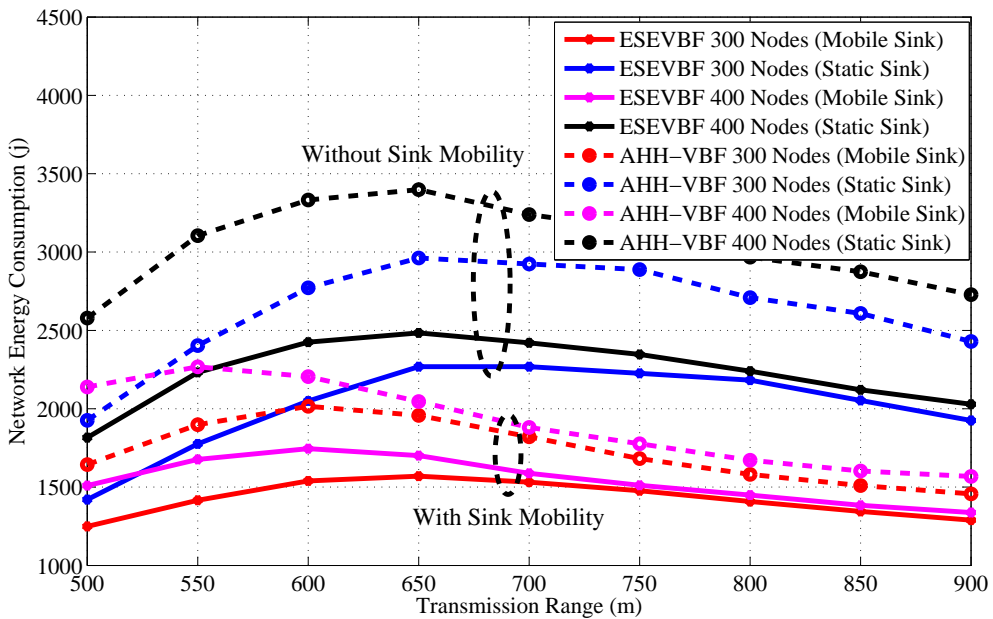


FIGURE 6.26: Network energy consumption in the static and mobile Sink network scenario for varying transmission range

of 200, 250, 300, ... %, and 450 nodes and all  $T_r$ . Notwithstanding, the AHH-VBF achieves 28.3%, 29.0%, 29.9%, ..., and 33.1% less end-to-end delay for the network of 200, 250, 300, ..., and 450 nodes, which is closer to ESEVBF's performance gain.

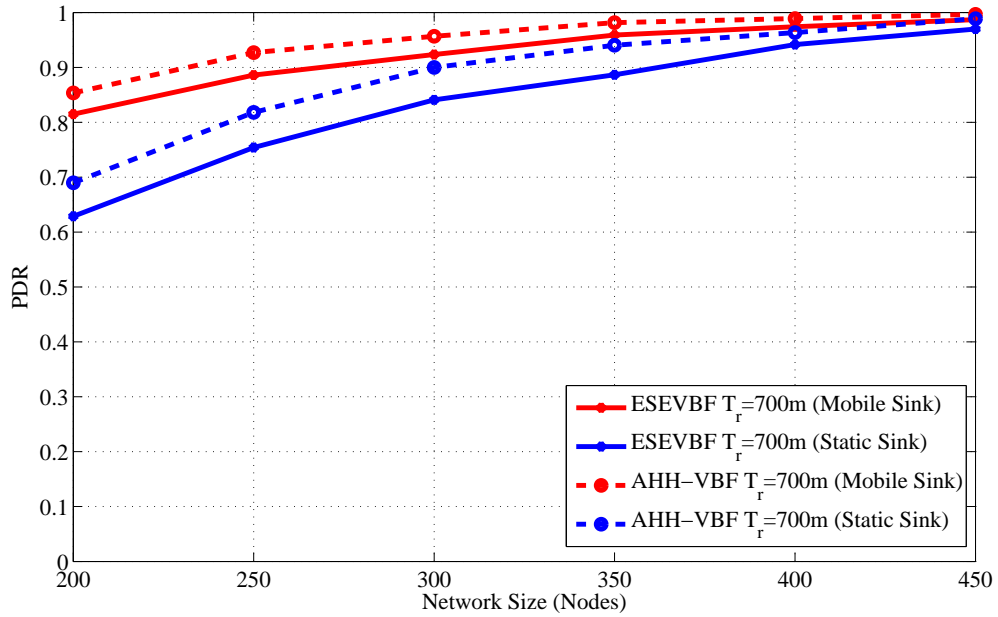


FIGURE 6.27: PDR in the static and mobile Sink network scenario for varying network size

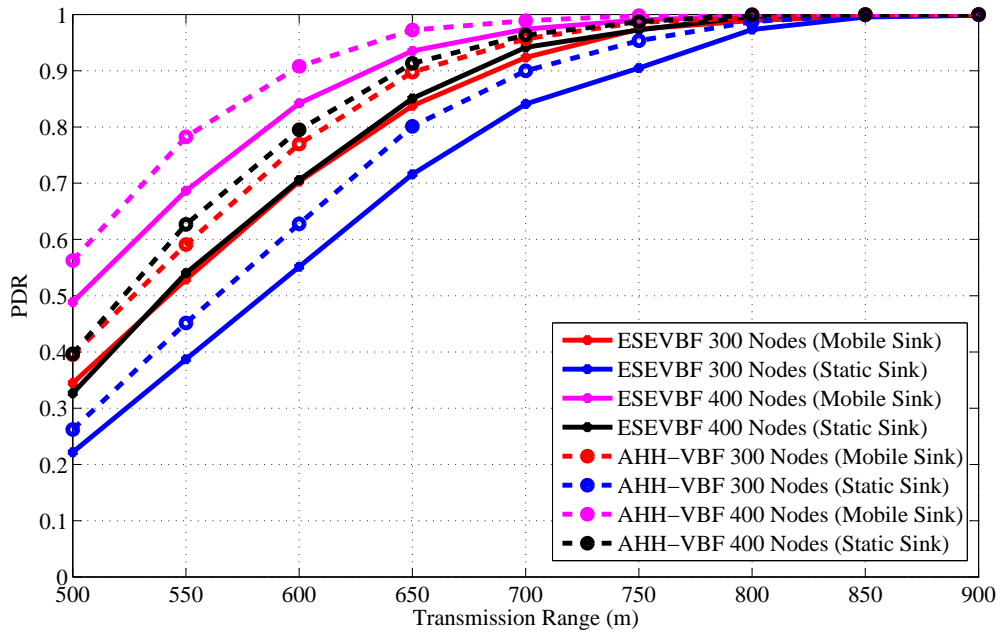


FIGURE 6.28: PDR in the static and mobile Sink network scenario for varying transmission range

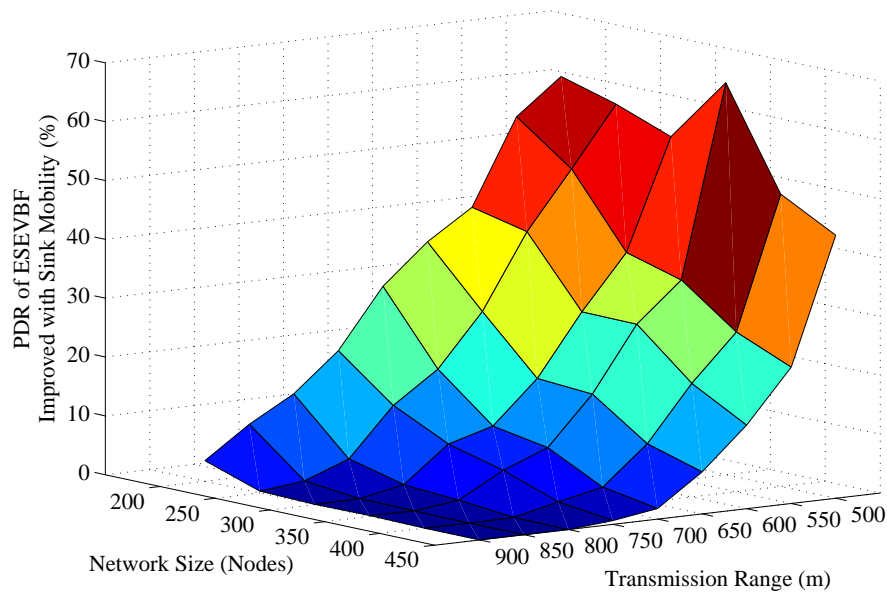


FIGURE 6.29: PDR alleviated after the introduction of the mobile Sink in ESEVBF

Next, the influence of Sink mobility on the overall network energy consumption is shown in Fig. 6.25 and 6.26. Results in that figure show the similar impact on the energy conservation as it has on the data copies processed in the network. It also verifies the claims in the literature that Sink mobility achieves energy efficiency in the network, which is about 36% more energy conserved than the static Sink scenario. Finally, the PDR improved by the proposed and conventional scheme is shown in Fig. 6.27 and 6.28. The overall PDR improved by the Sink mobility for ESEVBF and AHH-VBF Fig. 6.29 and 6.30, respectively. From the above discussion, it can easily conclude that the Sink mobility improves the performance of the routing protocols.

## 6.5 Conclusion

An energy scaled and expanded vector based routing (ESEVBR) scheme is presented in this chapter. ESEVBR provides energy fairness and reduces the packet broadcast by scaling and expanding the holding time with the residual energy and ratio of projection distance to vector and width of the virtual pipeline. The

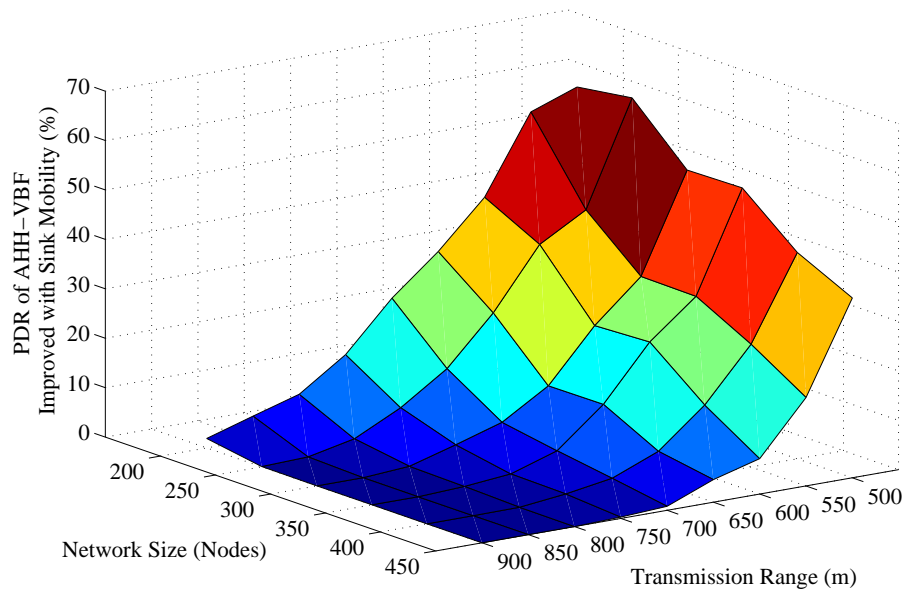


FIGURE 6.30: PDR alleviated after the introduction of the mobile Sink in AH-HVBF

new holding time signifies the difference between holding times of the potential forwarders, which reduces the data packet broadcast and maintains the energy fairness in the network. The simulation results show that the proposed ESEVBR is approximately 5% more energy efficient, experiences 14.6% less delay, and generates about 5% fewer data packets, compared to AHH-VBF. However, ESEVBR maintains similar PDR and very less number of nodes die in the network when ESEVBR is used as a forwarding technique in the underwater sensor network.

# Chapter 7

## Conclusion and Future Work

### 7.1 Conclusion

UWSNs are usually deployed sparsely in large 3D regions due to the expensive manufacturing and huge deployment cost. Moreover, the mobility of the sensor nodes with water current causes frequent topological changes. Consequently, the density of network nodes is observed to be different at different regions of the network. The routing protocol DOW-PR has been designed to enhance the reliability of the network in sparse regions and at the same time it provides energy efficient solution in dense network region. There are two versions of the routing protocol i.e. dolphin pod and whale pod. DOW-PR convincingly beat its counterpart routing protocol WDFAD-DBR in all performance metrics. It includes reduction in energy consumption, increasing PDR, and minimizing void and energy holes creation. DOW-PR explore the role of the parameters like number of PFNs, number of SUPs nodes and hops count value in designing the holding time equation. Moreover, the values of the above-mentioned parameters have been mapped (SET1, SET2 and SET3) into arbitrary values and that are also tested for simulations. The investigations through simulations showed that dolphin pods routing beats the WDFAD-DBR, on average improving by 31.5% of energy tax, 6% of PDR, and 24.6% of E2ED. However, certain performance trade-offs have been observed and listed in Table 2. It has been shown through critical analysis

from the results that, in order to improve PDR, end-to-end delay is compromised. Furthermore, the whale pods routing protocol outperformed the dolphin pod version and therefore improvement is seen in energy tax, PDR and fraction of void nodes. DOW-PR was designed to select forwarder from the upper hemisphere of transmission range in the direction of the nearest sink node. The advantage of spatial division was ignored in forwarder selection. Therefore, the requirement of communication range being spatially divided into logical subregions which is incorporated in GDGOR-IA. GDGOR-IA exploit geographic information to route data greedily towards sonobuoys and features opportunistic forwarding for improved data delivery. Three dimensional division has made network scalable and forwarding is directional because of selection of upward neighbor cubes of a sender cube. In this way, number of hops taken to execute a complete transmission from sender node to sonobuoy were found to be reduced significantly. Moreover, interference avoidance in GDGOR-IA helped in reduction of packet loss, thus it improved packet delivery ratio. In GRMC-SM, controlled sink mobility significantly improved network performance compared to the baseline scheme. Energy cost was significantly improved due to coping with communication voids by reducing fraction of void nodes in the network. Consequently, these schemes provided efficient solution for reliable communication. Mathematical problem formulation using linear programming resulted in feasible solution for minimizing the energy consumption, average delay and to maximize network throughput.

Transmission range adjustment and geo-spatial division were individually implemented in DOW-PR and GDGOR-IA respectively. In order to get benefit of both, this research incorporated the hybrid version of these two i.e. LETR. The novelty of location error prediction is also included while selecting the forwarder. The transmission range adjustment technique has helped to avoid void holes while depth adjustment and is only applied in extreme scenarios where a sensor node fails to find any neighbor within its maximum transmission range. A major contribution of this work is to tackle location errors in traditional geographic routing along with void hole avoidance. LETR, calculate MSE to mitigate the effects of localization errors on forwarder selection and data transmission. The controlled

depth adjustment significantly conserves energy consumption and contributes to more data transmissions in the network. Instead of node displacement towards bottom of water, LETR adjust node depth towards sinks at the surface. It reduces the distance of node with sink and the chances of frequent network topology readjustments, thus energy consumption is reduced and network lifetime prolongs. Another major contribution of this work is the MMS-LETR protocol which considers noise attenuation to eliminate retransmissions. This research defines sink mobility patterns provides maximum network coverage, which minimizes packet loss ratio. The simulation results prove that the location error resilient void hole avoidance technique increases network throughput and conserves energy as compared to traditional geographic routing techniques. This routing technique cope with localization errors, thus packet drop rate is reduced. It is therefore, LETR improves the network performance against a depth adjustment based geographic routing protocol, GEDAR at varying node densities. On the other hand, MS based protocols further improve the performance in terms of packet loss ratio and energy consumption.

All the above mentioned routing protocols were developed to achieve better lifespan of the network. It was however, ignored to realize the residual energy of the forwarding node. Along with this there are no mechanism incorporated to cope with the imbalance between the holding time difference and propagation delay of packet between nodes. For this reason, an Energy Scaled and Expanded Vector Based Forwarding (ESEVBF) scheme was proposed. ESEVBF provides energy fairness and reduces the packet broadcast by scaling and expanding the holding time with the residual energy and ratio of projection distance to vector and width of the virtual pipeline. The new holding time signifies the difference between holding times of the potential forwarders, which reduces the data packet broadcast and maintains the energy fairness in the network. The simulation results show that ESEVBF, is approximately 5% more energy efficient, experiences 14.6% less delay, and generates about 5% fewer data packets, compared to AHH-VBF. However, ESEVBF maintains similar PDR and very less number of nodes die in the network when ESEVBF is used as a forwarding technique in the underwater sensor

network.

## 7.2 Future Work

After critically reviewing the literature, it is well understandable that there are still numerous challenges which need to be resolved. The scope of this dissertation is extendable in future through investigation of new energy efficient parameters. Generally, all protocols proposed in this research can be additionally equipped with the phenomenon of duty cycle. The sensor nodes collaboratively schedule its sleep and wakeup time that helps in further reduction of energy consumption. Specifically, as for future work in DOW-PR routing, we plan to further investigate the optimum value of weighting coefficient  $\hat{\alpha}$  and to establish its relation with the topology changes and channel conditions. Residual energy parameters can be included while formulating the forwarding mechanism in DOW-PR, GDGOR-IA and LETR. The routing strategy proposed in ESEVBF can be extended and tested to two hop parameters, for example residual energy of expected forwarders at first and second level of forwarding . Furthermore, this research can be extended through deployment of heterogeneous nodes in all proposed routing protocols.



# Bibliography

- [1] O. Bello and S. Zeadally, “Intelligent device-to-device communication in the internet of things,” *IEEE Systems Journal*, vol. 10, no. 3, pp. 1172–1182, 2016.
- [2] P. S. Mann and S. Singh, “Energy-efficient hierarchical routing for wireless sensor networks: A swarm intelligence approach,” *Wireless Personal Communications*, vol. 92, no. 2, pp. 785–805, 2017.
- [3] B. Prabhu, N. Balakumar, and A. J. Antony, “Evolving constraints in military applications using wireless sensor networks,” 2017.
- [4] R. E. Mohamed, A. I. Saleh, M. Abdelrazzak, and A. S. Samra, “Energy-efficient routing protocols for solving energy hole problem in wireless sensor networks,” *Computer Networks*, vol. 114, pp. 51–66, 2017.
- [5] S. Maurya, V. Gupta, and V. K. Jain, “Lbrr: Load balanced ring routing protocol for heterogeneous sensor networks with sink mobility,” in *Wireless Communications and Networking Conference (WCNC), 2017 IEEE*. IEEE, 2017, pp. 1–6.
- [6] N. Sabor, S. Sasaki, M. Abo-Zahhad, and S. M. Ahmed, “A comprehensive survey on hierarchical-based routing protocols for mobile wireless sensor networks: Review, taxonomy, and future directions,” *Wireless Communications and Mobile Computing*, vol. 2017, 2017.
- [7] A. Kumar, H. Y. Shwe, K. J. Wong, and P. H. Chong, “Location-based routing protocols for wireless sensor networks: A survey,” *Wireless Sensor Network*, vol. 9, no. 01, p. 25, 2017.

- 
- [8] K. Langendoen and A. Meier, "Analyzing mac protocols for low data-rate applications," *ACM Transactions on Sensor Networks (TOSN)*, vol. 7, no. 2, p. 19, 2010.
- [9] C. Tunca, S. Isik, M. Y. Donmez, and C. Ersoy, "Ring routing: An energy-efficient routing protocol for wireless sensor networks with a mobile sink," *IEEE Transactions on Mobile Computing*, vol. 14, no. 9, pp. 1947–1960, 2015.
- [10] J. Heidemann, W. Ye, J. Wills, A. Syed, and Y. Li, "Research challenges and applications for underwater sensor networking," in *Wireless Communications and Networking Conference, 2006. WCNC 2006. IEEE*, vol. 1. IEEE, 2006, pp. 228–235.
- [11] U. M. Cella, R. Johnstone, and N. Shuley, "Electromagnetic wave wireless communication in shallow water coastal environment: theoretical analysis and experimental results," in *Proceedings of the Fourth ACM International Workshop on UnderWater Networks*. ACM, 2009, p. 9.
- [12] X. Che, I. Wells, G. Dickers, P. Kear, and X. Gong, "Re-evaluation of rf electromagnetic communication in underwater sensor networks," *IEEE Communications Magazine*, vol. 48, no. 12, pp. 143–151, 2010.
- [13] F. Hanson and S. Radic, "High bandwidth underwater optical communication," *Applied optics*, vol. 47, no. 2, pp. 277–283, 2008.
- [14] H. Kaushal and G. Kaddoum, "Underwater optical wireless communication," *IEEE Access*, vol. 4, pp. 1518–1547, 2016.
- [15] E. M. Sozer, M. Stojanovic, and J. G. Proakis, "Underwater acoustic networks," *IEEE journal of oceanic engineering*, vol. 25, no. 1, pp. 72–83, 2000.
- [16] M. Stojanovic and J. Preisig, "Underwater acoustic communication channels: Propagation models and statistical characterization," *IEEE communications magazine*, vol. 47, no. 1, pp. 84–89, 2009.

- 
- [17] J. Heidemann, M. Stojanovic, and M. Zorzi, "Underwater sensor networks: applications, advances and challenges," *Phil. Trans. R. Soc. A*, vol. 370, no. 1958, pp. 158–175, 2012.
- [18] R. W. Coutinho, A. Boukerche, L. F. Vieira, and A. A. Loureiro, "Geographic and opportunistic routing for underwater sensor networks," *IEEE Transactions on Computers*, vol. 65, no. 2, pp. 548–561, 2016.
- [19] A. Boukerche and A. Darehshoorzadeh, "Opportunistic routing in wireless networks: Models, algorithms, and classifications," *ACM Computing Surveys (CSUR)*, vol. 47, no. 2, p. 22, 2015.
- [20] D. Chen and P. K. Varshney, "A survey of void handling techniques for geographic routing in wireless networks," *IEEE Communications Surveys & Tutorials*, vol. 9, no. 1, pp. 50–67, 2007.
- [21] R. W. Coutinho, A. Boukerche, L. F. Vieira, and A. A. Loureiro, "Gedar: geographic and opportunistic routing protocol with depth adjustment for mobile underwater sensor networks," in *Communications (ICC), 2014 IEEE International Conference on*. IEEE, 2014, pp. 251–256.
- [22] M. Garcia, D. Carvalho, O. Zlydareva, C. Muldoon, B. Masterson, M. O'Grady, W. Meijer, J. O'Sullivan, and G. O'Hare, "An agent-based wireless sensor network for water quality data collection," *Ubiquitous Computing and Ambient Intelligence*, pp. 454–461, 2012.
- [23] E. M. Sozer, M. Stojanovic, and J. G. Proakis, "Underwater acoustic networks," *IEEE journal of oceanic engineering*, vol. 25, no. 1, pp. 72–83, 2000.
- [24] M. Stojanovic and J. Preisig, "Underwater acoustic communication channels: Propagation models and statistical characterization," *IEEE communications magazine*, vol. 47, no. 1, pp. 84–89, 2009.
- [25] P. K. Sahoo and W.-C. Liao, "Hora: A distributed coverage hole repair algorithm for wireless sensor networks," *IEEE Transactions on Mobile Computing*, vol. 14, no. 7, pp. 1397–1410, 2015.

- [26] R. Kacimi, R. Dhaou, and A.-L. Beylot, "Load balancing techniques for lifetime maximizing in wireless sensor networks," *Ad hoc networks*, vol. 11, no. 8, pp. 2172–2186, 2013.
- [27] M. A. Khan, A. Sher, A. R. Hameed, N. Jan, J. S. Abassi, and N. Javaid, "Network lifetime maximization via energy hole alleviation in wireless sensor networks," in *International Conference on Broadband and Wireless Computing, Communication and Applications*. Springer, 2016, pp. 279–290.
- [28] K. Li, "Optimal number of annuli for maximizing the lifetime of sensor networks," *Journal of Parallel and Distributed Computing*, vol. 74, no. 1, pp. 1719–1729, 2014.
- [29] M. B. Rasheed, N. Javaid, Z. Khan, U. Qasim, and M. Ishfaq, "E-horm: An energy-efficient hole removing mechanism in wireless sensor networks," in *Electrical and Computer Engineering (CCECE), 2013 26th Annual IEEE Canadian Conference on*. IEEE, 2013, pp. 1–4.
- [30] D. Jewel, P. Brundha, D. Wise, and G. A. Swaminathan, "Improved hole detection healing and replacing algorithm for optimal coverage in wireless sensor networks," 2016.
- [31] H. H. Ekal, J. Abdullah, A. Jamil, L. Audah, and R. Alias, "Energy balance mechanism for improving the lifetime in dense centric wireless sensor networks," in *Information Technology, Electronics and Mobile Communication Conference (IEMCON), 2016 IEEE 7th Annual*. IEEE, 2016, pp. 1–7.
- [32] T. Lu, G. Liu, and S. Chang, "Energy-efficient data sensing and routing in unreliable energy-harvesting wireless sensor network," *Wireless Networks*, pp. 1–15, 2016.
- [33] J. Kulshrestha and M. Mishra, "An adaptive energy balanced and energy efficient approach for data gathering in wireless sensor networks," *Ad Hoc Networks*, vol. 54, pp. 130–146, 2017.

- [34] V. Kumar and S. Kumar, "Energy balanced position-based routing for lifetime maximization of wireless sensor networks," *Ad Hoc Networks*, vol. 52, pp. 117–129, 2016.
- [35] C. Lin, G. Wu, F. Xia, M. Li, L. Yao, and Z. Pei, "Energy efficient ant colony algorithms for data aggregation in wireless sensor networks," *Journal of Computer and System Sciences*, vol. 78, no. 6, pp. 1686–1702, 2012.
- [36] X. Liu, "An optimal-distance-based transmission strategy for lifetime maximization of wireless sensor networks," *IEEE Sensors Journal*, vol. 15, no. 6, pp. 3484–3491, 2015.
- [37] A. Ghaffari, "An energy efficient routing protocol for wireless sensor networks using a-star algorithm," *Journal of applied research and technology*, vol. 12, no. 4, pp. 815–822, 2014.
- [38] S. Bhattacharjee and S. Bandyopadhyay, "Lifetime maximizing dynamic energy efficient routing protocol for multi hop wireless networks," *Simulation Modelling Practice and Theory*, vol. 32, pp. 15–29, 2013.
- [39] J. Ren, Y. Zhang, K. Zhang, A. Liu, J. Chen, and X. S. Shen, "Lifetime and energy hole evolution analysis in data-gathering wireless sensor networks," *IEEE transactions on industrial informatics*, vol. 12, no. 2, pp. 788–800, 2016.
- [40] P. G. V. Naranjo, M. Shojafar, A. Abraham, and E. Baccarelli, "A new stable election-based routing algorithm to preserve aliveness and energy in fog-supported wireless sensor networks," in *Systems, Man, and Cybernetics (SMC), 2016 IEEE International Conference on*. IEEE, 2016, pp. 002413–002418.
- [41] P. G. V. Naranjo, M. Shojafar, H. Mostafaei, Z. Pooranian, and E. Baccarelli, "P-sep: a prolong stable election routing algorithm for energy-limited heterogeneous fog-supported wireless sensor networks," *The Journal of Supercomputing*, vol. 73, no. 2, pp. 733–755, 2017.

- [42] Y.-x. Jin, F.-z. Chen, G.-f. Che, and W. Hu, "Energy-efficient data collection protocol for wireless sensor network based on tree," in *Wearable Computing Systems (APWCS), 2010 Asia-Pacific Conference on*. IEEE, 2010, pp. 82–85.
- [43] M. Stojanovic, "On the relationship between capacity and distance in an underwater acoustic communication channel," *ACM SIGMOBILE Mobile Computing and Communications Review*, vol. 11, no. 4, pp. 34–43, 2007.
- [44] T. Hafeez, N. Javaid, A. R. Hameed, A. Sher, Z. A. Khan, and U. Qasim, "Avn-ahh-vbf: Avoiding void node with adaptive hop-by-hop vector based forwarding for underwater wireless sensor networks," in *Innovative Mobile and Internet Services in Ubiquitous Computing (IMIS), 2016 10th International Conference on*. IEEE, 2016, pp. 49–56.
- [45] Y. Noh, U. Lee, S. Lee, P. Wang, L. F. Vieira, J.-H. Cui, M. Gerla, and K. Kim, "Hydrocast: pressure routing for underwater sensor networks," *IEEE Transactions on Vehicular Technology*, vol. 65, no. 1, pp. 333–347, 2016.
- [46] C. Carbonelli and U. Mitra, "Cooperative multihop communication for underwater acoustic networks," in *Proceedings of the 1st ACM international workshop on Underwater networks*. ACM, 2006, pp. 97–100.
- [47] H. Yang, B. Liu, F. Ren, H. Wen, and C. Lin, "Optimization of energy efficient transmission in underwater sensor networks," in *Global Telecommunications Conference, 2009. GLOBECOM 2009. IEEE*. IEEE, 2009, pp. 1–6.
- [48] S. Climent, A. Sanchez, J. V. Capella, N. Meratnia, and J. J. Serrano, "Underwater acoustic wireless sensor networks: advances and future trends in physical, mac and routing layers," *Sensors*, vol. 14, no. 1, pp. 795–833, 2014.
- [49] G. J. Pottie and W. J. Kaiser, "Wireless integrated network sensors," *Communications of the ACM*, vol. 43, no. 5, pp. 51–58, 2000.

- [50] M. O'Rourke, E. Basha, and C. Detweiler, "Multi-modal communications in underwater sensor networks using depth adjustment," in *Proceedings of the Seventh ACM International Conference on Underwater Networks and Systems*. ACM, 2012, p. 31.
- [51] M. Z. Abbas, K. A. Bakar, M. Ayaz, M. H. Mohamed, and M. Tariq, "Hop-by-hop dynamic addressing based routing protocol for monitoring of long range underwater pipeline." *KSII Transactions on Internet & Information Systems*, vol. 11, no. 2, 2017.
- [52] C. Maihofer, "A survey of geocast routing protocols," *IEEE Communications Surveys & Tutorials*, vol. 6, no. 2, 2004.
- [53] P. Xie, J.-H. Cui, and L. Lao, "Vbf: vector-based forwarding protocol for underwater sensor networks," in *Networking*, vol. 3976. Springer, 2006, pp. 1216–1221.
- [54] M. R. Jafri, M. M. Sandhu, K. Latif, Z. A. Khan, A. U. H. Yasar, and N. Javaid, "Towards delay-sensitive routing in underwater wireless sensor networks," *Procedia Computer Science*, vol. 37, pp. 228–235, 2014.
- [55] M. Ayaz, A. Abdullah, I. Faye, and Y. Batira, "An efficient dynamic addressing based routing protocol for underwater wireless sensor networks," *Computer Communications*, vol. 35, no. 4, pp. 475–486, 2012.
- [56] Y. Noh, U. Lee, P. Wang, B. S. C. Choi, and M. Gerla, "Vapr: void-aware pressure routing for underwater sensor networks," *IEEE Transactions on Mobile Computing*, vol. 12, no. 5, pp. 895–908, 2013.
- [57] H. Yan, Z. Shi, and J.-H. Cui, "Dbr: depth-based routing for underwater sensor networks," *NETWORKING 2008 Ad Hoc and Sensor Networks, Wireless Networks, Next Generation Internet*, pp. 72–86, 2008.
- [58] M. Zuba, M. Fagan, Z. Shi, and J.-H. Cui, "A resilient pressure routing scheme for underwater acoustic networks," in *Global Communications Conference (GLOBECOM), 2014 IEEE*. IEEE, 2014, pp. 637–642.

- [59] H. Yu, N. Yao, T. Wang, G. Li, Z. Gao, and G. Tan, “Wdfad-dbr: Weighting depth and forwarding area division dbr routing protocol for uasns,” *Ad Hoc Networks*, vol. 37, pp. 256–282, 2016.
- [60] R. W. Coutinho, L. F. Vieira, and A. A. Loureiro, “Dcr: Depth-controlled routing protocol for underwater sensor networks,” in *Computers and Communications (ISCC), 2013 IEEE Symposium on*. IEEE, 2013, pp. 000 453–000 458.
- [61] —, “Movement assisted-topology control and geographic routing protocol for underwater sensor networks,” in *Proceedings of the 16th ACM international conference on Modeling, analysis & simulation of wireless and mobile systems*. ACM, 2013, pp. 189–196.
- [62] Z. Li, N. Yao, and Q. Gao, “Relative distance based forwarding protocol for underwater wireless networks,” *International Journal of Distributed Sensor Networks*, vol. 10, no. 2, p. 173089, 2014.
- [63] S. K. Dhurandher, M. S. Obaidat, and M. Gupta, “A novel geocast technique with hole detection in underwater sensor networks,” in *Computer Systems and Applications (AICCSA), 2010 IEEE/ACS International Conference on*. IEEE, 2010, pp. 1–8.
- [64] N. Nicolaou, A. See, P. Xie, J.-H. Cui, and D. Maggiorini, “Improving the robustness of location-based routing for underwater sensor networks,” in *Oceans 2007-Europe*. IEEE, 2007, pp. 1–6.
- [65] H. Yu, N. Yao, and J. Liu, “An adaptive routing protocol in underwater sparse acoustic sensor networks,” *Ad Hoc Networks*, vol. 34, pp. 121–143, 2015.
- [66] J. M. Jornet, M. Stojanovic, and M. Zorzi, “Focused beam routing protocol for underwater acoustic networks,” in *Proceedings of the third ACM international workshop on Underwater Networks*. ACM, 2008, pp. 75–82.



- [67] T. Ali, L. T. Jung, and S. Ameer, "Flooding control by using angle based cone for uwsns," in *Telecommunication Technologies (ISTT), 2012 International Symposium on*. IEEE, 2012, pp. 112–117.
- [68] D. Hwang and D. Kim, "Dfr: Directional flooding-based routing protocol for underwater sensor networks," in *OCEANS 2008*. IEEE, 2008, pp. 1–7.
- [69] E. A. Carlson, P.-P. J. Beaujean, and E. An, "Location-aware source routing protocol for underwater acoustic networks of auvs," *Journal of Electrical and Computer Engineering*, vol. 2012, p. 5, 2012.
- [70] Z. Guo, G. Colombi, B. Wang, J.-H. Cui, D. Maggiorini, and G. P. Rossi, "Adaptive routing in underwater delay/disruption tolerant sensor networks," in *Wireless on Demand Network Systems and Services, 2008. WONS 2008. Fifth Annual Conference on*. IEEE, 2008, pp. 31–39.
- [71] T. Ali, L. T. Jung, and I. Faye, "Diagonal and vertical routing protocol for underwater wireless sensor network," *Procedia-Social and Behavioral Sciences*, vol. 129, pp. 372–379, 2014.
- [72] A. Wahid, S. Lee, H.-J. Jeong, and D. Kim, "Eedbr: Energy-efficient depth-based routing protocol for underwater wireless sensor networks," *Advanced Computer Science and Information Technology*, pp. 223–234, 2011.
- [73] J. Xu, K. Li, G. Min, K. Lin, and W. Qu, "Energy-efficient tree-based multi-path power control for underwater sensor networks," *IEEE Transactions on Parallel and Distributed Systems*, vol. 23, no. 11, pp. 2107–2116, 2012.
- [74] B. Peng and A. H. Kemp, "Energy-efficient geographic routing in the presence of localization errors," *Computer Networks*, vol. 55, no. 3, pp. 856–872, 2011.
- [75] A. M. Popescu, N. Salman, and A. H. Kemp, "Geographic routing resilient to location errors," *IEEE Wireless Communications Letters*, vol. 2, no. 2, pp. 203–206, 2013.

- [76] N. Salman, M. Ghogho, and A. H. Kemp, "On the joint estimation of the rssi-based location and path-loss exponent," *IEEE Wireless Communications Letters*, vol. 1, no. 1, pp. 34–37, 2012.
- [77] Z. Zhou, Z. Peng, J.-H. Cui, Z. Shi, and A. Bagtzoglou, "Scalable localization with mobility prediction for underwater sensor networks," *IEEE Transactions on Mobile Computing*, vol. 10, no. 3, pp. 335–348, 2011.
- [78] O. Cayirpunar, E. Kadioglu-Urtis, and B. Tavli, "Optimal base station mobility patterns for wireless sensor network lifetime maximization," *IEEE Sensors Journal*, vol. 15, no. 11, pp. 6592–6603, 2015.
- [79] Y.-S. Chen and Y.-W. Lin, "Mobicast routing protocol for underwater sensor networks," *IEEE Sensors journal*, vol. 13, no. 2, pp. 737–749, 2013.
- [80] M. Akbar, N. Javaid, A. H. Khan, M. Imran, M. Shoaib, and A. Vasilakos, "Efficient data gathering in 3d linear underwater wireless sensor networks using sink mobility," *Sensors*, vol. 16, no. 3, p. 404, 2016.
- [81] S. Yoon, A. K. Azad, H. Oh, and S. Kim, "Aurp: An auv-aided underwater routing protocol for underwater acoustic sensor networks," *Sensors*, vol. 12, no. 2, pp. 1827–1845, 2012.
- [82] W. Liang, J. Luo, and X. Xu, "Prolonging network lifetime via a controlled mobile sink in wireless sensor networks," in *Global Telecommunications Conference (GLOBECOM 2010), 2010 IEEE*. IEEE, 2010, pp. 1–6.
- [83] P. Baruah, R. Urgaonkar, and B. Krishnamachari, "Learning-enforced time domain routing to mobile sinks in wireless sensor fields," in *Local Computer Networks, 2004. 29th Annual IEEE International Conference on*. IEEE, 2004, pp. 525–532.
- [84] S. Basagni, A. Carosi, E. Melachrinoudis, C. Petrioli, and Z. M. Wang, "Controlled sink mobility for prolonging wireless sensor networks lifetime," *Wireless Networks*, vol. 14, no. 6, pp. 831–858, 2008.

- [85] A. Sher, N. Javaid, I. Azam, H. Ahmad, W. Abdul, S. Ghouzali, I. A. Niaz, and F. A. Khan, "Monitoring square and circular fields with sensors using energy-efficient cluster-based routing for underwater wireless sensor networks," *International Journal of Distributed Sensor Networks*, vol. 13, no. 7, p. 1550147717717189, 2017.
- [86] F. Al-Salti, N. Alzeidi, K. Day, B. Arafeh, and A. Touzene, "Grid-based priority routing protocol for uwsns," *International Journal of Computer Networks and Communications*, vol. 9, no. 6, pp. 1–20, 2017.
- [87] K. Anupama, A. Sasidharan, and S. Vadlamani, "A location-based clustering algorithm for data gathering in 3d underwater wireless sensor networks," in *2008 International Symposium on Telecommunications*. IEEE, 2008, pp. 343–348.
- [88] G. Liu and C. Wei, "A new multi-path routing protocol based on cluster for underwater acoustic sensor networks," in *2011 International Conference on Multimedia Technology*. IEEE, 2011, pp. 91–94.
- [89] P. Xie, Z. Zhou, Z. Peng, J.-H. Cui, and Z. Shi, "Void avoidance in three-dimensional mobile underwater sensor networks," in *International Conference on Wireless Algorithms, Systems, and Applications*. Springer, 2009, pp. 305–314.
- [90] J. Khan and H.-S. Cho, "A distributed data-gathering protocol using auv in underwater sensor networks," *Sensors*, vol. 15, no. 8, pp. 19 331–19 350, 2015.
- [91] W. Raza, F. Arshad, I. Ahmed, W. Abdul, S. Ghouzali, I. Niaz, and N. Javaid, "An improved forwarding of diverse events with mobile sinks in underwater wireless sensor networks," *Sensors*, vol. 16, no. 11, p. 1850, 2016.
- [92] G. Han, J. Jiang, N. Bao, L. Wan, and M. Guizani, "Routing protocols for underwater wireless sensor networks," *IEEE Communications Magazine*, vol. 53, no. 11, pp. 72–78, 2015.

- [93] N. Li, J.-F. Martínez, J. M. Meneses Chaus, and M. Eckert, “A survey on underwater acoustic sensor network routing protocols,” *Sensors*, vol. 16, no. 3, p. 414, 2016.
- [94] S. M. Ghoreyshi, A. Shahrabi, and T. Boutaleb, “Void-handling techniques for routing protocols in underwater sensor networks: Survey and challenges,” *IEEE Communications Surveys & Tutorials*, vol. 19, no. 2, pp. 800–827, 2017.
- [95] J. E. Garcia, “Accurate positioning for underwater acoustic networks,” in *Oceans 2005-Europe*, vol. 1. IEEE, 2005, pp. 328–333.
- [96] J. U. Khan and H.-S. Cho, “A distributed data-gathering protocol using auv in underwater sensor networks,” *Sensors*, vol. 15, no. 8, pp. 19 331–19 350, 2015.
- [97] M. C. Domingo and R. Prior, “Energy analysis of routing protocols for underwater wireless sensor networks,” *Computer communications*, vol. 31, no. 6, pp. 1227–1238, 2008.
- [98] U. Lee, J. Kong, M. Gerla, J.-S. Park, and E. Magistretti, “Time-critical underwater sensor diffusion with no proactive exchanges and negligible reactive floods,” *Ad Hoc Networks*, vol. 5, no. 6, pp. 943–958, 2007.
- [99] V. Raghunathan, C. Schurgers, S. Park, and M. B. Srivastava, “Energy-aware wireless microsensor networks,” *IEEE Signal processing magazine*, vol. 19, no. 2, pp. 40–50, 2002.
- [100] I. Vasilescu, K. Kotay, D. Rus, M. Dunbabin, and P. Corke, “Data collection, storage, and retrieval with an underwater sensor network,” in *Proceedings of the 3rd international conference on Embedded networked sensor systems*. ACM, 2005, pp. 154–165.
- [101] N. Xu, S. Rangwala, K. K. Chintalapudi, D. Ganesan, A. Broad, R. Govindan, and D. Estrin, “A wireless sensor network for structural monitoring,”

- in *Proceedings of the 2nd international conference on Embedded networked sensor systems*. Acm, 2004, pp. 13–24.
- [102] R. Szewczyk, A. Mainwaring, J. Polastre, J. Anderson, and D. Culler, “An analysis of a large scale habitat monitoring application,” in *Proceedings of the 2nd international conference on Embedded networked sensor systems*. ACM, 2004, pp. 214–226.
- [103] R. W. Coutinho, A. Boukerche, L. F. Vieira, and A. A. Loureiro, “A novel void node recovery paradigm for long-term underwater sensor networks,” *Ad Hoc Networks*, vol. 34, pp. 144–156, 2015.
- [104] —, “Enor: Energy balancing routing protocol for underwater sensor networks,” in *Communications (ICC), 2017 IEEE International Conference on*. IEEE, 2017, pp. 1–6.
- [105] M. Liu, F. Ji, Q. Guan, H. Yu, F. Chen, and G. Wei, “On-surface wireless-assisted opportunistic routing for underwater sensor networks,” in *Proceedings of the 11th ACM International Conference on Underwater Networks & Systems*. ACM, 2016, p. 43.
- [106] V. G. Menon and P. J. Prathap, “Comparative analysis of opportunistic routing protocols for underwater acoustic sensor networks,” in *Emerging Technological Trends (ICETT), International Conference on*. IEEE, 2016, pp. 1–5.
- [107] J. Janardanan Kartha and L. Jacob, “Delay and lifetime performance of underwater wireless sensor networks with mobile element based data collection,” *International Journal of Distributed Sensor Networks*, vol. 11, no. 5, p. 128757, 2015.
- [108] M. Erol, L. F. Vieira, and M. Gerla, “Localization with dive’n’rise (dnr) beacons for underwater acoustic sensor networks,” in *Proceedings of the second workshop on Underwater networks*. ACM, 2007, pp. 97–100.

- [109] M. O'Rourke, E. Basha, and C. Detweiler, "Multi-modal communications in underwater sensor networks using depth adjustment," in *Proceedings of the Seventh ACM International Conference on Underwater Networks and Systems*. ACM, 2012, p. 31.
- [110] Z. Yu, C. Xiao, and G. Zhou, "Multi-objectivization-based localization of underwater sensors using magnetometers," *IEEE Sensors Journal*, vol. 14, no. 4, pp. 1099–1106, 2014.
- [111] A. Kleerekoper and N. Filer, "Revisiting blacklisting and justifying the unit disk graph model for energy-efficient position-based routing in wireless sensor networks," in *Wireless Days (WD), 2012 IFIP*. IEEE, 2012, pp. 1–3.
- [112] T. Melodia, D. Pompili, and I. F. Akyildiz, "Optimal local topology knowledge for energy efficient geographical routing in sensor networks," in *INFOCOM 2004. Twenty-third Annual Joint Conference of the IEEE Computer and Communications Societies*, vol. 3. IEEE, 2004, pp. 1705–1716.
- [113] S. Lee, B. Bhattacharjee, and S. Banerjee, "Efficient geographic routing in multihop wireless networks," in *Proceedings of the 6th ACM international symposium on Mobile ad hoc networking and computing*. ACM, 2005, pp. 230–241.
- [114] A. Khasawneh, M. S. B. A. Latiff, O. Kaiwartya, and H. Chizari, "A reliable energy-efficient pressure-based routing protocol for underwater wireless sensor network," *Wireless Networks*, pp. 1–15, 2017.
- [115] Y. Han, C. Zheng, and D. Sun, "Localization of large scale underwater sensor networks based on recursive position estimation," in *OCEANS'15 MT-S/IEEE Washington*. IEEE, 2015, pp. 1–4.
- [116] K. M. Kwak and J. Kim, "Development of 3-dimensional sensor nodes using electro-magnetic waves for underwater localization," *Journal of Institute of Control, Robotics and Systems*, vol. 19, no. 2, pp. 107–112, 2013.

- 
- [117] M. Stojanovic, "On the relationship between capacity and distance in an underwater acoustic communication channel," *ACM SIGMOBILE Mobile Computing and Communications Review*, vol. 11, no. 4, pp. 34–43, 2007.
- [118] L. Brekhovskikh and Y. P. Lysanov, "Fundamentals of ocean acoustics," *The Journal of the Acoustical Society of America*, vol. 116, no. 4, pp. 1863–1863, 2004.
- [119] C. Carbonelli and U. Mitra, "Cooperative multihop communication for underwater acoustic networks," in *Proceedings of the 1st ACM international workshop on Underwater networks*. ACM, 2006, pp. 97–100.
- [120] T. S. Rappaport *et al.*, *Wireless communications: principles and practice*. prentice hall PTR New Jersey, 1996, vol. 2.
- [121] J. So and H. Byun, "Load-balanced opportunistic routing for duty-cycled wireless sensor networks," *IEEE Transactions on Mobile Computing*, vol. 16, no. 7, pp. 1940–1955, 2017.
- [122] X. Liu, "A transmission scheme for wireless sensor networks using ant colony optimization with unconventional characteristics," *IEEE Communications Letters*, vol. 18, no. 7, pp. 1214–1217, 2014.
- [123] N. Javaid, M. Shah, A. Ahmad, M. Imran, M. I. Khan, and A. V. Vasilakos, "An enhanced energy balanced data transmission protocol for underwater acoustic sensor networks," *Sensors*, vol. 16, no. 4, p. 487, 2016.
- [124] P. Casari, M. Stojanovic, and M. Zorzi, "Exploiting the bandwidth-distance relationship in underwater acoustic networks," in *OCEANS 2007*. IEEE, 2007, pp. 1–6.
- [125] D. Walker, "Micro autonomous underwater vehicle concept for distributed data collection," in *OCEANS 2006*. IEEE, 2006, pp. 1–4.